UNIVERSITÀ DEGLI STUDI DI CATANIA

IN ASSOCIATION WITH

ISTITUTO NAZIONALE DI FISICA NUCLEARE (INFN)
SEZIONE DI CATANIA

DOTTORATO DI RICERCA IN
FISICA - XXXIII CICLO

BEHNAM ALI MOHAMMADZADEH

PMT'S ICARUS APPARATUS and ITS SLOW CONTROL SYSTEM.

SUPERVISORS
PROF. VINCENZO BELLINI
PROF. GIUSEPPE ANDRONICO
PROF CORRADO SANTORO

COORDINATORE DI DOTTORATO
PROF. SEBASTIANO ALBERGO

To my Wife

NASIM

This thesis is dedicated to my wife for her love, endless support and encouragement.

GLOBAL INDEX

CHAPTER 1

A BRIEF INTRODUCTION TO NEUTRINO

Contents

1.1 History

The significant effects of elusive neutrinos in nuclear physics, particle physics, astronomy and cosmology are undeniable. They are present in everywhere of the Universe and are called nature's mysterious messengers.

In the beginning of the 20^{th} century, the physics world was fronting considerable information coming from the atomic and subatomic realm, that did not fit with classical mechanics and would have given birth to quantum mechanics.

One of the issues was to understand data related to beta decay, connected to the problem of statistics for ^{14}N nucleus. James Chadwick was the first person who discovered the continuous energy spectrum of the beta decay in 1914 [1]. The final state of the beta decay of an unstable nucleus was assumed to consist of only two particles: the daughter nucleus and the electron.

The analysis of this two-body decay mode led to the conclusion that the emitted electron might be monoenergetic.

In 1930, Pauli proposed the following scheme: the beta decay might be a three-body decay, in which an electrically neutral and extremely light particle should have a small magnetic moment such that it could be bound in the decaying nucleus. The results of Pauli's hypothesis are summarized as follows:

1. In the final state of the beta decay, the available energy of the electron should be shared with the new particle, and hence its energy spectrum should be continuous.
2. Because each electron is accompanied by a spin ½ new particle, the spin of ^{14}N must be an integer and subsequently should obey the Bose-Einstein statistics.

In 1932, Chadwick [2] discovered the neutron, which is the counterpart of the proton in a nucleus (Heisenberg, 1932). Years later, Fermi called Pauli's neutral particle "neutrino" and formulated the quantum theory of the beta decay (Fermi, 1933) [3].

Questioning the validity of parity conservation in weak interactions, Tsung-Dao Lee and Chen Ning Yang proposed an experiment to test the angular distribution of the beta rays emitted from the ^{60}Co nuclei with spins polarized along an external magnetic field (Lee and Yang, 1956). If parity was conserved, there should be no correlation between the spin and momentum of every electron emitted in the decay. Chien-Shiung Wu and her collaborators performed the proposed experiment and discovered that the electrons were almost always emitted in the direction opposite to the nuclear spins, which is apparently a signature of maximal parity violation (Wu *et al.*, 1957). Other experimental groups in different weak processes (Garwin et al., 1957; Friedman and Telegdi, 1957) afterwards obtained more evidence for maximal parity non-conservation. Soon after the observation of parity violation, several influential theorists put forward the idea that neutrinos might simply be massless and could naturally be explained in terms of the two component Weyl spinor (Lee and Yang, 1957; Landau, 1957; Salam, 1957). In such a two-component neutrino theory the helicity of a neutrino must be identical with its handedness or chirality. The aforementioned ^{60}Co experiment indicated that the emitted electron and its accompanying electron antineutrino should have left ($h = -1/2$) and right ($h = +1/2$) helicities, respectively, the helicity h of a particle being defined as the projection of its spin vectors in the direction of its impulse (momentum) **p**,

$$\mathbf{h} = \mathbf{s} \cdot \mathbf{p} / |\mathbf{s}| \cdot |\mathbf{p}| \qquad (1)$$

. Direct helicity measurements confirmed $h = -1/2$ for neutrinos and $h = +1/2$ for antineutrinos (Goldhaber *et al.*, 1958; Bardon *et al.*, 1961). That is why neutrinos (antineutrinos) have commonly been accepted to be exactly massless and purely left-handed (right-handed) for several decades before the phenomena of atmospheric and solar neutrino oscillations were firmly established at the end of the 1990's and the beginning of the 2000's [4].

1.2 Neutrino Oscillation

For a long time, it was assumed that Pauli's neutrinos had zero mass. To date direct measurements are no more consistent with this assumption. It is impossible to prove that a quantity, the neutrino mass in this case, is exactly zero. Subsequent experiments required the introduction of a second neutrino, ν_μ, different from the neutrino of β-decay, ν_e; afterwards it was realized that neutrinos could exhibit new interesting phenomena, mixing and oscillations, if their mass is not exactly zero. There is much evidence that this is indeed the case. Together with the three neutrino flavors, ν_e ν_μ and ν_τ, (electron, muon and tau neutrinos), three different lepton numbers have been introduced, which appear to be conserved in any weak interaction. This implies that in β-decay, only ν_e are emitted, while in pion decays almost only, ν_μ are produced (suppression factor of the electron channel is 1.283×10^{-4}).

It is possible however to conceive a situation in which:

1. The neutrinos have masses.

2. The mass eigenstates do not coincide with flavor eigenstates.

Then it's possible to introduce a unitary mixing matrix **U** which connects flavor and mass eigenstates through:

$$V_f = U\,V_m \qquad V_m = U^{\dagger}V_f \ . \tag{2}$$

in which

$$V_f = (\nu_e\,,\nu_\mu\,,\nu_\tau)$$

$$V_m = (\nu_1,\nu_2,\nu_3) \tag{3}$$

are the flavor and mass neutrino eigenstates. If the masses of the three different neutrinos are different then a neutrino beam which at t=0 shows a pure flavor state, may oscillate into another flavor state.

1.3 Hypothesis of the existence of the neutrino (Pauli and Fermi)

In 1914 J. Chadwick discovered that, in addition to electrons produced by internal conversion, and therefore with well-defined energy, since conversion is a two-body process, nuclei emit electrons with a continuous energy spectrum.

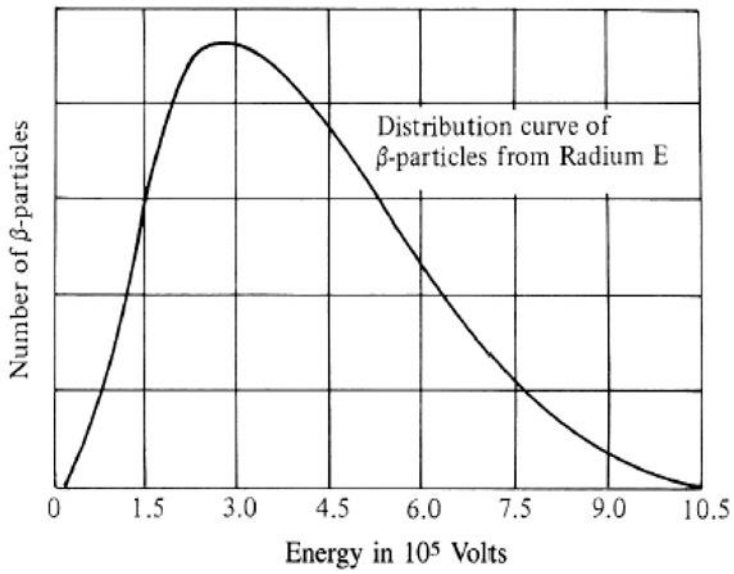

Fig 1: Energy distribution of the electrons emitted in the decay of Radium E, i.e. $_{210}$Bi, a radioactive isotope produced in the $_{238}$U decay chain.

$$ {}_{A}X_{Z} \rightarrow {}_{A}Y_{Z-1} + e^{-} \tag{4} $$

$$ {}_{1}n_{0} \rightarrow {}_{1}p_{1} + e^{-} + \bar{\nu}_{e} \tag{5} $$

In 1930 W. Pauli re-established all conservation laws, hypothesized that in the β decay, together with the electron, a neutral and spin 1/2 particle was also emitted, which does not interact either electromagnetic or nuclear force, that he called “neutron” and Fermi renamed "neutrino" after the discovery of the neutron. The neutrino hypothesis solves the problem of missing energy (the neutrino in practice does not interact in the detectors and goes unnoticed), statistics and conservation of angular momentum. Furthermore, the observed value of the electron's maximum energy, E^{e}_{max}, tells us that the neutrino must

have a very small mass. In 1934, Fermi, taking as a model the description of electron-proton diffusion provided by quantum electrodynamics, also proposed a type of interaction for β decay based on a field theory, in which the particles emitted in the decay are not present in the nucleus before their emission, but they are created at the instant of decay. Fermi used the mathematical formalism of the creation and destruction operators of particles introduced by Jordan for electrodynamics. In this case, however, the interaction is point-like and is called a four fermion interaction, constituting a "contact" interaction between the four spin 1/2 particles involved in the reaction, the neutron (which constitutes the initial state), the proton, the electron and the antineutrino (which constitute the final state).

1.4 Experimental discovery of the neutrino (Cowan-Reines)

The success of Fermi's theory in describing nuclear decays (beta decays) was a convincing "indirect" evidence of the existence of the neutrino; from the Pauli hypothesis, however, it took more than 25 years to detect the effects of a neutrino interaction in an experiment. This is due to the incredibly small values of the cross sections of the neutrino-matter interactions. Indeed, from Fermi's theory we have $\sigma(\nu_e) \approx 10^{-43}\ \mathrm{cm}^2\ \mathrm{MeV}^{-2}\ E_\nu{}^2$. To detect these interactions, it is therefore necessary to have a neutrino source with a very high flux and a target with a very high mass. The simplest neutrino or antineutrino interactions are those of inverse β decay,

$$\nu_e + n \rightarrow e^- + p \quad (6)$$

$$\bar{\nu}_e + p \rightarrow e^+ + n \quad (7)$$

In 1956, G. Cowan and F. Reines proposed to exploit the high flow of $\bar{\nu}_e$ produced by the fission of uranium in the 1 GW reactor of the Savannah-River plant. Nuclear reactors are very intense sources of $\bar{\nu}_e$ that derive from the β decay of the neutrons of which the fragments of nuclear fission are rich. The neutrino flux from the reactor can be estimated considering that on average a fission reaction provides about 200 MeV of thermal energy and produces 6 $\bar{\nu}_e$ per fission. For a 1 GW reactor the estimate of the flow is $\Phi_\Omega \sim 1.9 \cdot 10^{20}$ antineutrinos / s, with a continuous energy spectrum and an average energy of ~ 3 MeV.

The apparatus designed by Cowan and Reines consisted of a target of about 1000 liters of aqueous solution of cadmium chloride, $CdCl_2$, contained in two containers alternating with three other containers filled with a liquid scintillator that acted as a detector.

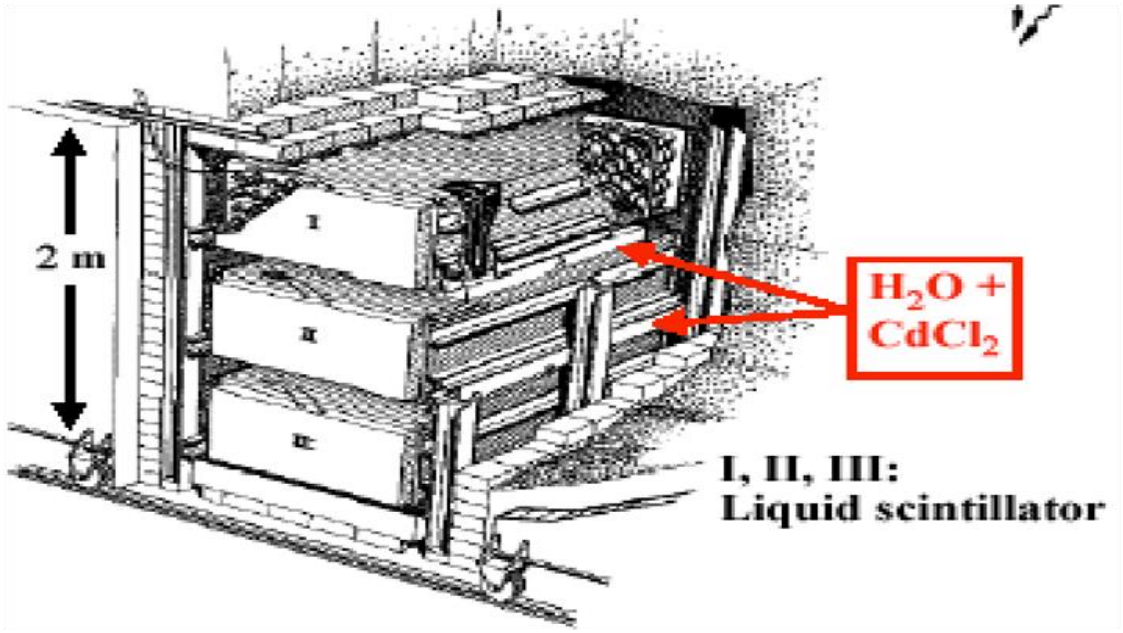

Fig 2: Cowan and Reines experimental setup.

The experimental signature of the neutrino reaction is as follows: the positron produced by the reaction is rapidly annihilated with a water electron in a pair of photons, which produce light due to the Compton effect in the scintillators surrounding the water. The light is detected with photomultipliers. The characteristic time is about 10^{-9} s and the coincidence between two scintillators (I and II or II and III in figure 2) represents the t_0 of the measurement; the neutron is slowed down ("moderated") by collisions with water and in a time of $\sim 10^{-5}$ s it is captured by cadmium. From the capture, photons of $\sim$ 6 MeV are emitted. There is therefore a delayed γ- γ coincidence with respect to t_0 in the same pair of scintillators and this defines the data taking strategy. The signature that distinguishes the searched events is therefore a double coincidence in the same pair of scintillators, separated by a time of a few microseconds. In a first series of measurements lasting 200 hours, 567 such events were collected. The estimated background with the reactor off was 209 events. The expected fluctuation of the fund is therefore $\sqrt{209}$, so the

observation of 567 events is very significant. The result of the measurement is $\sigma(\bar{\nu}_e p \rightarrow n e^{+)} = (1.1 \pm 0.3)\ 10^{-43}\ cm^2$.

1.5 Neutrino: Dirac or Majorana particle?

The Standard Model was formulated in the 1960s accordingly to the knowledge available at that time about existing elementary particles and their properties. Neutrinos had to be massless following Landau's so-called two-component theory (Lee & Yang and Salam), in which massless neutrinos are described by left-handed Weyl spinors. A particle can be left-handed, spinor ψ_L (right-handed, spinor ψ_R) if its helicity is -1 (+1),

This description was adopted in the Standard Model of Glashow, Weinberg and Salam, assuming the non-existence of right-handed neutrinos, necessary to generate the mass of the Dirac neutrino with the same Higgs mechanism that generates the Dirac masses for charged quarks and leptons. However, in recent years, experiments have shown compelling evidence for the existence of neutrino oscillations, which are a consequence of the non-zero masses of neutrinos and their flavor mixing. So, it is time to revise the Standard Model, taking into account the non-zero mass of neutrinos.

In 1937 Majorana discovered that a neutral fermion with finite mass, such as the neutrino, can be described by a spinor with only two independent components, imposing the so-called Majorana condition: $\psi = \psi^c$, where $\psi^c = C\psi^T$, with the matrix C equal to quantum operator of charge conjugation, which in quantum mechanics transforms a particle to its antiparticle and vice versa. Without going into detail in the formalism, Majorana's condition is equivalent to imposing that $\psi_R = \psi_L^c$. Therefore, the dextrorotatory component ψ_R of the Majorana neutrino is not independent, but it can be obtained from the left-handed component through the charge conjugation operation and the Majorana spinor can therefore be written as $\psi = \psi_L + \psi_L^c$. In this way, what we now call antineutrino, would be only the dextrorotatory neutrino, while the real antineutrino would be a particle with a very large mass, yet to be discovered experimentally. Whether the neutrino is described by the Dirac equation or by that of Majorana is currently an open problem. In my thesis I

will not deal with the measurements of possible neutrino-free double beta decay, the existence of which would prove that Majorana is right about the nature of the neutrino.

1.6 Generalities on Neutrino Oscillations

The Standard Model provides three families of neutrinos with zero mass:

$$\binom{\nu_e}{e^-}_L \binom{\nu_\mu}{\mu^-}_L \binom{\nu_\tau}{\tau^-}_L \tag{8}$$

$$\binom{\bar{\nu}_e}{e^+}_R \binom{\bar{\nu}_\mu}{\mu^+}_R \binom{\bar{\nu}_\tau}{\tau^+}_R \tag{9}$$

Neutrinos couple only through the weak charge and interact with two different modes: charged current (CC), with exchange of W^+ or W^- and neutral current (NC) with exchange of Z^0.

Assuming that, neutrinos have mass, we can express the weak-tasting neutrino eigenstates $|\nu_\alpha>\ (\alpha = e, \mu, \tau)$ as a linear combination of $|\nu_k>$ (k = 1,2,3). Neutrino oscillations -> the neutrino eigenstates of weak flavor do not exactly correspond to the mass eigenstates, but are mixtures of one and the other: |

$$|\nu_\alpha>=\sum_{k=1,2,3} U_{\alpha k}^{*}\ |\nu_k> \tag{10}$$

A mass eigenstate $|\nu_k>$with mass m_k and impulse p evolves over time according to

$$|\nu_k(t)>= e^{-iE_k t}|\nu_k> \tag{11}$$

where $E_k = \sqrt{P^2 + {m_k}^2}$ and the units of measurement are used for which c = 1.

The temporal evolution of a weak flavor eigenstate $|\nu_\alpha>$is given by

$$|\nu_\alpha(t)>=\sum_{k=1,2,3} U_{\alpha k}^{*}\ |\nu_k> \tag{12}$$

Combining equations (8), (9) and (10) we find:

$$|\nu_\alpha(t)>=\sum_{\beta=e,\mu,\tau}\left(\sum_{k=1,2,3} U_{\alpha k}^{*}\, e^{-iE_k t}\, U_{\beta k}\right)|\nu_\beta> \tag{13}$$

The probability that a neutrino created as a weak eigenstate ν_α will be detected as a weak eigenstate ν_β after time t is:

$$P(\nu_\alpha \to \nu_\beta)(t) = \left|\langle \nu_\alpha | \nu_\beta(t) \rangle\right|^2$$

$$= \sum_{k=1,2,3} \sum_{j=1,2,3} U_{\alpha k}{}^* U_{\beta k} U_{\alpha j} U_{\beta j}{}^* e^{-i(E_k - E_j)t} \quad (14)$$

An ultra-relativistic neutrino covers a distance L in time t and has $E \approx p + m^2 / 2p$. Assuming that all neutrinos have the same momentum we can set $E = |\mathbf{p}| \cdot E_k - E_j \approx \Delta m_{kj}{}^2 / 2E$ where $\Delta m_{kj}{}^2 = m_k{}^2 - m_j{}^2$

It is thus obtained:

$$P(\nu_\alpha \to \nu_\beta)(L, E) = \sum_{k=1,2,3} \sum_{j=1,2,3} U_{\alpha k}{}^* U_{\beta k} U_{\alpha j} U_{\beta j}{}^* exp\left(-i \frac{\Delta m_{kj}{}^2 L}{2E}\right) \quad (15)$$

The unitary matrix U is known as the PMNS matrix (Pontecorvo-Maki-Nakagawa-Sakata). A representation of it is:

$$U = \begin{pmatrix} c_{12}c_{13} & s_{12}c_{13} & s_{13}e^{-i\delta} \\ -s_{12}c_{23} - c_{12}s_{13}s_{23}e^{i\delta} & c_{12}c_{23} - s_{12}s_{13}e^{i\delta} & c_{13}s_{23} \\ s_{12}s_{23} - c_{12}s_{13}c_{23}e^{i\delta} & -c_{12}s_{23} - s_{12}s_{13}c_{23}e^{i\delta} & c_{13}c_{23} \end{pmatrix} \quad (16)$$

By measuring the change in the flavor composition of neutrino sources over long distances, as a function of L / E, neutrino oscillations can be experimentally detected, with results that are different from the predictions of the Standard Model. [5]

Why will I present mainly high energy data on muon neutrinos and antineutrinos (ν_μ) in the following?

$$\nu_\mu \to \mu^- \,,\ \bar{\nu_\mu} \to \mu^+ \quad (17)$$

Because high-energy neutrino beams are generally produced by pion decay:

$$\pi^+ \to \nu_\mu + \mu^+ \ , \quad \pi^- \to \bar{\nu_\mu} + \mu^- \quad (18)$$

In these beams, including that of the Fermilab booster where the Short Baseline Neutrino) SBN experiment will take data, the electron's neutrinos are a few percent. They come from the decay of the muon, which has an average life (t_μ = 2.197 μs), about one hundred times longer than that of the pion (t_μ = 26 ns), and from the modest contamination of K in

the π beams. The $K^{\pm}$ (particle with strangeness) have a hadron production cross section much smaller than that of the pion and decays mainly with emission of ν_μ.

$$\mu^- \rightarrow \nu_\mu + e^- + \bar{\nu}_e \qquad \mu^+ \rightarrow \bar{\nu}_\mu + e^+ + \nu_e \tag{19}$$

$$k^+ \rightarrow \mu^+ + \nu_\mu \quad , BR = 63{,}43\% \tag{20}$$

$$k^+ \rightarrow \pi^0 + e^+ + \nu_e \quad , BR = 4{,}87\% \tag{21}$$

1.7 Experiments in progress: the road to massive liquid Argon detectors

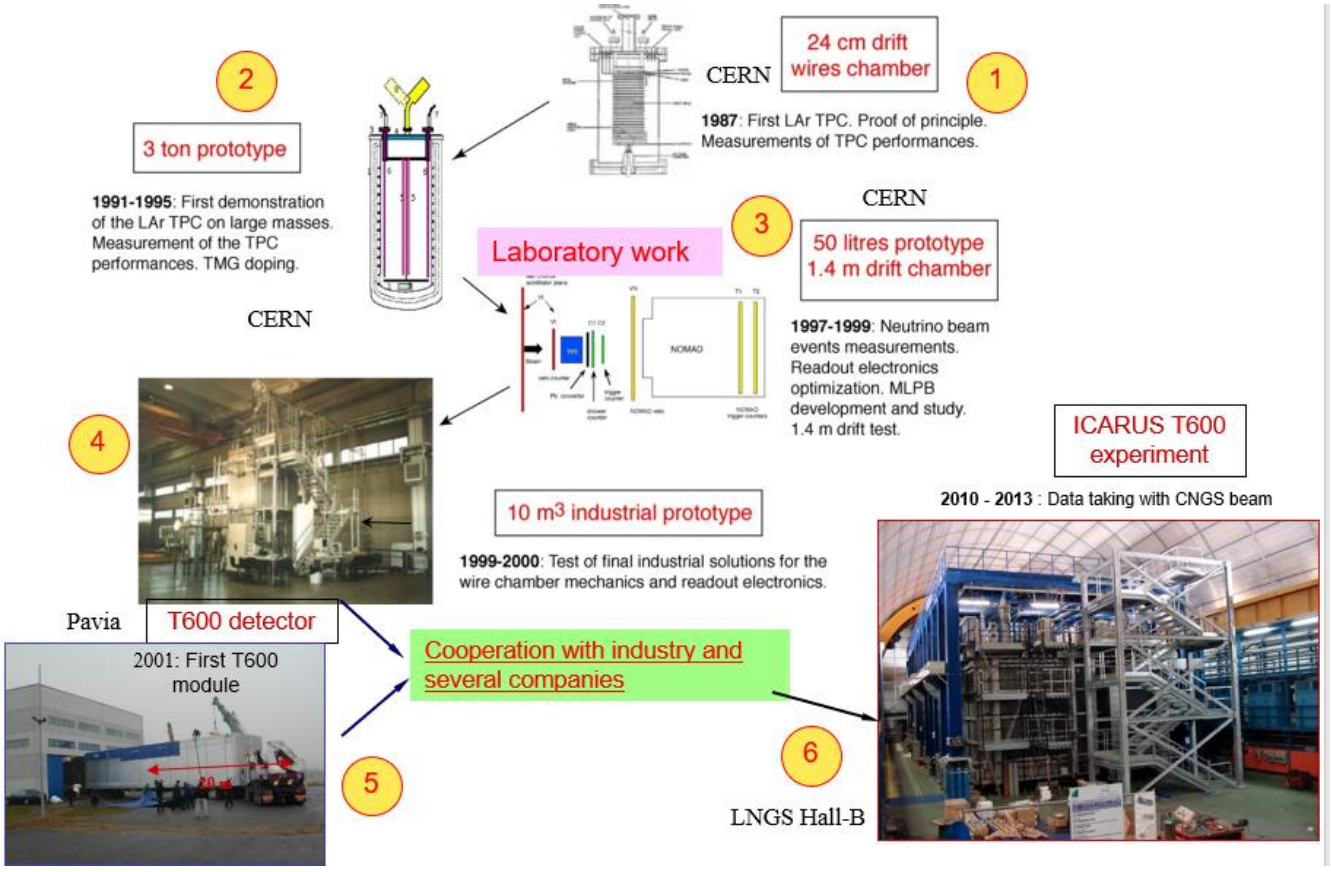

This road map has been essentially developed by C. Rubbia and collaborators at CERN (Switzerland), Pavia and LNGS (Assergi) Italy.

1.8 Experiments in progress: 3D identification of particles

($k^+ \rightarrow \mu^+ \rightarrow e^+$)

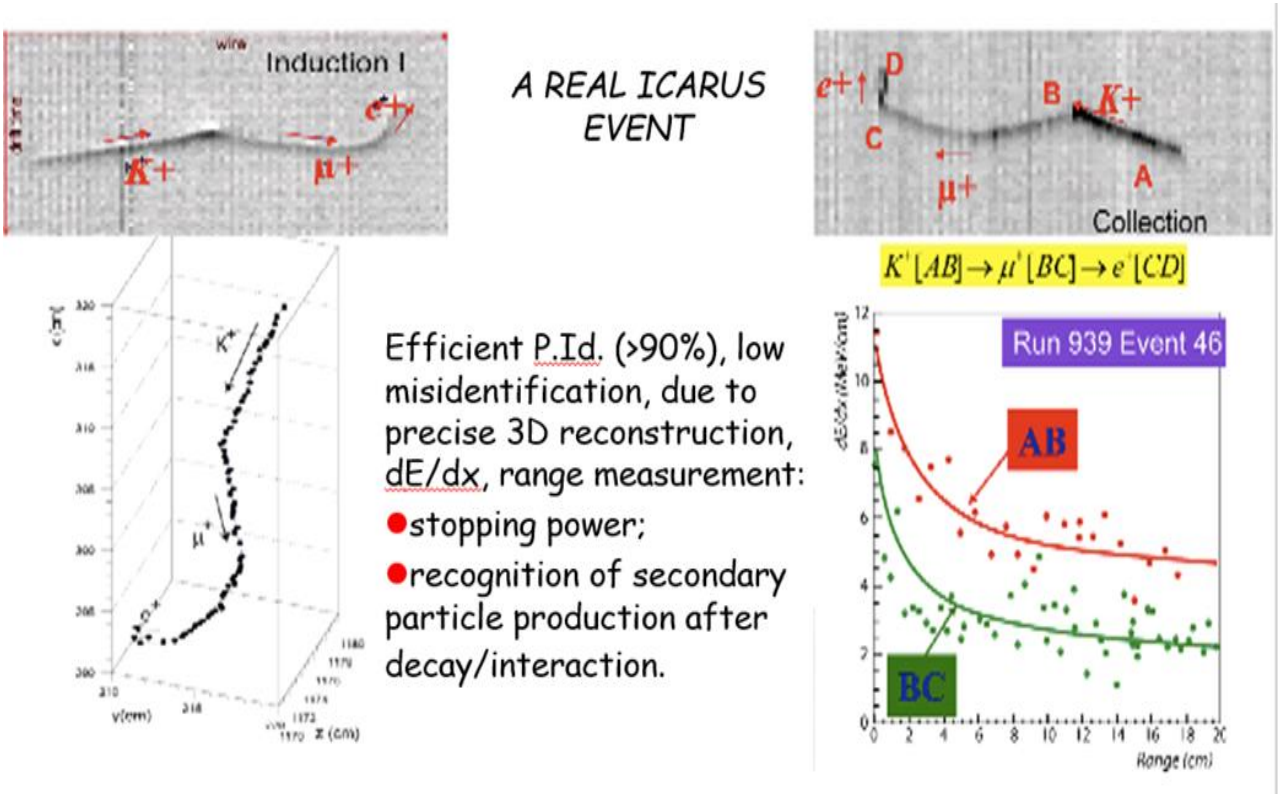

Example of K^+ decay imaging in ICARUS T600 Time Projection Chamber.

Induction and collection are two modes to collect the charge produced inside a TPC. So, there is the first layer of wires that operates using the phenomenon of electrical induction. This is an event of a kaon decay to muon and electron. The same event is also displayed using the charge collection.

In three dimensions, it is the decay of the kaon and reconstruction of the track. The kaon decays and we can see $\mu^+$and e^+at the end of the track. So, this is the reconstruction of kaon decay track. In the right diagram, we can see the identification mode of the particle. AB is related to the kaon. In the classical banana plot, $\frac{dE}{dX}$, the relative points are higher in this plot. The green track is the same, but for the path BC. It is normal that in this banana plot we identify the particle by following the ratio mass charge.

1.9 Experiments in progress: the "short baseline" neutrino physics

Are neutrinos a simple “carbon copy” repetition of quarks? Neutrino oscillations have established a picture consistent with the mixing of three physical neutrino ν_e, ν_μ and ν_τ with mass eigenstates ν_1, ν_2 and ν_3. In particular $\Delta {m_{31}}^2 \approx 2.4 \times 10^{-3}$ eV^2 and $\Delta {m_{21}}^2 \approx 8 \times 10^{-5}$ eV^2 are relatively small and mixing angles very large. There are however several anomalies which, if confirmed experimentally, could hint to the presence of additional, larger squared mass differences in the framework of more than 3 neutrinos with additional “sterile” neutrinos or other effects. See ref. [5], for instance.

- ✓ *Three angles (θ_{12}, θ_{13}, θ_{23})*
- ✓ *Two mass differences (Δm^2_{12}, Δm^2_{23})*

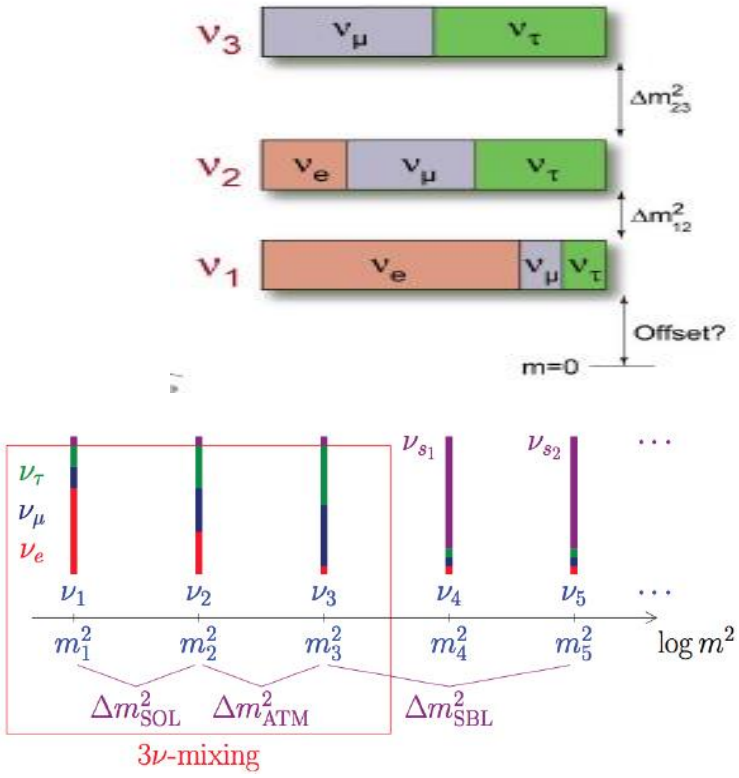

Neutrino oscillation can give us information only about the squared mass difference between two different families, 1-2, 2-3 (or 1-3), which are the auto-states of the neutrino masses and we can see what the mixing is between the flavor and the masses 1-2, 2-3 (or 1-3) auto-states.

In the diagram the normal hierarchy is assumed for the neutrino masses. We don't assume that the inverse hierarchy is still valid for the neutrino masses.

The source of the information is the experimental neutrino oscillation. Every neutrino oscillation is related to the nature of the phenomenon that we investigate. As an example, the solar neutrino gives us information about the difference between the lightest auto-state m_1 and the second intermediate auto-state m_2. This is obtained from solar neutrino oscillation. Another needed information is the squared mass difference between the second auto-state and the third one. This is obtained by atmospheric neutrinos. Atmospheric neutrino gives us information also about Δm^2_{23}. If we combine these two, we have information about the three-neutrino mixing. Newly, it has been found that the short baseline neutrino oscillation cannot be explained by using a three neutrino's scheme. It is

needed to introduce at least 1 or maybe 2 neutrinos, the so-called sterile neutrinos, which has a mass larger than the normal neutrino. So, the normal scheme is with three neutrino mixing, but if we go to short baseline neutrino oscillation, it seems that we need to introduce at least one more neutrino which is not interacting weakly.

1.10 Experiments in progress: anomalies persist in the neutrino sector.

Three main classes of anomalies have been reported, namely the apparent disappearance signal in the anti-ν_e events detected from:

(1) nearby nuclear reactors and

(2) Mega-Curie k-capture calibration sources in the experiments to detect solar ν_e,

and, in addition,

(3) observation of presumed excess signals of ν_e electrons in the decay of muon neutrinos from particle accelerators (the LSND effect).

The most popular direction is the one of sterile neutrinos, although also other alternatives are possible. These three independent phenomena may all point out to the possible existence of at least a fourth non-standard and heavier neutrino state driving oscillations at small distances, with $\Delta m_{new}{}^2$ of the order of ≈ 1 eV^2 and relatively small $\sin^2(2\theta_{new})$ mixing angles.

1.11 Experiments in progress: 1. the anomaly of the disappearance of (anti) neutrinos from the nuclear reactor.

A re-evaluation of all the nuclear reactor antineutrino spectra has increased the expected flux: the ratio R between observed and predicted rates of previous experiments has been decreased to R = 0.938 ± 0.023, leading to a deviation of 3.0 σ from unity.

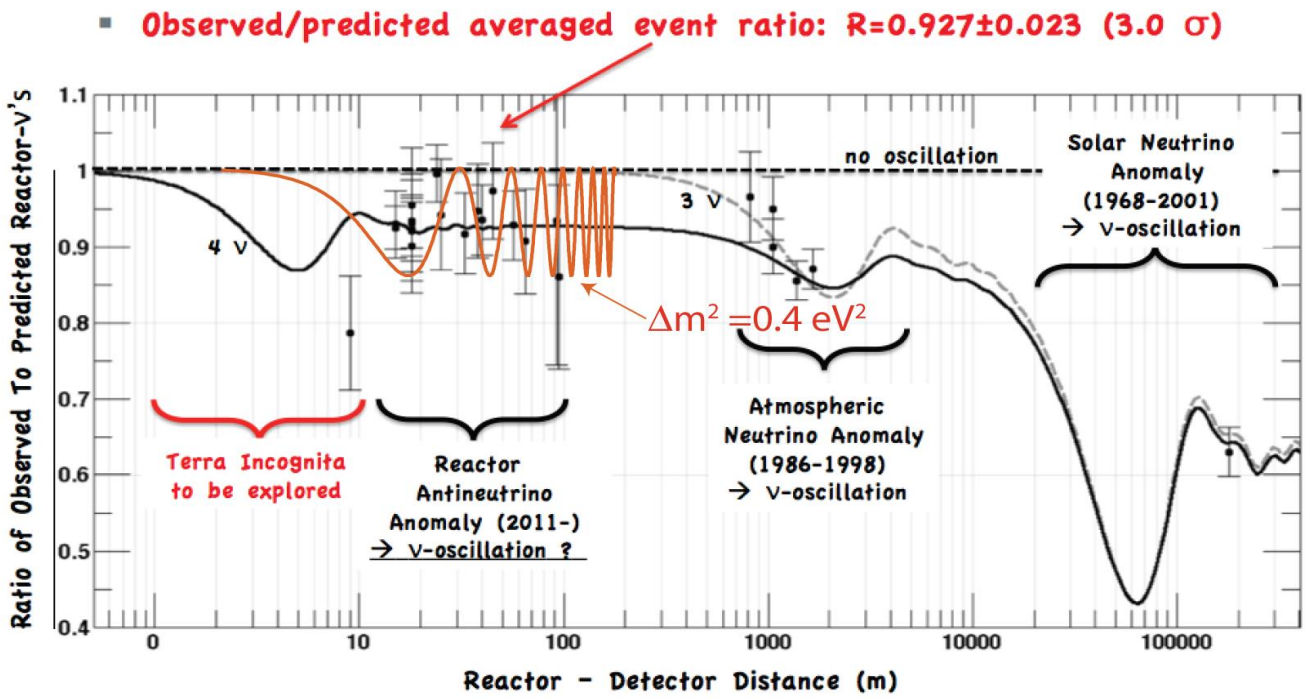

Reactor experiments explored distances far away from the perspective oscillation region, with perhaps the exception of ILL at ~9 m, but with modest statistical impact (68% CL).

The sterile neutrino can be investigated in two different phenomena. One possible phenomenon is the neutrino oscillation of the electron neutrino from nuclear reactors. So, anti-neutrinos which oscillate and the phenomenon of oscillation which are not predicted both by the three neutrinos scheme could be explained. If we go very near the to the core of the reactor in a nuclear power plant we will have a lot of problems related to the flux of neutrinos from the core and we need heavy protection, which is not so easy. So, the information of the anti-neutrino oscillation can be deduced using the electron anti-neutrinos from the nuclear reactors. However there is also possibility to investigate the short range oscillation of the μ neutrinos, which is not reported in the previous plot.

Only the reactor neutrino anomaly is reported. In the central plot we see the atmospheric neutrino anomaly which has been reported 20 years ago. And in the last part, in the very low energy which is forever for electron neutrino.

So, what is the meaning of this plot?

The first part on the left is related to the muon neutrino oscillation because the atmospheric neutrino that we observe comes from the decay of the pion when the cosmic ray impinges on the higher layer of atmosphere. It produces a pion. This pion decays and from the decay muon and muon antineutrino are originated. So, this is an oscillation related to the atmospheric neutrino that cannot be explained just by using the scheme with three neutrinos. From this experiment, Δm^2_{31}can be found. The rightest part, the existing neutrino oscillation is the oscillation of electron neutrino because from the sun we observe electron neutrino. This has been explained by imagining that we have the oscillation between masses 1 and 2.

1.12 Experiments in progress: 2. The anomaly of the disappearance in Gallium

SAGE and GALLEX experiments [6]recorded the calibration signal produced by intense artificial k-capture sources of ^{51}Cr and ^{37}Ar.

$$^{71}\mathrm{Ga} + \nu_e \rightarrow {}^{71}\mathrm{Ge} + e^-$$

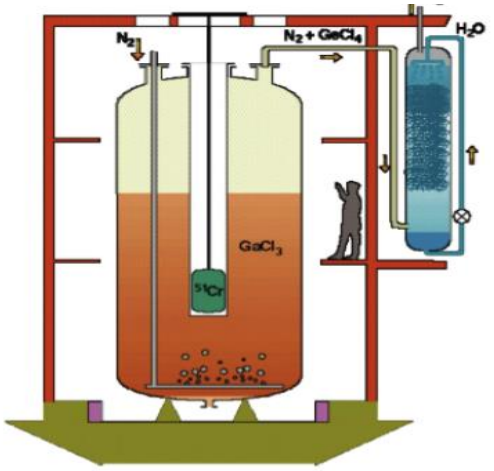

30.3 tons of Gallium
in an aqueous solution : $GaCl_3$ + HCl

The averaged result of the i icted neutrino rates are consistent with ea σ from unity.

These best fitted values ma e neutrino with an evidence of 2.3σ and a bro 2 eV^2 and $\sin^2(2\theta_{new}) \approx 0.3$.

1.13 Experiments in progress 3. The LSND anomaly: (appearance of events ν_μ -> ν_e)

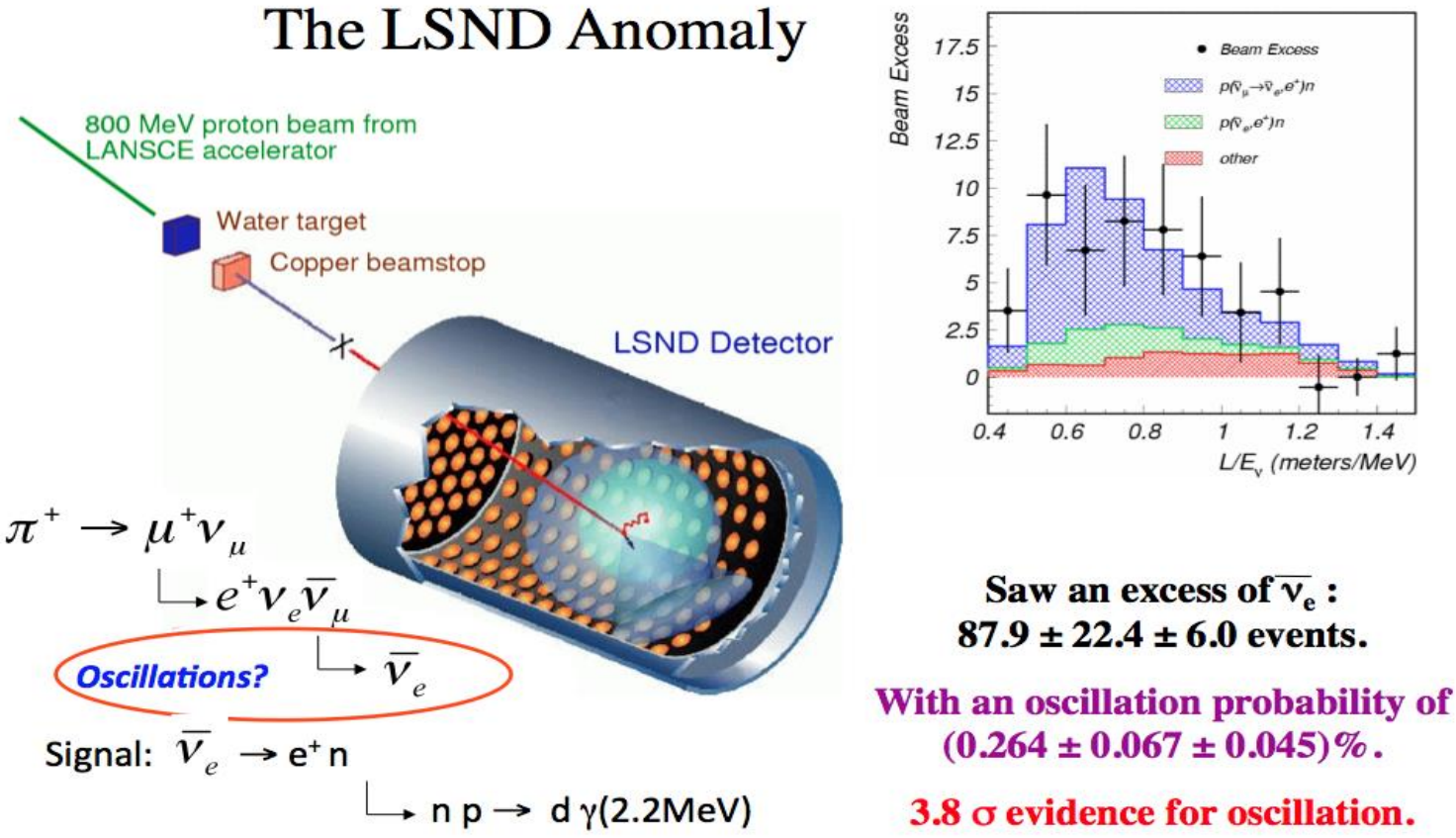

This unexpected result from LSND experiment [7] is worth an experimental confirmation and it appears among the main goals of the SBN Collaboration at Fermilab.

1.14 Perspectives of the SBN experiment: a "naïve" expectation.

The Big Bang cosmology does predict at most one single sterile neutrino of $\Delta m^2 < 0.5$ eV^2 and in the general formula (3+1 model) [8]

$$P_{\nu\alpha\rightarrow\nu\beta} = \delta_{\alpha\beta} - 4|U_{\alpha 4}|^2\left(\delta_{\alpha\beta} - |U_{\beta 4}|^2\right)\sin^2\left(\frac{\Delta m^2_{41} L}{4E}\right) \qquad (22)$$

With such model, the most relevant and solid result is obtained by LSND experiment, given by

$\sin^2 2\theta_{e\mu} = 4|U_{e4}|^2|U_{\mu 4}|^2 \approx 1.5\times10^{-3}$.

If LSND result is confirmed as true, this product implies within the model also the disappearance of both ν_e and ν_μ, since $\sin^2 2\theta_{ee} = 4|U_{e4}|^2 (1-|U_{e4}|^2)$ and $\sin^2 2\theta_{\mu\mu} = 4|U_{\mu 4}|^2 (1-|U_{\mu 4}|^2)$.

With no LSND effect there should be no other disappearances.

Reactor experiments presently claim $\sin^2 2\theta_{ee} \approx 0.12$, $|U_{e4}|^2 = 0.03$.

From LSND results and assuming naively muon-electron universality, we expect at FNAL $\sin^2 2\theta_{ee} = \sin^2 2\theta_{\mu\mu} \approx 0.08$, about ½ of the present reactor data and Mega-sources effects much smaller than claimed.

In the SBN measurements ν_e's will be reduced significantly by two effects:

1) LSND signal + 2) Intrinsic disappearance of ν_e beam at FNAL booster.

The intrinsic ν_e signal may be reduced by a factor 2 using a horn in the primary ν_μ beam.

\

References in Chapter 1

[1] J. Chadwick 1914 **Verh. der Deutschen Physikalischen Ges.** 16 383

[2] J. Chadwick **Possible existence of a neutron** Nature, 129 (1932), p. 312

[3] Yang, C. N. (2012). "Fermi's β-decay Theory". **Asia Pacific Physics Newsletter. 1** (1): 27–30.

[4] S. Fukuda, Y Fukuda, M Ishitsuka,Y Itow, T Kajita -**Phys. Rev. Lett. 85, 3999**

Published 6 November 2000

[5] C. Giunti and C.W. Kim **Fundamentals of Neutrino Physics and Astrophysics, 2007 – Oxford Eds.**

[6] A Bellerive – REVIEW OF SOLAR NEUTRINO EXPERIMENTS
https://doi.org/10.1142/S0217751X04019093

[7] J.E. Hill - An Alternative Analysis of the LSND Neutrino Oscillation Search Data on $\bar{\nu}_{\mu} \rightarrow \bar{\nu}_{e}$ **Phys.Rev.Lett**.75:2654-2657,1995

[8] V. Bellini et al: **Communication to Accademia Gioenia, Catania – Italy (unpublished)**

CHAPTER 2

THE ICARUS TIME PROJECTION CHAMBER TPC T600

Contents

2.1 Introduction to ICARUS experiment

The ICARUS T600 detector is the largest Liquid Argon Time Projection Chamber (LAr-TPC) ever operated on a neutrino beam for oscillation studies. It took data from 2010 to 2013 in the INFN Gran Sasso Laboratory (Italy), both with atmospheric neutrinos and with the CERN Neutrinos to Gran Sasso (CNGS) beam. After an intense refurbishing operation, carried out at CERN in the framework of the Neutrino Platform activities (WA104/NP01), the entire apparatus was moved to Fermilab (IL, USA), where it is operated as far detector of the Short Baseline Neutrino (SBN) program [1]: three liquid argon detectors, placed along the Booster Neutrino Beam (BNB) line and operating at shallow depth, will investigate the possible presence of sterile neutrino states.

The realization of a new light detection system, sensitive to the photons produced by the LAr scintillation, is a fundamental feature for the T600 operation at shallow depth. A threshold of 100 MeV of deposited energy, a time resolution of the order of ≈ 1 ns and a high granularity are required to effectively identify the events associated with the neutrino beam and handle the expected huge cosmic background. The T600 scintillation light detection system was significantly upgraded at CERN from summer 2015 to summer 2017, after preliminary studies based on simulations and laboratory tests, devoted to optimizing the performance of the apparatus.

2.2 The ICARUS T600 detector

The ICARUS T600 detector is made of two identical cryostats, filled with about 760 ton of ultra-pure liquid argon [2]. Each cryostat houses two TPCs with 1.5 m maximum drift path, sharing a common central cathode made of punched stainless-steel panels. The cathode plane and field cage electrodes, composed by stainless-steel tubes, generate an ideally uniform electric field E = 500 V/cm.

Charged particles interacting in liquid argon produce both scintillation light and ionization electrons. Electrons are drifted by the electric field to the anode, made of three parallel wire

planes. A total of 53248 wires are deployed, with 3 mm pitch, oriented on each plane at a different angle (0°, $\pm 60^{\circ}$) with respect to the horizontal direction. By appropriate voltage biasing, the first two wire planes record signals in a non-destructive way, while the ionization charge is collected and measured on the last plane. The electronics was designed to allow continuous read-out, digitization and independent waveform recording of signals from each wire of the TPC, with 400 ns sampling time and 12-bit dynamic range [3]. The information about the ionization track occurrence time, combined with the electron drift velocity ($v \approx 1.6$ mm/μs at $E = 500$ V/cm) provides the event coordinate in the drift direction. The composition of the three views from the TPC wires yields the track projection on the anode plane. This information allows obtaining a full 3D reconstruction of the tracks, with a spatial resolution of about 1 mm^3 [4].

The precise information of the event occurrence time is given by the LAr scintillation light , which permits the generation of a light-based trigger signal and a preliminary identification of event topology for fast selection purposes [5]. The light information is a fundamental feature for the identification of signals related to the neutrino beam induced events. This requires a high-performance light detection system, as described in the following sections.

2.3 Aspects of light detection

Information about the detected particle is carried by light and transformed by photon detectors into an analog electrical signal. A light signal primarily contains information on the following items:

- ✔ time relative to some initiating event;
- ✔ intensity in terms of the photon number;
- ✔ position of a detected signal on the photocathode and
- ✔ wavelength.

Not all this information is necessarily investigated by a user, and some detectors have some advantages with respect to others, concerning a particular performance attribute. Intensity can be referred to the number of photons per event, or per time unit, with regard to detector area. Photon rates may be constant with time (DC detection), slowly changing,

or transient in nature. The detector time response is generally specified in terms of some property of the pulse shape, such as its rise time; or the response may be explained in terms of bandwidth. The sensitivity of most detectors is related to the wavelength of a signal, but without the capability for its direct determination: it requests additional instrumentation, such as a monochromator.

The process of light detection is a quantum mechanical phenomenon of absorbing the energy of a photon to produce a free electron.

Given the generation of enough photoelectrons per time unit, it is feasible to quantify the related charge in terms of a current or voltage to provide a measure of the light input. The ability to detect a light signal depends mainly on two considerations: the first one is the sensitivity of the photocathode, in terms of quantum efficiency (QE), "η", which is the ratio of the number of photoelectrons produced to the number of incident photons; the second one is the level of background.

QE is always less than unity, although in certain solid-state detectors the QE approaches unity over a limited wavelength band. Other detectors, such as photomultipliers (PMT's), are often used at infrared wavelengths, where QE's are very low. It is, however, still possible to perform measurements under these circumstances since PMT's are capable of detecting single photoelectrons, by virtue of their high and relatively noiseless gain. Until the 1970's PMT's were the only commercially available devices with this capability, but now solid state PMT's, SiPM's (Silicon PhotoMultipliers), with intrinsic gain are readily available.

A brief introduction to the terminology is appropriate at the outset, to remove possible confusion. The following terms are faced throughout the scientific literature: signal current and signal counts, whose meanings are obvious. Associated with these two variables we have dark current and dark counts, or equivalently, background current, and background counts. The words dark and background apply to the output from a detector in the absence of light input, but the terms really refer to signals, albeit unwanted ones. Noise is reserved for the description of statistical aspects of light, such as shot noise; it is not a signal but rather a fluctuation within an existing one. 'Noise in signal' and 'noise in background' are the appropriate terms for the shot noise inherent in the current produced by a light signal, and that produced by a background signal, respectively.

2.3.1 SiPM

There are currently more than ten manufacturers of SiPMs: among them we find Hamamatsu, Photonique, STM, SensL, RMD, and Perkin Elmer. As stated in the literature: 'Every producer has invented a name for their device, amongst which we have MRS, MRSAPD, MAPD, SiPM, SSPM, SPM, G-APD'. The first single pixel G-Mode APD (Avalanche Photo Diode), manufactured by EG&G, is the one described by Haitz et al. (1963) [6]. Micropixel APDs (MTS APD) were patented by Golovin et al. (1989) [7], and the first commercial devices followed a few years later in Russia. The SiPM is a multi-pixel APD with all channels terminating on a common substrate. A 2-D array of pixels, as small as 10 μm, constitutes a packaged detector of typically 1 × 1 mm^2. The number of pixels per unit area ranges from 100 to 100,000. Each pixel operates at a bias voltage of about 50 V, which corresponds to ~15 % above the breakdown voltage in the so-called Geiger mode. A quenching resistor is included in each pixel to terminate the discharge. Pixels generate signals with common amplitude because every avalanche runs into saturation. Hence, a multi-photon flash produces a comb-shaped response by separating individual photon detections, depicted in Figs 1 and 2.

Sensitivity is usually quoted in terms of photon detection efficiency (PDE), which is the product of QE, fill factor (dead space), and avalanche probability.

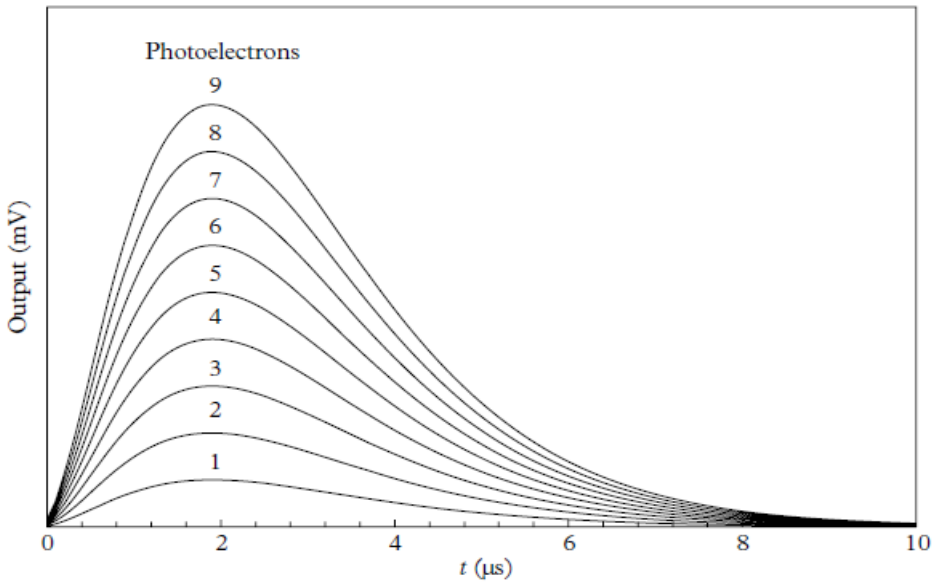

Fig. 1: A representation of the output after shaping and filtering, as seen on an oscilloscope. In reality there are signals in the valleys between the traces, but their number is small.

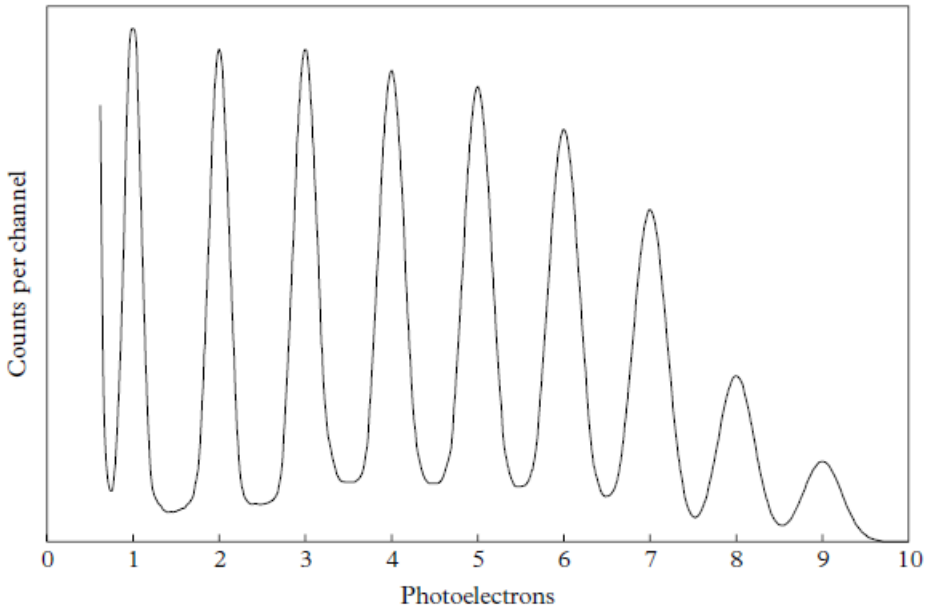

Fig. 2: A multi-photoelectron pulse height distribution for which the mean number of photoelectrons per flash is
4. The steeply falling edge on the left of the distribution is referred to as the pedestal or noise edge.

The realizable QE is about half of that of a single-channel APD. The original SiPM's showed high red sensitivity with similar spectral response to single-channel APD's. A significant development was the enhanced blue-green response introduced to match the light output from scintillators; PDE curves are shown in Fig. 3 for N-type Hamamatsu devices and the P-type detector from CPTA. It is worth noting that the N-type has similar sensitivity to a vacuum PMT in the blue green region of the spectrum, but with a superior response to red light. Linearity with respect to light input ameliorates by increasing the number of pixels, and with uniformity of illumination. The signal output of an individual pixel is fixed, regardless of the number of coincident photons received; hence the improvement in dynamic range which follows from uniform illumination. Linearity, for the Hamamatsu C12661 modular series, extends to 10^7 single-photon counts/s, for 15 μm pixels.

Dark count rates are high in these devices, especially at room temperature: 100 kHz to several megahertz per square millimeter is not uncommon. They reduce by a factor of 2 per 8°C drop in temperature. The time distribution for dark counts shows an excess of undersized intervals below 1 μs because of correlations. After pulse rates in the Hamamatsu S12571-050C were initially high but modified designs reduced this contribution to 1-2%, provided that overvoltage is kept below 3 V. Dark count rates are strongly dependent on threshold, with a decrease of four orders at a threshold of 2.5 photoelectrons equivalent. This sensor has not been selected for ICARUS experiment, because of the very large surface needed to cover in the Time Projection Chamber T600.

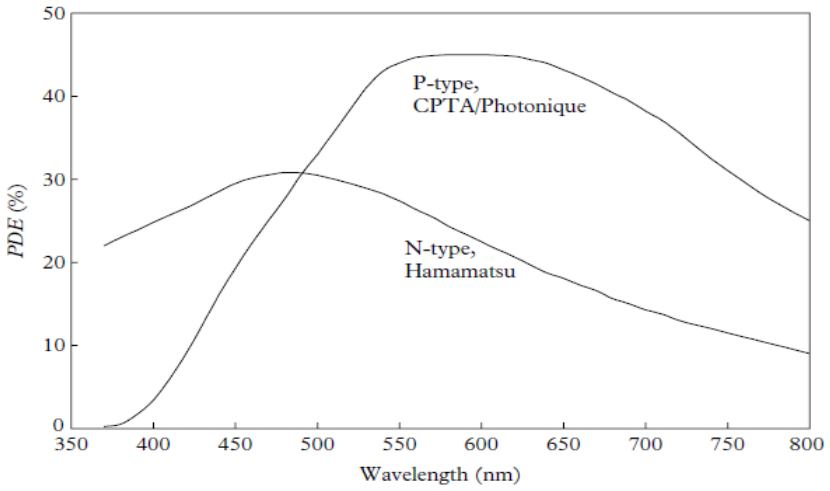

Fig. 3: PDE (Photon Detection efficiency) is similar in concept to QE as defined for a PMT, but includes collection efficiency; P-type detectors are best suited to applications involving red and infrared light, while the N-type is preferred for scintillator applications.

2.3.2 Photomultiplier Tubes (PMT's)

A photomultiplier tube, useful for detecting very weak light signals, is a photo emissive device in which the absorption of a photon results in the emission of an electron. These detectors work by amplifying the electrons generated by a photocathode exposed to a photon flux.

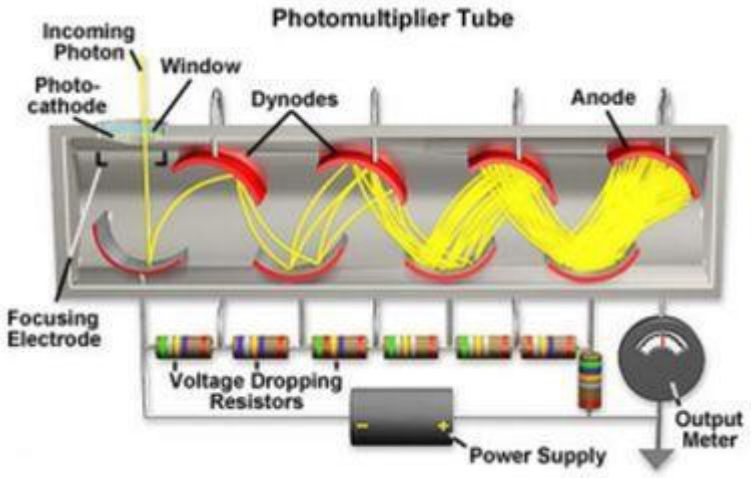

Fig4. Photomultiplier Tube photo

It should also be mentioned that PMT's are useful for applications which require:

High **Low** **High**

There are many types of photomultiplier tubes with different characteristics in:

Shape **Struct** **Spectral** **Effective**

PMT modules consist of a photomultiplier tube to convert light into electrical signals, a high-voltage power supply circuit, and a voltage divider circuit to distribute the optimum voltage to each dynode. All components are assembled into a single compact case. Also, modules are provided with various additional functions such as signal processing, cooling, and circuitry to interface to a PC.

2.4 Design and optimization of the scintillation light detection system

2.4.1 Scintillation light emission in liquid argon

Scintillation light emission in LAr is due to the radiative decay of excimer molecules Ar^{*2} produced by ionizing particles, releasing monochromatic VUV photons ($\lambda \approx 128$ nm) in transitions from the lowest excited molecular state to the dissociative ground state. The emitted light is characterized by a fast ($\tau \approx 6$ ns) and a slow ($\tau \approx 1.5$ μs) decay components. Their relative intensity depends on dE/dx, ranging from 1:3 for minimum ionizing particles, up to 3:1 for alpha particles. This isotropic light signal propagates with negligible attenuation throughout each TPC volume. Indeed, LAr is fully transparent to its own scintillation light, with measured attenuation length in excess of several tens of meters and Rayleigh-scattering length of about 1 m [8]. Because of their short wavelength the scintillation photons are absorbed by all detector materials without reflection, leaving time and amplitude information unaffected during the photon path to the light detectors.

2.4.2 Scintillation light detection in ICARUS T600

A scintillation light detection system based on 74 ETL9357FLA (8″ diameter) PMT's, mounted behind the wire chambers, was adopted in the T600 detector for the LNGS run [9]. Instead for the Short Baseline Neutrino (SBN) experiment at Fermilab with the BNB (Booster Neutrino Beam), 360 Hamamatsu R5912-MOD PMT's will be used. The sand-blasted glass window of each device is coated with about 200 $\mu g/cm^2$ of TetraPhenyl Butadiene (TPB), to convert the VUV photons to visible light. ICARUS at Fermilab will take data at shallow depth, facing more challenging experimental conditions than at LNGS, where it was located underground.

The light detection system will complement the 3D track reconstruction performed with the use of the TPC wires, thus contributing to identify neutrino interactions occurring in the BNB

spill gate structure and rejecting the expected ≈ 10 kHz cosmic background. This new environment requires a number of improvements, namely the adoption of a PMT model with better performances, an improvement of the neutrino energy sensitivity down to 100 MeV, a time resolution about 1ns and an increase of the light detection granularity. This last requirement is needed to localize the track associated with every light pulse along the ≈ 20 m of the longitudinal detection direction, with accuracy better than 1 m, namely shorter than the expected average spacing between cosmic muons in each TPC image. In this way, the light detection system would be able to unambiguously provide the absolute timing for each track, and to identify, among the several tracks in the LAr TPC image, the event in coincidence with the neutrino beam spill.

The adoption of large area PMT's coated with TPB was considered the best solution for the light detection system upgrade. The use of alternative devices, such as SiPM detectors, was considered not mature enough for applications in large volume LAr-TPC, because of their small sensitive surface.

2.4.3 Optimization by Monte Carlo simulation

Dedicated Monte Carlo simulations were realized to design and optimize the light detection system for the refurbishing of the T600 detector [10]. Initially, the focus was put on the geometrical properties of the propagation of the VUV scintillation light in ICARUS, with some simplifications on the features of the topology of the considered class of events:

i. electromagnetic (e.m.) showers, mimicking Neutral Current (NC) and ν_e Charged Current (CC) interactions from BNB (Booster Neutrino Beam).

ii. single crossing cosmic muons, which represent the most abundant source of background muons with respect to the muons generated from ν_μ CC interactions from BNB.

Fine details of physical events, such as e.m. showers shape or particle multiple scattering, were found to be less important than the spatial resolution achieved with 8″ diameter devices spaced by 1 m distance. Muons were schematized as straight lines, while e.m events as clusters of points with 1 MeV deposited energy each. Shower energy spanned from 100 MeV

to 1 GeV, to cover all the expected energy range in the SBN configuration. Muons generated from ν_μ CC interactions were a superposition of the other two event topologies. From each point along the simulated track, the proper number of photons was generated isotropically; due to the short wavelength, LAr scintillation light is absorbed by all the detector material, so no reflection was assumed. A Rayleigh scattering length of 90 cm was considered, slightly different with respect to the 99.8 cm measured by Babicz et al [2]. A 5% overall Quantum Efficiency (QE) was conservatively assumed for the PMT's, which includes wavelength shifting conversion efficiency and geometrical factor: about 50% of the light is lost during conversion. An error of ±1 ns on the arrival time and a ±10% uncertainty on the number of collected photons were assumed, to take into account the PMT response uncertainties, according to experimental measurements results [10]. Different PMT positioning layouts with 8″ and 5″ diameter PMT's were considered to study the performance both for cosmic muons and for e.m. showers in the T600 detector. Configurations with a different number of PMT's were also considered, starting from 27 devices (8″ PMT's) up to 210 devices (5″ PMT's) per TPC. The pattern of each layout was constrained by the existing mechanical structure of the T600: the requirement was not to change it, exploiting the free space already available in this structure.

For what concerns the event position reconstruction, simulations were carried out to evaluate the capabilities of the different configurations to localize the e.m. showers, mainly along the 18 m length on the beam direction (z axis). The error on the event position reconstruction was calculated as the difference between the actual geometrical center of the event and the one derived from the average on the PMT coordinates, weighted on the light collected by each PMT. The best results were obtained by the set of geometries with the highest numbers of PMT's, as shown in Fig.1 for *a)* 27 (8″) PMT's, *b)* 90 (8″) PMT's, and *c)* 210 (5″) PMT's. However, the difference among them is not significant and performance improvements can be obtained just by refining the reconstruction algorithm. For example, just considering in the average on the PMT position only those devices with a signal above a threshold of 10 phe, as shown in Fig 1 *d*), the 90 (8″) PMT configuration shows a localization capability which is better than the one obtained with the 210 (5″) PMT's configuration. A more detailed study of the PMT system performance was then carried out within LArsoft, which is a framework supporting a shared base of physics software across LAr-TPC experiments. In particular, the

ICARUS T600 detector description and the particle generation and propagation in the ICARUS volume are determined within Geant4 software, which is implemented in LArsoft. The ICARUS T600 inner detectors main components (wires, PMT's, cathode, field cage) are faithfully reproduced. Both single BNB ν_μ and ν_e interactions and cosmic ray samples were generated inside the active volume of one of the two modules of ICARUS. LAr soft framework covers basic components of the real scintillation detector system and includes all relevant physical processes. With the full simulation, individual physical factors that can affect the performance of the detector system, such as detector geometry, surface finishing, decay time and scintillation yield of scintillator as well as responses of PMT's and front-end electronics, are included [11].

The impact of the layout with 90 (8″) PMT's for each TPC in terms of neutrino vertex localization, as obtained from LArsoft simulation of BNB ν_eCC and ν_μCC events, is shown in Fig.6: provided the timing information from all PMT's is available, an accuracy of less than 15 cm and a precision of about 30 cm (70 cm) for ν_eCC (ν_μCC) was obtained by estimating the neutrino vertex position from the light barycenter of the first three hit PMT's.

Finally, this analysis opens the possibility to directly match the event position as determined by the analysis of the charge with light information coming from PMT's. This could help in developing a quick first level event tagging using the light signals. As an example of the localization capability, two neutrino events reconstructed from the TPC wires are shown superimposed with the map of PMT's in Fig.7.

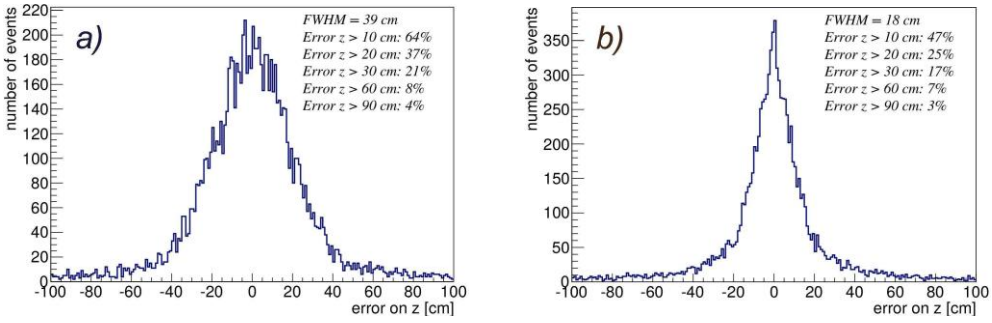

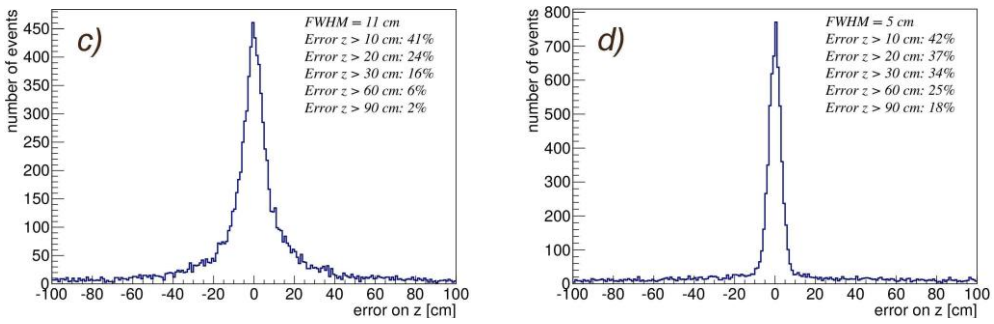

Fig 5. Evaluation of the precision of the localization of the actual interaction position along the beam direction z for e.m. showers as determined with the custom simulation. The considered layouts are: *a)* 27 (8″) PMTs; *b)* 90 (8″) PMT's; *c)* 210 (5″) PMTs. Figure *d)* shows the result obtained with the layout with 90 (8″) PMT's by considering only those devices with a signal above a threshold of 10 phe. The FWHM and the percentage of events localized with an error greater than 10, 20, 30, 60 and 90 cm are indicated in each figure.

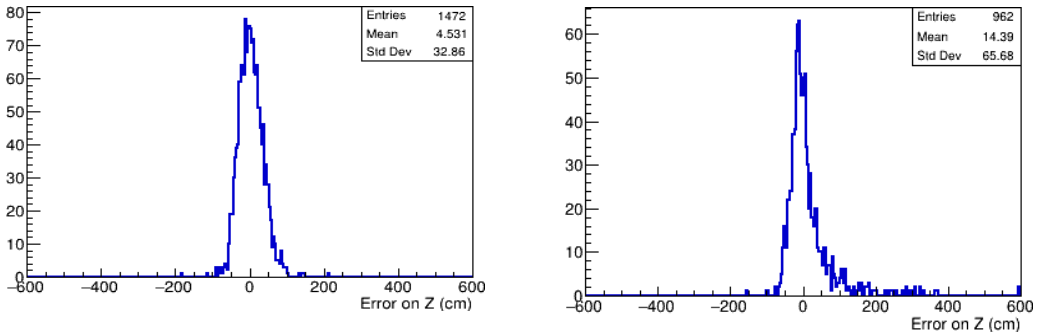

Figure 6. LArsoft evaluation of the precision of the localization of the actual neutrino vertex position, along the beam direction z, for ν_e (*Left*) and ν_μ (*Right*) for the layout with 90 (8″) PMTs: a precision of about 30 cm (70 cm) for ν_eCC (ν_μCC) is obtained.

The described MC simulations led to select the 90 (8″^{J}) PMT's layout for installation on the ICARUS T600 TPCs. This layout implies the use of 360 PMT's with 8″ diameter, corresponding to a coverage of 5% of the wire plane surface. The estimation of the number of photo-electrons collected per MeV of deposited energy in a single TPC gives an average of about 15 phe/MeV (9 phe/MeV for events close to the cathode).

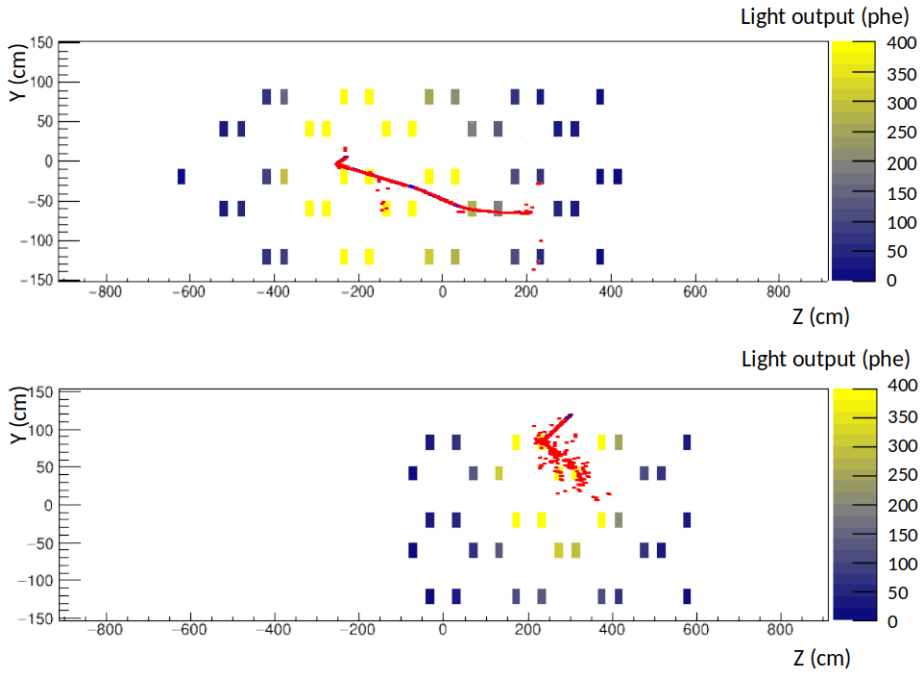

Fig 7. Examples of neutrino events simulated with LArsoft and reconstructed from the TPC wires superimposed with the color map of PMT's having a light signal exceeding 10 photoelectrons. Top: ν_μCC, 1.2 GeV deposited energy. Bottom: ν_eCC 0.9 GeV deposited energy.

The possibility to adopt the scintillation light for triggering and timing purposes with events down to 100 MeV is then assured in the whole TPC volume.

2.5 Hardware implementation

The realized PMT layout, shown in Fig.16, features 360 total Hamamatsu R5912-MOD PMT's deployed in groups of 90 devices behind each wire chamber. As told before, since the PMT glass window is not transparent to the scintillation light produced in liquid argon, each unit was coated with a proper wavelength shifter (TPB) re-emitting in the visible. The PMT's were installed using dedicated mechanical supports. A laser calibration system permits the timing calibration of the single units.

In this section the ICARUS T600 scintillation light detection system is described, presenting the main characteristics of its different components.

2.5.1 Photomultiplier tubes

In order to identify the most suitable model to the requirements of the light detection system of ICARUS T600, a test campaign was carried out on different PMT samples manufactured by different producers, such as Hamamatsu and ETL [12–14]. All the PMT's taken into consideration feature an 8″ hemispherical glass window with bialkali photocathode on platinum undercoating, to guarantee high performance at cryogenic temperatures. The evaluation of their conformity was based on the following considerations:

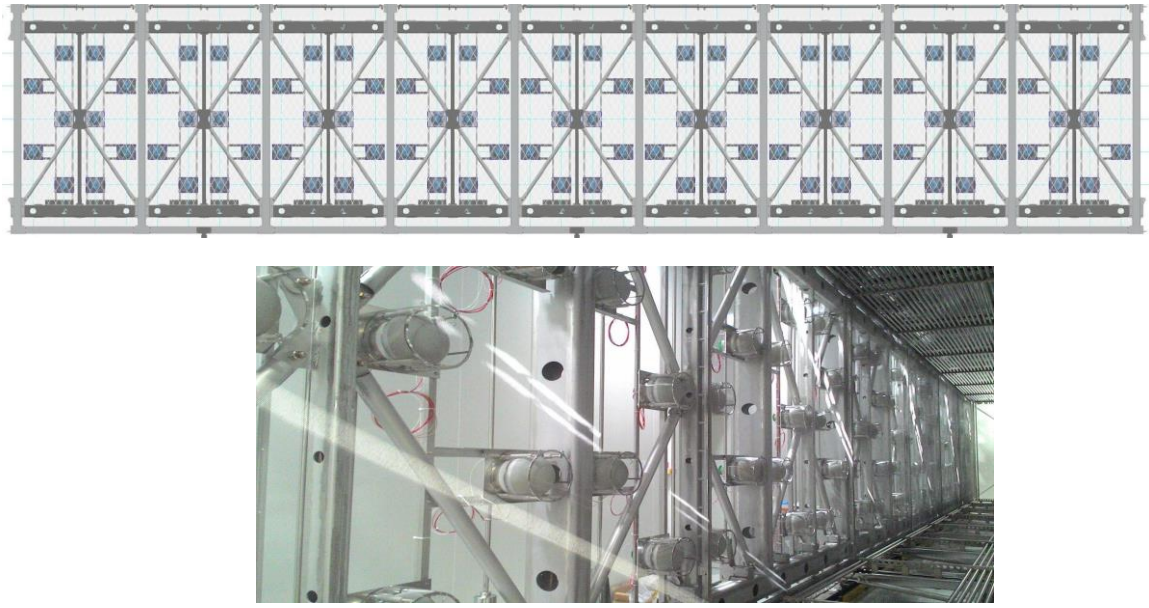

Fig 8. Scheme of the adopted geometry with 90 PMT's behind each wire plane and picture of the actual configuration.

-The scintillation light detection system should guarantee a good sensitivity to ionizing interactions in LAr down to an energy deposition of 100 MeV. To this end the quantum efficiency and its uniformity over the sensitive surface of PMT's have a strong impact on the global efficiency of the system. The effective values of these parameters resulting from actual measurements on PMT prototypes are considered distinguishing features for the model selection.

The dynamics of the scintillation light detection system should permit the recording of the scintillation light fast component pulses and, at the same time, of single photons arriving from

the slow component de-excitation. In addition, it must cope with the expected wide variation of light intensity which depends on the deposited energy and on the geometry of interactions inside the LAr volume. Reckoning the standard electronics for PMT signal recording without pulse amplification, a gain $G \approx 10^7$ at cryogenic temperature is necessary to detect single photons. Moreover, the PMT dynamics should permit the generation of anode pulses without remarkable saturation up to hundreds of photoelectrons.

-The light collection system should be able to unambiguously provide the absolute timing of each interaction and identify, among the several tracks in the LAr-TPC image, the event in coincidence with the neutrino beam spill. In order to achieve O(1 ns) timing resolution, fast PMT pulses are

Fig 9. The PMT Hamamatsu R5912-MOD.

needed. Moreover, good stability of the transit time as a function of temperature and applied voltage, low time spread and a good uniformity over the PMT sensitive windows surface are required.

-Since a PMT's large number is used, the presence of a high dark count rate can affect the detector performance inducing stochastic coincidences at trigger level. From each PMT a single photoelectron physical background rate of tens of kHz is expected in LAr. This rate consists of residual photons produced from the decay of ^{39}Ar or other radioactive

contaminates. Therefore, an intrinsic dark count rate of a few kHz at cryogenic temperatures is judged acceptable. On the other hand, the absence of bursts, sparkling, lightening effects or other noise generating pulses above the single photon level is considered mandatory.

-ICARUS T600 will operate in absence of external magnetic fields, except for the earth's intrinsic field. Therefore, the main PMT performances should not be degraded by external magnetic fields (about 1 gauss) at different axial orientations.

-The adopted devices should withstand low temperatures and the relative high pressure as expected in LAr immersion. All the considered PMT models were subjected to a series of thermal shocks to highlight possible mechanical or cracking problems.

Best results were obtained with the Hamamatsu R5912-MOD device (see Fig 9) which was therefore selected for installation. The main features and the characteristics resulting from the tests are summarized in table1.

For the upgrade of the ICARUS T600 scintillation light detection system, 400 Hamamatsu R5912-MOD PMT's were procured in 2016. All the samples were tested at room temperature and 60 of them were also characterized at cryogenic temperature, in liquid argon bath during a test campaign carried out at CERN in 2016 and 2017 [15]. All the 400 PMT's were rated compliant with the requirements for installation in the T600.

Each device was equipped with a proper base voltage divider directly welded on the PMT flying leads. The base circuits, entirely passive, were manufactured with SMD (Surface Mounted Device) resistors and capacitors,

Table 1. Main acceptance requirements for the Hamamatsu R5912-MOD

Spectral Response	$300 \div 650$ nm
Window Material	Borosilicate glass (sand blasted)
Photocathode	Bialkali with Pt under-layer
Max suppy voltage (anode-cathode)	2000 V
Photocathode Q.E. at 420nm	$\geq 16\%$
Photocathode Q.E. surface uniformity at 420nm	within $\pm 5\%$ of mean value
Number of dynodes	10
Typical Gain	1×10^7 at 1500 V
Nominal anode pulse rise time*	≤ 4 ns
Nominal P/V ratio*	2.5
Max. dark count rate*	5000 s^{-1}
Max. transit time variation	2.5 ns (center-border)
Transit time spread (RMS)	0.7 ns

* Values for $G = 1 \times 10^7$

able to withstand the LAr temperature. The reference voltage distribution ratio is the standard one recommended by Hamamatsu. A particular care was devoted to the choice of damping resistors to improve the PMT time response. Detailed design and specifications are presented in reference [15].

2.5.2 Wavelength shifter deposition

The glass window of this PMT model is not transparent to the scintillation light produced by liquid argon. The sensitivity to vacuum-ultraviolet (VUV) photons was achieved by depositing a layer of a proper wavelength shifter on the PMT windows.

1,1,4,4-Tetraphenyl-1,3-butadiene, or TPB, is an organic fluorescent chemical compound generally used as wavelength shifter, thanks to its extremely high efficiency to convert ultraviolet photons into visible light. To obtain effective TPB layers on a large number of PMT's, ensuring at the same time a high repeatability and reliability of the operation, a dedicated thermal evaporator was instrumented, by specifying the relative evaporation procedure [16].

The thermal evaporator consists of a vacuum chamber, 68 cm high and 64 cm diameter, closed at both sides by means of two large flange plates[1]. The PMT to be coated is fastened to a specific rotating support looking downwards and inclined of 40° angle with respect to the vertical direction, as shown in Fig.6 . The rotating structure, fixed below the chamber top plate, is connected to an external motor by a ferrofluid-based feedthrough allowing a rotation speed of 10 turns/min. The vacuum chamber houses a "temperature controlled" *Knudsen cell*, placed on the bottom plate at distance of about 14 cm below the PMT surface. For each deposit the cell crucible was filled with about 0.8 g of TPB and left to evaporate at a temperature of 220° for about 10 min, yielding a uniform TPB coating of about 220 $\mu g/cm^2$ on the PMT sensitive

[1] The thermal evaporator and the optical test system cited in this paper were funded by the Italian INFN (Istituto Nazionale di Fisica Nucleare)

surface.

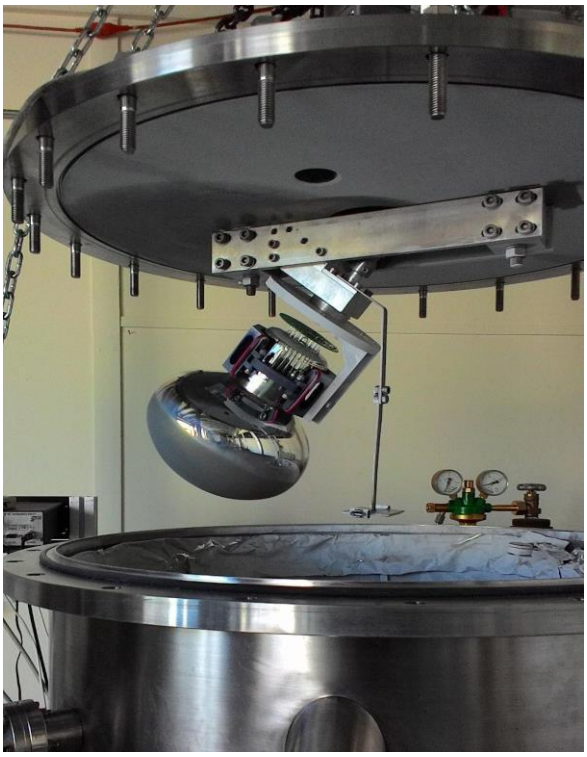

Fig 10. Picture of the instrumented evaporator with a PMT fastened on the rotating support.

This density value was proven to guarantee a high conversion efficiency and the absence of adhesion instabilities onto sand-blasted glass at cryogenic temperatures after immersion in LAr [17].

The effectiveness of this technique from the point of view of deposition uniformity and light conversion efficiency was validated by simulations and experimental tests before being accepted for the TPB coating of the 360 Hamamatsu R5912 of ICARUS T600 light detection system. The treatment of a total of 365 PMT's was carried out at CERN Technology Department in around 120 working days. The distribution of the resulting TPB coatings is shown in Fig.11.

The effective value of the quantum efficiency at λ = 128 nm and its uniformity as a function of the position on the photocathode window was measured by means of an optical test system on 10 PMT samples. The quantum efficiency was evaluated by comparing the currents given by

the PMT under VUV illumination and by a reference calibrated photodiode [2]. Values are distributed in the 0.11 ÷ 0.15 range, with an average value of 0.12, while for each PMT the uniformity results to be within ±5 % around the mean value, as shown in Fig 20, in agreement with

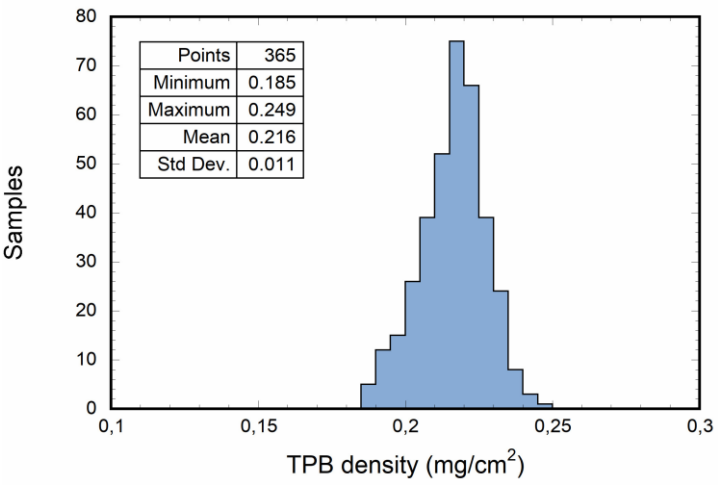

Fig 11. Distribution of the resulting TPB coating densities. Each sample is related to a PMT evaporation run of the series production. In addition to the needed 360 PMT's, 5 more samples were coated as spare units.

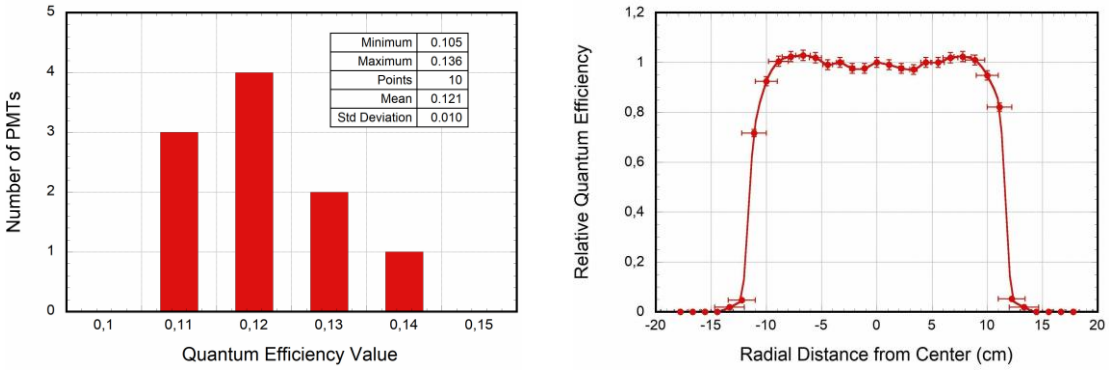

Fig 12. (Left) Distribution of quantum efficiency resulting from the measurement of 10 PMT samples after the TPB coating by evaporation. (Right) Example of measurement of quantum efficiency variation as a function of the radial distance from the center.

the nominal surface uniformity at 420 nm without TPB.

[2] Light at λ = 128 nm is generated by a 30 W deuterium lamp (McPherson 632) and selected by a monochromator (McPherson 234/302). The reference is a NIST calibrated photodiode.

2.5.3 Deployment and installation of the PMT's

Each of the two T600 LAr cryostats features a mechanical structure that sustains the different internal detector subsystems and the control instrumentation. The three wire-planes of each TPC are held by a sustaining/tensioning frame positioned onto the longitudinal side walls of the cryostat. The stainless-steel supporting structure has dimensions of 19.6 m in length, 3.6 m in width and 3.9 m in height, subdivided in 9 sectors, 2 m long each. PMT's are located in the 30 cm space behind the wire planes, 10 units for each frame sector, as shown in Fig.13.

The PMT's are mounted onto the mechanical frames by means of PEEK^{TM} holders in the form of slabs with dimensions of 350 × 250 mm^2, 10 mm thick, held up by stainless-steel bars 3 m long, as shown in Fig. 21. The support system allows the PMT positioning behind the collection planes ≈ 5 mm far from the wires.

The electron multiplication process inside the PMT gain region can induce a fake signal on

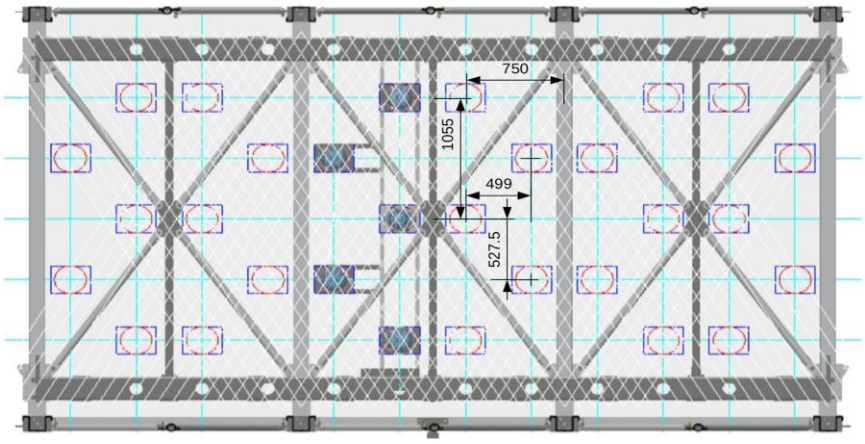

Fig 13. Drawing of the PMT positioning behind the wire planes. Units of measurement are millimiters. Three frame sectors are displayed.

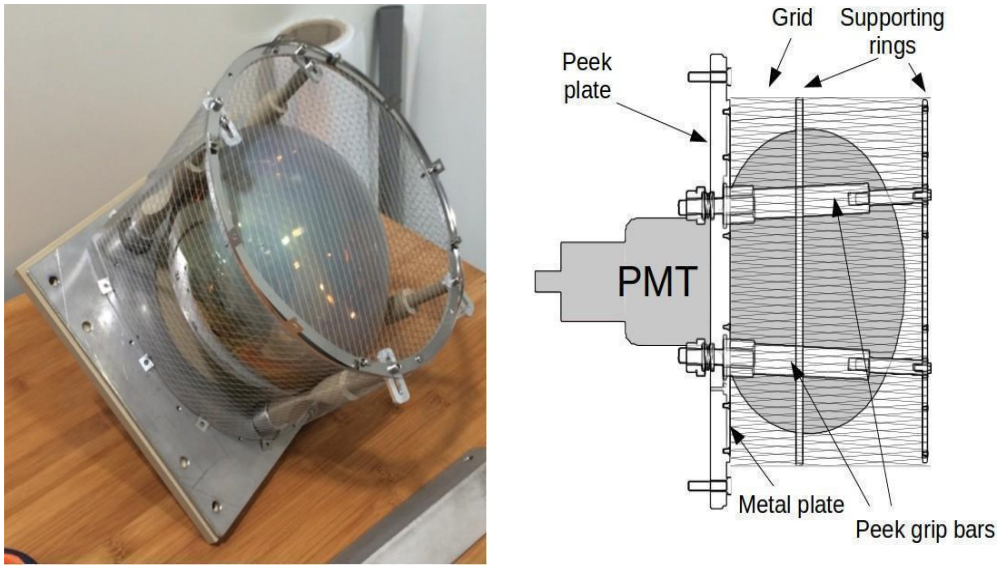

Fig 14. Picture (left) and CAD drawing (right) of the PMT support.

the wire plane areas facing them. These induced signals appear as fuzzy smeared blobs on a group of wires spanning the PMT diameter. The effect was witnessed continuously on ICARUS data from LNGS run, but it was negligible and easily identifiable, given the low number of PMT's and tracks per event. At Fermilab, the larger number of PMT's, coupled with higher background track multiplicity, calls for a mitigation of this phenomenon. A stain less steel grid cage is mounted around each device as shown in Fig. 14. The cage is connected to the detector ground, as well as the wire polarization system. Pictures of the supporting system are shown in Fig. 15 .

Fig 15. Picture of the PMT supporting system.

2.5.4 PMT cabling and feedthrough installation

A negative power supply and two independent coaxial cables are used to provide each PMT with high voltage and to read out the anode signals. Signal cables are RG316/U, 7 m long with a BNC connector on one end. High voltage cables are HTC-50-1-1, 7 m long, with a SHV connector on one end. The non-terminated ends of the cables are directly soldered on the PMT bases.

For each group of 10 PMT's mounted in the same frame sector, two bundles of 10 signal cables and 10 power supply cables are deployed along the mechanical structure up to the frame top, as outlined in Fig. 16. Each bundle is then driven through a stain less steel chimney (20 cm diameter, 1 m long), vertically mounted on the detector roof. The top edge of each chimney hosts a set of feedthrough flanges for the interconnection of various elements of the detector

(PMT signal and power supply, wire signals and biasing, optical fibers and sensors). The PMT flanges are from Allectra Ltd., each hosting 10 SHV-SHV or 10 BNC-BNC feedthrough connectors mounted on stainless-steel DN100CF high vacuum flanges. A photo showing the assembly of the PMT flanges is reported in Fig. 17 and Fig18. The main characteristics of the flanges are listed in Table 2.

The electrical connection between PMT flanges and electronics, located in a building alcove

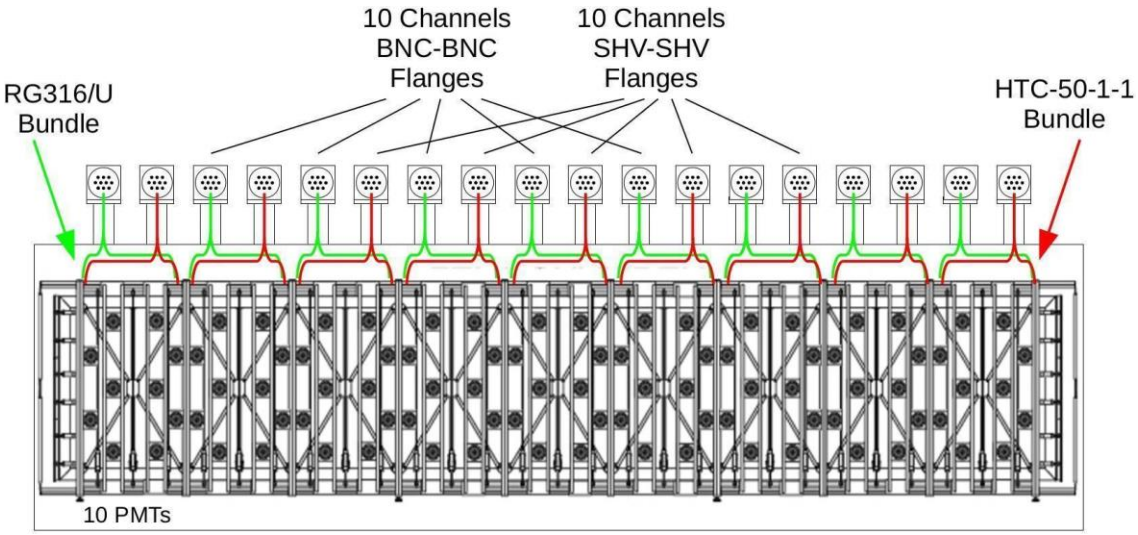

Fig 16. Outline of the PMT cables deployment along the mechanical structure and their distribution on the top chimneys.

Table 2. Flange main characteristics

Flange type	DN100CF	DN100CF
Number of feedthroughs	10	10
Connection type (Int/Ext)	BNC/BNC	SHV/SHV
Impedance	50 Ohm	50 Ohm
Shield type	Grounded	Grounded
Voltage	1000 V	6000 V
Min. temperature	−200°C	−200°C
Vacuum	UHV	UHV

adjacent to the detector, consists of 360 signal cables (RG316/U with BNC-MCX termination) and 360 high voltage cables (RG58/U with SHV-SHV termination) deployed on cable-trays. In order to guarantee uniformity among the different channels, all the cables are 37 m in length. The actual total cable length from PMT base to electronic channel input is 44 m. A detailed study on the effects of the use of these extremely long cables shows a reduction of the high frequency components of the PMT signal resulting in an increase of the rise-time to 8 ns [18]. These effects are included in Monte Carlo simulations described in section 2.4.3, to evaluate possible effects on the system performance.

2.5.5 PMT electronics

PMT electronics is designed to allow continuous read-out, digitization and independent waveform recording of signals coming from the 360 PMT's of the light detection system. This operation is performed by 24 V1730B digitizers. Each module consists of a 16-channel 14-bit 500-MSa/s FLASH ADC with 2 Vpp input dynamic range. In each board 15 channels are used for the acquisition of PMT signals, while a channel is left for possible future implementations. During the acquisition, the data stream of each channel is continuously written every 2 ns in a circular memory.

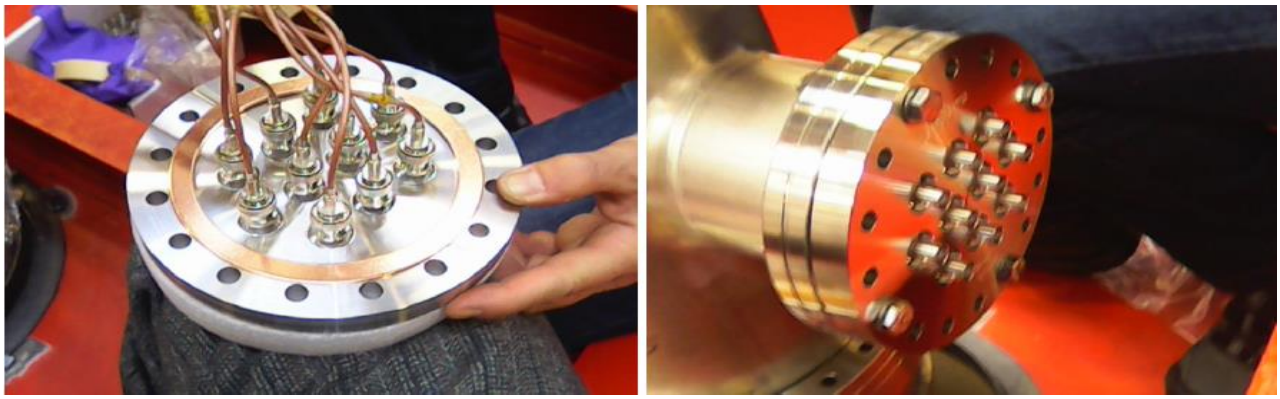

Fig 17. Pictures showing the assembly of the PMT flanges. Signal cables and BNC flanges are shown in the top pictures.

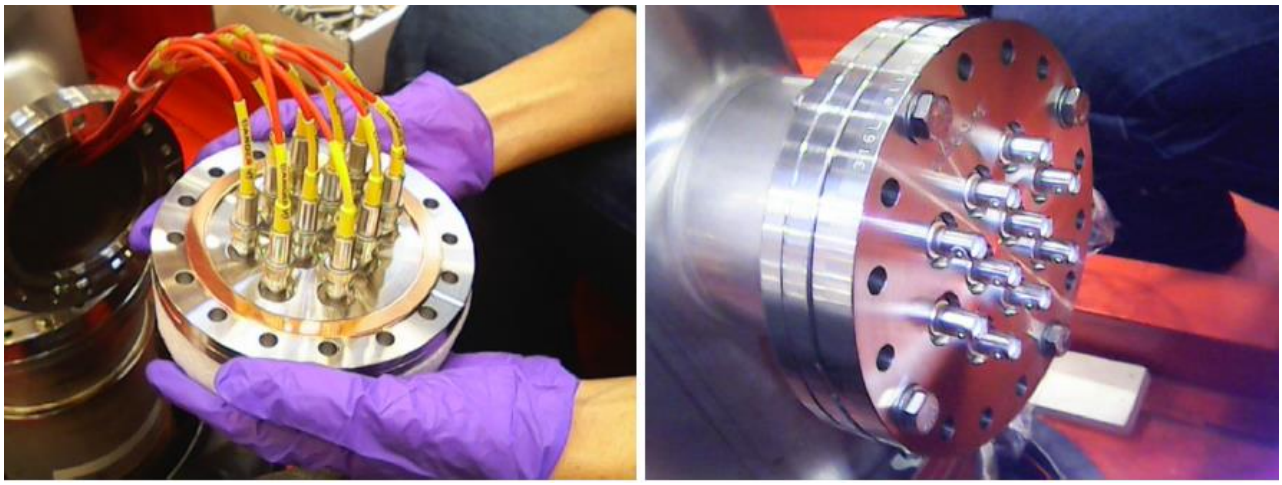

Fig 18. Pictures showing the assembly of the PMT flanges. HV cables and SHV flanges are presented in the bottom pictures.

buffer of 5kSa, corresponding to 10 μs[3], allowing the recording of both components of the LAr scintillation light, i.e. photons from fast and slow decays of excited excimers to ground state, as described in Section 2.4.1. When a board receives an external trigger request, the active buffers are frozen, writing operations are moved to the next available buffers and stored data are available for download via optical link[4]. Trigger pulses are generated by the ICARUS Trigger System every time an ionizing interaction is recognized in the detector on the base of information coming from neutrino beams and other apparatus subsystems. To this aim, V1730B boards generate trigger-request logical patterns through LVDS (Low Voltage Differential Signal) outputs showing the presence of signals with amplitude overcoming digitally programmed thresholds [19].

For generation and distribution of high voltages, the same power supply system designed by ICARUS for the LNGS run is adopted. For each cryostat, housing 180 PMT's, a primary -2000 V is generated by a BERTAN 210-02R. The primary voltage is finely regulated and distributed to 180 PMT's by four CAEN A1932AN boards, 48 channels each, housed in a CAEN SY1527 crate. The linear technology employed in this system results in extremely low output ripple, as demonstrated during the ICARUS data taking at LNGS. This is a fundamental feature required for the light detection system to prevent the induction of PMT noise onto the wire planes. To perform a study on the performance of the ICARUS PMT electronics and other detector subsystems before the final detector operation at Fermilab, a LAr test facility was instrumented at CERN[5] [20].

2.5.6 Layout of the laser calibration system

To identify interactions associated with the neutrino beam and reject the expected huge cosmic background, the occurrence time of each event should be reconstructed with a resolution better than 1 ns, as aforesaid. This can be achieved by means of a precise determination of the time delay of the response of each PMT, that may drift in time for temperature excursions, power supply variations or other reasons.

[3] The total memory available for each channel is 5.12 MSa, divisible into a maximum of 1024 buffers.

[4] Data read out is based on the CAEN proprietary CONET2 (Chain162 able Optical NETwork) protocol allowing up to 80 MB/s data transfer.

[5] This work was carried out in the framework of the CERN Neutrino Platform WA104/NP01 activities.

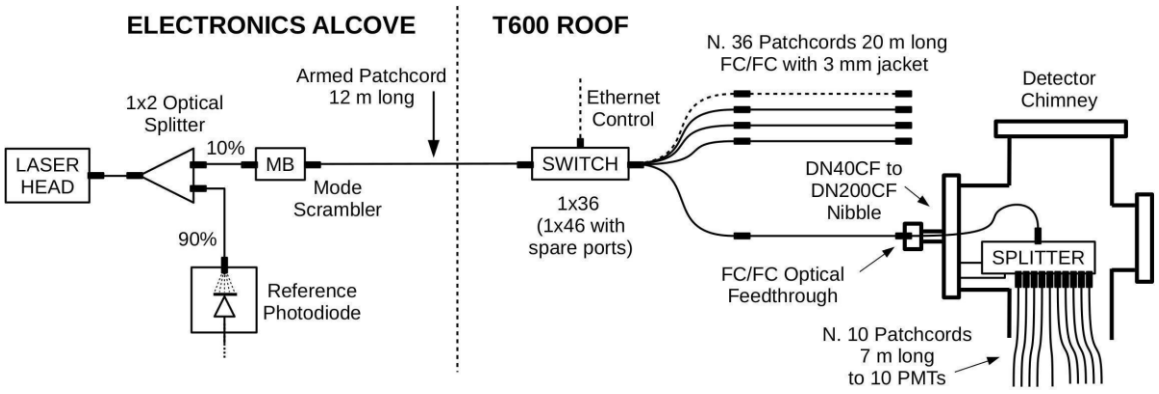

Fig 19. Diagram of the laser calibration system.

Table 3. Optical flange main characteristics

Manufacturer	VACOM GmbH
Flange type	DN40CF
Connection type (Int/Ext)	FC/FC
inside fiber	MM 50 μm core; NA 0.2
Min. temperature	−25°C
Max. temperature	75°C
Vacuum	UHV

The monitoring of the timing values during data-taking can be accomplished with cosmic rays or by delivering a fast calibration pulse to each individual channel.

A fast laser-based calibration system has been developed for the time calibration and monitoring of each PMT channel. Its layout is outlined in Fig. 27 , while additional information on the employed components can be found in reference [21]. Fast light pulses (60 ps FWHM, 120 mW peak power, emission at 405 nm) are generated by a laser diode (Hamamatsu PLP10) settled in the building electronics alcove. Light pulses feed, through 50 μm patch cables and an optical switch (Agiltron Inc.), 36 optical flanges mounted in the same 36 chimneys used for the PMT signal cables, on the opposite site of the BNC flanges. The main characteristics of the optical flanges are shown in Table 3. Inside each chimney, a 1 × 10 optical splitter (Lightel Technologies Inc.) delivers the input laser signal to 10 (50 μm, 7 m long) injection fibers deployed along the mechanical frames, to convey the calibration signal to each PMT, as shown in Fig. 20.

A specially shaped stainless steel pipe (2.5 mm diameter, 20 cm long), fixed inside the PMT sustaining structure, drives the end section of each optical fiber and allows the light focusing on the device windows, as shown in Fig. 21.

The laser pulses should be delivered to the PMT photocathodes with minimal attenuation and without deterioration of the original timing characteristics. Extensive tests were performed on the different components at both room and cryogenic temperatures, to ensure that selected items comply with these requirements [21]. Fig. 14 in chapter 3 shows the distributions of time delay and fraction of transmitted light, obtained from measurements at room temperature on the initial sample of 410

Fig 20. Left picture: DN200CF side of one nibble with a 1 10× splitter (on the right) and a 10-channel patch panel to connect the internal patches to the outputs of the splitter (on the left). Right picture: front view of the DN200CF to DN40CF nibble with a mounted FC/FC optical feedthrough.

Fig 21. Picture showing the stainless steel pipe which drives the end section of the calibration optical fiber toward the PMT window. A blue-light laser spot on the PMT surface can be noticed.

injection patches, using the laboratory setup of reference [22]. The delay dispersion over the 7 m cable length is within 90 ps, with an average value of about 45.59 ns, while the dispersion on the transmission is around 8% with an average value of ≈ 88%. The used sample of 360 injection

patches was then selected, requiring fibers with the highest transmission and similar delays. Measurement at cryogenic temperatures (with a LN_2 bath) shows that transmission and delay are like the ones measured at room temperature.

Test results indicate that the expected performances of the laser calibration system, such as a resolution of about 100 ps, fit well the calibration requests for timing at the level of 1 ns.

References in Chapter 2

[1] MICROBooNE, LAR1-ND, ICARUS-WA104 collaboration, A Proposal for a Three Detector Short-Baseline Neutrino Oscillation Program in the Fermilab Booster Neutrino Beam, arXiv:1503.01520.

[2] ICARUS collaboration, S. Amoruso, M. Antonello, P. Aprili, F. Arneodo, A. Badertscher,

A. Baiboussinov et al., Design, construction and tests of the ICARUS T600 detector, Nucl. Instrum. Meth. A527 (2004) 329–410.

[3] ICARUS/NP01 collaboration, L. Bagby, B. Baibussinov, V. Bellini, M. Bonesini, A. Braggiotti et al., New read-out electronics for ICARUS-T600 liquid Argon TPC. Description, simulation and tests of the new front-end and ADC system, JINST 13 (2018) P12007.

[4] M. Antonello, B. Baibussinov, P. Benetti, E. Calligarich, N. Canci, S. Centro et al.,

Precise 3D track reconstruction algorithm for the ICARUS T600 liquid argon time projection chamber detector, Adv. High Energy Phys. 2013 (2013) 260820.

[5] M. Antonello, B. Baibussinov, P. Benetti, F. Boffelli, A. Bubak, E. Calligarich et al., The trigger system of the ICARUS experiment for the CNGS beam, JINST 9 (2014) P08003.

[6] Journal of Applied Physics **34**, 1591 (1963); https://doi.org/10.1063/1.1702640

[7] Journal of Applied Mechanics and Technical Physics **volume 30**, pages 602–609(1989)

[8] M. Babicz, S. Bordoni, A. Fava, U. Kose, M. Nessi, F. Pietropaolo et al., Light propagation in liquid argon, submitted to JINST (2020 submitted to JINST) , [arXiv:2002.09346].

[9] A. Ankowski, M. Antonello, P. Aprili, F. Arneodo, A. Badertscher, B. Baiboussinov et al., Characterization of ETL 9357FLA photomultiplier tubes for cryogenic temperature applications, Nucl. Instrum. Meth. A556 (2006) 146–157.

[10] A. Falcone, Studies and tests for the new light collection system of the ICARUS T600 detector. PhD thesis, University of Pavia, 2017.

[11] D. Garcia-Gamez, Developing Scintillation Light Readout Simulation for the SBND experiment, JINST 11 (2016) C01080.

[12] P. Agnes, G. L. Raselli and M. Rossella,Characterization of large area PMT's at cryogenic temperature for rare event physics experiments, JINST 9 (2014) C03009.

[13] A. Falcone, R. Bertoni, F. Boffelli, M. Bonesini, T. Cervi, A. Menegolli et al.,

Comparison between large area photo-multiplier tubes at cryogenic temperature for neutrino and rare event physics experiments, Nucl. Instrum. Meth. A787 (2015) 55–58.

[14] A. Falcone, F. Boffelli, M. Bonesini, T. Cervi, R. Mazza, A. Menegolli et al.,

Performance of large area PMT's at cryogenic temperatures for neutrino and rare event physics experiments, PoS PhotoDet2015 (2016) 019.

[15] ICARUS/NP01 collaboration, M. Babicz, L. Bagby, B. Baibussinov, V. Bellini, M. Bonesini,

A. Braggiotti et al., Test and characterization of 400 Hamamatsu R5912-MOD photomultiplier tubes for the ICARUS T600 detector, JINST 13 (2018) P10030.

[16] M. Spanu, Study on the TPB as wavelength shifter for the ICARUS T600 light detection system in the Fermilab SBN program. PhD thesis, University of Pavia, 2018.

[17] P. Benetti, C. Montanari, G. Raselli, M. Rossella and C. Vignoli, Detection of the VUV liquid argon scintillation light by means of glass-window photomultiplier tubes, Nucl. Instrum. Meth. A505 (2003) 89 – 92.

[18] M. Diwan, "Photo-multiplier and cable analysis."

URL:https://www.phy.bnl.gov/~diwan/talks/pedagogy/pmt/pmt-cable-analysis.pdf, 2019.

[19] CAEN S.p.A., "V1730/VX1730 & V1725/VX1725 16/8-channel 14-bit 500/250 MS/s Waveform Digitizer." User Manual UM2792, 2016.

[20] ICARUS/NP01 collaboration, M. Babicz, M. Diwan, A. Fava, A. Guglielmi, W. Ketchum, G. Meng et al., A particle detector that exploits liquid argon scintillation light, Nucl. Instrum. Meth. A (2019) 162421.

[21] ICARUS collaboration, M. Bonesini, R. Benocci, R. Bertoni, A. Falcone, R. Mazza, M. Torti et al., The laser diode calibration system of the Icarus T600 detector at FNAL, JINST 15 (2020) C05042.

[22] R. Bertoni, M. Bonesini, A. de Bari and M. Rossella,

A laser diode based system for calibration of fast time of flight detectors, JINST 11 (2016) P05024.

Chapter 3

TEST RUN at CERN of A SAMPLE of ICARUS PMT's

Contents

3.1 Characterization of PMT's during the test run at CERN.

Hamamatsu R5912-MOD series (8", 10 dynodes) are rated for cryogenic temperature, as they feature a cathode with platinum under-layer. They are supplied with sandblasted glass windows. In ICARUS there are 360 PMT's with a spare of 40 PMT's.
The characterization of all 400 such devices focused on these points:

- gain and linearity;
- effective Quantum Efficiency: i.e. with Tetra Phenyl Butadiene used as WLS, (WaveLength Shifter) on window;
- response uniformity on the photocathode surface;
- peak-to-valley ratio of the SER (Single Electron Response) distribution.

Measurements have been done both at room and at cryogenic temperature.

An ICARUS Hamamatsu PMT R5912-MOD is described in the following pictures (no number for them):

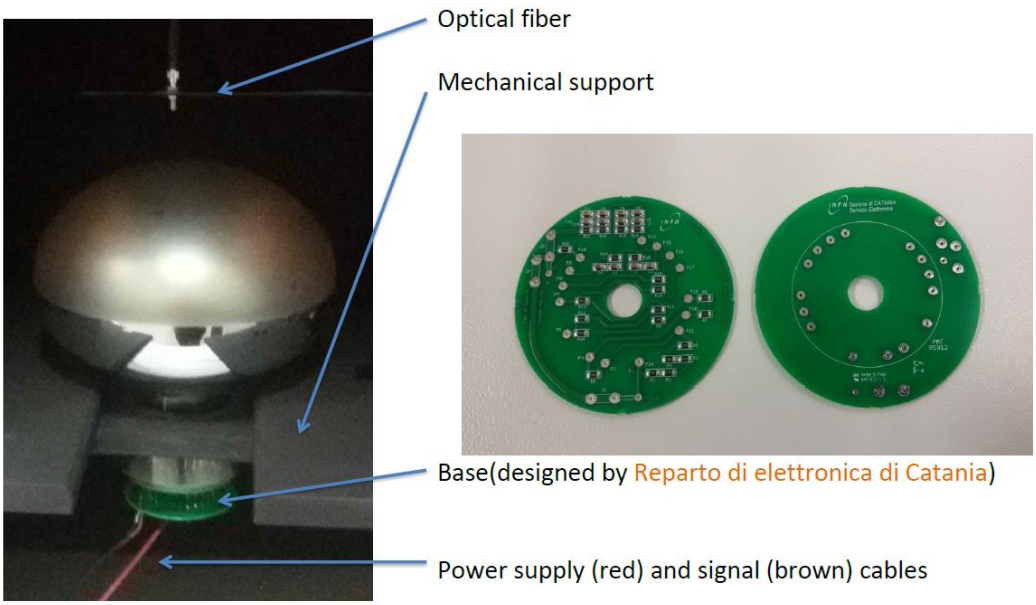

Dark room (test at room temperature)

Ideasquare building @ CERN

Control room (test at room temperature)

Ideasquare building @ CERN

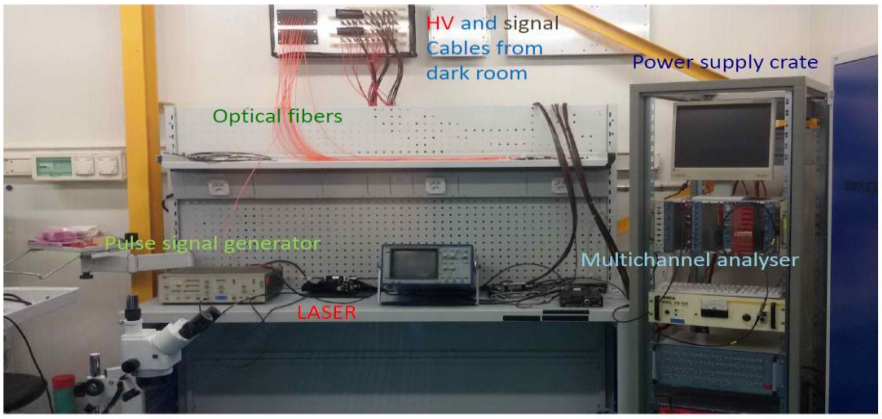

Cryo tests mechanical support

Building 220 @ CERN

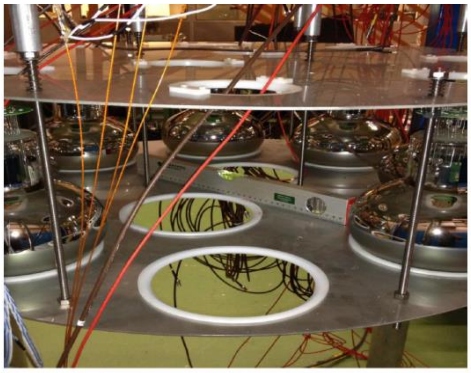

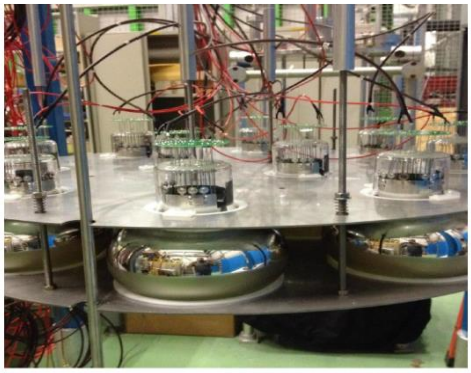

3.2 The CERN 10-PMT Test Facility.

The whole experimental setup has been implemented inside LAr which is the same scintillator used for the ICARUS T600 TPC (Time Projection Chamber). According to figure 1, the CERN 10-PMT facility consists of a double-wall, vacuum-insulated 1.5m^3 cryostat. The geometry of the PMT setup has been designed in a way that cryostat is instrumented with 10 Hamamatsu R5912-MOD PMT's, in which 8 of them are peripheral and two of them are central. It should be mentioned that, by means of evaporation, 6 of these PMT's have been coated with TPB as a wavelength shifter. This is while other 4 PMT's have not been equipped with a wavelength shifter, in order to study the visible photons detection efficiency [1].

The internal translation and rotation of the setup, consisting of an alpha source and a SiPM-based detection system, can be accomplished by means of a mechanical extendible handler (Kenosistek S.r.l., Binasco (MI), Italy) as shown in Fig 2.

To furthermore explain the experimental setup, it can be said that among the existing PMT's in the setup, only one of them is placed in front of the SiPM. For every particular position,we get a lot of data, since the signal of the SiPM goes over the threshold for many times, which means many acquisitions.

It is important to highlight that the distance between the SiPM and alpha source is always the same, because they are fixed in the same frame. What changes is the distance between a selected PMT and the alpha source, because the alpha source and SiPM move together. When the position of the alpha source is changed, what is to be measured is the delay between the SiPM signal (near the alpha source) and the signal of the PMT's (far from the source).

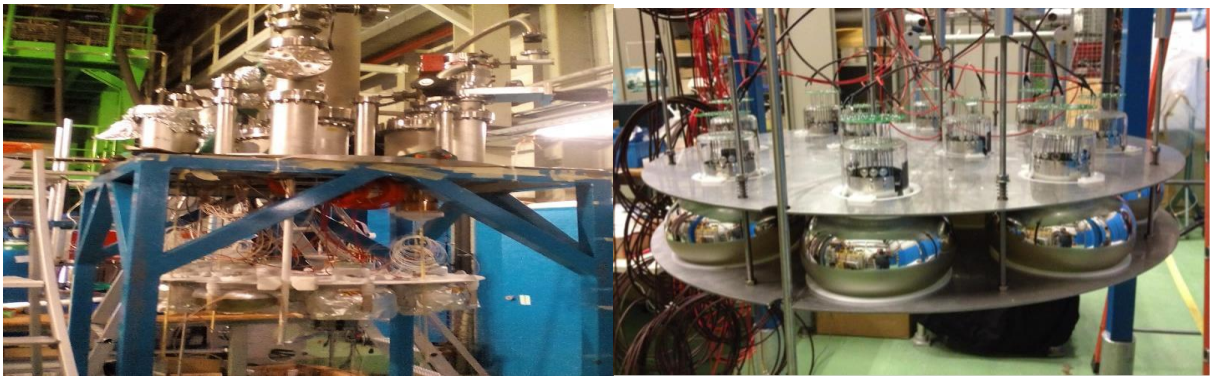

Fig 1. CERN 10-PMT Facility Experimental Setup

Fig 2. The adopted mechanical extendible handler

3.3 The alpha source and SiPM Properties.

The alpha source, as shown in Fig. 3, consists of a 22mm diameter, 4mm thick, stainless steel disk with an active surface of about 2cm^2. The light emission can be considered pointlike, due to the very short stopping power of the alpha particle in LAr. The general goal is to build a trigger starting from the PMT's signals produced by the scintillation light inside the LAr from both cosmic rays and the source, which is inserted in the body of the LAr. A dedicated support with hexagonal shape (110 mm width, 60 mm high), made of ABS by a 3D printer, hosts the source and holds up 6 SiPM arrays (16 Hamamatsu S12572-050P for each array) used for the data acquisition trigger and for the definition of the t0 (will be discussed later) of the light generation. The 16-SiPM arrays are electrically coupled in parallel in two groups, in order to get two independent trigger lines. In this experiment, the distance between the SiPM detector and the alpha source is always the same, because they are fixed in the same frame. What changes is the distance between a selected PMT and the alpha source because the alpha source and the SiPM detector move together.

Fig 3. Picture of the used alpha source

3.4 Brief Remarks of the Experimental Setup.

An oscilloscope (Tekronix MSO64, 2.5GHZ bandwidth, 12bit 25 GSa/s) has been used for checking the quality of the produced signals (as seen in the Fig. 4).

The used oscilloscope for the setup has four channels, namely , c1, c2, c3, c4 in which three of them are related to PMT's and the other is related to SiPM (detector). Only one of the PMT's has been placed in front of the SiPM. Channel 1 is SiPM and channel 2 is PMT. When SiPM level is over a threshold, we acquire data. So, we obtain the SiPM itself plus the signal of the PMT. We accomplish this task in different positions. For every particular position, we get a lot of data since the signal of the SiPM goes over the threshold for many times which means many acquisitions.

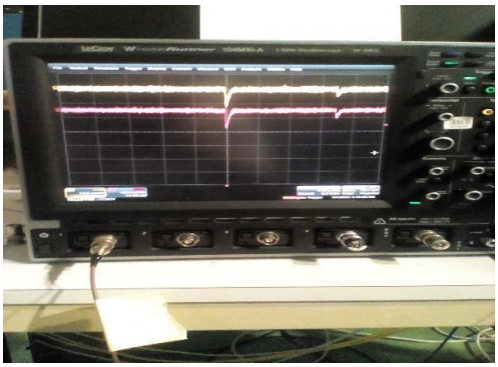

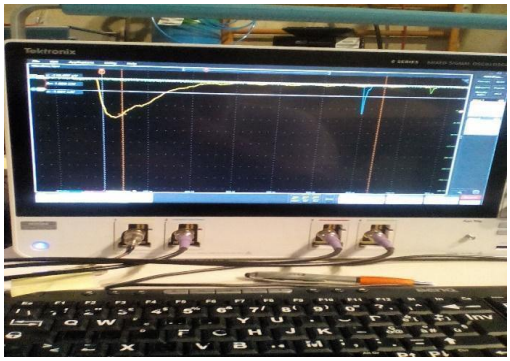

Fig 4. Shapes of the produced signals in the oscilloscope

3.5 Results of Data Analysis.

During the experiment runs, a great amount of data was obtained for data analysis. Here, it is worth noting that the horizontal position of the source is maintained. The source itself is under the vertical line of one of the 3 recorded PMT's. Quality of the signals which are produced by PMT's depends extremely on the number of the detected photons. In order to characterize experimental apparatus effectiveness, some important properties such as signal shapes, amplitude of the signals, t_0 , and delay have been discussed completely through data analysis, which will be presented in the following subsections.

3.5.1 Signal shapes

In the following, the signal shapes for both SiPM and PMT have been shown, respectively for different distances. The first purple line stands for the baseline. It is obtained by averaging in time the first points of the waveform. For baseline calculation, an interval has been taken before the start of the signal. The part of the line is established by averaging the red points in the interval of the times between -0.2 and -0.1. In fact, we are averaging the signals in a time interval which is before the start of the real signal. The other red and blue lines are related to 10% and 90% of the signal and they will be needed in the subsequent parts of the analysis. In order to specify good and bad signals, we can specify a threshold in which it can be said that what is under threshold can be considered as a bad signal and what is above it will be a good

one. This is specified since the baseline cannot specify whether a signal is good or bad and therefore a threshold will be needed. It is also worth mentioning that what is between threshold and baseline can be considered as a noise.

Here signal shapes of the SiPM have been presented and in the subsequent part the ones of PMT.

Reading=100

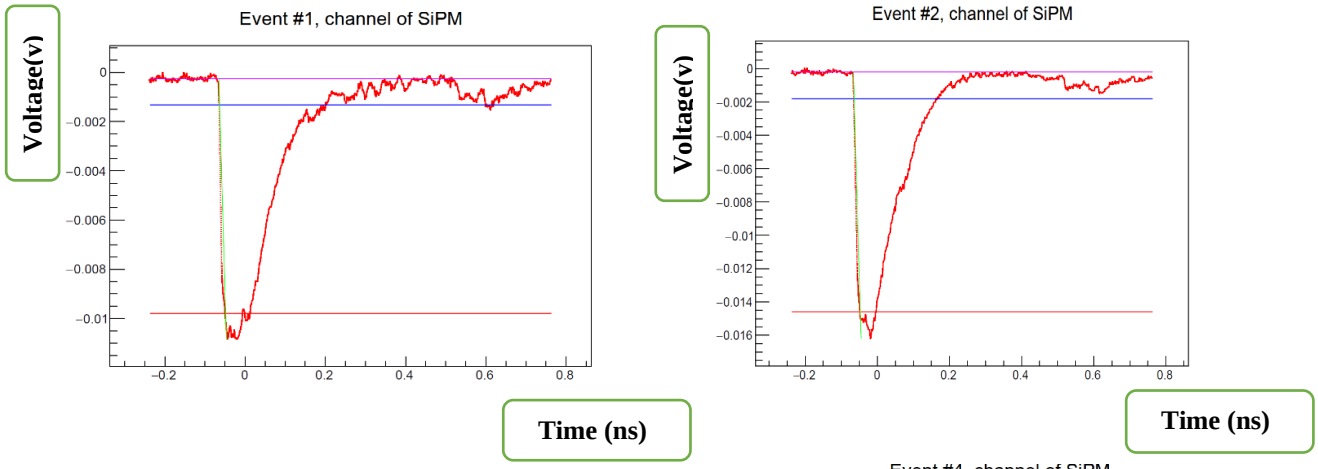

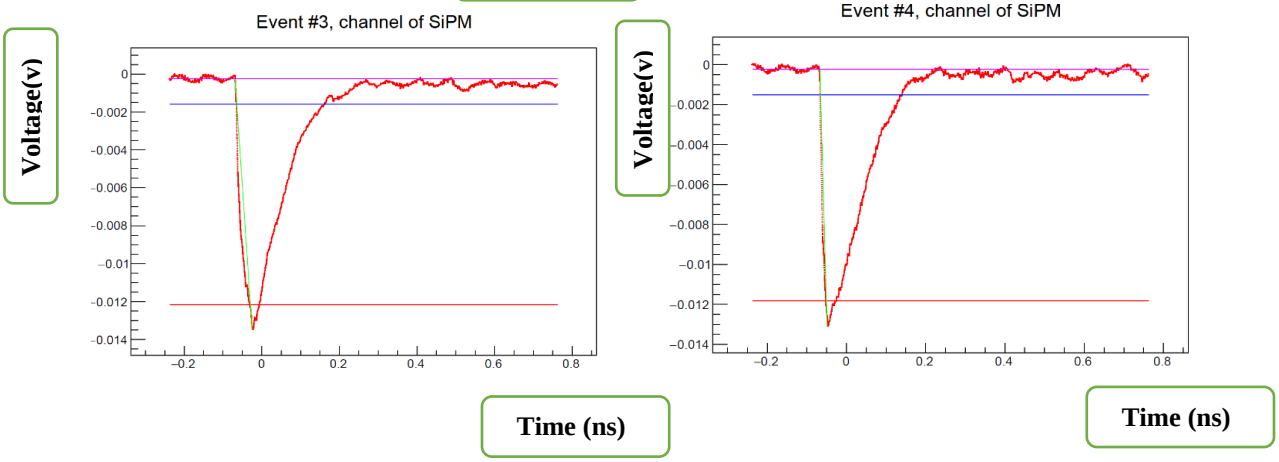

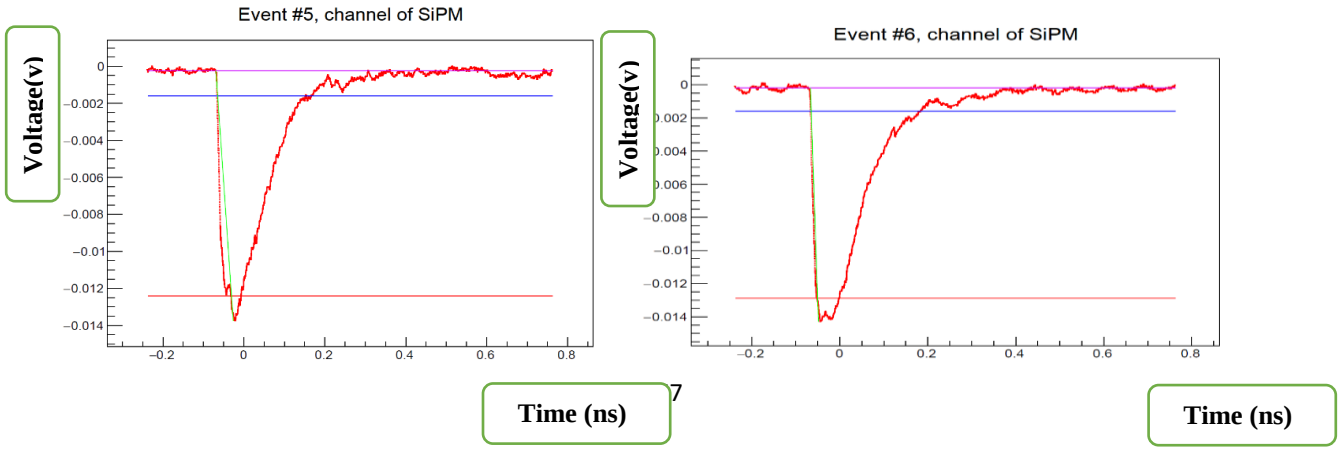

In this part, signal shapes of the PMT for the same distance alpha source-PMT are shown,

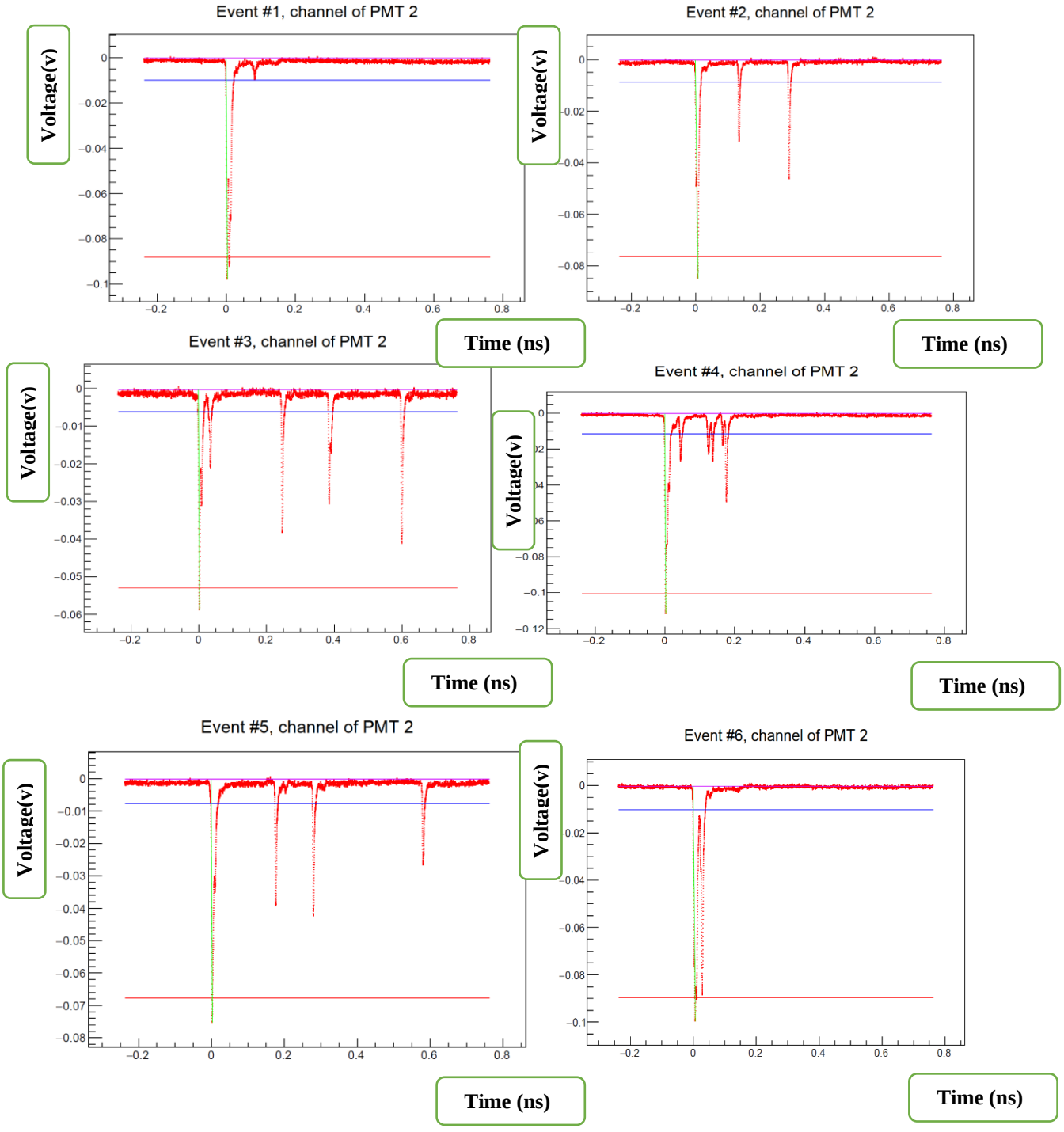

Fig 5. Signal shapes of SiPM and PMT

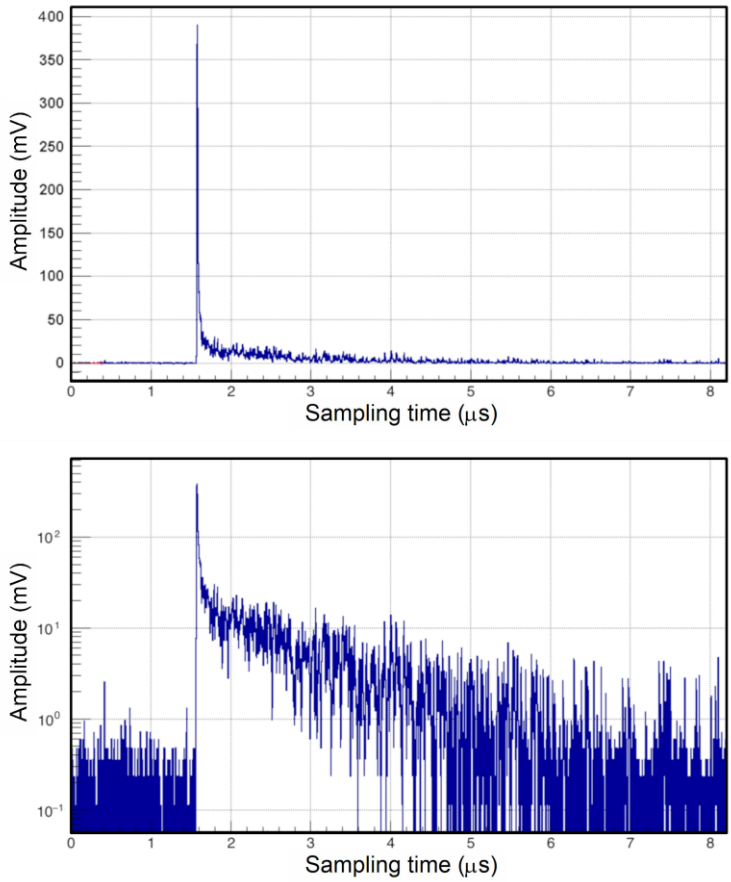

Fig 6. Example of PMT signal (absolute value) recorded with the CERN 10-PMT facility in linear (*Up*) and logarithmic (*Down*) scale in a previous experiment. The presence of both the slow and the fast Components of the scintillation light can be noticed.In this picture the PMT's signal is positive.

3.5.2 Area vs peak of the signals.

As shown in the plots of the signal shapes, we need height of the signal for calculating 10% and 90% of the signal. Height of a signal is a number which is the difference in voltages between the deepest point where the signal has a minimum value of the voltage and the baseline. In other words, height is the difference between baseline and minimum peak. After the specification of the signal, we can speak about 10% and 90% of the signal.

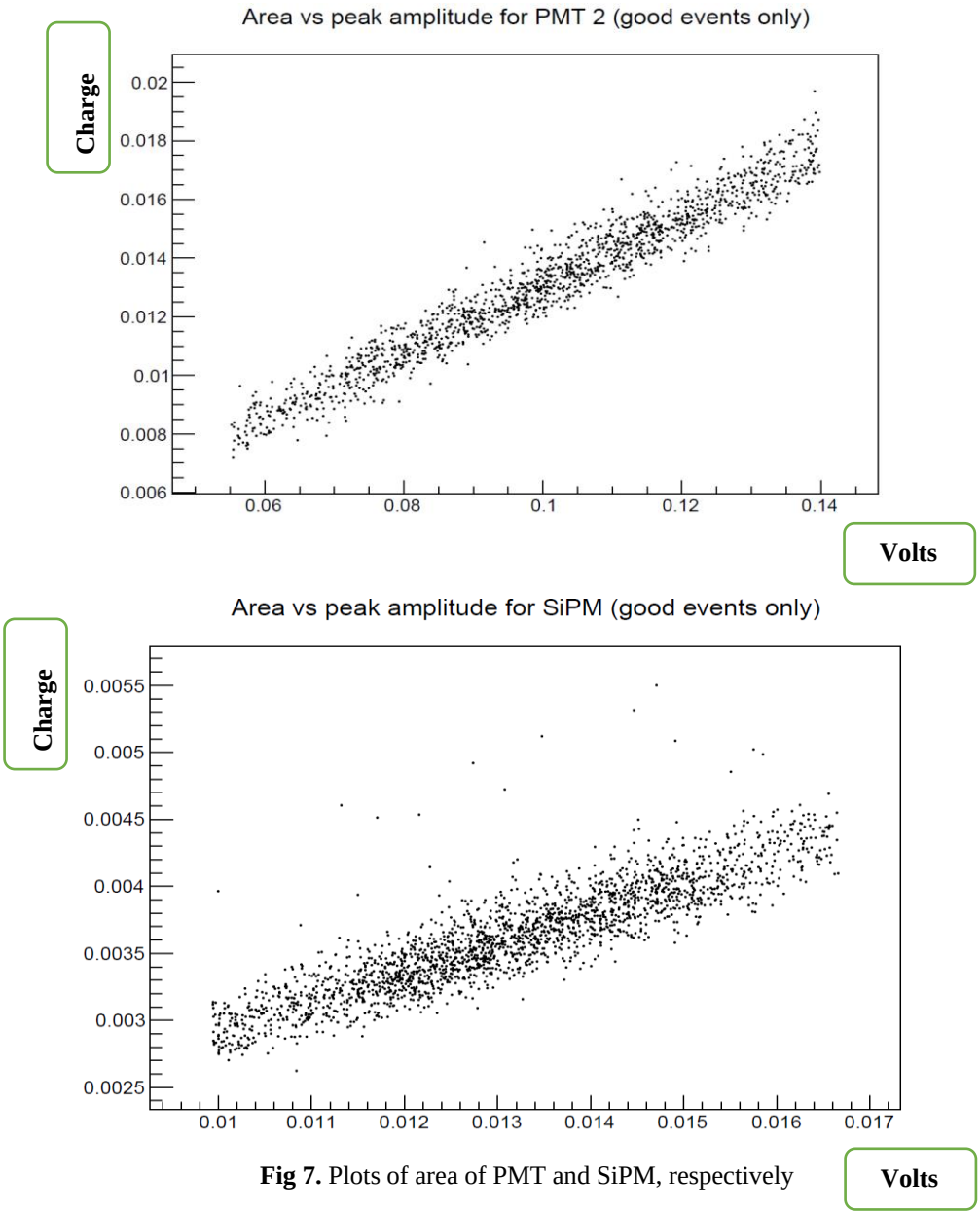

Fig 7. Plots of area of PMT and SiPM, respectively

3.5.3 Height Distribution of the signals.

In the following plots, the blue plot is related to all events consisting of bad (discarded) and good (selected) ones while the red one is only related to good events.

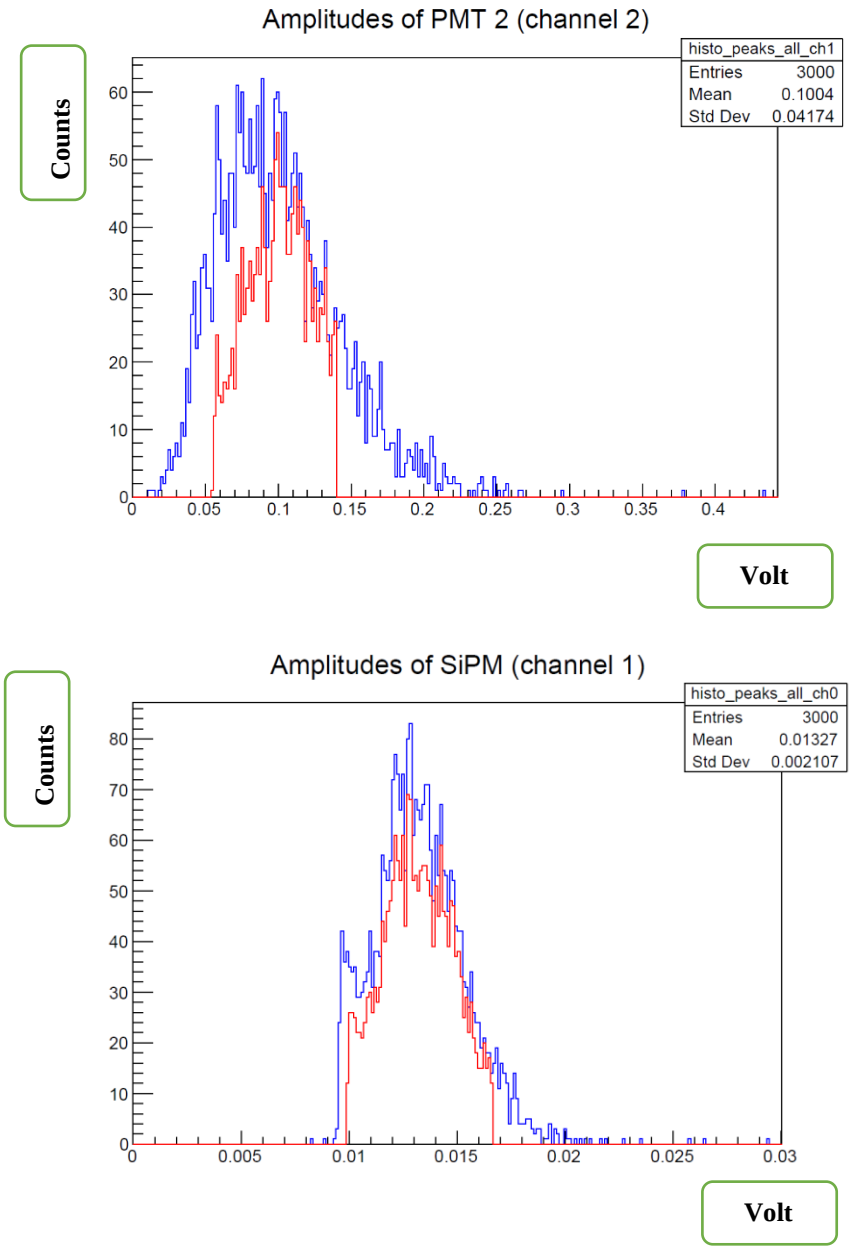

Fig 8. Spectrum plots

3.5.4 t_0.

As seen in the following plots of t_0 and according to what has been shown in the previous signal amplitude plots, two points of 10% and 90% are connected to each other by a straight

green line. This straight line crosses the baseline at some time called t_0. In fact, this algorithm is related effectively to the time when light reaches a single phototube.

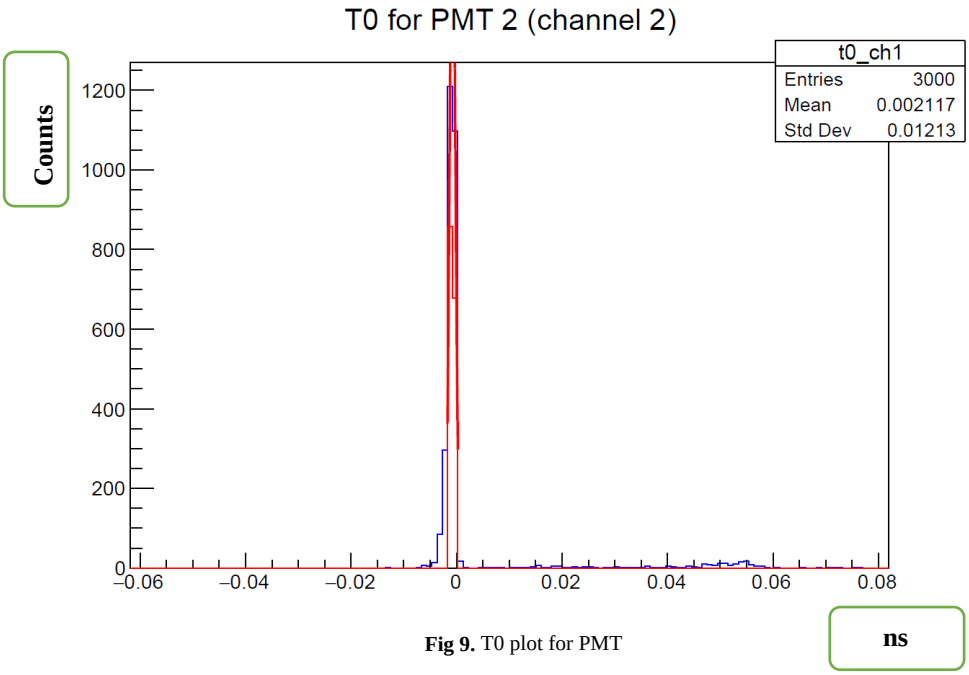

Fig 9. T0 plot for PMT

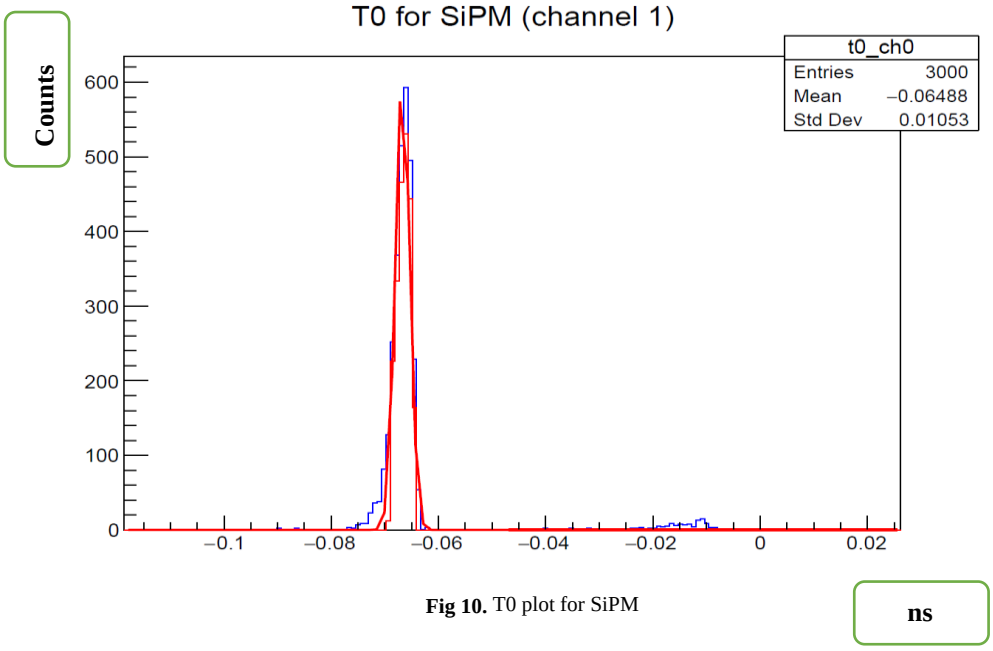

Fig 10. T0 plot for SiPM

3.5.5 Delay:

In this experiment two different methods have been used for determination of the delay (t_1-t_0) between the PMT and SiPM acquired signals:

1. By using a constant fraction discriminator which is an electronic module measuring the time when every signal reaches a constant fraction of its peak, event by event.
2. Determining the intersection point between the baseline and the extrapolated line (10%- 90%), traced in the leading edge of the signal waveform, event by event. .

A new time t_1 is determined for each distance of the PMT from the alpha source.

The time delay distributions are extremely affected by an asymmetric shape which can be due to the different number of photons reaching the PMT surface.

As it is seen in the following delay plots, the scope of the straight line fitting the delay for different positions gives an estimation of the velocity of VUV photons in LAr. Results of measurement for the inverse of the speed of the light in argon gives values spanning from 7.1 to 8.2 ns/m. A comparison between the published results in reference [2], compared to the exact value which has been reported as 7.5±0.07 ns/m shows that our results are compatible with those reported therein.

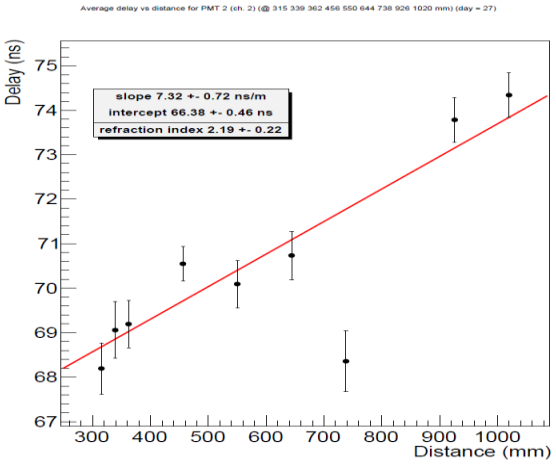

Fig11: Delay Plot (of the PMT2 and SiPM)

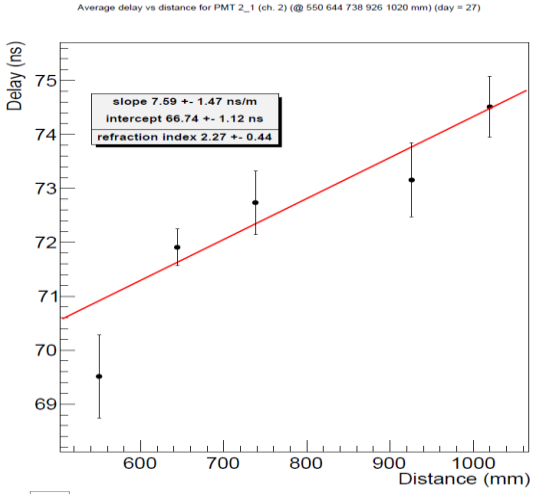

Fig12: Delay Plot (of the PMT2_1 and SiPM)

According to what has been reported about the speed of light, it has been found that for λ = 128 nm , refractive index is n = 1.357±0.001 which fits our results.

3.6 Final system tests

The full light detection system was tested at Fermilab after installation, in order to check the functioning of all the PMT channels, evaluate their performance before cooling down, evaluate the effectiveness of the internal optical-fiber light-distribution system. To this purpose, a subset of the final electronic chain was used. This allowed gaining experience on how to program the new electronics and how to synchronize it with other detector subsystems, such as the trigger and the TPC electronics. Test data were recorded with triggers generated by means of a pulse generator with and without the combination of laser light pulses through the optical-fiber light-distribution system. An example of PMT signal shape recorded in combination with a Laser light pulse and a 10 μs random trigger acquisition are shown in Fig. 14.

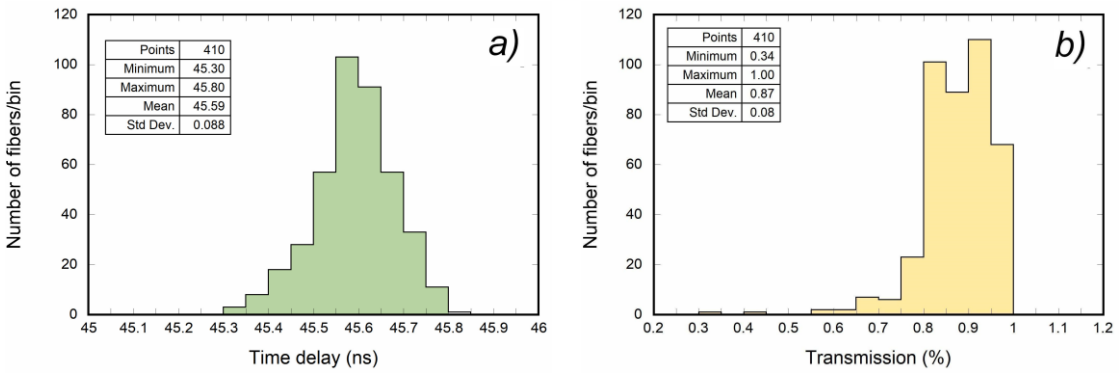

Fig 13. *a)* distribution of 7 m injection patches time delay; *b)* distribution of transmission for the same sample.

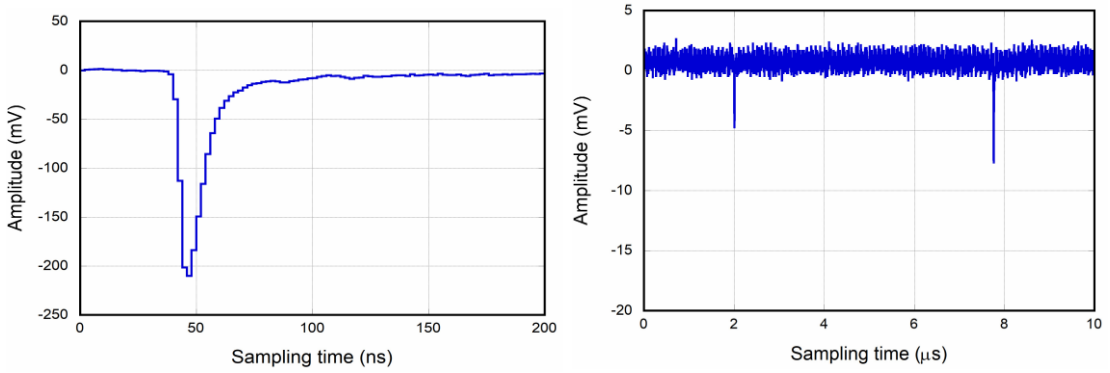

Fig 14. *Left*: example of actual PMT signal shape recorded in combination with a Laser pulse. *Right*: a 10 μs off-light recording showing two random single-electron pulses.

A first quick check was carried out to highlight possible problems related to the detector transfer to Fermilab. They have been found 351 working PMT's, a PMT sparking when applied voltage exceeded 957 V, two dead PMT's, and 6 PMTs with some issue when illuminated with the laser source. These PMTs are undergoing further investigation.

The PMT signal analysis was mainly focused on the gain calibration and dark count rate. The gain calibration of the working PMT's was carried out by acquiring PMT waveforms at a minimum of 3 voltage points. The gain was evaluated by fitting the charge distribution with the analytical expression described in [3]. In Fig. 15, the distribution of the applied voltage needed to attain a gain of $G = 10^7$ for the 351 working PMT's is shown. Results are consistent with a standard deviation of about 5% with respect to the calibration performed at CERN [4].

The dark rate of PMT's was evaluated at Fermilab by counting the number of random single photoelectron pulses using light off data and dividing the total number by the effective acquisition time. An overall average rate of about 1.6 kHz was found. This value is consistent with the average rate of 2.1 kHz previously measured at room temperature before the installation of the PMT's, taking into account that a different measurement technique was adopted at CERN [4].

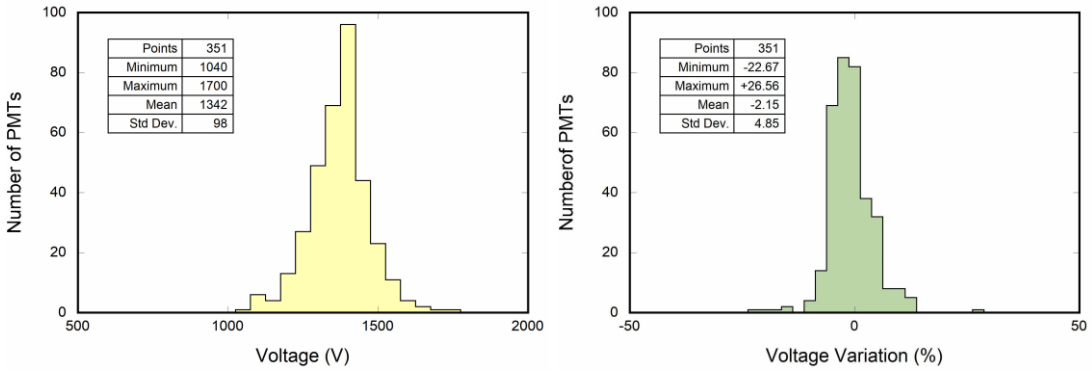

Fig 15. *Left*: distribution of voltages to attain a gain $G = 10^7$ for a set of 351 PMT's. *Right*: distribution of voltage variation (percentage) with respect to the calibration performed at CERN [4]. The results are consistent with a standard deviation of about 5%.

3.7 Final remarks

The new scintillation light detection system for the ICARUS T600 LAr-TPC, realized for its operation at Fermilab in the context of the SBN program, includes the use of 360 large area PMT's mounted behind the wire planes and a fast-laser calibration system. The high performance of this detection system in terms of sensitivity, granularity and time resolution, will allow ICARUS to cope with the large cosmic ray background by identifying the events associated with the neutrino beam.

To this purpose the system was extensively simulated, the components were precisely characterized and the installation procedures and techniques were carefully defined.

Preliminary tests carried out after transport and installation of the apparatus at Fermilab verified the performances of the light detection system required for the identification of signals related to neutrino beam induced events.

3.8 Publication Abstracts

Measurement of Liquid Argon Scintillation Light Properties by means of an Alpha Source inside the CERN 10-PMT Facility

B. Ali-Mohammadzadeh,[a] M. Babicz,[b,c] V. Bellini,[a] A. Fava,[d] U. Kose,[c] F. Pietropaolo,[c,e] M.C. Prata,[f] G.L. Raselli,[f] F. Resnati,[c] M. Rossella,[f] C. Scagliotti,[f] F. Tortorici[a] and A. Zani[c,f]

[a]*University of Catania and INFN, Catania, Italy* [b]*Institute of Nuclear Physics PAN, Cracow, Poland*

[c]*CERN, Geneva, Switzerland*
[d]*Fermi National Laboratory, Batavia IL, USA*

[e]*University of Padova and INFN, Padova, Italy*

[f] *University of Pavia and INFN, Pavia, Italy*

E-mail: gianluca.raselli@pv.infn.it

Abstract: A particle detection system which exploits the scintillation light produced by ionizing particles in liquid argon (LAr) has been assembled at CERN. The system is based on a dewar housing 10 large-area photomultiplier tubes (PMT). The system is instrumented with an alpha source mounted on an extendible mechanical handler which permits to vary the distance between the source and the PMT plane vertically and to change the source position below the PMT's horizontally. Arrays of silicon photomultiplier (SiPM) photodetectors, integrated in the source support, are used for the data acquisition trigger and to define the t_0 of the light generation. PMT and SiPM signals can be recorded at different distances and different positions allowing the measurement of some properties of the LAr scintillation light.

Keywords: Photon detectors for UV, visible and IR photons (vacuum) (photomultipliers, HPDs, others); Noble liquid detectors; Scintillators, Scintillation and Light emission processes.

Design and implementation of the new scintillation light detection system of ICARUS T600

B. Ali-Mohammadzadeh,[a] M. Babicz,[b,c] W. Badgett,[d] L. Bagby,[d] V. Bellini,[a] R. Benocci,[e] M. Bonesini,[e] A. Braggiotti,[f,g] S. Centro,[f] A. Chatterjee,[h,d] A.G. Cocco,[i] M. Diwan,[l] A. Falcone,[e] C. Farnese,[f] A. Fava,[d] D. Gibin,[f] A. Guglielmi,[f] W. Ketchum,[d] U. Kose,[c] A. Menegolli,[m] G. Meng,[f] C. Montanari,[m,d] M. Nessi,[c] F. Pietropaolo,[c,f] A. Rappoldi,[m] G.L. Raselli,[m,6] M. Rossella,[m] C. Rubbia,[c,n,o] P. Sala,[p,c] A. Scaramelli,[m] F. Sergiampietri,[c,q] M. Spanu,[e] D. Torretta,[d] M. Torti,[e] F. Tortorici,[a] F. Varanini,[f] S. Ventura,[f] C. Vignoli,[o] A. Zhang[l,7] and A. Zani[p] for the ICARUS Collaboration

[a] *University of Catania and INFN, Catania, Italy* [b] *Institute of Nuclear Physics PAN, Cracow, Poland*

[c] *CERN, Geneva, Switzerland* [d] *Fermi National Laboratory, Batavia IL, USA*

[e] *University of Milano Bicocca and INFN, Milan, Italy*

[f] *University of Padova and INFN, Padova, Italy* [g] *CNR, Padova, Italy* [h] *University of Pittsburgh, Pittsburgh PA, USA*

[i] *University of Napoli and INFN, Napoli, Italy*

[l] *Brookhaven National Laboratory, Brookhaven NY, USA* [m] *University of Pavia and INFN, Pavia, Italy*

[m] *Gran Sasso Science Institute, L'Aquila, Italy* [o] *INFN, Laboratori Nazionali del Gran Sasso, Assergi, Italy* [p] *University of Milano and INFN, Milan, Italy* [q] *INAF, Torino, Italy*

E-mail: gianluca.raselli@pv.infn.it

Keywords: Photon detectors for UV, visible and IR photons (vacuum) (photomultipliers, HPDs,

[6] Corresponding author.

[7] now at Stony Brook University, Stony Brook NY, USA

others); Noble liquid detectors (scintillation, ionization, double phase); Scintillators, scintillation

References in chapter 3:

[1] M. Bonesini et al., An innovative technique for TPB deposition on convex window photomultiplier 110 tubes, JINST **13** (2018) P12020, [1807.07123].

[2] M. Babicz et al., Experimental study of the propagation of scintillation light in Liquid Argon, Nucl. Instrum. Meth. **A936** (2019) 178–179.

[3] E. Bellamy, G. Bellettini, J. Budagov, F. Cervelli, I. Chirikov-Zorin, M. Incagli et al., Absolute calibration and monitoring of a spectrometric channel using a photomultiplier, Nucl. Instrum. Meth. A339 (1994) 468 – 476.

[4] ICARUS/NP01 collaboration, M. Babicz, L. Bagby, B. Baibussinov, V. Bellini, M. Bonesini,

A. Braggiotti et al., Test and characterization of 400 Hamamatsu R5912-MOD photomultiplier tubes for the ICARUS T600 detector, JINST 13 (2018) P10030.

CHAPTER 4

SLOW CONTROL SYSTEM FOR ICARUS PMT's

Contents

4.1 Introduction

Slow control systems are used to monitor a wide variety of experimental equipment. This is especially critical for experiments that must operate autonomously over long periods of time or are installed in remote locations. In contrast to the “fast” data acquisition system (DAQ), which is designed to read out the scientific data from the detector once they occur at usually rather high rates, the slow control system usually reads and processes auxiliary sensors and devices at regular intervals, ranging from seconds to hours. Typical slow control parameters are high voltages, temperatures, pressures, gas flows, but also include digital on/off states, e.g., of crates. Typical slow control systems in particle physics, as for example described in ref. [1, 2, 3], set the parameters of various instruments (“configuration” and “control”), record and store the measurements of the instrument’s sensors for online and offline use (“monitor”), and provide an automated feedback to the user in case of parameters falling outside a predefined range (“exception”). The latter is of particular importance for safety relevant applications. While some large projects employ industrial SCADA (Supervisory Control And Data Acquisition) standards and systems [1], similar efforts can usually not be afforded for considerably smaller laboratory projects with their limited scientific scope, operation time and manpower. A full SCADA performance, where complex modifications of a detector’s state are managed by the system, is often also not required. Open-source slow control solutions, such as Experimental Physics and Industrial Control System toolkit (EPICS, Argonne) [4], NOMAD (ILL) [5] or Midas (PSI/TRIUMF) [6] exist for large [7, 8] to medium-sized experiments (e.g., [9]) or research centers with many experiments with similar instrumentation. However, also these tools are often too complex for small R&D projects with only a few different instruments. As a consequence such systems are often either operated without slow control, or with custom solutions with limited functionality. To fill this gap, Doberman has been developed (Detector OBsERving and Monitoring ApplicatioN). It is a simple and extendable opensource slow control system designed for small projects [10].

EPICS SCADA is a platform that let users to interface directly with control system and get values to be monitored. These values are provided by means of Process Variables (PV), i.e., named control system data points that have values and a set of metadata as time stamp, alarm state, units, display ranges, a status/severity (OK, alarm, error) and more.

EPICS is usually complemented with a graphical interface, Control System Studio (CSS). A first look at CSS could be overwhelming. CSS interfaces to a control system by means of tools collection as alarm handler, archive engine, and as well as several operator interface and control system diagnostic tools. Most of them deal with PV in a large different way. One tool displays the value of a PV (Parameter Value), one displays details of the PV configuration, while another concentrates on the alarm state of a PV. Each individual tool deserves some attention and EPICS, indeed, offers each functionality as a separate tool. A key point of CSS is the integration of such functionalities.

To build a control system, users would typically select certain tools, configure them, deploy them in the control room, and then offer operators with some way of integrated access. For example, icons for the individual tools are placed on the desktop, or a Launcher application implemented in Python/TkInter is created to allow access to all control system tools from one top-level user interface. The same desktop computer used to access the control system might also run an Email application, and most sites also have some type of Electronic Logbook, maybe with a web browser interface.

Integration of fundamentally separate tools via a Launcher still leaves users with stand-alone tools, running in parallel. CSS offers an integrated approach that might become more obvious in the following example scenario.

While CSS includes server tools like the Alarm Server, this in turn is again a client to the control system. When installing or learning to use CSS, a certain familiarity with the control system is assumed. For example, we will need to know PV names that CSS can read or write. We might want to create new PVs that can serve as alarm triggers.

Like other control system client tools, CSS can use the metadata that comes with PV's. We need to understand what metadata our control system provides, and how to configure it. In the absence of a real control system, a few initial steps with CSS will be possible by using simulated PVs like sim://noise which is shown in Fig 1.

.

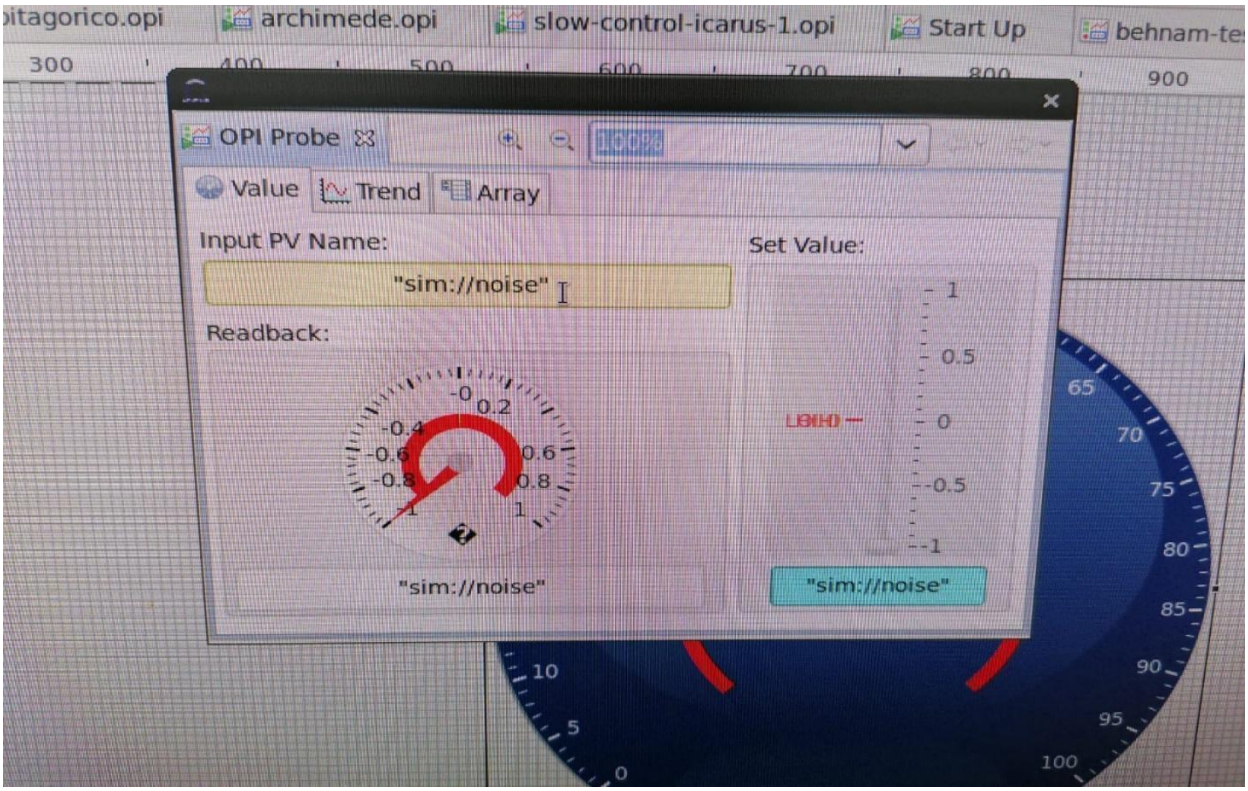

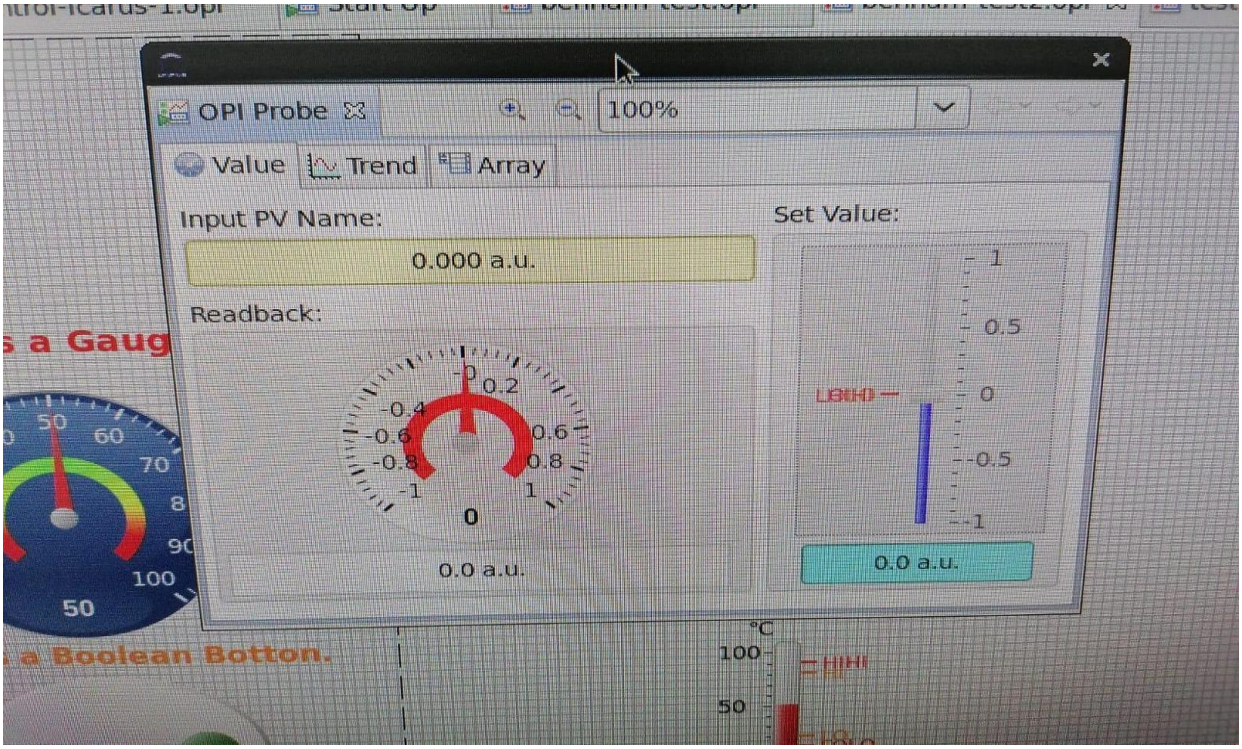

Fig 1. Typical examples of creating a PV.

The detector controls and monitoring team should (broadly) provide the following items:

- The ability to monitor (either directly or indirectly) any system of the experiment that can provide useful information on the health of the detector or conditions important to the experiment.
- A full control capability for systems that do not already have a fully developed independent control system (either inherited from a previous experiment or developed by the sub-system experts themselves).
- An integrated operator interface that
  - provides display panels for controls and monitoring (GUI interface).
  - archives the sampled data (archiver).
  - displays warnings and alarms to alert the operator (alarm server).

4.2 EPICS and CSS

4.2.1 General

EPICS (Experimental Physics and Industrial Control System) is based on a client/server network model.

- ✔ Data collection/providing devices run as *servers*, other processes run as *clients*.
- ✔ EPICS servers hold information in the form of Records (also known as process variables (PVs) or channels) which can be accessed by clients.
- ✔ Records are interfaced to devices (software/hardware) which allow them to input/output data into EPICS records.
- ✔ Clients access data using the *EPICS Channel Access (CA) protocol*

An EPICS system consists of *any number of server programs* implementing the EPICS Channel Access (CA) protocol to provide *client programs* access to *any number of process variables.*

The EPICS base distribution provides a standard type of channel access server called an Input/Output Controller (IOC), which can be extended to support specific hardware as desired.

The CSS Toolkit, based on Java's Eclipse environment, provides necessary applications to develop operator panel interfaces (OPI) such as displays and control panels

The CSS BOY (Best OPI Yet) application allows one to develop an OPI in a few minutes.

CSS also provides Alarm and Archiver applications. Archived data are stored in a PostgreSQL Database. Some of the most prevalent tools existing in CSS have been depicted in Fig. 2.

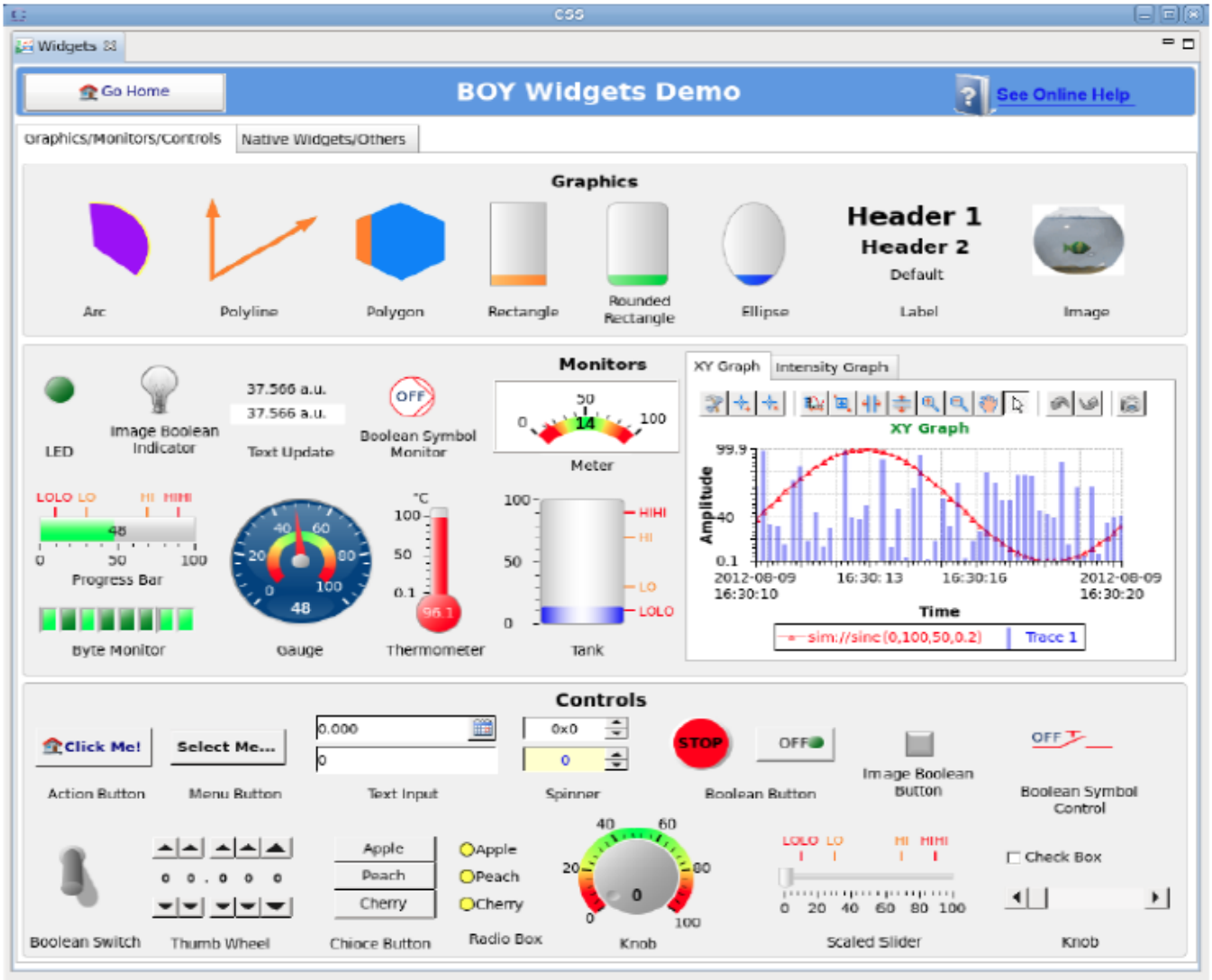

Fig 2. Some examples of the existing widget samples in CSS used in slow control

About the necessity and importance of slow control, we should say that normally we have many pieces of hardware, so we lack the time to access physically different parts of the apparatus for different operations such as: turning on/off, controlling voltage, monitoring. This makes the importance of the slow control very significant. In fact, it is here where the slow control system enters.

4.2.2 To compile EPICS

The present work was based on Linux operating system, where it is usual to have a large number of commands executed from command line, as for example compilers, that usually are external applications.

The C++ compiler, needed to compile EPICS, in Linux is usually called **g++.**

EPICS source code is quite complex. In cases like this compilation relays on another external application called **make**, to handle the complex compiling rules can be requested.

Compiling EPICS in Linux is not so difficult. Once sources are available, we have to verify that our system has **g++**, **make** and **readline** header files to successfully compile EPICS from a terminal. Once compilation is completed, a folder called **bin** will be present, where executables and utilities are and also another one, **lib**, where EPICS libraries are, in order to develop user software on top of EPICS.

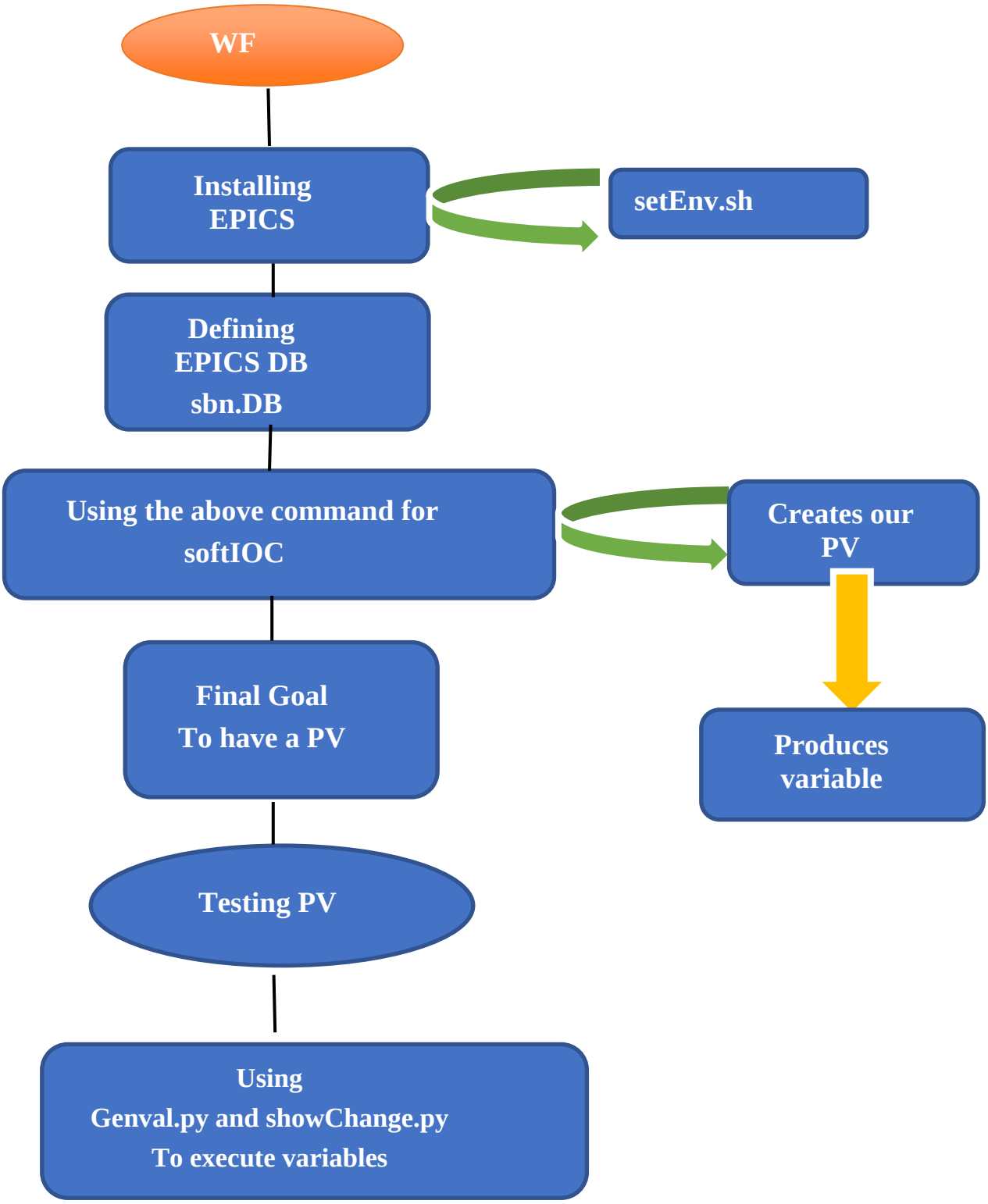

Fig. 3 Flowchart used to test EPICS installation.

In Table 1, the concept of the mentioned commands has been summarized briefly:

Command	Meaning
setEnv.sh	A shell script to set environment variables required from EPICS
sbn.DB	Demo epics DB scheme used for tests defining a PV; text file.
soft.IOC	Program part of EPICS, to start a software IOC defined by the user.
genVal.py	Python script that at random time steps change, in a random way, the PV value making use of PyEpics
showChange.py	Python script that checks if the PV changes making use of PyEpics and, in this case, print it on screen

Table 1 Elements for EPICS test flowchart.

First step in this procedure was the installation of EPICS. Once EPICS is installed, we should set up some environment variables correctly. To do this the related commands were placed in **setEnv.sh**. Then, an EPICS DB should be defined. In our case we use **sbn.db**. This database has been used for soft.IOC to create process variables as parameter values (PV).

Next step is testing PV. We need three terminals. In terminal 1 we set environment variables and start our IOC by means of soft.IOC and sbn.db issuing the command **soft.IOC -d sbn.db**. In terminal 2 we set environment variables and execute the python script genVal.py. Finally, in terminal 3 we set environment and execute the python script showChange.py; at this point we should see a succession of printed values while genVal.py is changing PV value.

4.2.3 Slow Control and DAQ

As it seems, it is mandatory to have a collection of commands inside a system with which we can operate on the hardware of the apparatus. In Table 2 a comparison between slow control and DAQ is reported: it will appear that they are totally different subjects.

DAQ	Slow Control
Is used for reading data such as signals from the PMT's	Is used to control and monitor functionality
Is the collection of data that the hardware gives us	Is a set of instant data to provide status information
problem of rate	No problem regarding to rate
is fast	is slow

Table 2 DAQ versus Slow Control.

One of the main differences between DAQ and slow control is related to **rate**.

To further explain Table 2, we first address the following very basic and important questions:

- What is slow control?
- Why do we need slow control?
- How is slow control organized in a big experiment?

Let us imagine a hardware such as a PMT array. With slow control, we need to control and monitor the functionality of every PMT. They, can be switched on/off, or monitored to asses if the voltage is good or if the current is too much higher. In case of a dangerous situation, we can immediately try to correct it or, if not possible, turn off. Here is exactly the point where slow control enters the game. DAQ is supposed to read the signal that a PMT generates in case some photons hit, hopefully related to a particle like, α, β, γ, ν etc, crossing through the

detector and gives us some information. This information may be in the form of a number. DAQ is the collection of all the information that the hardware provides about the presence of a crossing particle.

So, in DAQ, we have a big amount of data arriving at a very fast rate and that we need to collect in a (usually) big data storage system. DAQ is really complicated since we need to project a data acquisition handling an enormous amount of data, also using very powerful computing, fast switching and fast network interfaces.

From the slow control point of view, such types of problems do not exist! The problem of rate is not present, and generally every good server or PC is enough.

In Fig.4 there is a typical example of a slow control system, which is the basic idea. There is a power supply, a piece of hardware that we can switch on/off directly. We can do so only if we are near the apparatus. If we are far from the power supply, or if we are near the whole set where there is a big experiment, we have not only one power supply, but many of them and of other hardware components, of the order of many hundreds. So, it is impossible to control and to monitor all this hardware in a short time. Also, it is impossible to control manually some characteristics such as temperature, voltage or current, while all such controls should be performed in a reasonably short time.

For all these reasons, it is necessary to have a software system with which we can control all these hundreds of hardware simultaneously and in a comfortable way with a dedicated monitor(s).

This process is repeated for hundreds of pieces of hardware. By EPICS and CSS we can build a GUI and with it some parameters can be defined as well. At the end of the process, we can control and command power-supply by the GUI.

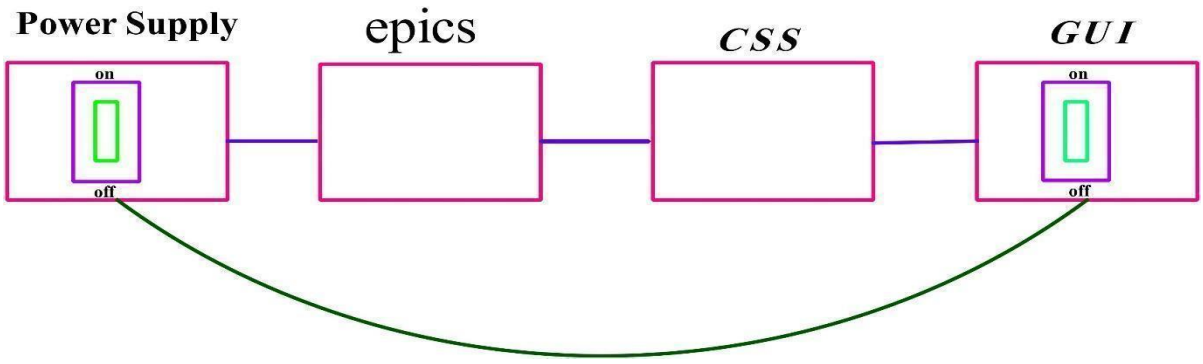

Fig 4. A Simple and descriptive example of a slow control system.

In Fig 5, another example, similar to the one already illustrated. We can design a very simple GUI with just a widget, a Boolean switch, connected to a PV: this will command the crate. Inside the crate, we are supposing 3 boards. By the GUIs, we can command the single board or single channel inside every single board.

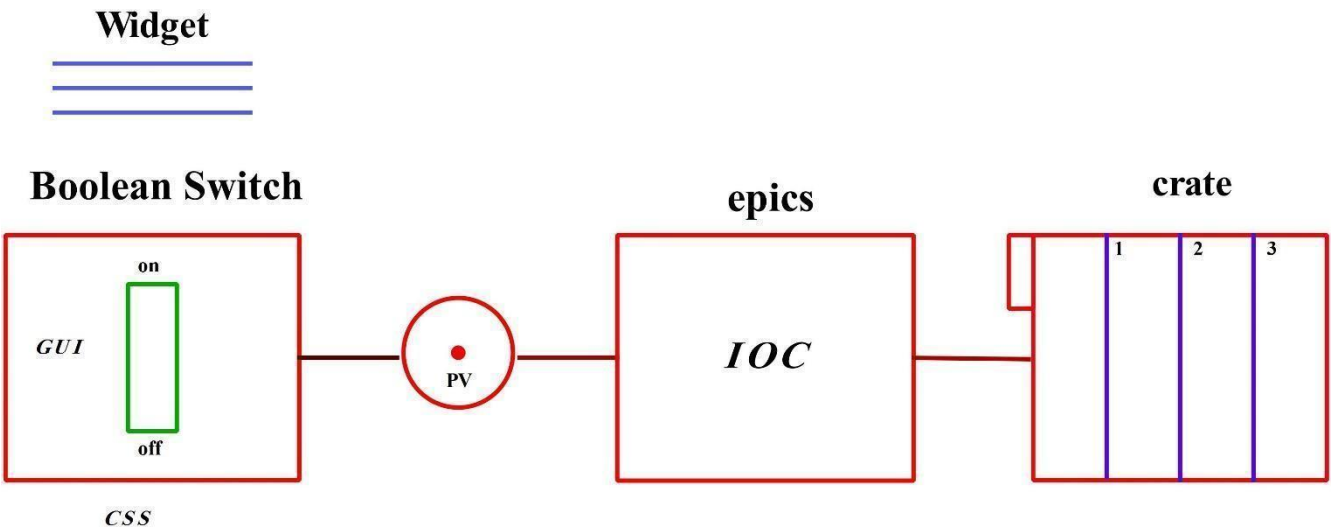

Fig 5. Second example of a slow control system

4.3 Icarus Slow Control Architecture by location.

The ICARUS top level slow control layout is shown in Fig. 6. Subsequent photos show the several levels.

The physical location of the various ICARUS experimental equipment is mapped in the several layouts, to let operators to navigate the system acting with respect to apparatus physical location. For example, if we want to turn on/off a power supply that we know is in given rack we need to navigate the slow control layout to locate the rack where we can operate the power supply.

Level 1 or top level (Fig 6) is the entry point of our slow control procedure. From here we can navigate in the system to reach the present functionalities.

Also, from the top level we look at the general architecture of the apparatus, where two tanks, namely T300-1 and T300-2, are present. Near the apparatus there are seven racks (blue boxes). It should be mentioned that these racks are not the only ones, there are many other racks, but the other racks contain hardware which is out of our interest in this work. Of these seven racks, the central rack contains hardware to create the trigger and we are not interested in it.

The second level (Fig 8) consists of a description of crates in given rack and the rack is visible frontally. From here, we can go to level three, only with the first and last rack. The other four racks (DIG) contain two crates that hold many pieces of hardware that controls digitizing. We are not interested in operating digitizers but, instead, we are interested in monitoring voltages from the two crates contained in each of these racks as shown in Fig 9-12, as requested by the collaboration.

From the top level, we can go to the level two by clicking, we can directly go to PMT 1 and PMT 2 (Fig 8, 13). In the shown racks, there is a power supply. We can operate on it, by switching on/off, and we can monitor voltage and current produced by the power supply.

Instead, clicking on the VM Crate box we access level 3 (Fig 14), where we can operate on this set of PMT’s. We can choose between three operations.

If we choose the first operation, namely manual, we go to the level four (Fig 15), where finally we can operate directly on each group of each board.

If we choose the second possibility, we can turn on/off a single board or all the crate, with the general switch.

If we click on the option Automatic, we can give EPICS the command to run a command file.

In level three, we will decide how to turn on the PMT's. The most important task regarding the previous statement is that we should decide about the essential needs, such as what do we want to do with PMT's or what are the operations that we need. Once these questions were addressed and clarified, a preview can be written and then the layout design. Then, it has been shown that the better way to proceed in this level is to give three possibilities to turn on/off all the PMT's or a part of them. First choice is to turn off all the single groups of PMT's.

By clicking on the proper item, we can go to the level 4, whose preparation has been completed. There we can decide that, for example, in the group 1 at the channel 4 we want to set a specific voltage and then to turn on all that group. This operation can be repeated for all the groups of these 4 boards of 6 groups. So, manually we can turn on or off the selected channels. It should be remembered that we cannot turn on or off the single channel, but only a group of minimum 6 channels. Due to hardware limitations. The second choice is also manual like the first choice, however it is more rapid, because in this choice it isn't necessary to specify what groups of channels are supposed to be turned on. So, in this situation, we want, for example, to turn on board 1 made by 6 groups of channels of the mentioned board. For board 2, we are not interested in turning on. For the third board, we want to turn on all the groups, but this is not the same story for board 4. After specification of these, we can turn on the source as well as turning on all the boards that we want.

In the third choice, which is named automatic, we need only click on the supposed choice and CSS gives command to EPICS to run a file. Of course, the name and the type of the file should also be specified. By clicking on given icon, the command is given to EPICS by CSS to run that file. Before this operation, it is very important to be sure about the configuration of the file.

The range offered by these choices is the better way to operate with the PMT's.

All the previous items regard a single crate. Inside it, four boards have been specified. Each board has 48 channels, but because of the hardware and software configuration inside each board, named AN1932A, we can turn on/off only a group of eight channels and not the single channel. Each small circle in Fig 15, the last one, is the LED for the status on or off for a

channel. It is also worth mentioning that Bertran module prepared the power supply for the whole system.

We can write six groups for each board, (in total 48) and for each group we can indicate single channels, which are typically eight. For each channel, we have a LED in the mode of turning on/off, the number of corresponding PMT's [N.B.: PMT number is in a specific PV in the real ICARUS EPICS database]. VMON is required for monitoring the voltage as well as IMON for current. Then, we can see the status provided us by EPICS, directly connected to the hardware. If we want to set the maximum voltage, and then to switch all the single group, VSET is used. The last observed status shows all the groups and not just one. Software of the board gives us the information on not only a single channel, but on a specified group.

Alle these concepts have been implemented, as shown by figures 6 through 15, that are reported in the following.

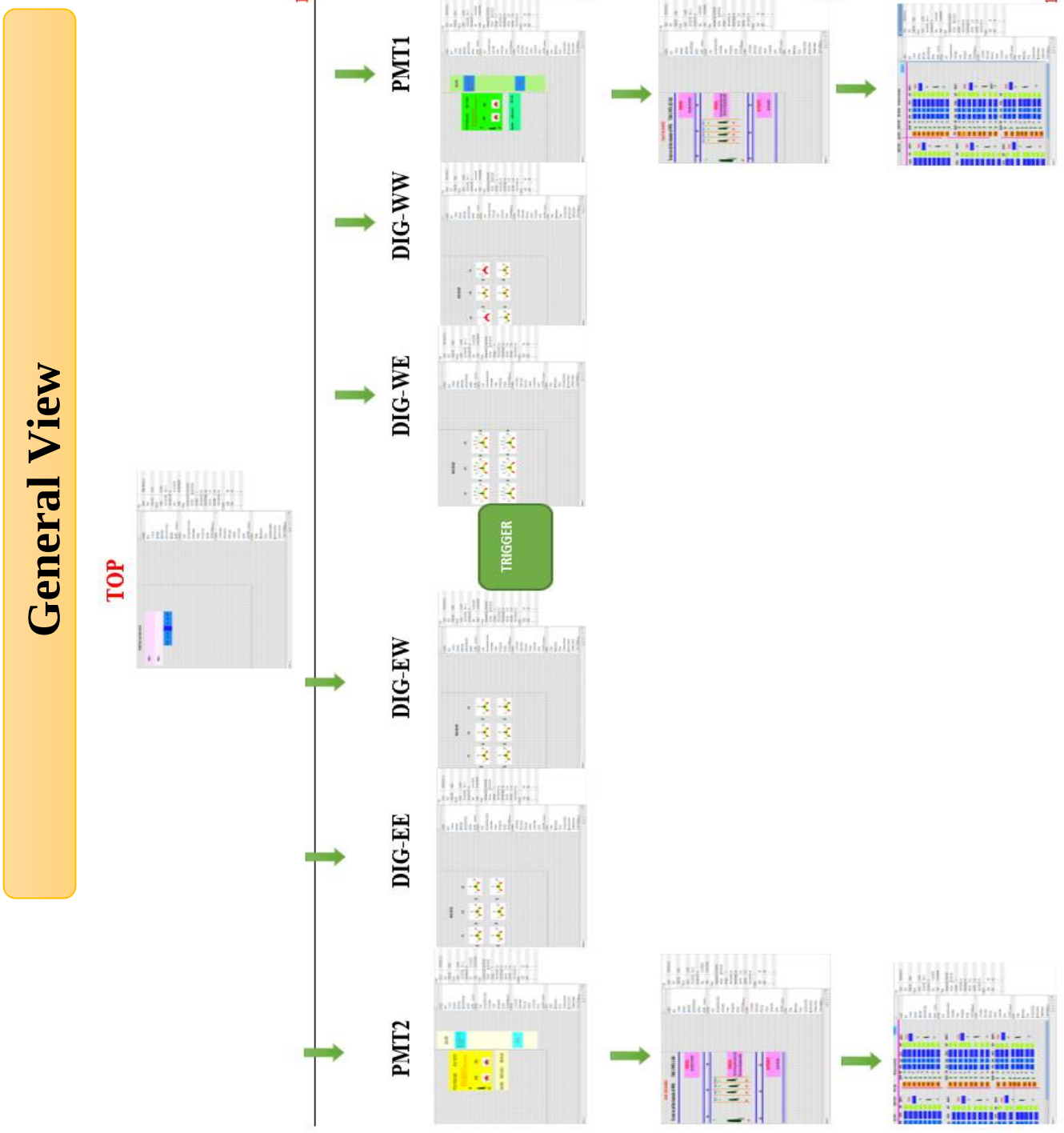

Fig .6 General view slow control.

Layout of Level 1

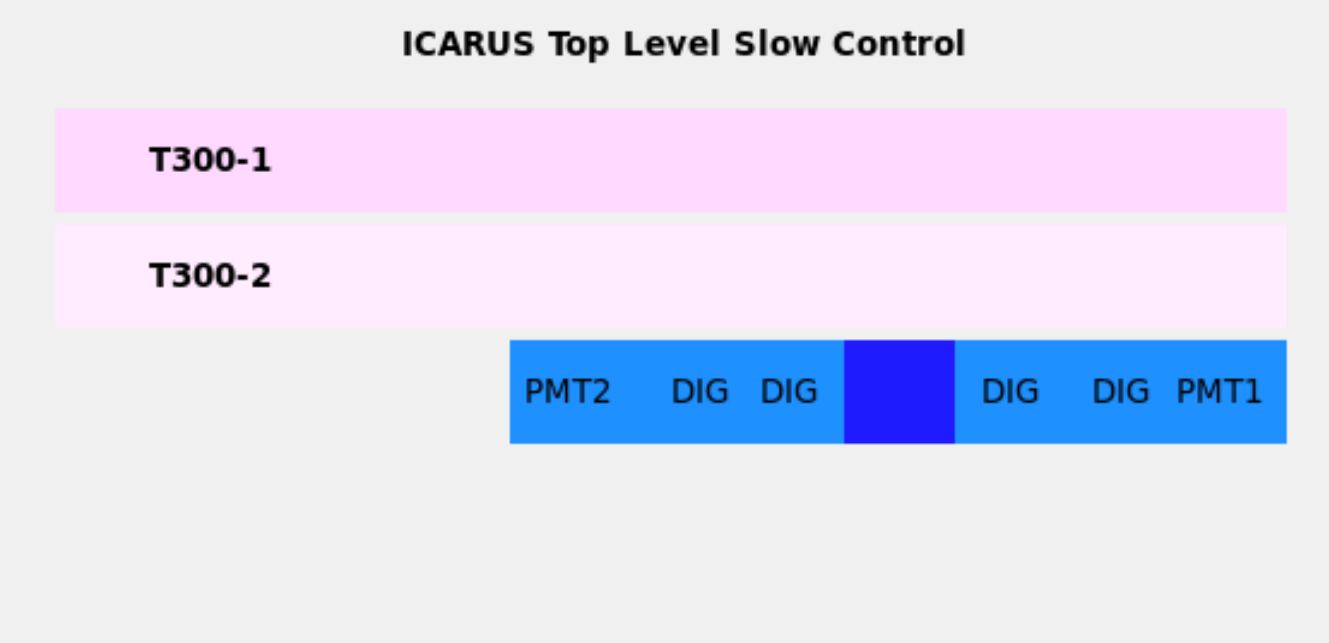

Fig 7. layout of the slow control interface at the top level

Layout of Level 2

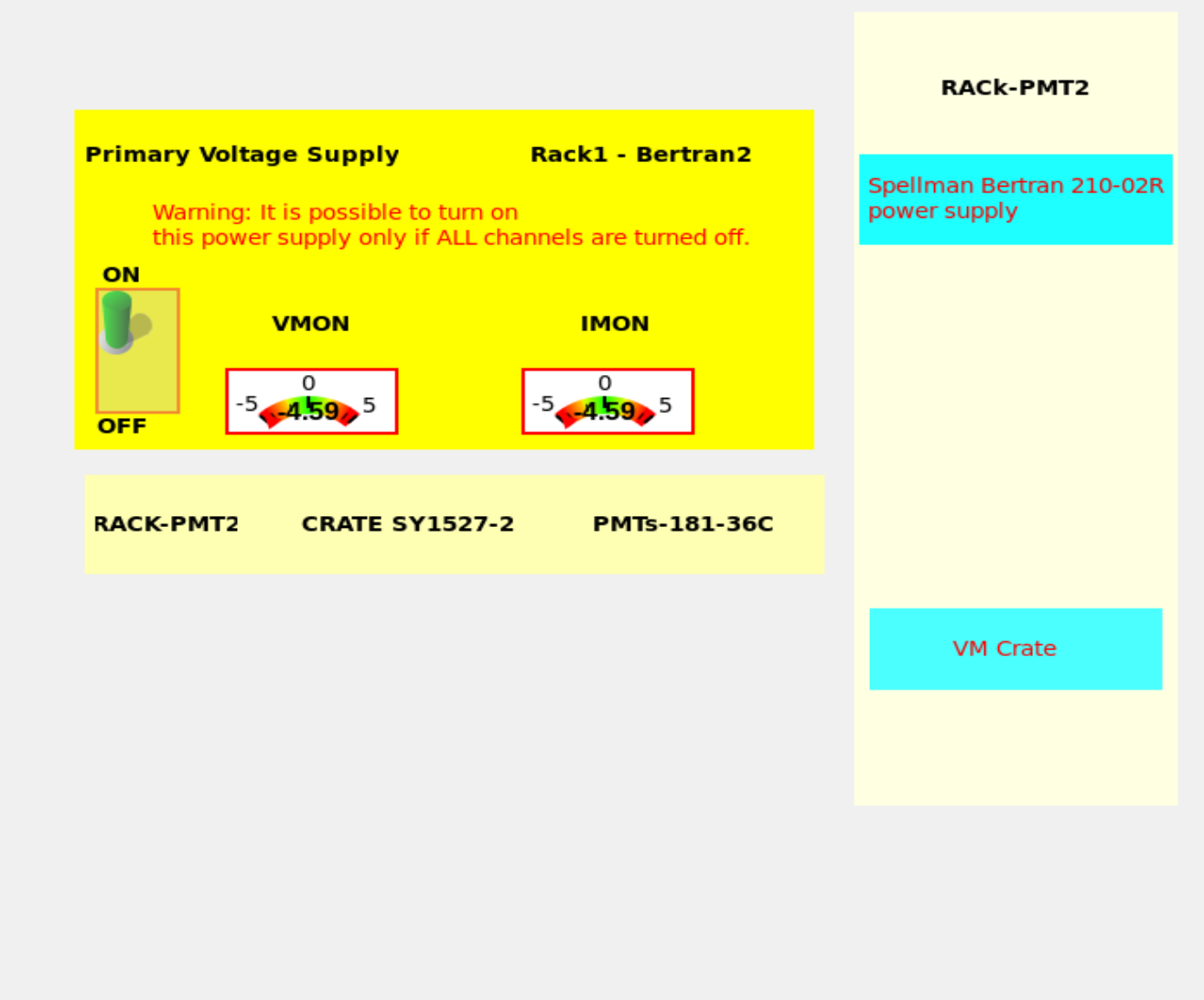

Fig 8. Layout of level 2

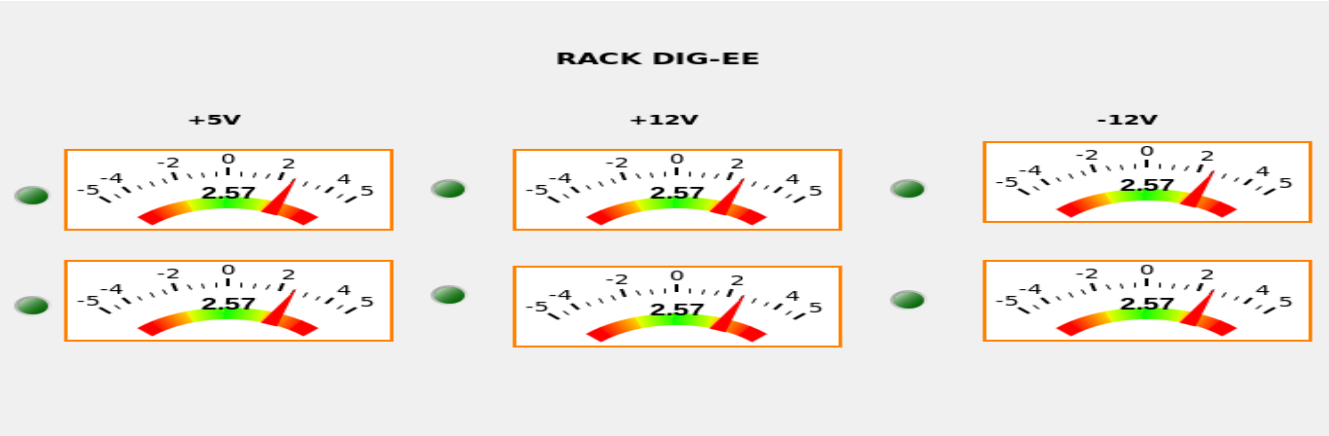

Fig 9. layout of Rack Dig- EE

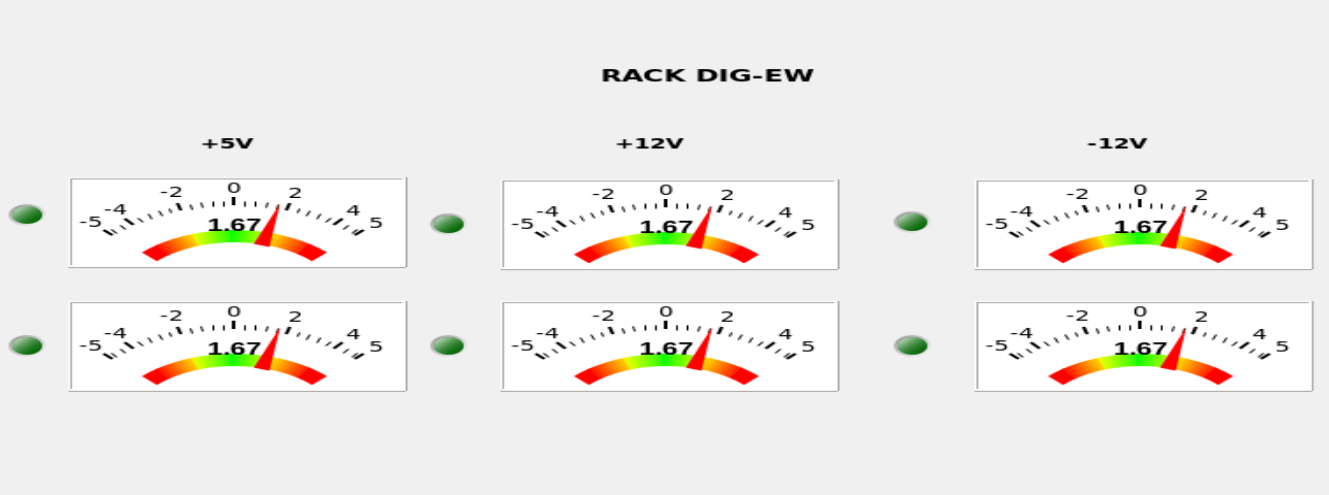

Fig 10. layout of Rack Dig- EW

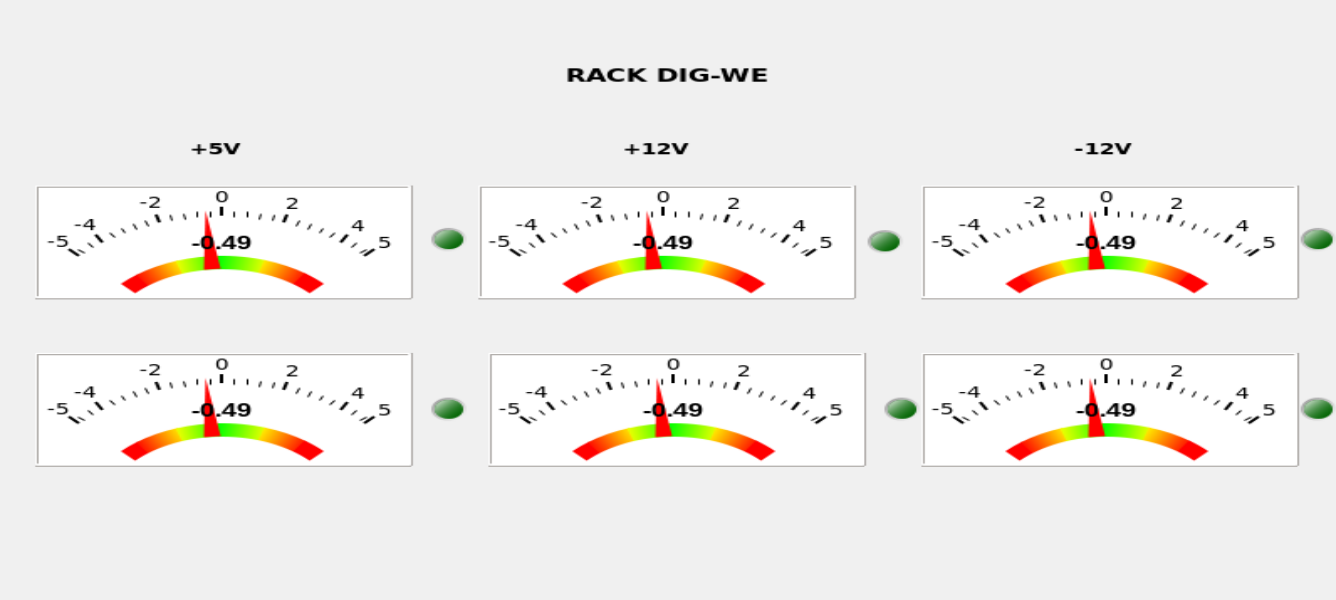

Fig 11. layout of Rack Dig- WE

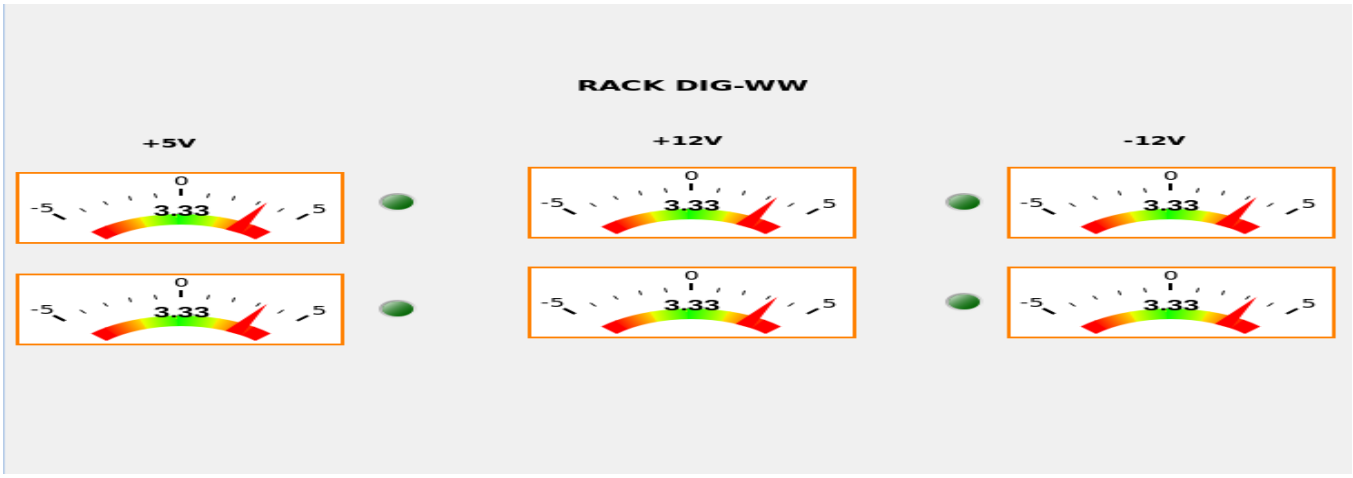

Fig 12. layout of Rack Dig- WW

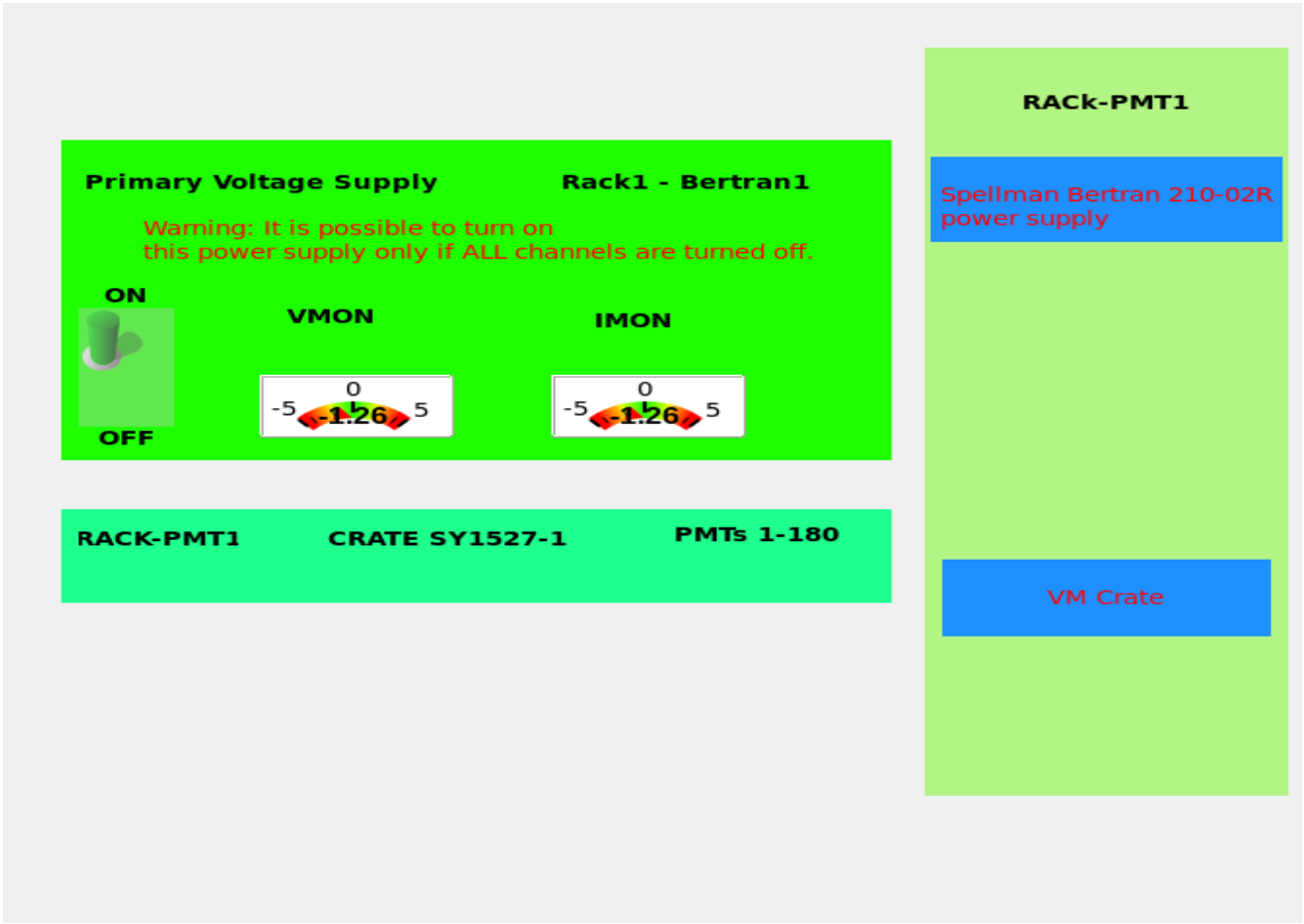

Fig 13. Layout of level 2

Layout of Level 3

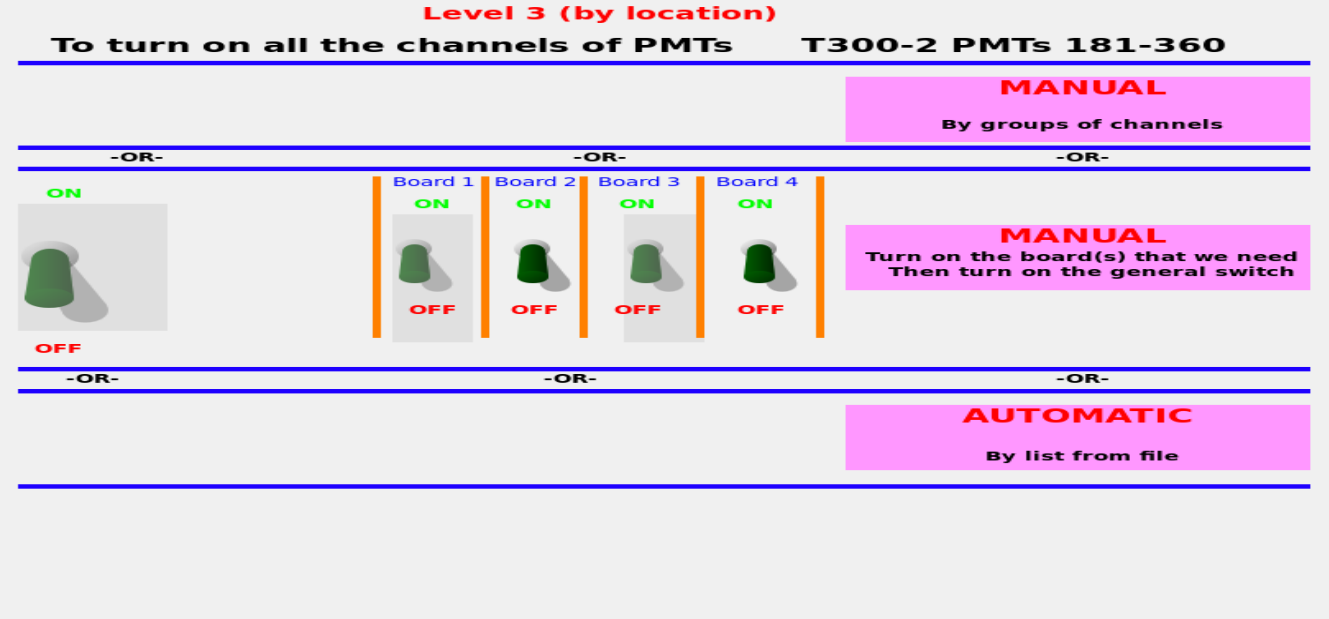

Fig 14. Layout of level 3

Layout of Level 4

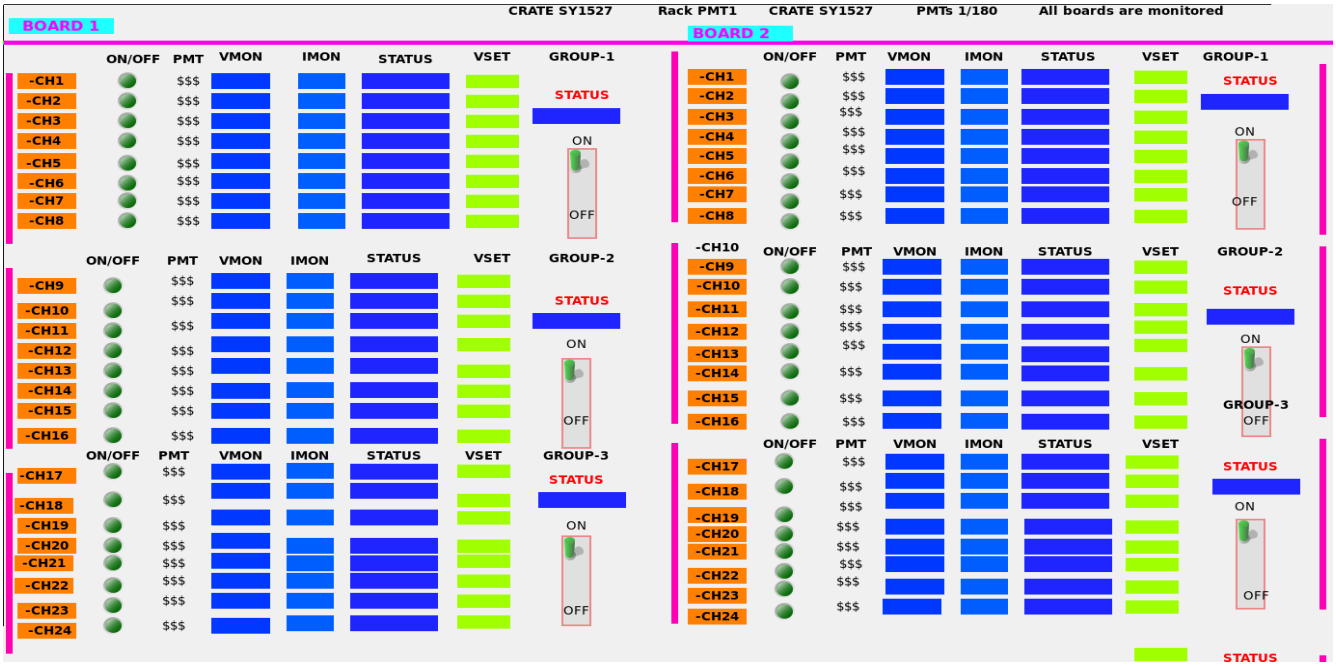

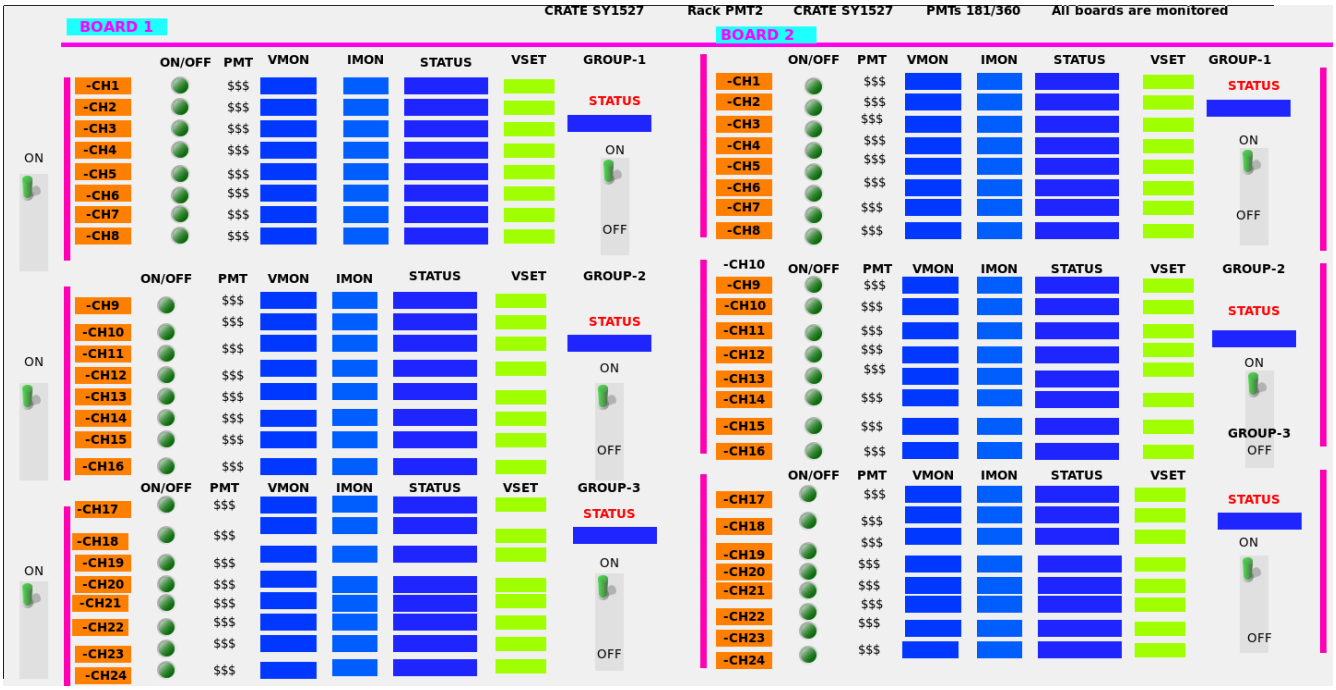

Fig 15. Layout of level 4

4.4 Icarus Slow Control Architecture by functionality.

In this section, we are interested in the functionality of ICARUS hardware. This is a different way to obtain similar results than working by location.

By location, we know that in given rack there is some hardware, such as power supply. The location is clear, and we only know that there is hardware only in that rack. If we want to operate with one of these two hardware's, we know that we should go near that rack and operate with it. From the slow control point of view, this means that we must click on the rack item and operate on that. Location is clear for us in such rack and hence we go to operate on that.

From the functionality point of view, the final product is important. We only want to operate with, for example, power supply, independently of where it is physically located, without any need to know where it is located.

By functionality, we can independently work on where the materials are. For example, we know that there are some Power Suppliers, we want, for example, to operate with these to switch ON/OFF or monitor the voltage or current of these Power Suppliers. Let us focus on the first example, to switch ON/OFF the Power Supply.

In the top level (Fig. 16) we click on the PMT HV distribution. The system will propose the level 2 (Fig. 17a-17c). At level2, Fig. 17a-17c, we can choose which group we are interested. If we click on the first, the system sends us to the related layout to organize how to switch ON/OFF all the PMT's of that part. If we want to operate with PMT 1 or some, we should begin from the top and go to the last layout, that is level 4. But, if we proceed in such a way, we lose a lot of information. So, we should design a path to do so in order to get all the information. If we want to operate on PMT's, we can click on the second item in Fig 16, but before arriving at the last image, the slow control system asks us: what group of PMT's do you want to operate with? And we can choose the first group or second group. After we choose the desired group, for example, the first group, the arisen question will be: in what way can we operate? Normally the system shows us the three following options:

Manual

Manual (but by groups)

Automatic (which file has been configured).

If we choose the first or second option, the system leaves us to Fig 19. So, we want to imagine these four levels like a flowchart. The steps of the flowchart take us to the last operation which is a real operation that we want to do, for example turning on or turning off the Power Supply.

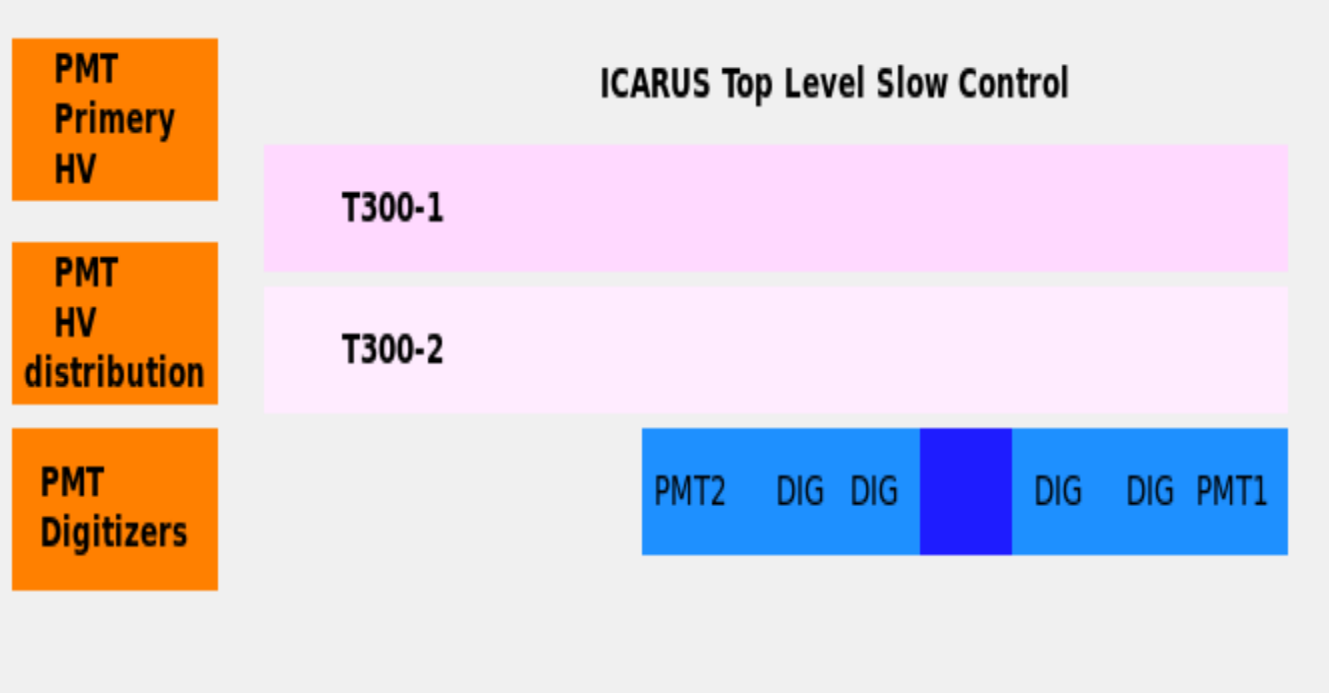

Fig 16. Layout of level 1

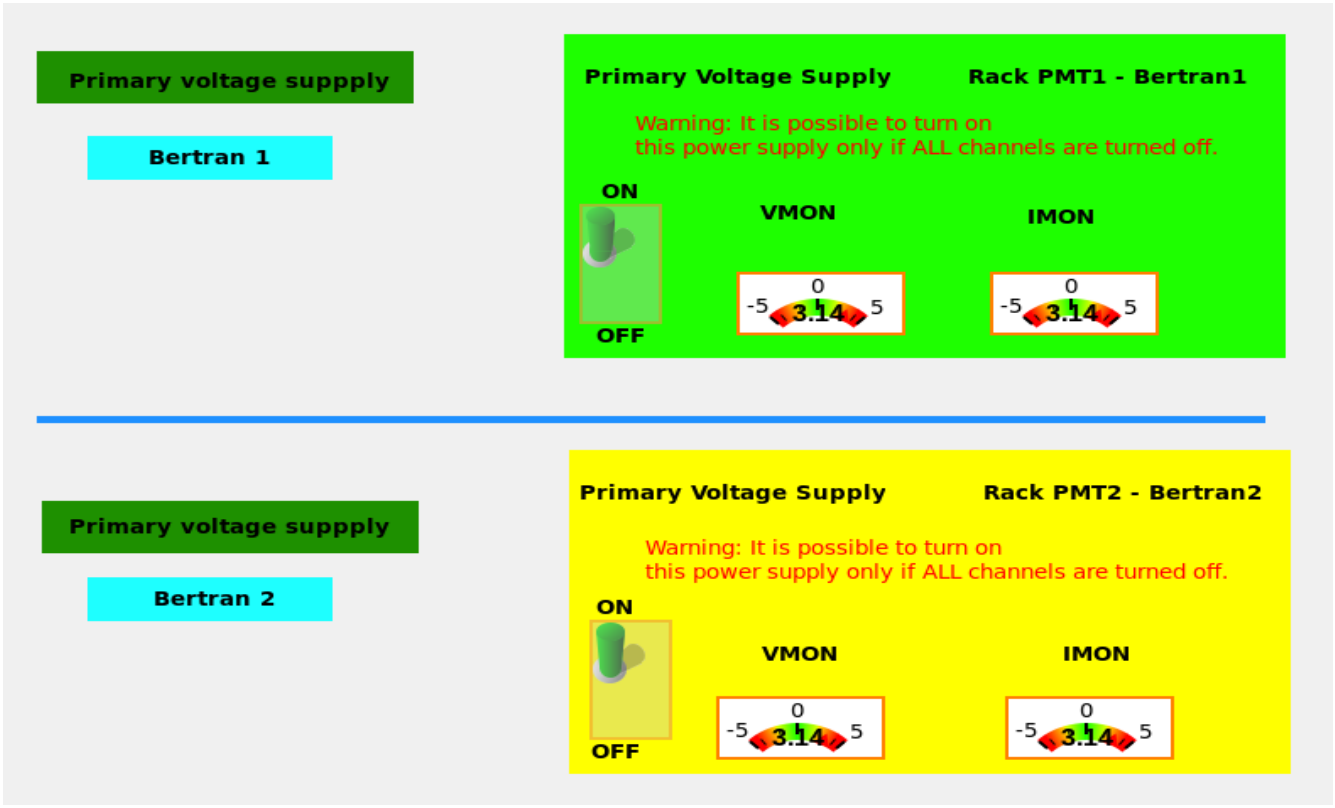

Fig17a. Layout of level 2: block 1

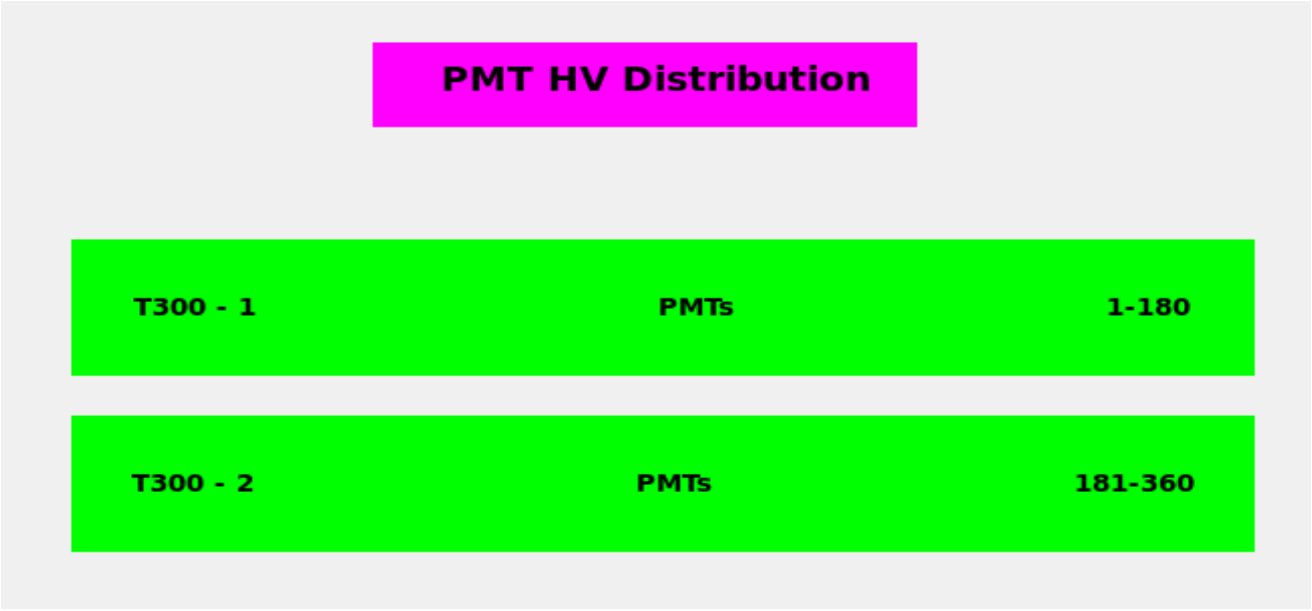

Fig 17b. Layout of level 2: block 2

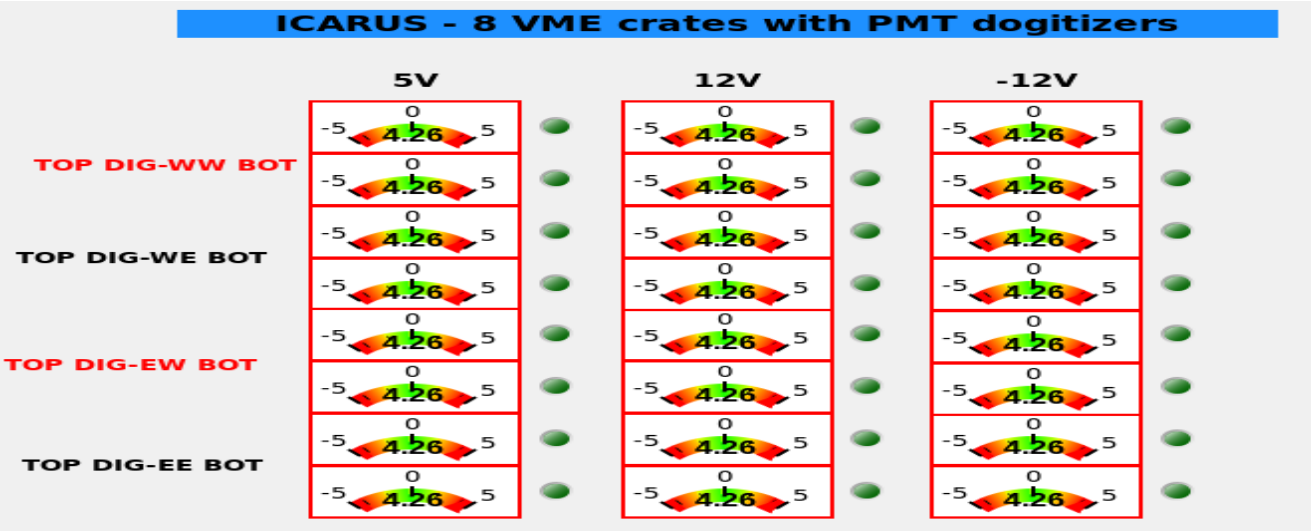

Fig 17c. Layout of level 2 : block 3

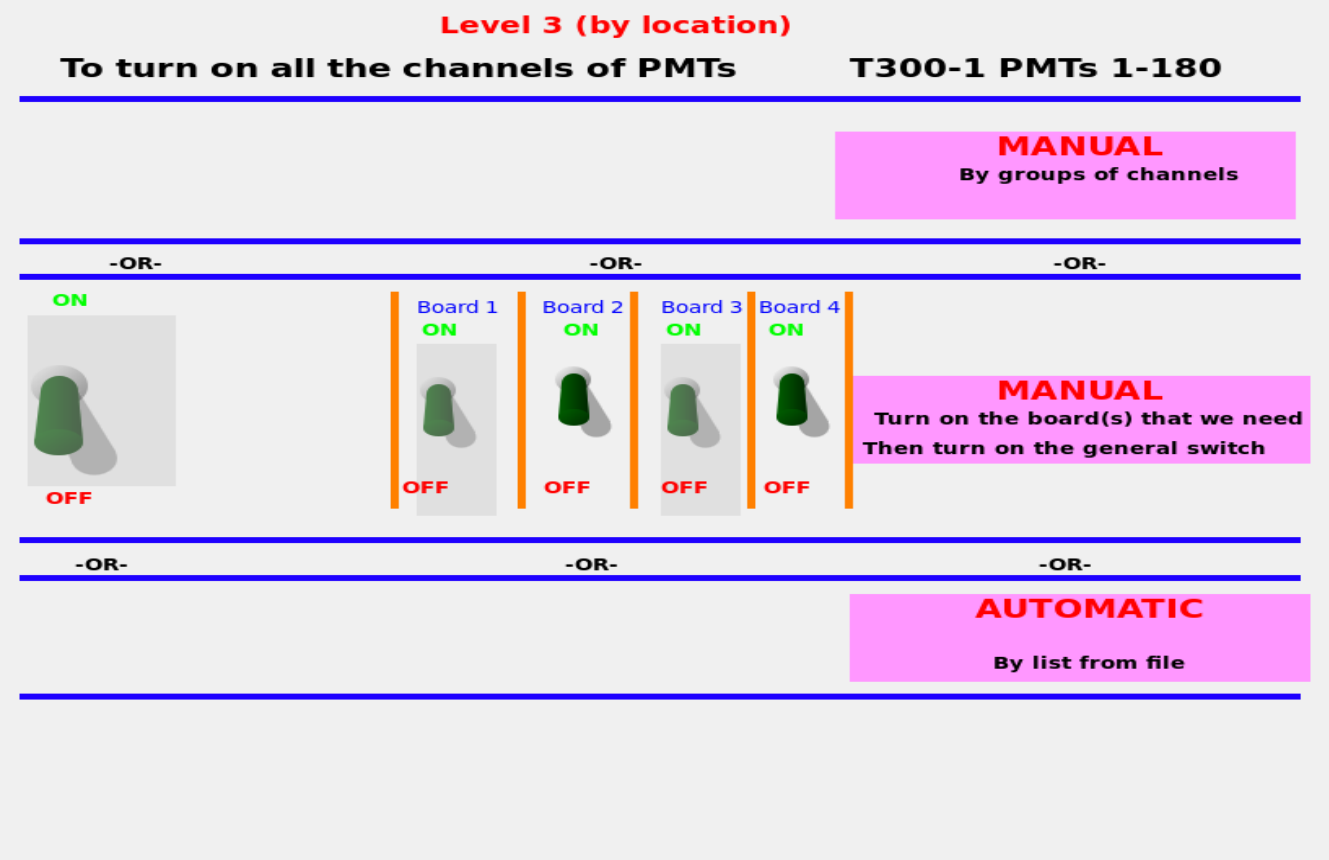

Fig 18a. Layout of level 3: block 1

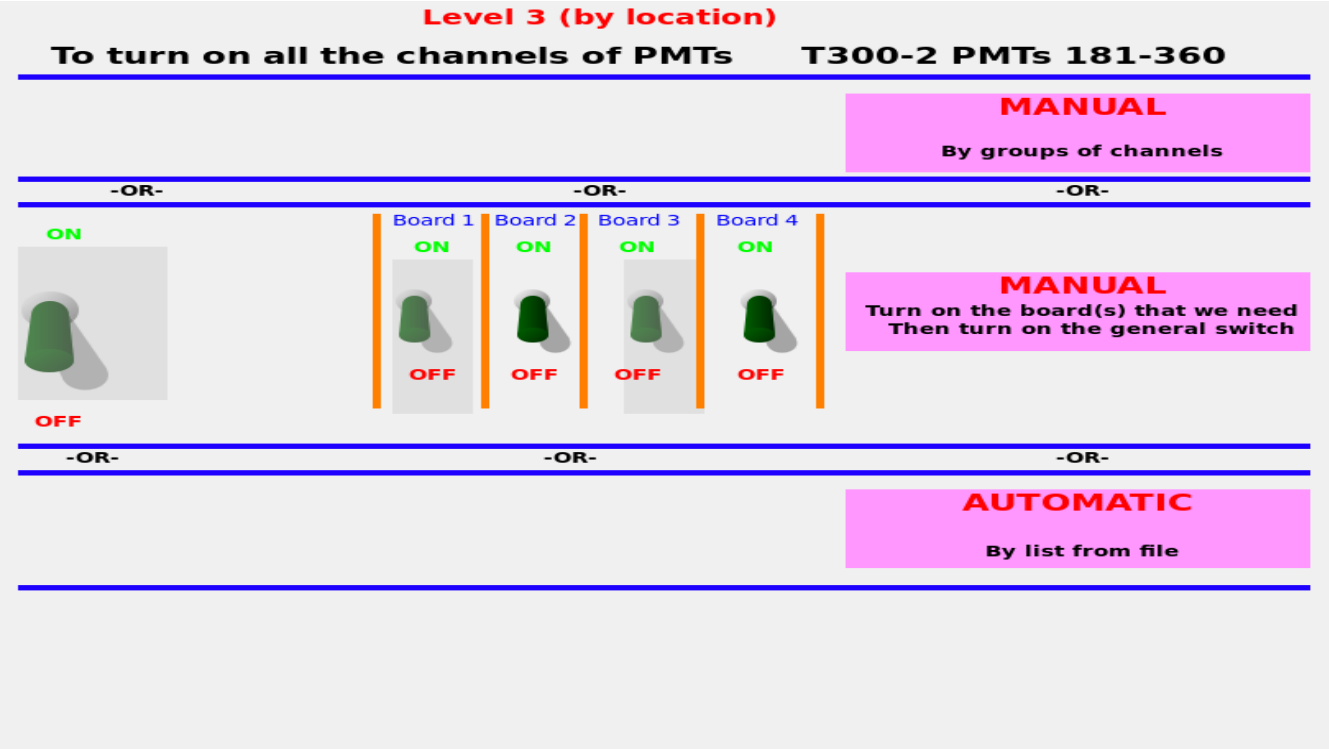

Fig 18b. Layout of level 3 : block 2

Fig 19a. Layout of level 4: block 1

Fig 19b. Layout of level 4. Block 2

The above figures (16 through 19b) are summarized in Fig 20.

ICARUS @ Fermilab
General View

Level 1

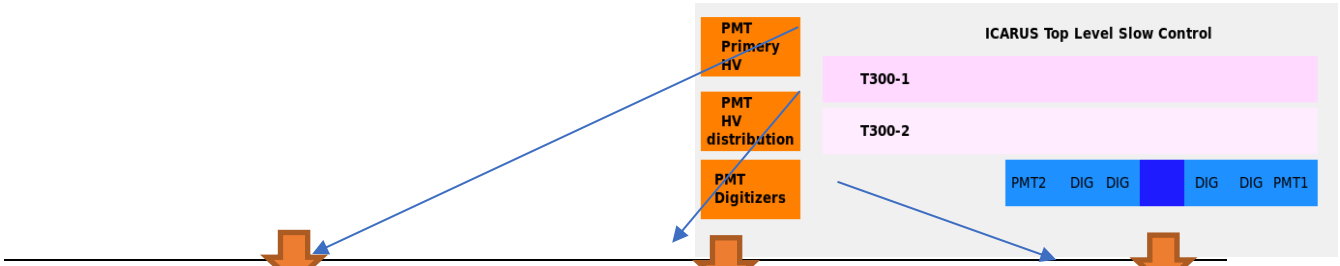

Level 2 **PMT Primary HV** **PMT HV distribution** **PMT digitizer**

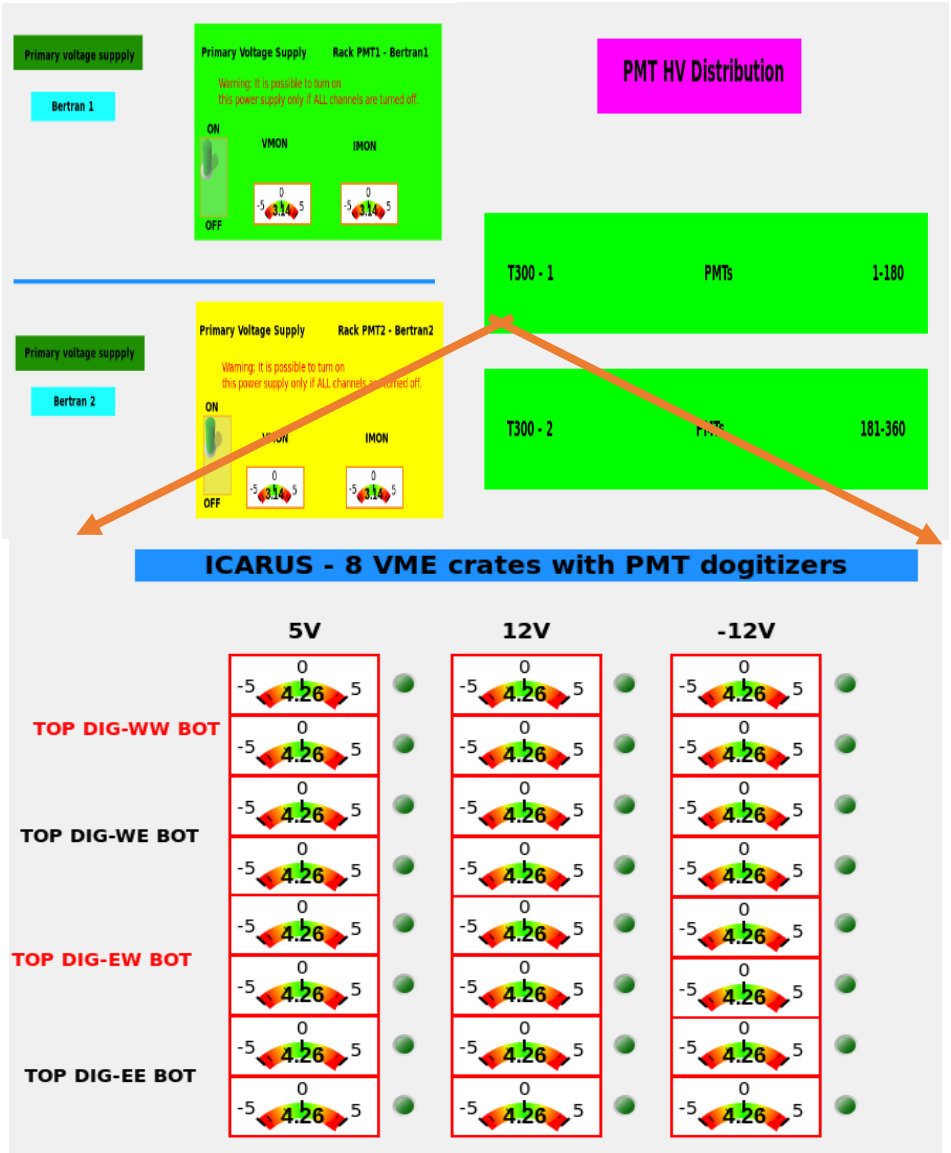

Level 3

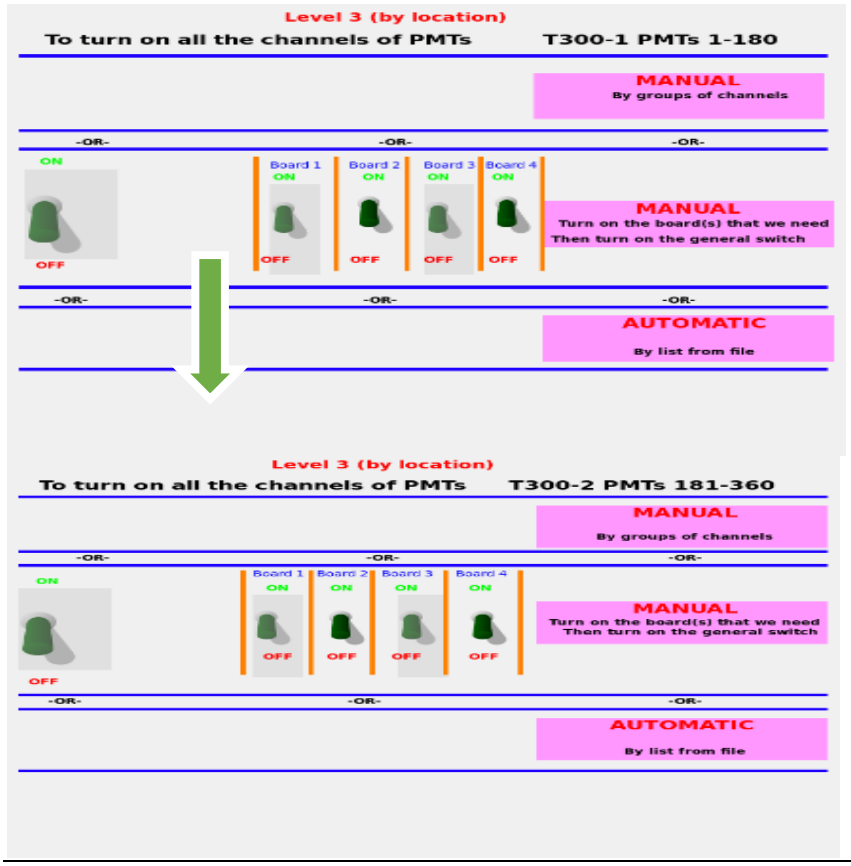

Level 4

Fig 20. Complete flowchart

4.5 Final diagnosis of status of PMT's

As already said, in the ICARUS experiment there exist 2 tanks, named T300-1 and T300-2 (ICARUS T600). As we know, there is a neutrino beam that enters inside the T600 apparatus. We can imagine looking at such apparatus from top. As shown in Fig 23, in each of this tank there are two sides full of PMT's. Each side contains 90 PMT's. The layouts in Fig. 24 show an improved layout. At the top level a new box was added for PMT Diagnostics. Clicking on this another layout is shown, with both cryostats and for each cryostat we have right and left side of T300-1 and the same for T300-2. Following designs are representative of distribution of PMT's in the structure. All the Boolean circles show PMT's. If the circle is green, the PMT is in the ON mode and if it is red, it is in OFF mode. With the shown layouts, we can see how many PMT's are OK and how many are not. Therefore, with such a configuration, we can control if PMT's are operative or not.

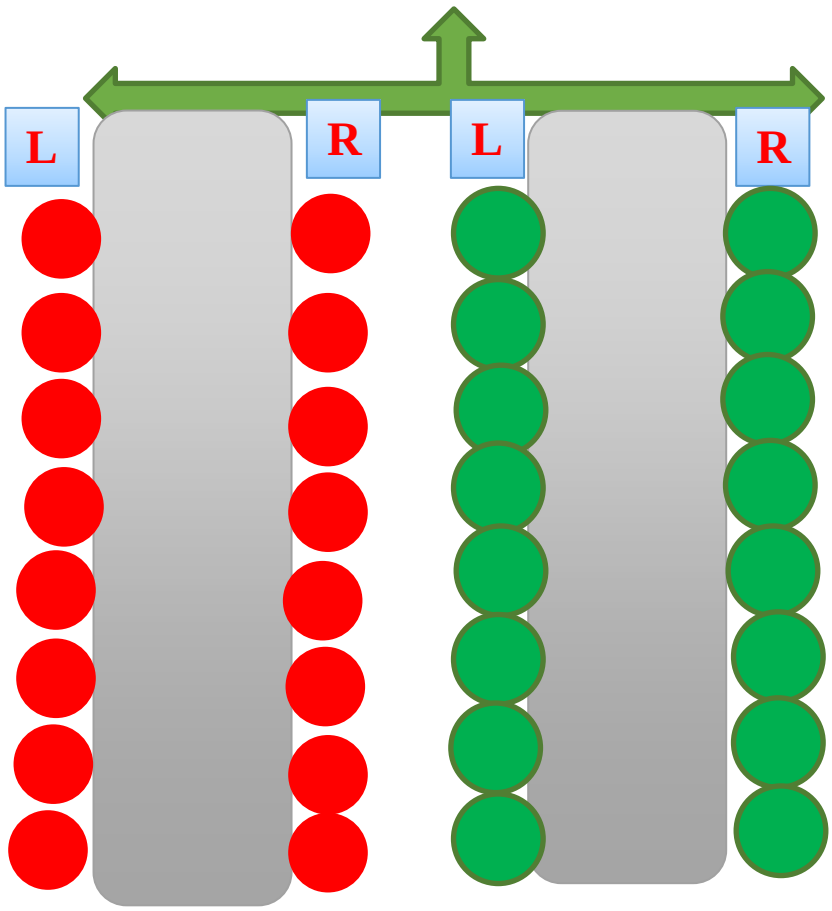

Fig21. Representation of PMT's

New Top Level with PMT Diagnostics key

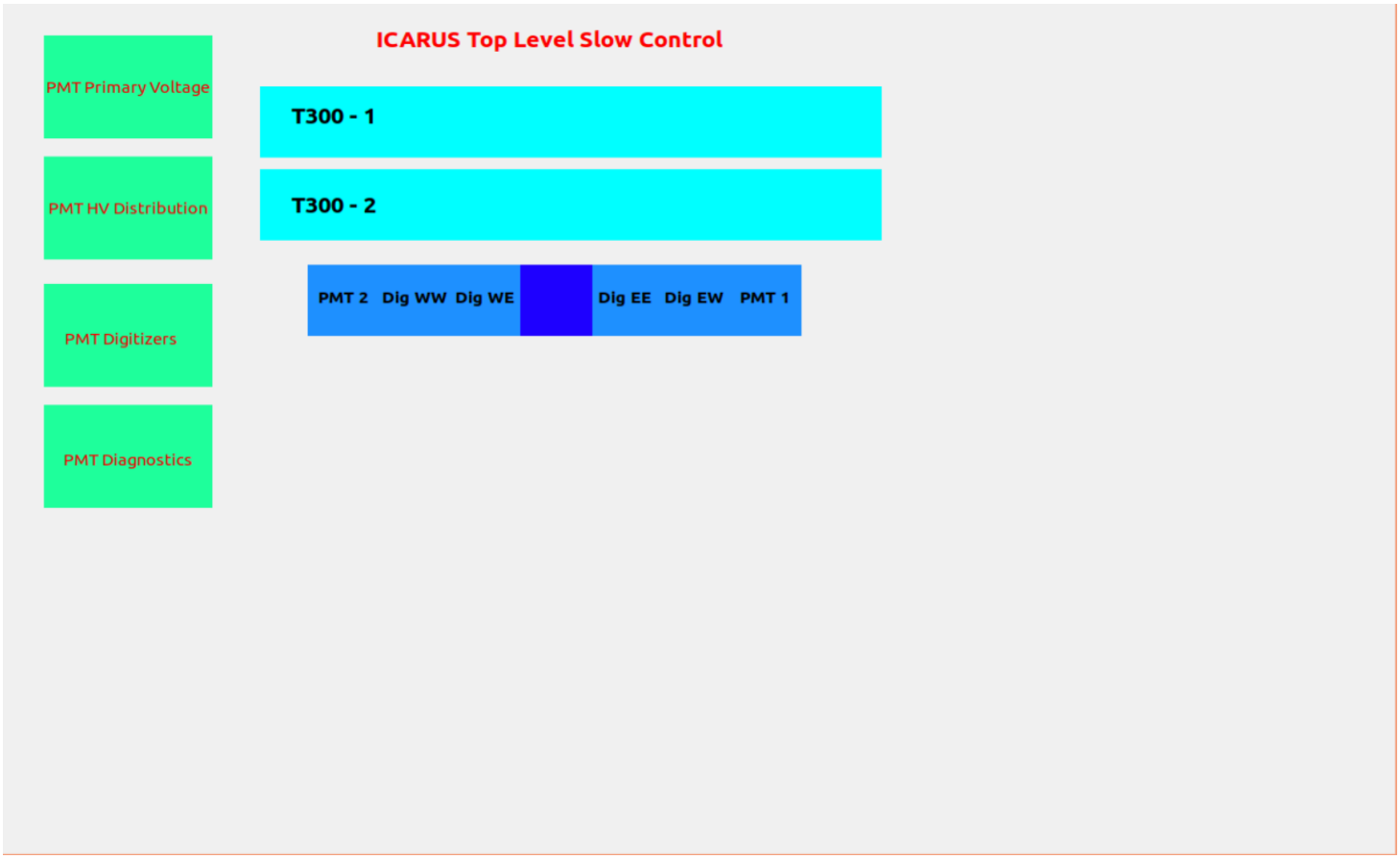

Second level layout from PMT Diagnostics


Diagnostic Side Views
T300 - 1
Left Side
Right Side
T300 - 2
Left Side
Right Side

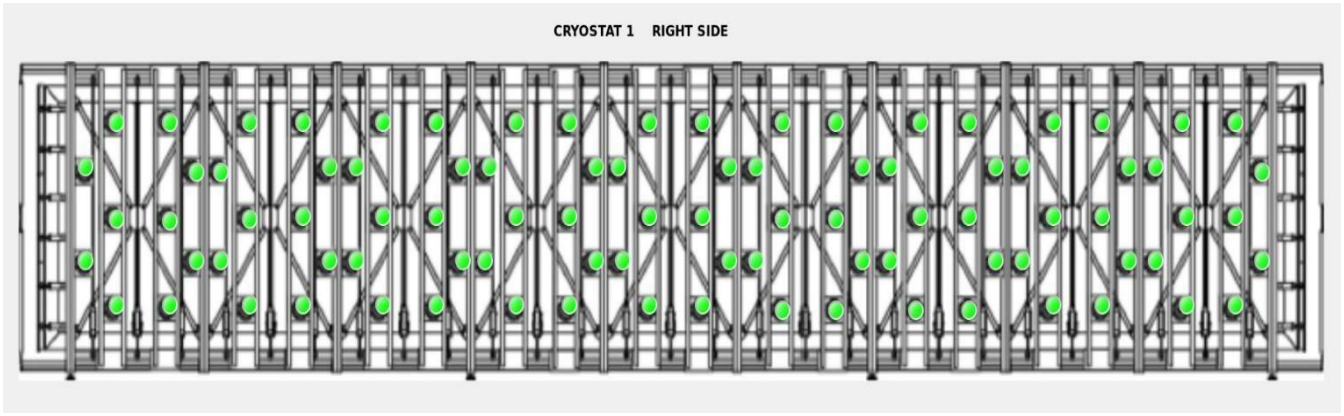
CRYOSTAT 1 RIGHT SIDE

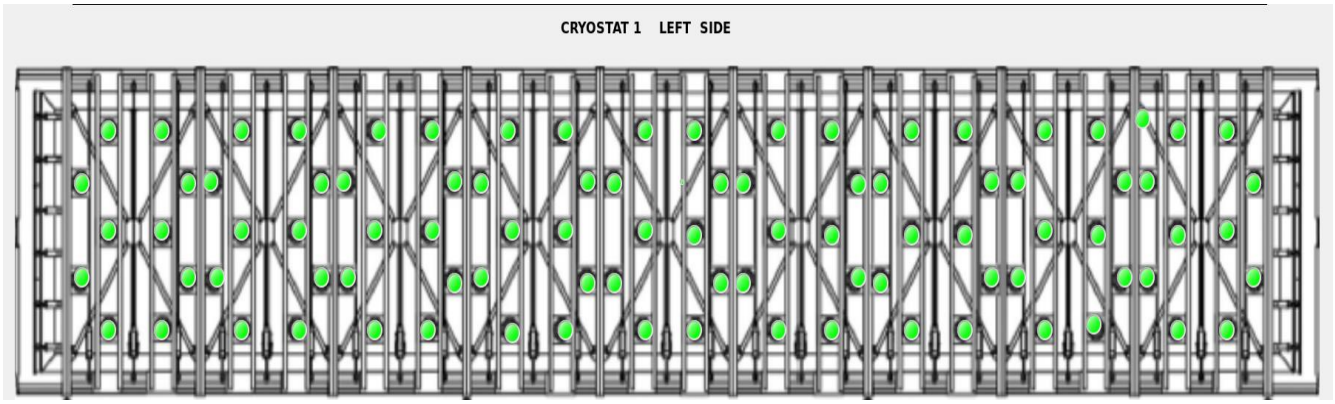
CRYOSTAT 1 LEFT SIDE

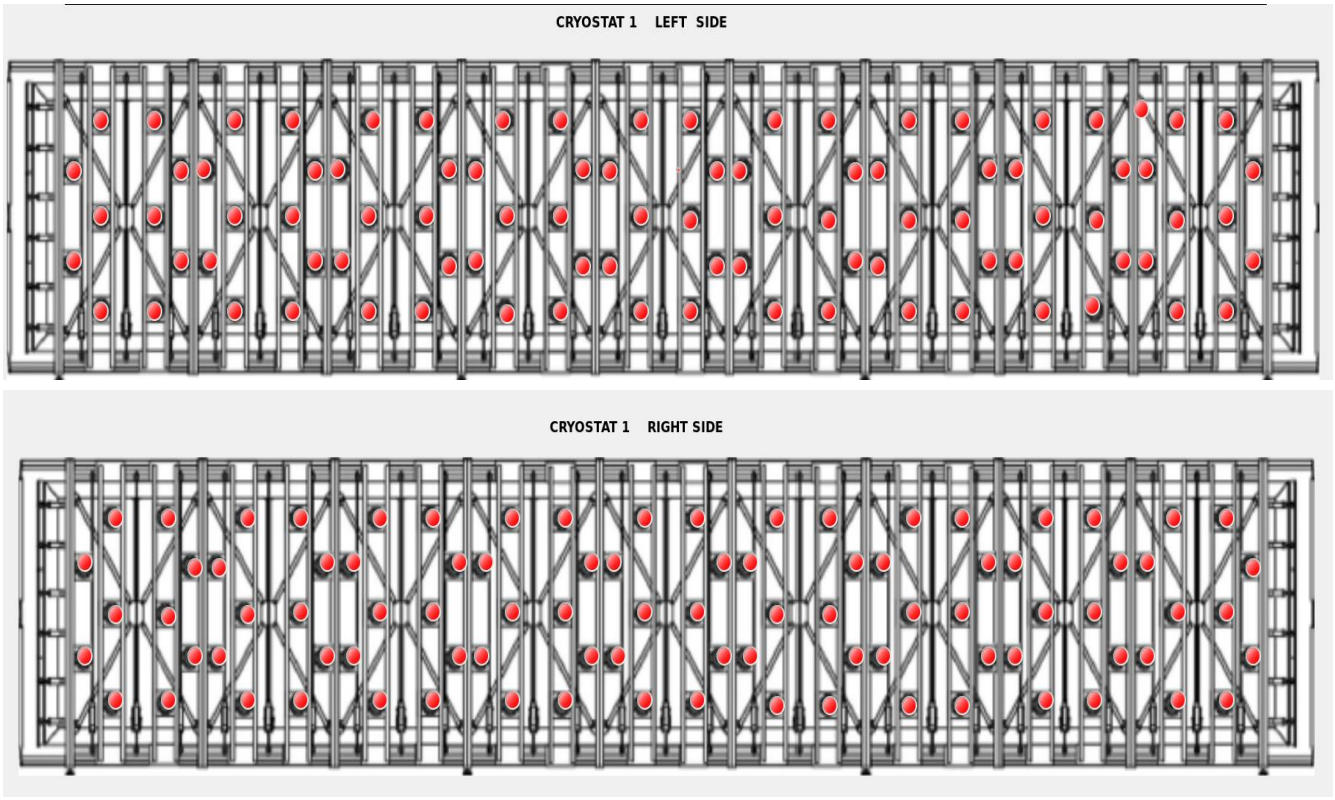

Fig22. General view of the two sides of cryostat 1, when PMT's are all turn on (green) or turn off (red)

The slow control tool proposed in this paragraph 4.5 by Catania group has been accepted by the collaboration and constitutes a further method of checking the functionality of all the PMT's of the Icarus apparatus.
In fact, when one or more PMT's may break down, the alarm system (which is not the subject of this thesis) and the consultation of the layouts (fig. 20) of the two PMT's groups (1-180 and 181-360) will allow to intervene in the best possible way as defined by the procedures of use and maintenance of the apparatus under the neutrino beam.
In such an event, consulting the "PMT diagnostics" layout will also allow to have a landscape view of the situation.
This can also be useful for a single PMT in failure, but it will be even more useful in the case of the simultaneous failure of several PMT's.
It is also necessary to consider that, apart from the malfunction of the single PMT, the unexpected disconnection of one or more cables or the failure of an entire board of power supply channels of the PMT's, could also occur.
When designing such a complex experimental apparatus, maintenance procedures must also be envisaged when unforeseen 'hardly predictable' events with different monitoring and even 'disaster recovery' techniques happen, not only in the IT sector but also in the mechanical and electronic one.

Should a cluster of PMT fail to function properly, researchers and operation personnel would be immediately notified of the presence of an area which is not affected by the transit of particles to be detected.
In view of these considerations, it is suggested that the collaboration needs keep in the control room always on a monitor, dedicated only to the layout of fig. 22, in such a way that the four sides of the two PMT, are visible and monitored 24 h a day.
This facility should be refined by inserting the possibility of positioning the cursor on each of the 360 colored Boolean dots, i.e. on each of the 360 PMT's, to see further information displayed such as exact position of any PMT on the single side of the single tank, according to the system of positioning chosen by the installers of the PMTs and all the others that the researchers should deem useful to request as the data taking will proceed.
However, this upgrade can only be finalized in the hall hosting the apparatus, because the required information to achieve it, are retrievable only in that location.

References for Chapter 4

[1] A. Barriuso Poy et al., The detector control system of the ATLAS experiment, JINST 3 (2008) P05006.

[2] E. Aprile et al. (XENON100), The distributed Slow Control System of the XENON100 Experiment,
JINST 7 (2012) T12001.

[3] J. H. Choi et al. (RENO), Slow Control Systems of the Reactor Experiment for Neutrino Oscillation, Nucl. Instrum. Meth. A 810 (2016) 100.

[4] http://www.aps.anl.gov/epics/index.php

[5] https://www.ill.eu/instruments-support/instrument-control/software/nomad/

[6] http://midas.psi.ch

[7] J. Frederick Bartlet et al., The Control architecture of the D0 experiment, eConf C011127 (2001)
TUCT005.

[8] P. Paolucci et al., The IFR online detector control at the BaBar experiment at SLAC, Nucl. Instr. Meth. A 456 (2000) 137.

[9] J. Adam et al. (MEG), The MEG detector for $\mu^+ \to e^+\gamma$ decay search, Eur. Phys. J. C73 (2013) 2365.

[10] https://bitbucket.org/Doberman_slowcontrol/

Summary

The new scintillation light detection system for the ICARUS T600 LAr-TPC, realized for its operation at Fermilab in the context of the SBN program, includes the use of 360 large area Hamamatsu R5912-MOD PMT's, mounted behind the TPC wire planes and a fast-laser calibration system. The high performance of this detection system in terms of sensitivity, granularity and time resolution, together with the Cosmic Ray Tagger detector, will allow ICARUS to cope with the large cosmic ray background, by identifying the events associated with the neutrino beam. The incoming Cosmic Ray flow will be reduced by a 2.85 m concrete roof, built on the top of the CRT apparatus. To this purpose all the ICARUS detectors have been extensively simulated, their components precisely characterized and the installation procedures and techniques carefully defined.

To get a better understanding of the ICARUS PMT's operation, a sample of 10 PMT's has been tested at CERN, using an alpha source as a trigger for data acquisition. This system has been placed inside a dewar, containing Liquid Argon (LAr) for the sake of evaluating light speed in such a medium. The distance between the PMT's and the source was variable. The alpha source has been housed under the PMT's. Triggering was accomplished by means of Silicon Photomultiplier (SiPM), whose signals were also recorded, together with the PMT's for several different distances. Some important properties such as area, t_0, amplitude of the signals have been investigated through the data analysis. Moreover, the delay measurement has been performed between the PMT's signal (far from the alpha source) and SiPM signal (near the alpha source) as the fundamental criterion for light speed evaluation inside Lar.

Preliminary tests carried out after transport and installation of the ICARUS apparatus at Fermilab verified the performances of the light detection system required for the identification of signals related to neutrino beam induced events.

Furthermore, work on the ICARUS operation has been done and completed for its slow control from two points of view, namely by location and functionality. By location, the exact place of the apparatus is important and by functionality, the performance of the apparatus is important. The work considered for both methods and the related layouts in different levels were represented. Also, by taking advantage of EPICS (a software package which plays a crucial role in slow control activities) some commands have been defined, as well as some

variables and their final tests through different commands were achieved successfully and obtained eye catching results. Finally, these algorithms were shown using the CSS package. In the last section a general view of the sides of two cryostats were represented to complete the diagnosis of all the PMT's. Some perspective on how using this CSS package has been given as a conclusion of my work on "slow control".

APPENDIX (1)

As aforesaid in this part some more plots will be represented regarding data analysis.

SiPM signal shapes for

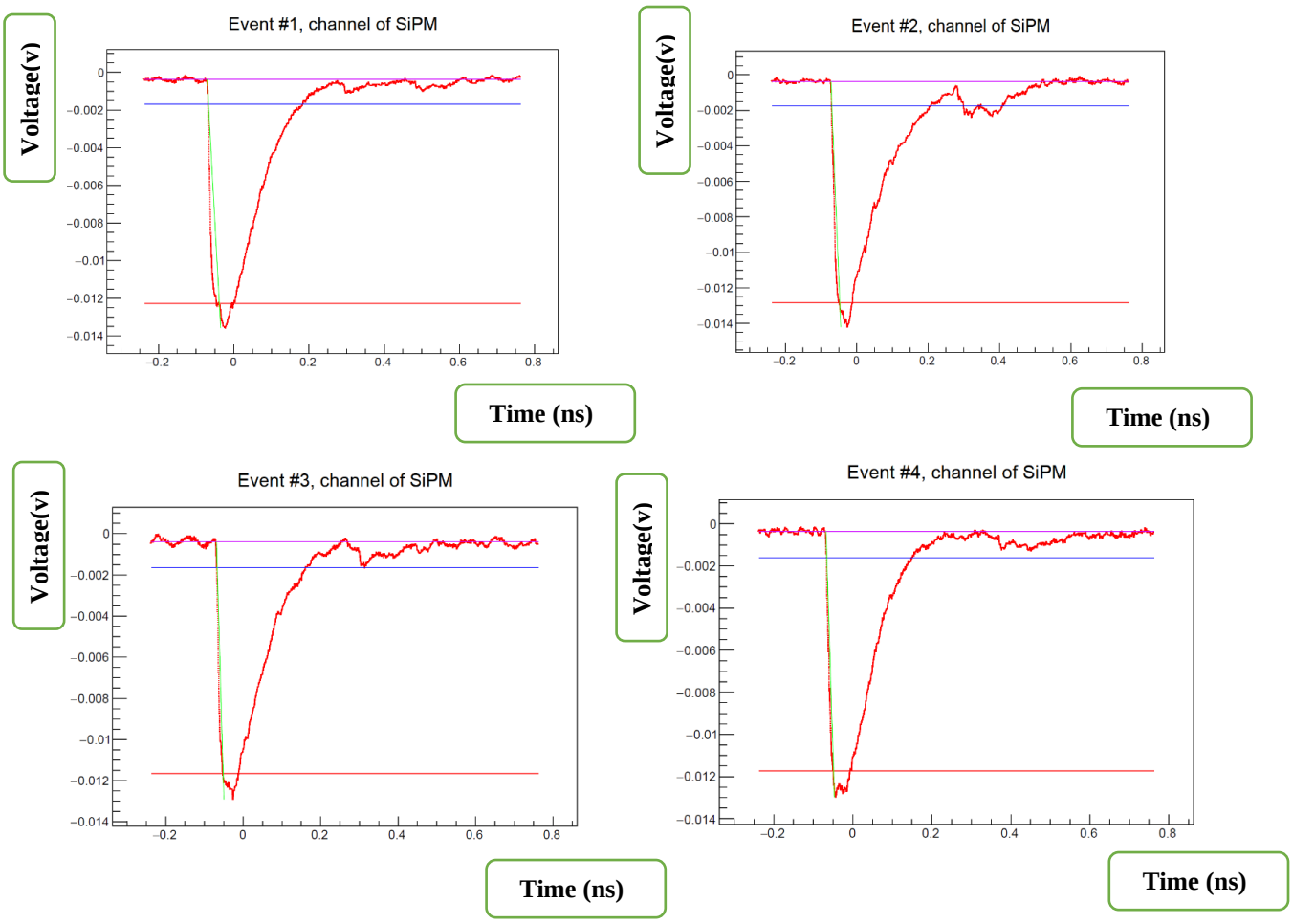

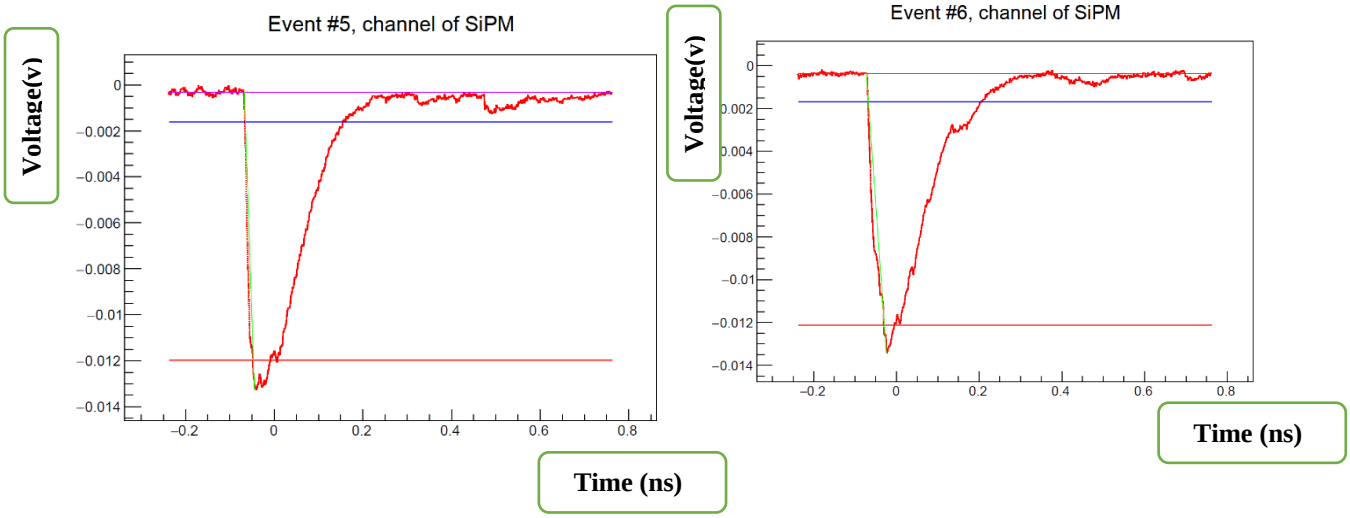
Event #5, channel of SiPM
Voltage(v)
Time (ns)
Event #6, channel of SiPM
Voltage(v)
Time (ns)

PMT signal shapes for

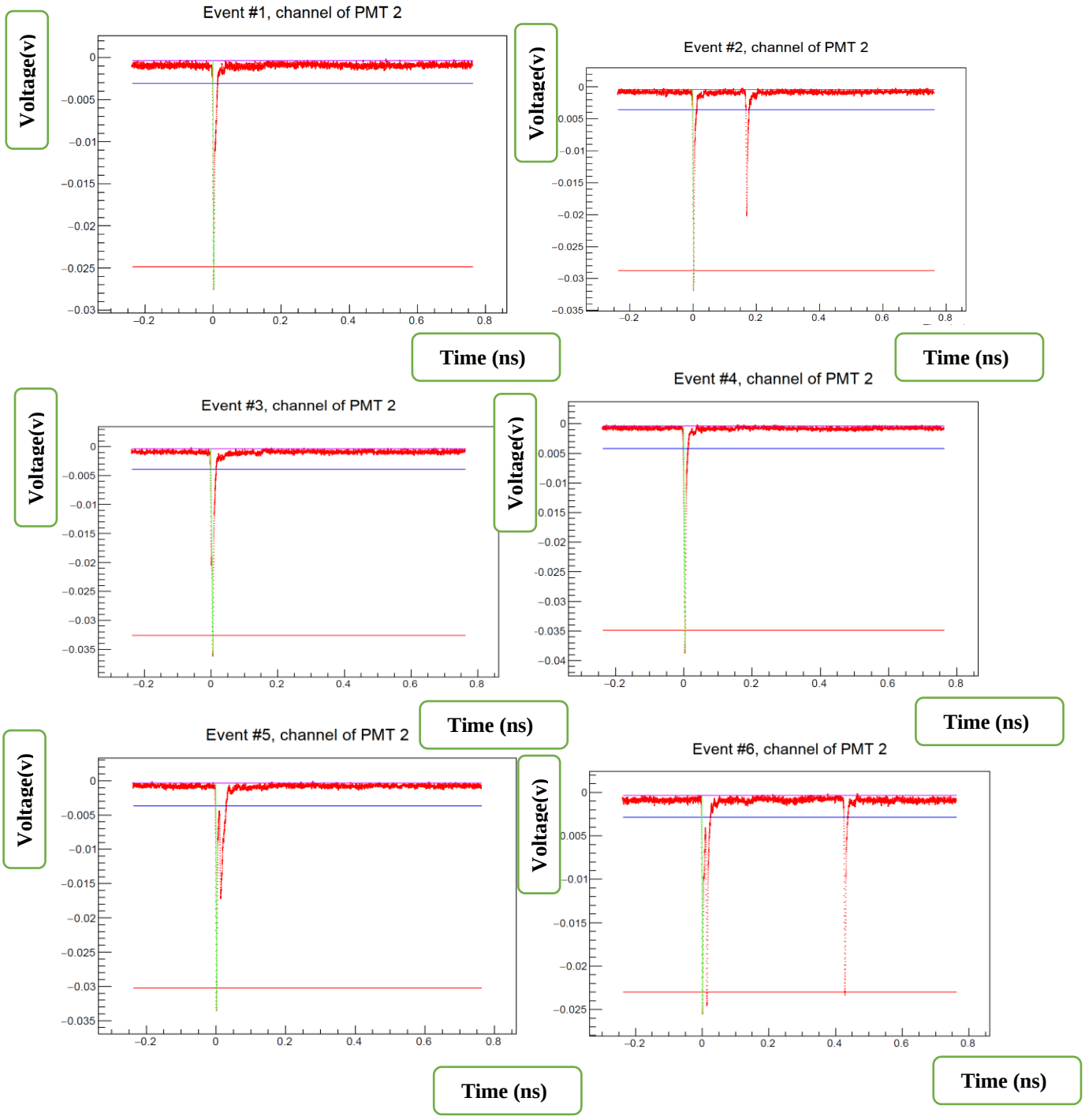

SiPM signal shapes for

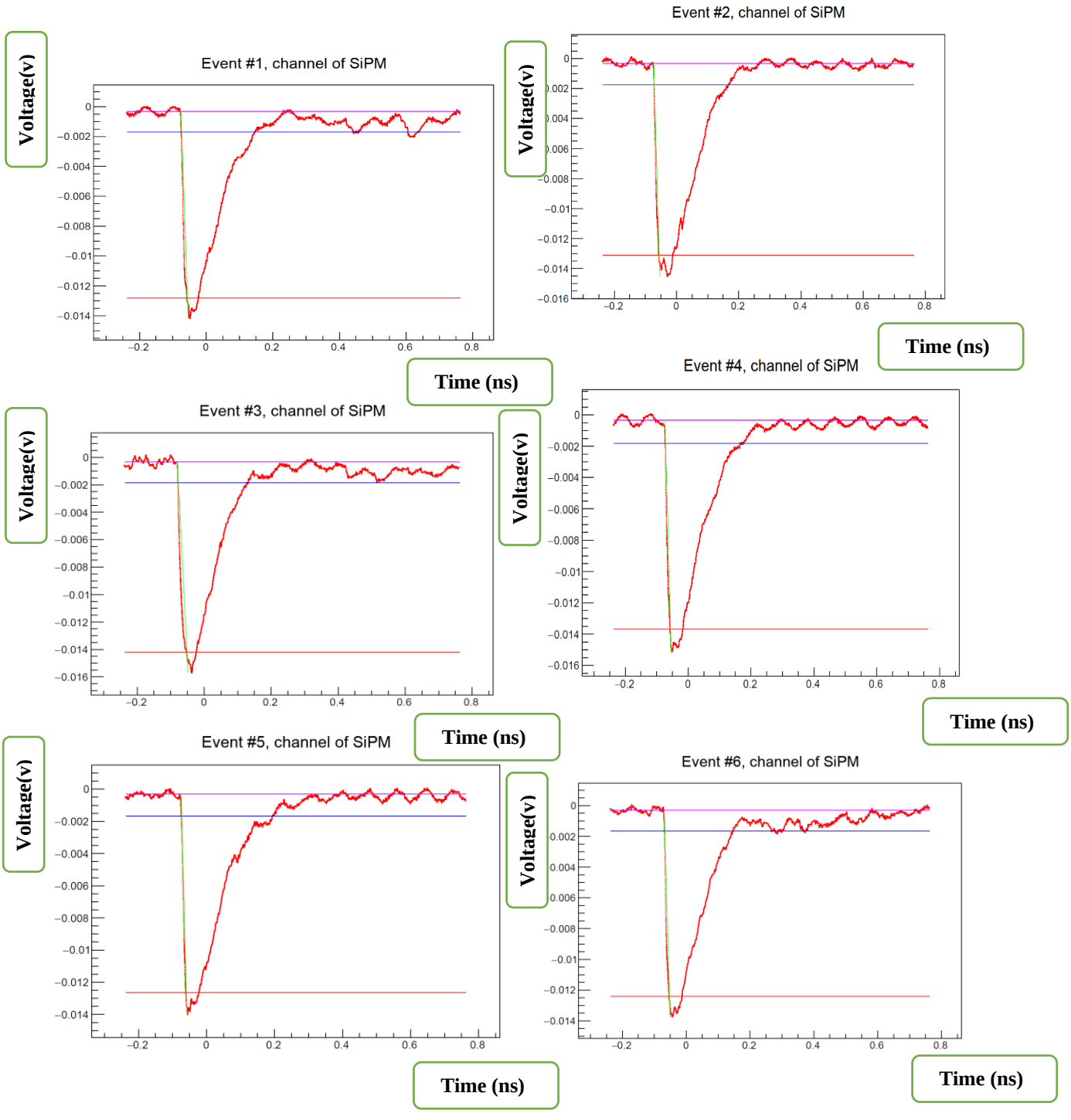

PMT signal shapes for reading

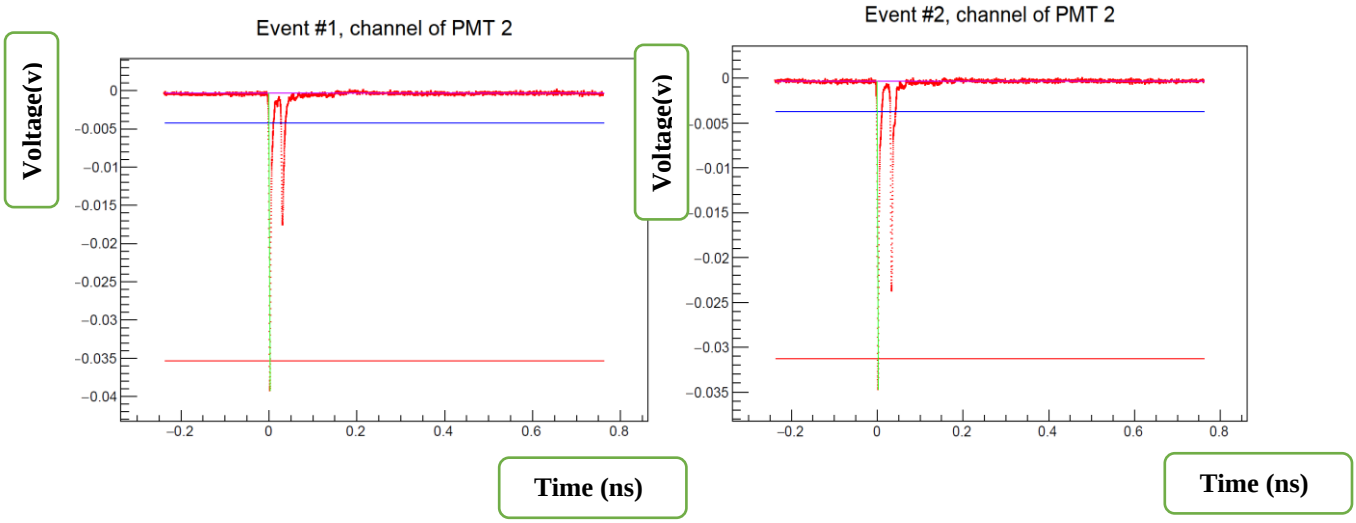

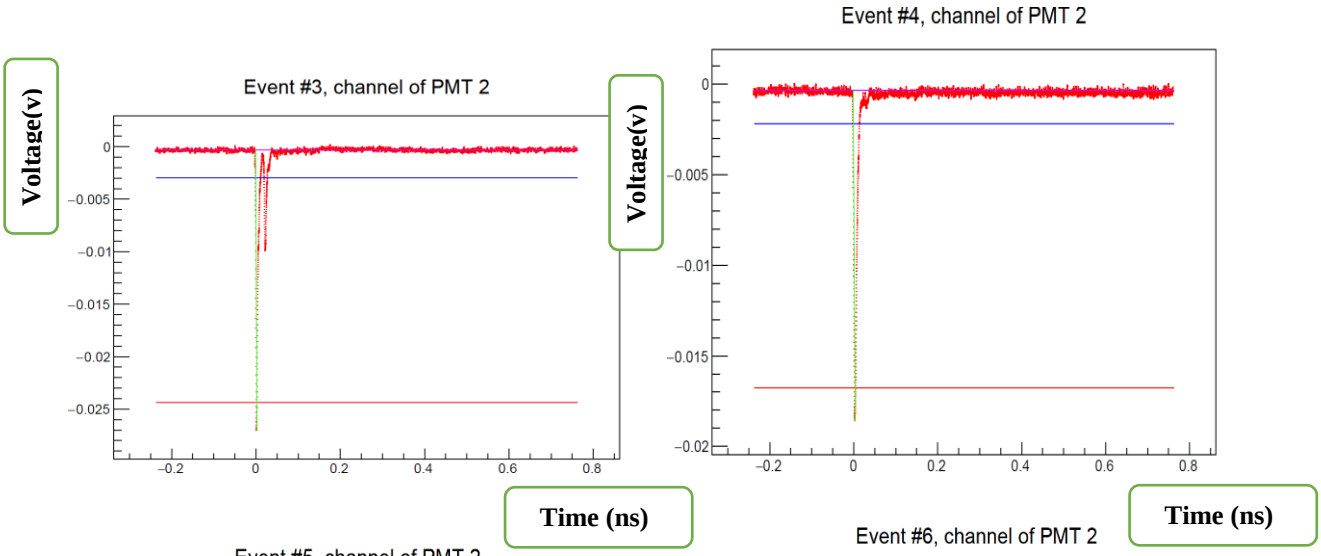

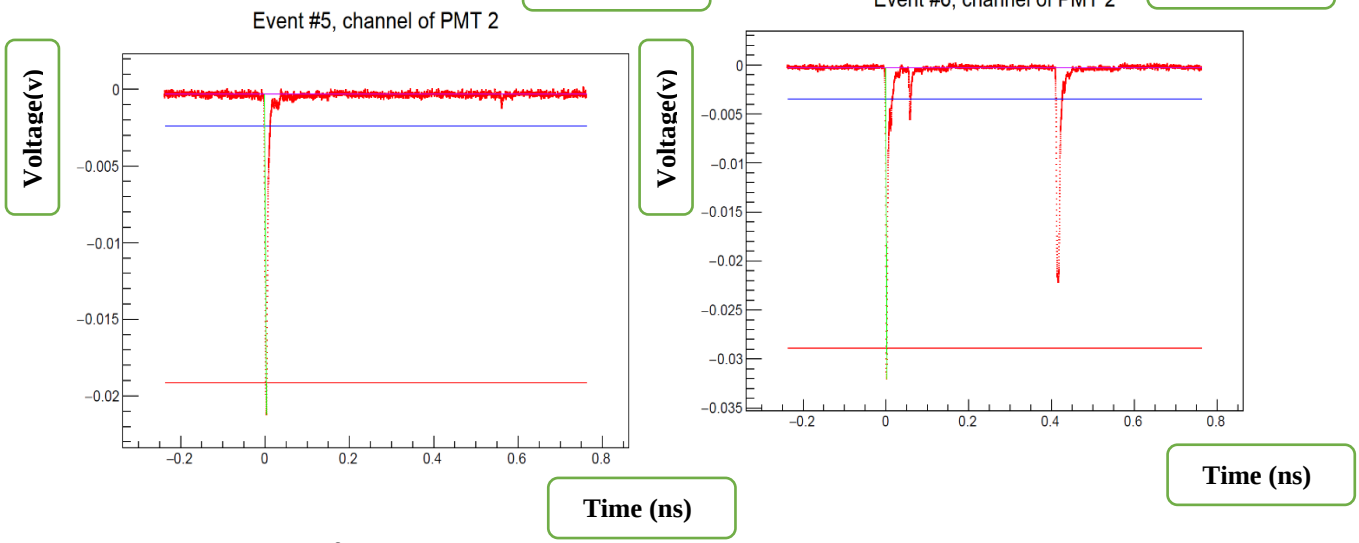

Here the analysis of the reading 400 has been shown.

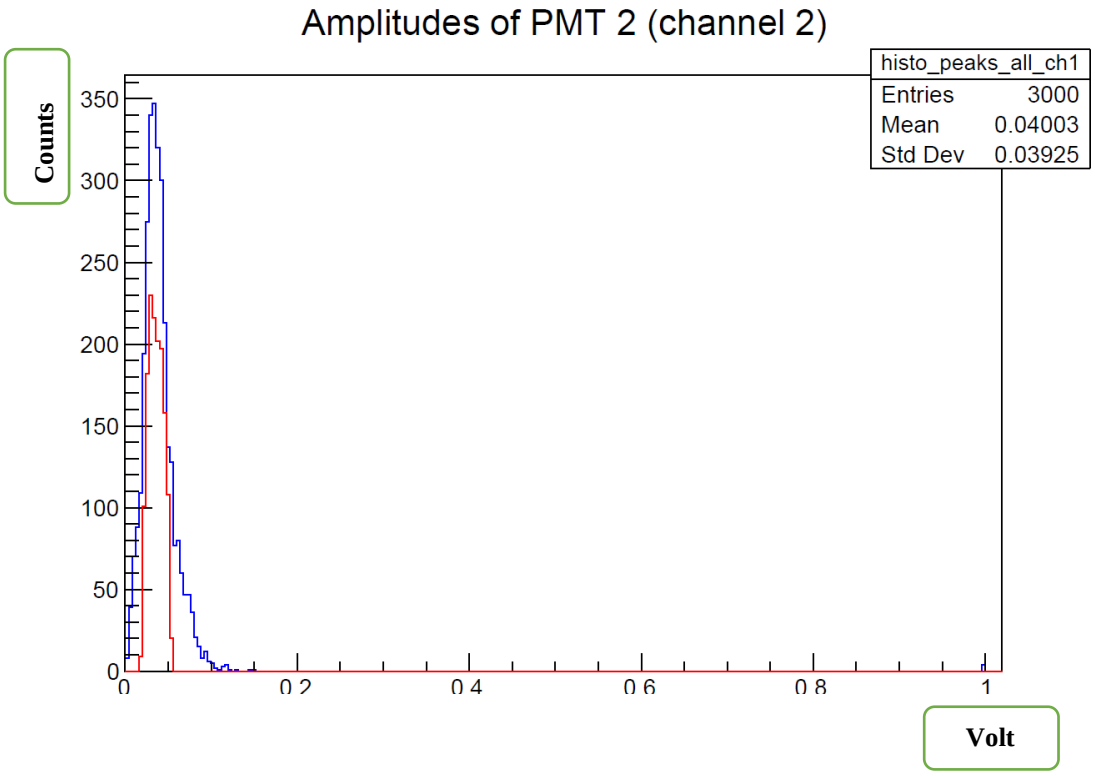
Amplitudes of PMT 2 (channel 2)
histo_peaks_all_ch1
Entries 3000
Mean 0.04003
Std Dev 0.03925
Counts
Volt
0
50
100
150
200
250
300
350
0.2
0.4
0.6
0.8
1

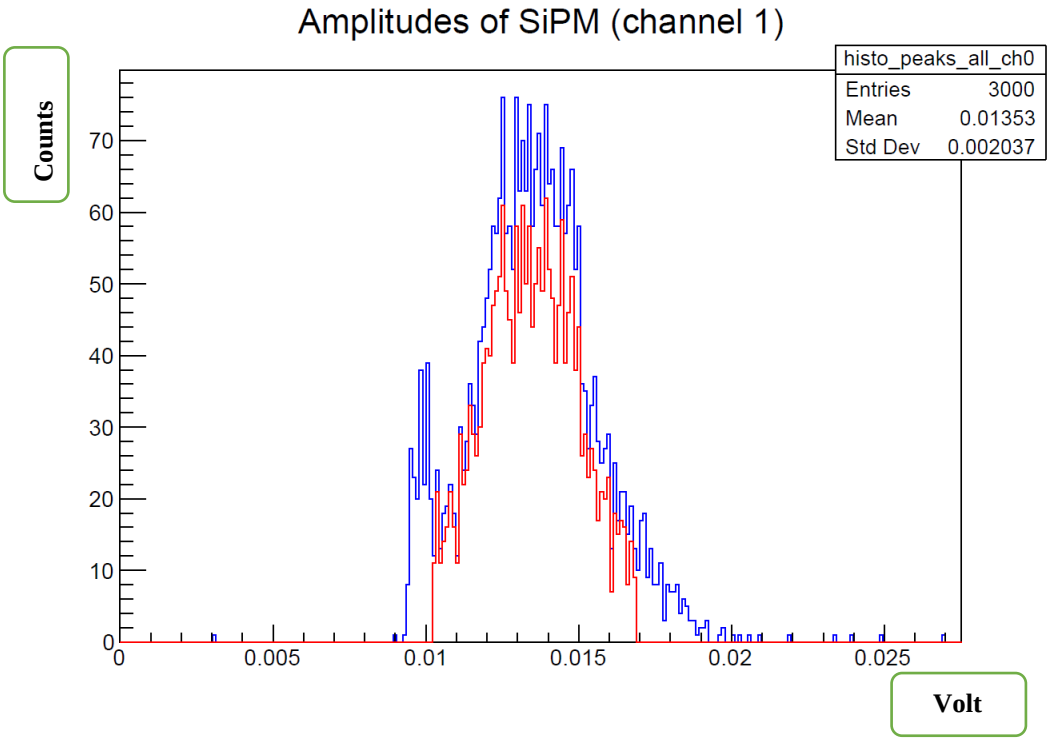
Amplitudes of SiPM (channel 1)
histo_peaks_all_ch0
Entries 3000
Mean 0.01353
Std Dev 0.002037
Counts
Volt
0
10
20
30
40
50
60
70
0.005
0.01
0.015
0.02
0.025

Area vs peak amplitude

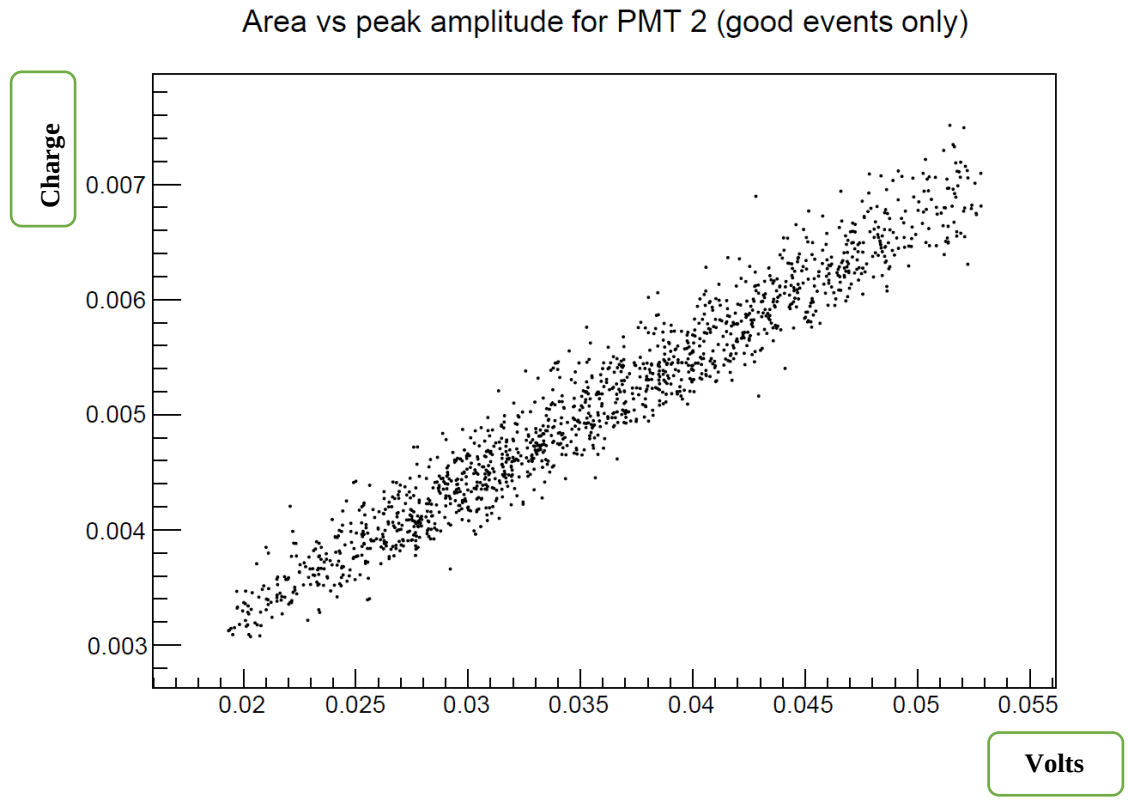

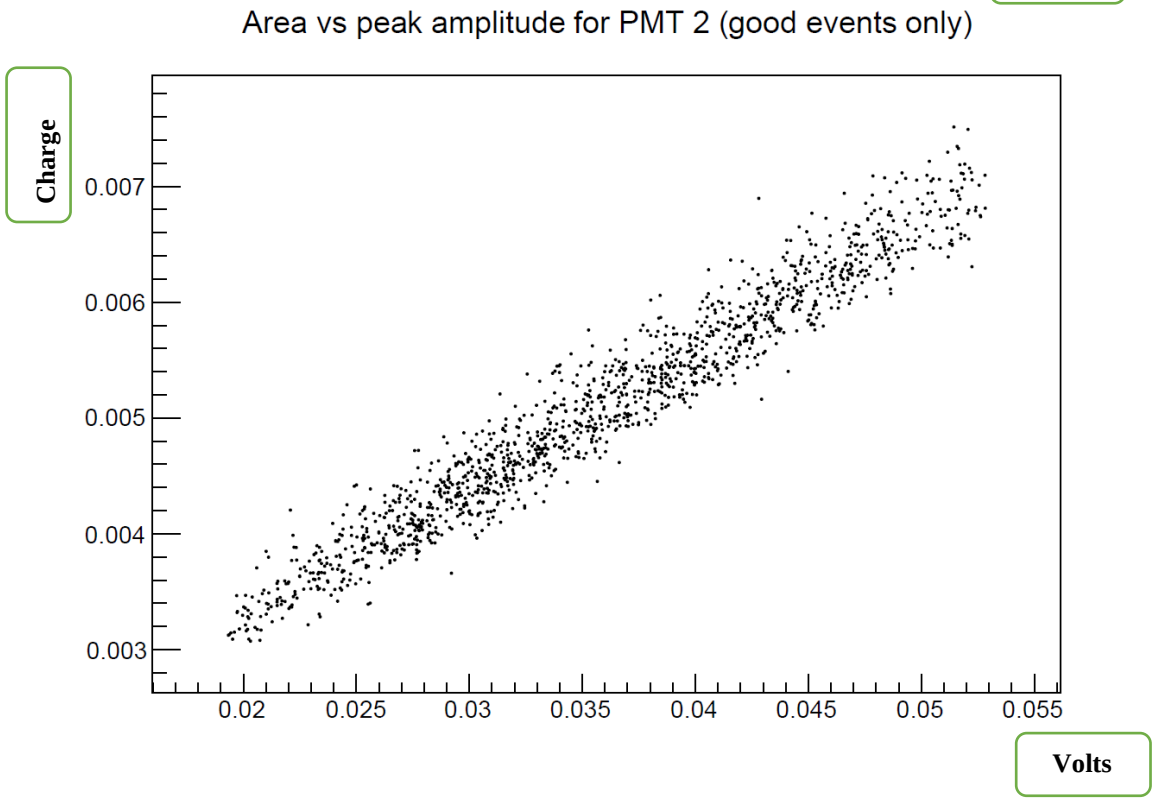

t0

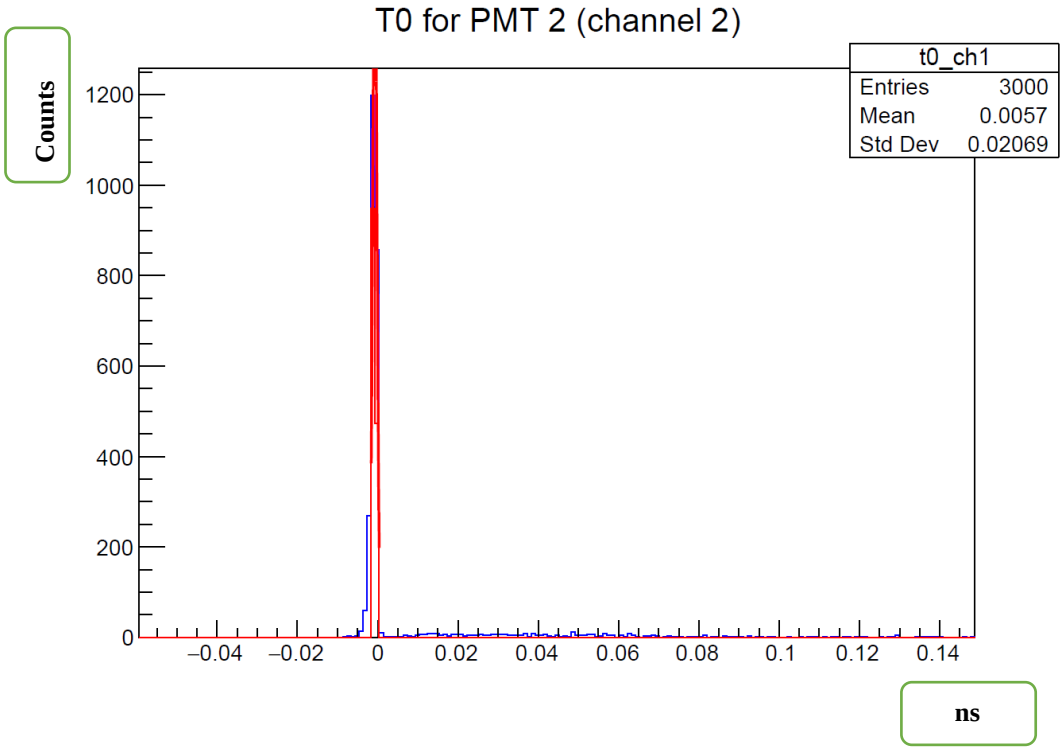
T0 for PMT 2 (channel 2)
Counts
t0_ch1
Entries 3000
Mean 0.0057
Std Dev 0.02069
1200
1000
800
600
400
200
0
−0.04
−0.02
0
0.02
0.04
0.06
0.08
0.1
0.12
0.14
ns

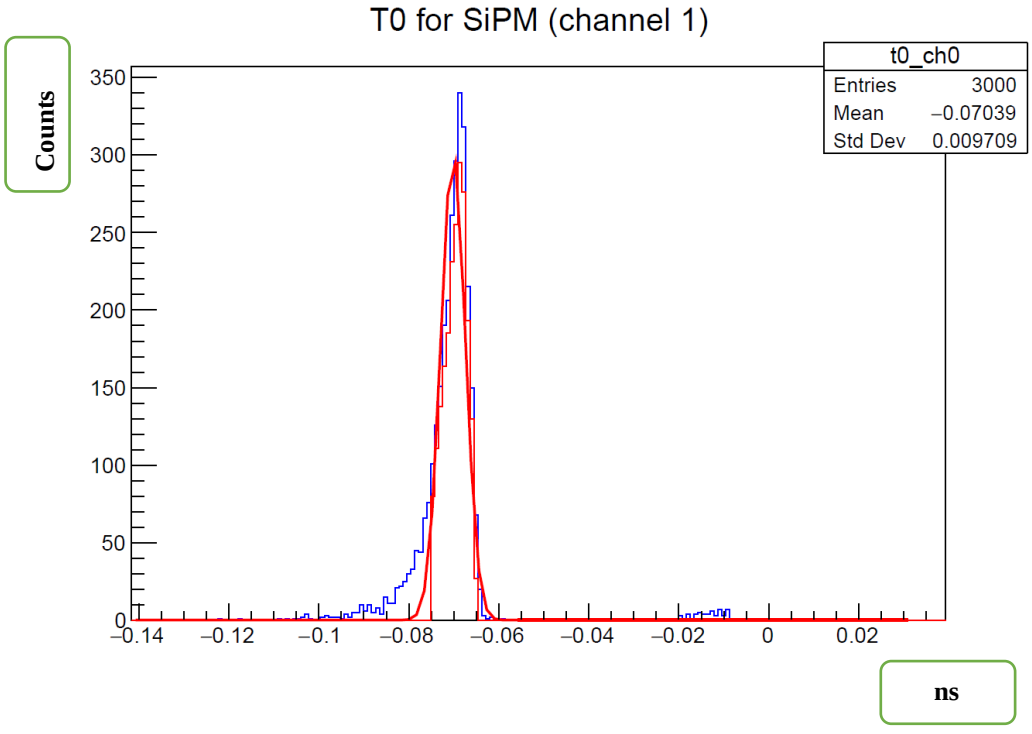
T0 for SiPM (channel 1)
Counts
t0_ch0
Entries 3000
Mean −0.07039
Std Dev 0.009709
350
300
250
200
150
100
50
0
−0.14
−0.12
−0.1
−0.08
−0.06
−0.04
−0.02
0
0.02
ns

Here the analysis of the reading 800 have been presented.

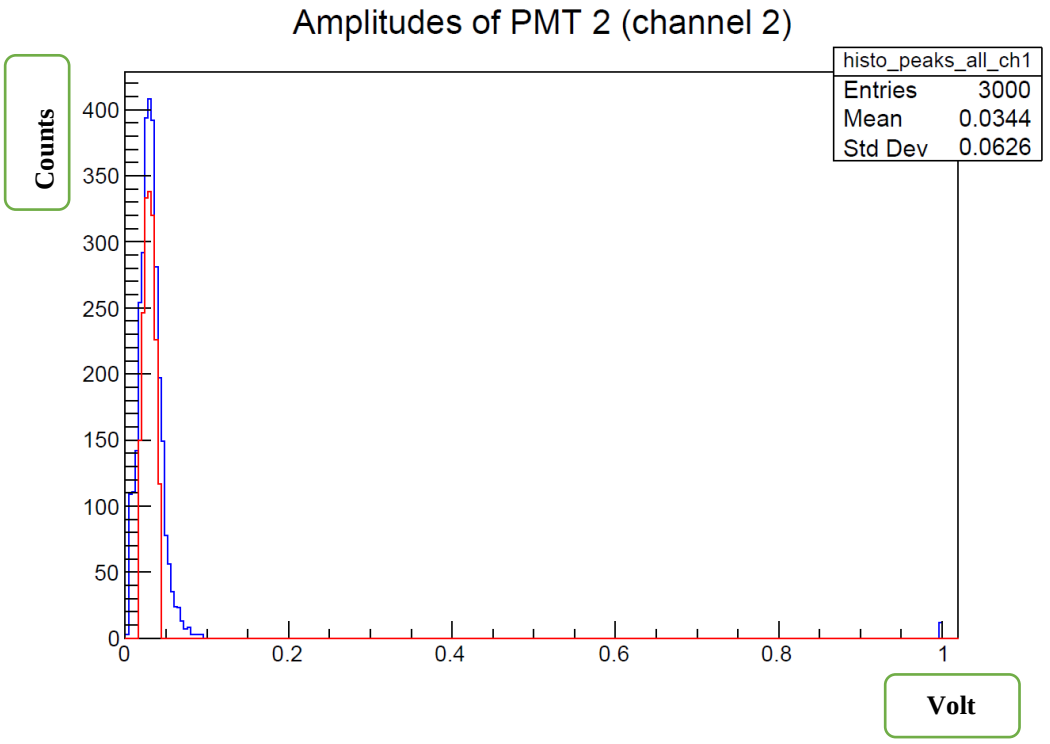

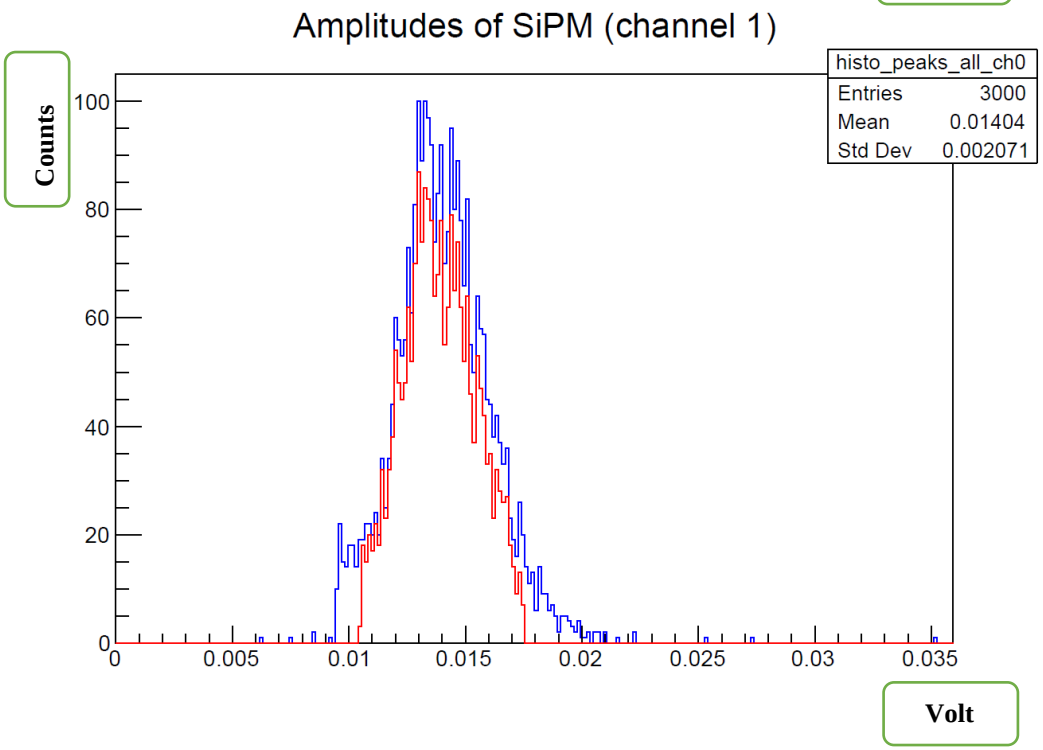

Area vs peak

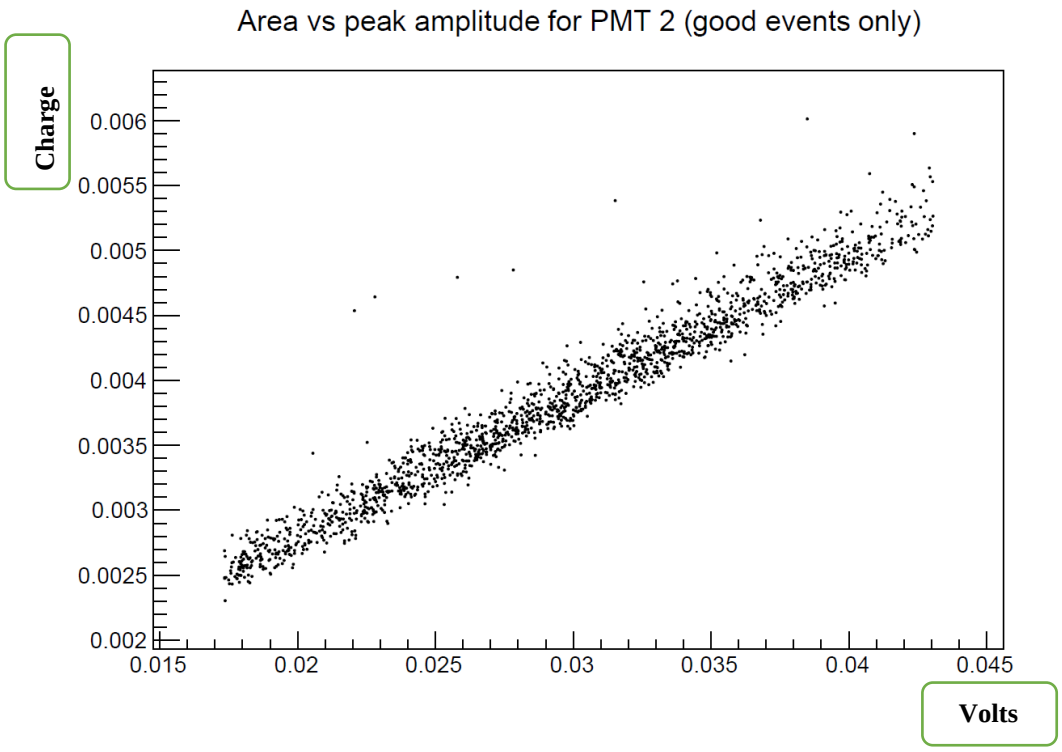
Area vs peak amplitude for PMT 2 (good events only)
Charge
0.006
0.0055
0.005
0.0045
0.004
0.0035
0.003
0.0025
0.002
0.015
0.02
0.025
0.03
0.035
0.04
0.045
Volts

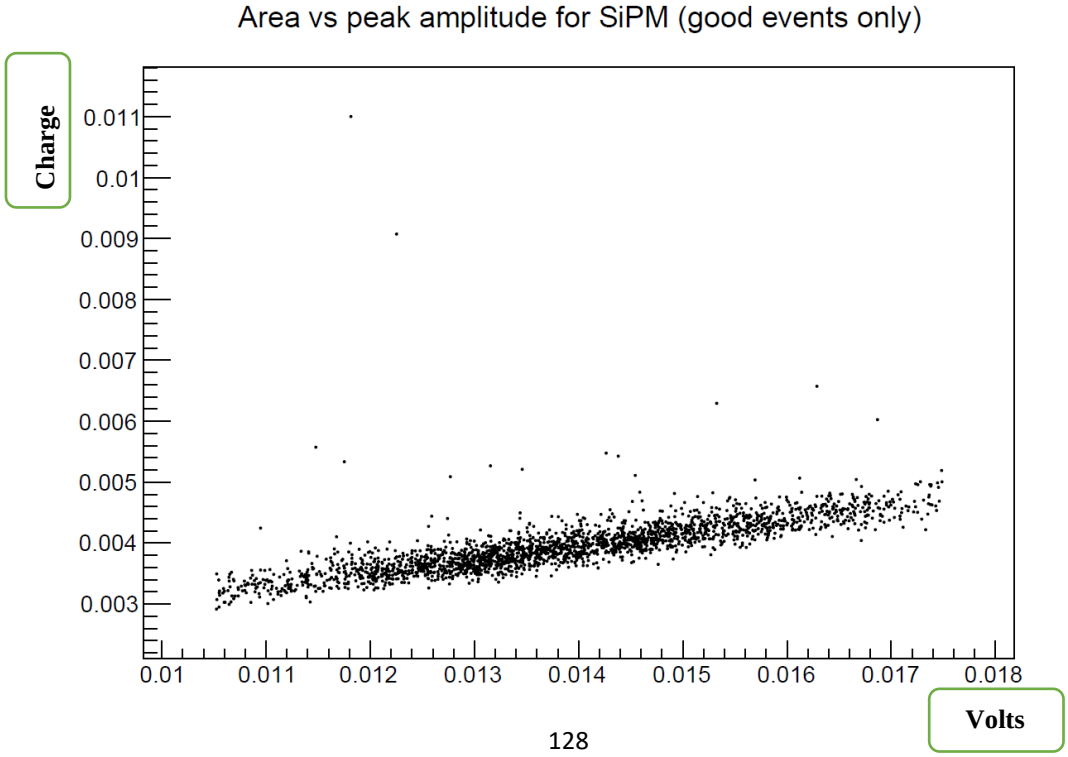
Area vs peak amplitude for SiPM (good events only)
Charge
0.011
0.01
0.009
0.008
0.007
0.006
0.005
0.004
0.003
0.01
0.011
0.012
0.013
0.014
0.015
0.016
0.017
0.018
Volts

t_0

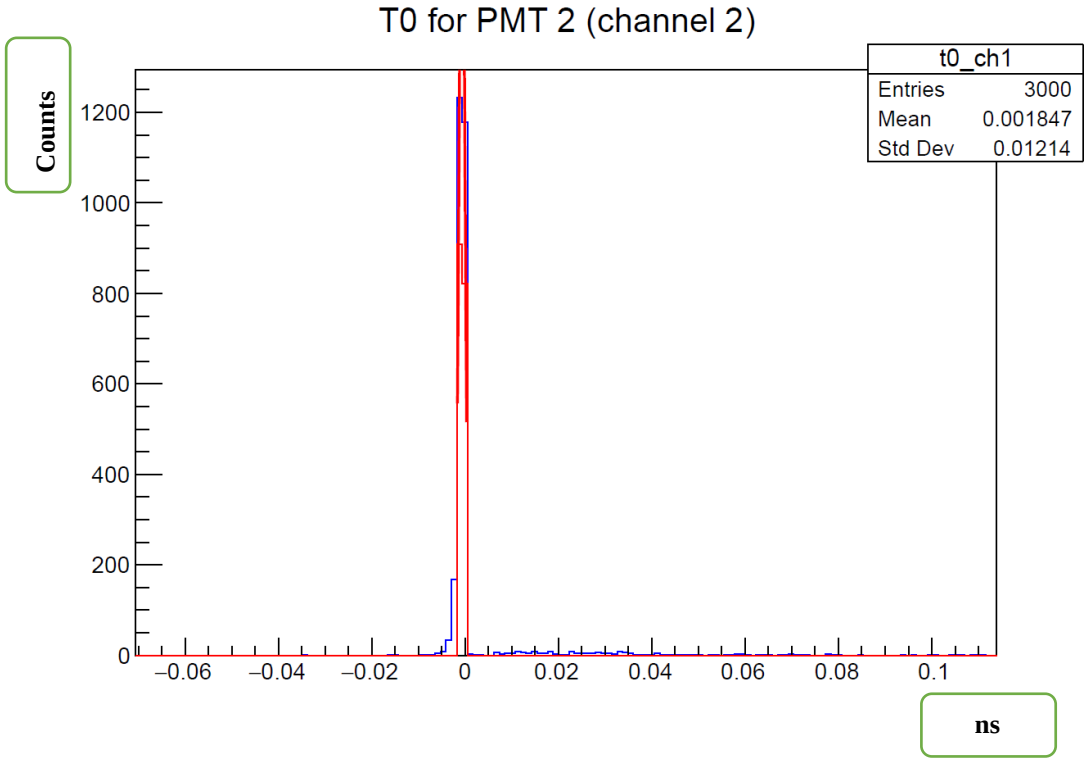
T0 for PMT 2 (channel 2)
t0_ch1
Entries 3000
Mean 0.001847
Std Dev 0.01214
Counts
ns

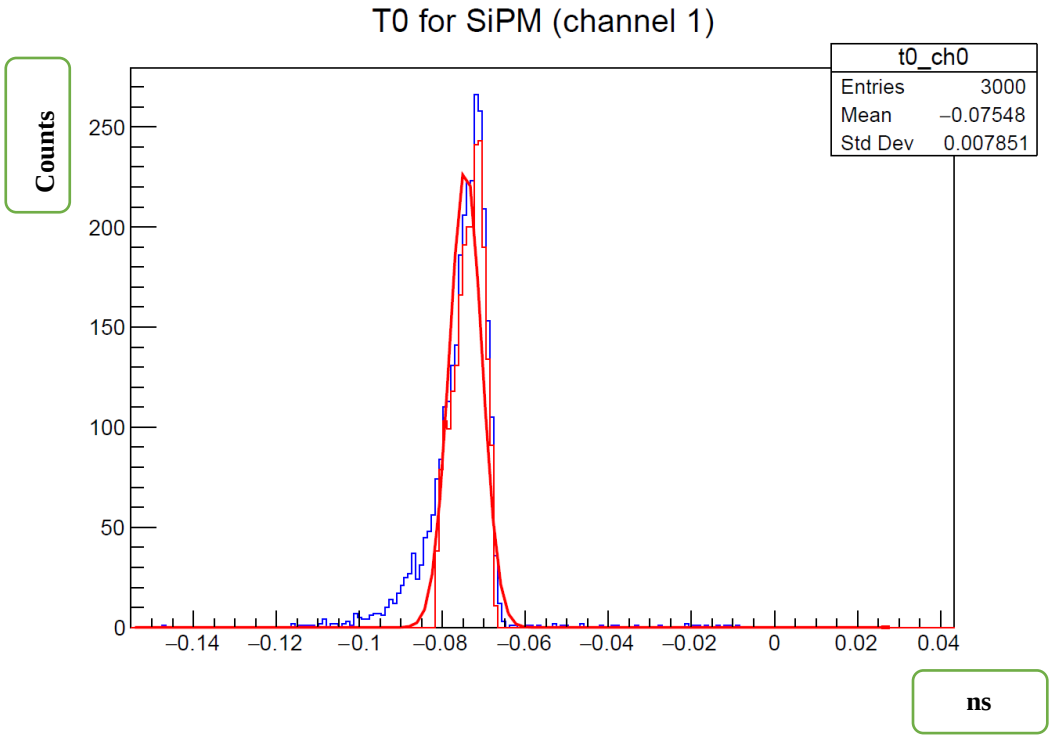
T0 for SiPM (channel 1)
t0_ch0
Entries 3000
Mean −0.07548
Std Dev 0.007851
Counts
ns

APPENDIX (2)

Here an exact layout of ICAUS top level with further details have been presented through two photos beside some other ones in an operative way. The work has accurately been done by very exact and complex software with complicated codes in which in the subsequent part is visible. The designs which have been provided in this thesis consist all these complex codes in which due to avoid repeating, a very small part of that has been represented here which can be true for the other parts as well.

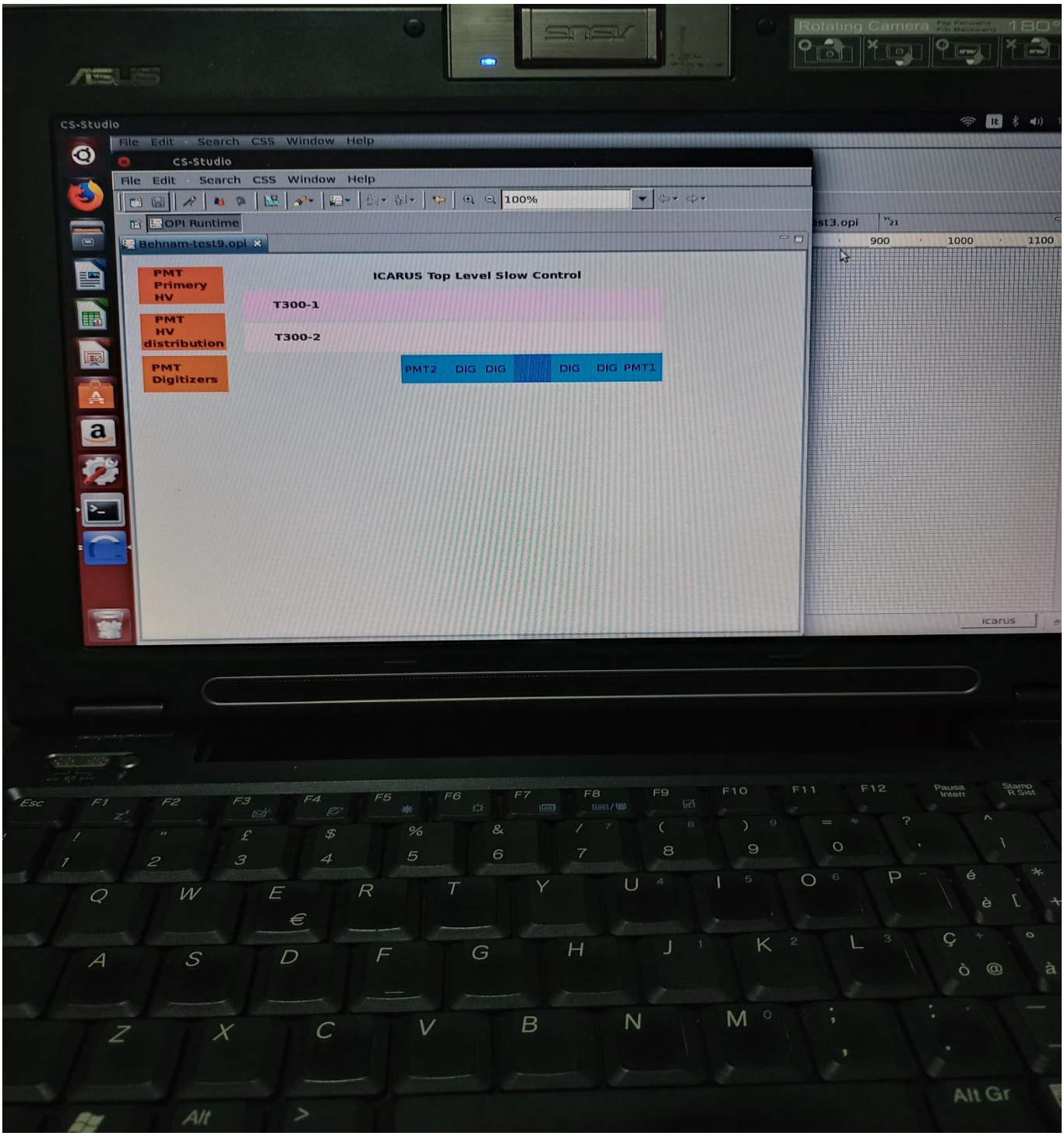
Rotating Camera
CS-Studio
File Edit Search CSS Window Help
CS-Studio
File Edit Search CSS Window Help
100%
OPI Runtime
Behnam-test9.opi
PMT Primery HV
PMT HV distribution
PMT Digitizers
ICARUS Top Level Slow Control
T300-1
T300-2
PMT2 DIG DIG DIG DIG PMT1
900
1000
1100
icarus

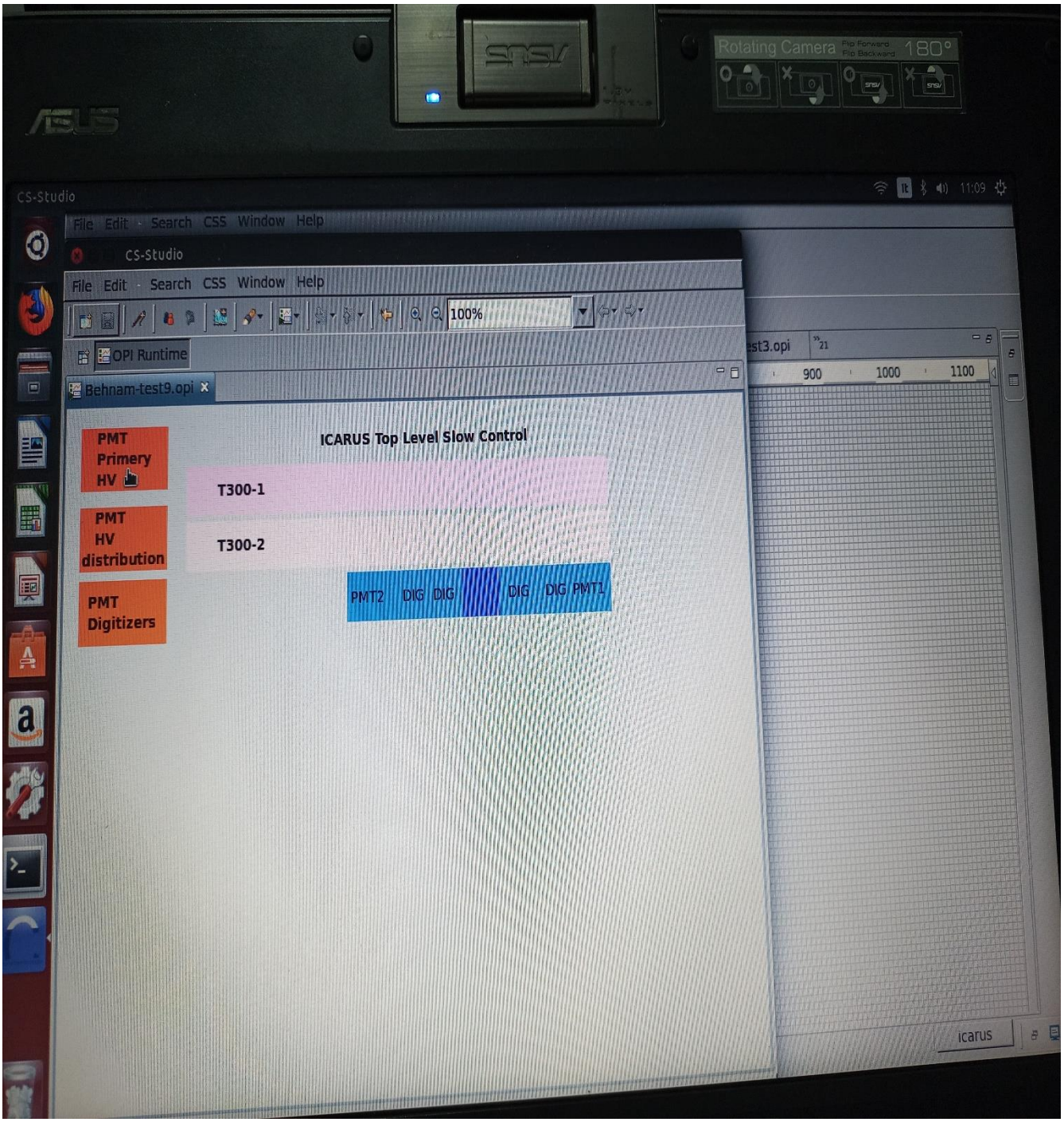
Rotating Camera
Flip Forward
Flip Backward
180°
CS-Studio
File Edit Search CSS Window Help
CS-Studio
File Edit Search CSS Window Help
100%
OPI Runtime
Behnam-test9.opi
ICARUS Top Level Slow Control
PMT Primery HV
T300-1
PMT HV distribution
T300-2
PMT Digitizers
PMT2 DIG DIG DIG DIG PMT1
900
1000
1100
icarus

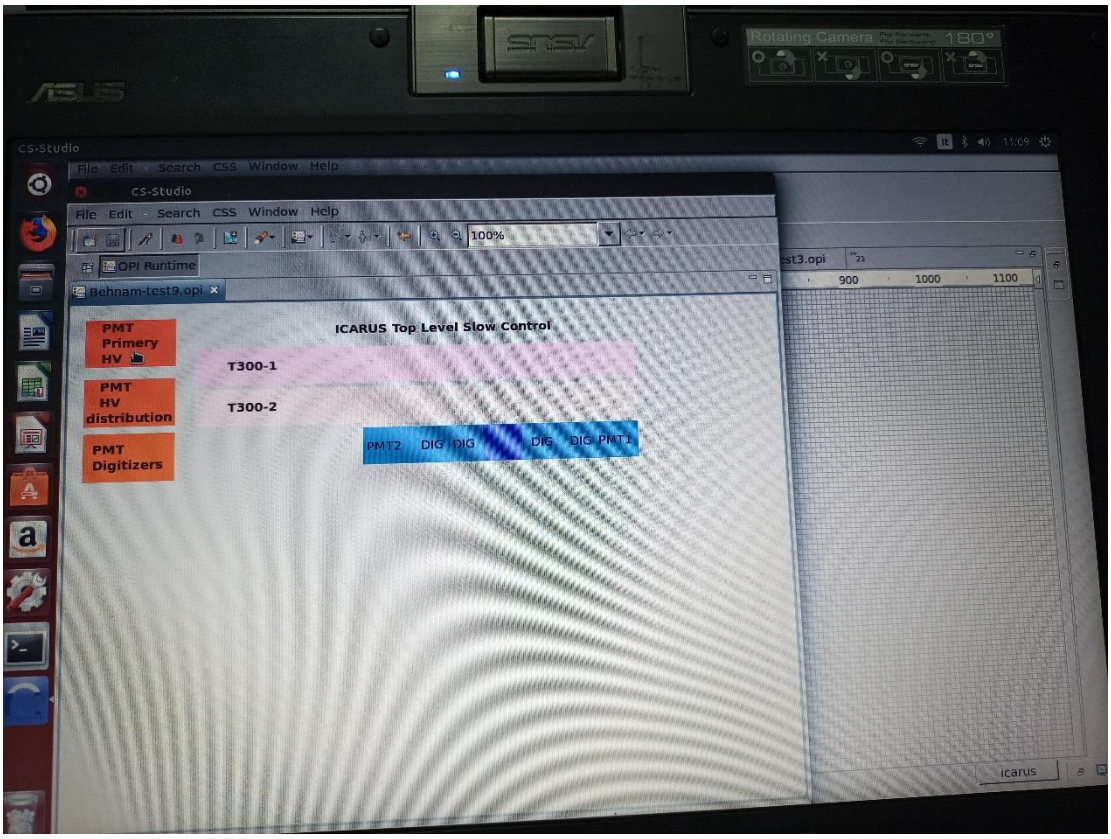
Rotating Camera
180°
CS-Studio
File Edit Search CSS Window Help
OPI Runtime
Behnam-test9.opi
ICARUS Top Level Slow Control
PMT Primery HV
PMT HV distribution
PMT Digitizers
T300-1
T300-2
PMT2 DIG DIG DIG DIG PMT1
icarus

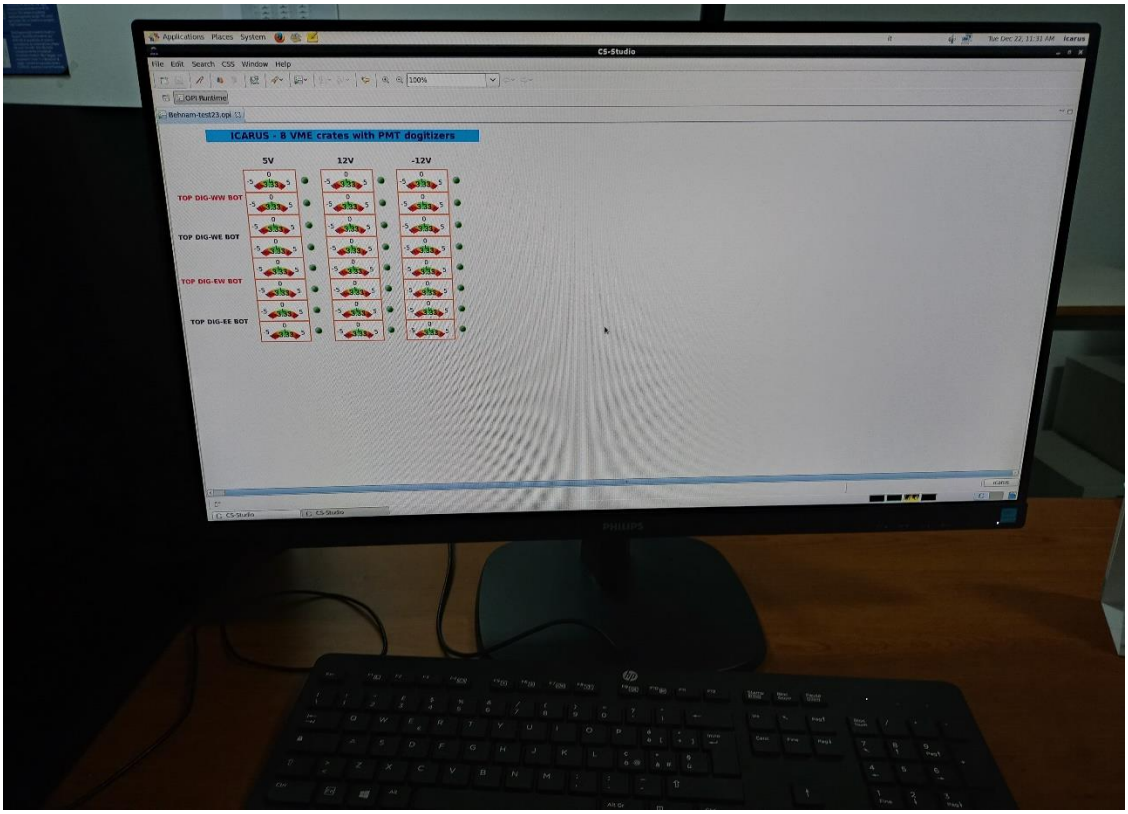
CS-Studio
ICARUS - 8 VME crates with PMT dogitizers
5V
12V
-12V
TOP DIG-WW BOT
TOP DIG-WE BOT
TOP DIG-EW BOT
TOP DIG-EE BOT

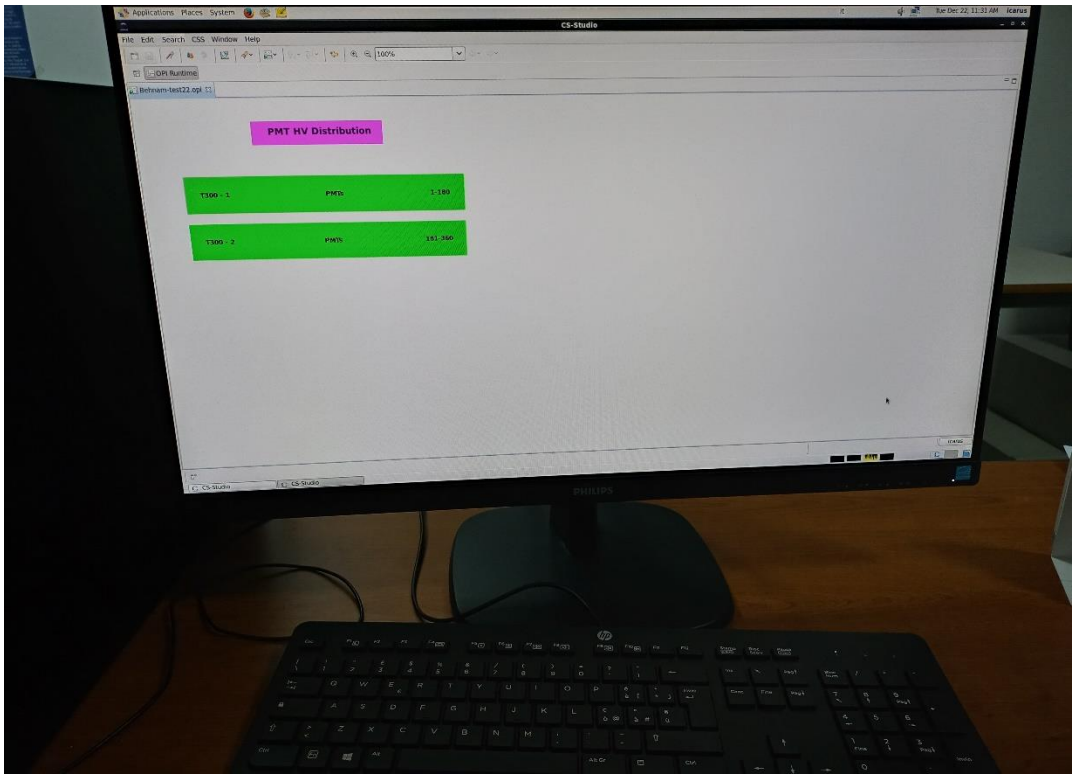
CS-Studio
PMT HV Distribution
T300 - 1
PMTs
1-180
T300 - 2
PMTs
181-360

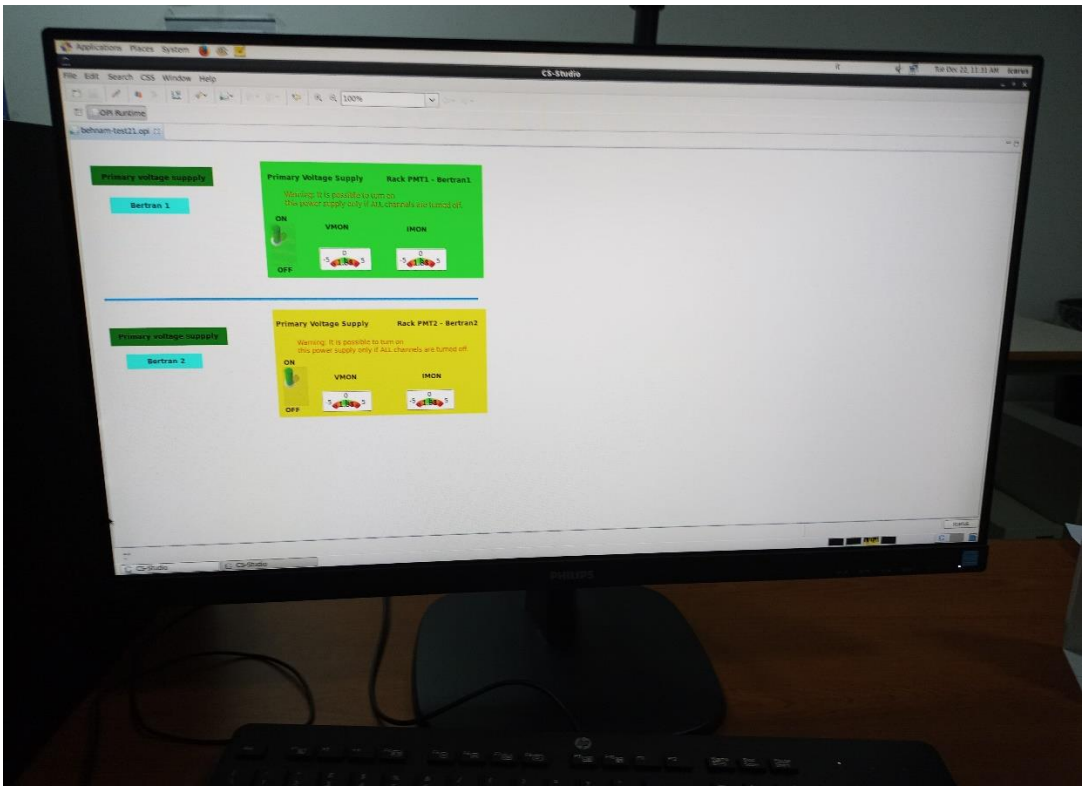
CS-Studio
Primary voltage supply
Bertran 1
Primary Voltage Supply
Rack PMT1 - Bertran1
ON
OFF
VMON
IMON
Primary voltage supply
Bertran 2
Primary Voltage Supply
Rack PMT2 - Bertran2
ON
OFF
VMON
IMON

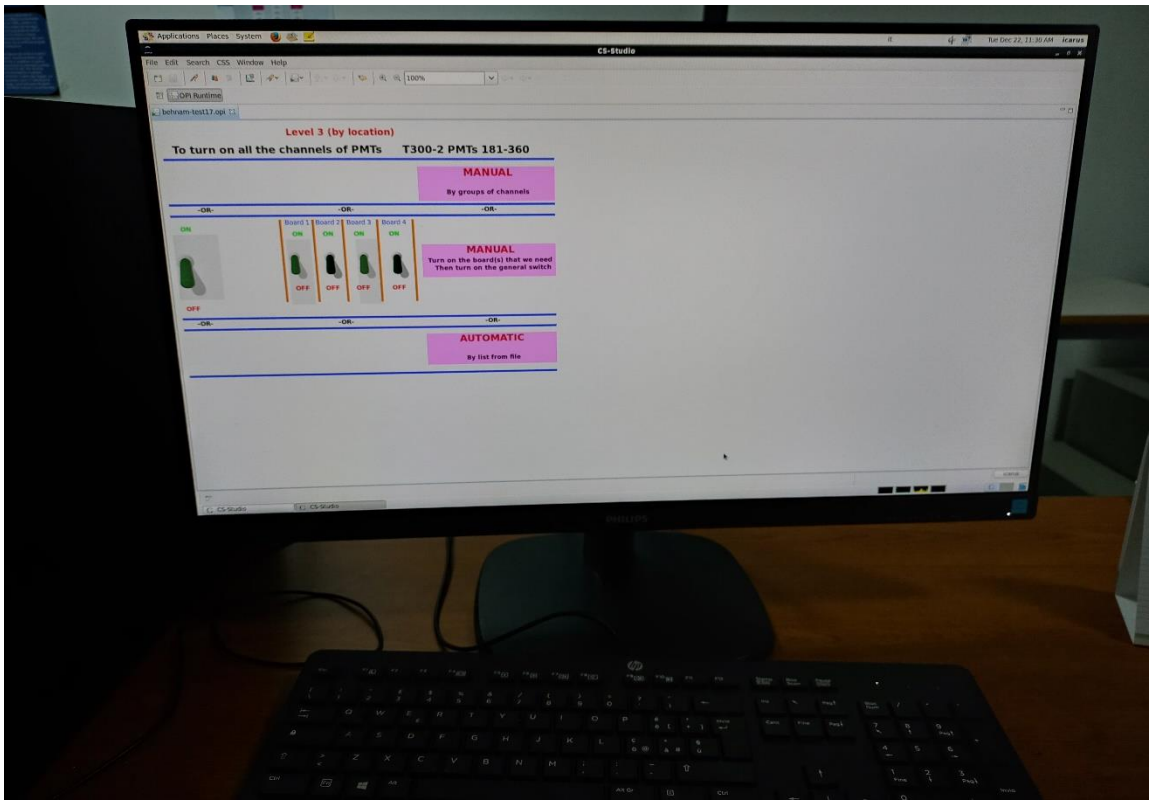
CS-Studio
Level 3 (by location)
To turn on all the channels of PMTs T300-2 PMTs 181-360
MANUAL
By groups of channels
-OR-
-OR-
-OR-
Board 1
Board 2
Board 3
Board 4
ON
OFF
MANUAL
Turn on the board(s) that we need
Then turn on the general switch
-OR-
-OR-
-OR-
AUTOMATIC
By list from file

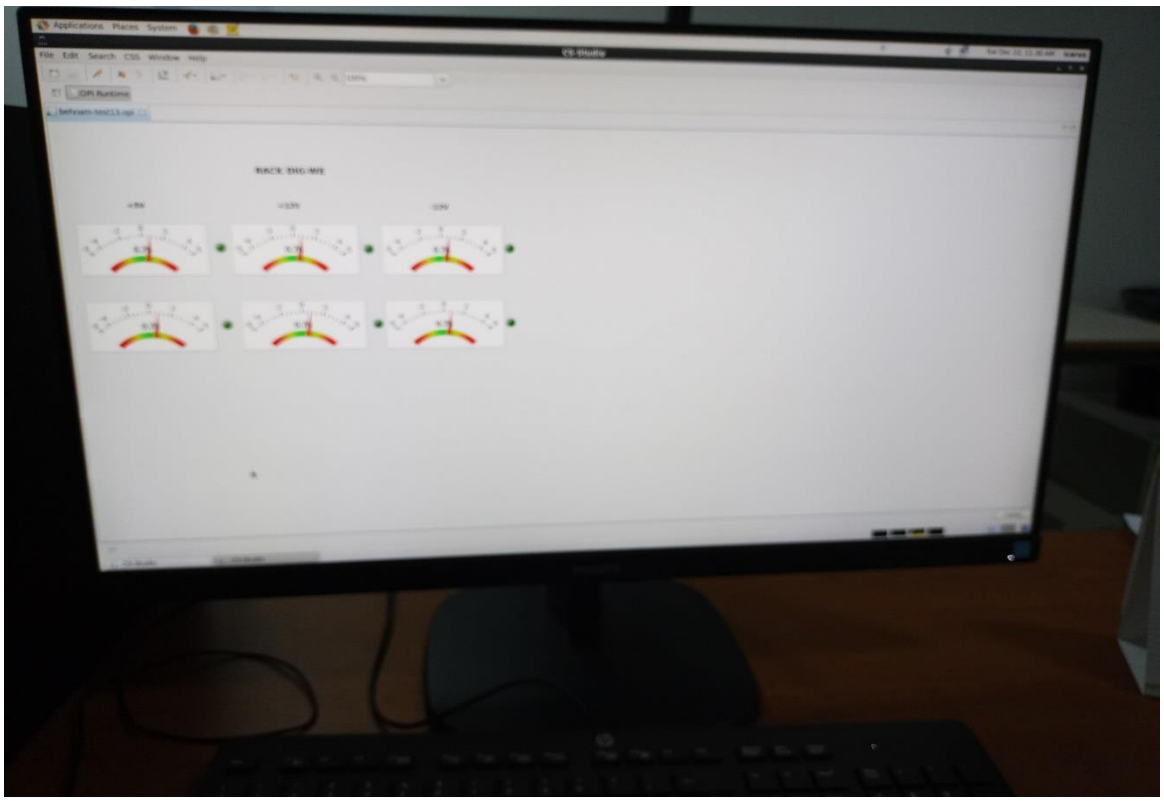

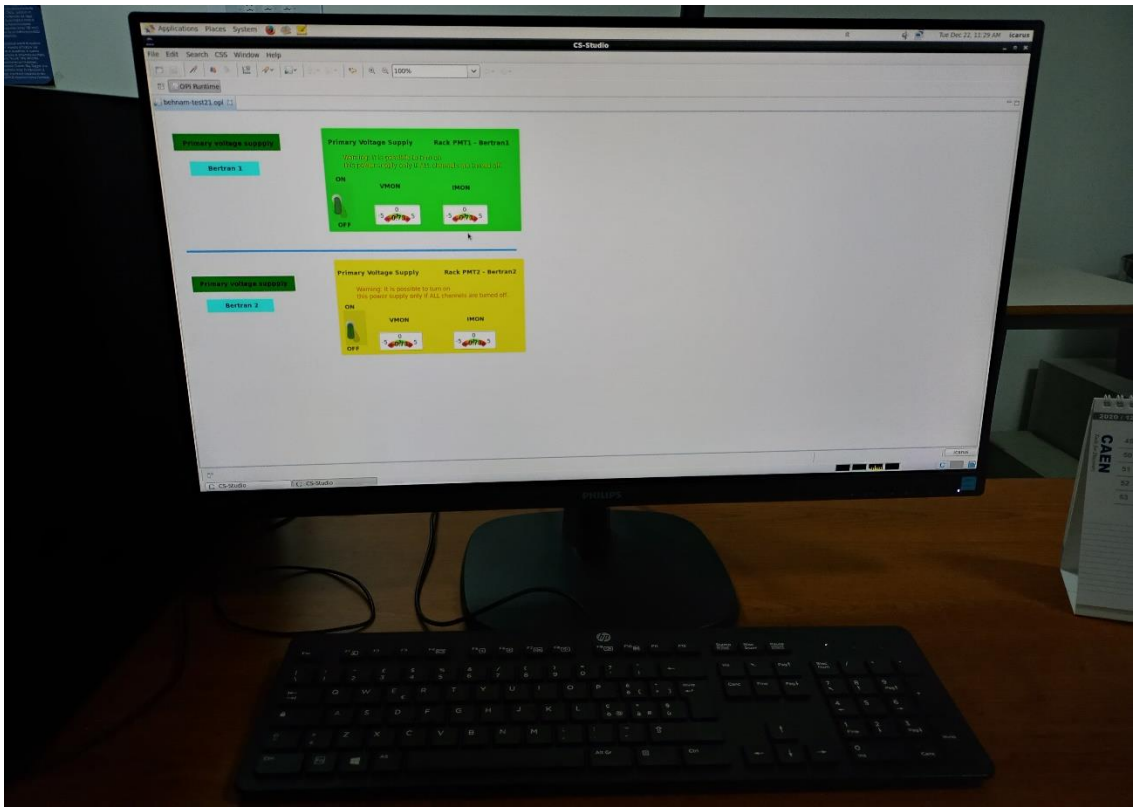
CS-Studio
Primary voltage supply
Bertran 1
Primary Voltage Supply
Rack PMT1 - Bertran1
ON
VMON
IMON
OFF
Primary voltage supply
Bertran 2
Primary Voltage Supply
Rack PMT2 - Bertran2
ON
VMON
IMON
OFF

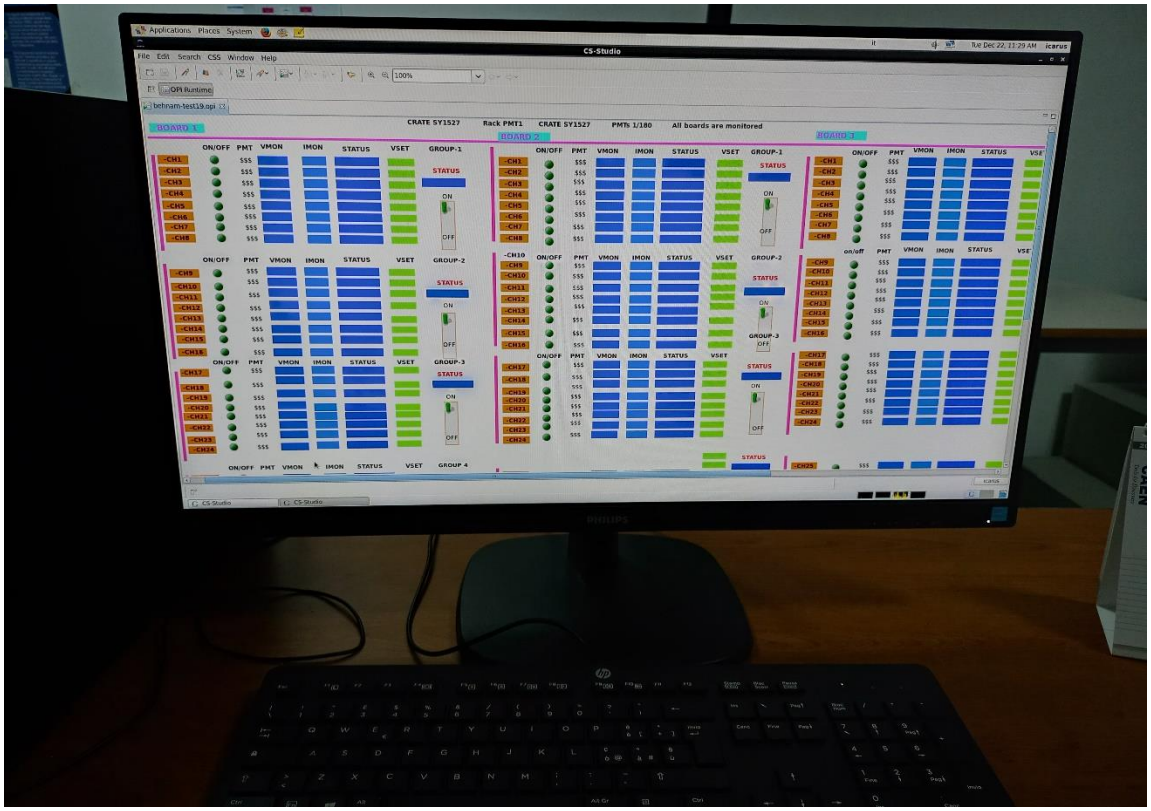
CS-Studio
CRATE SY1527
Rack PMT1
CRATE SY1527
PMTs 1/180
All boards are monitored
BOARD 1
BOARD 2
BOARD 3
ON/OFF
PMT
VMON
IMON
STATUS
VSET
GROUP-1
GROUP-2
GROUP-3
GROUP 4

The following code has produced the ICARUS top level design.

```
<?xml version="1.0" encoding="UTF-8"?>
<display typeId="org.csstudio.opibuilder.Display" version="1.0.0">
  <auto_zoom_to_fit_all>false</auto_zoom_to_fit_all>
  <macros>
    <include_parent_macros>true</include_parent_macros>
  </macros>
  <wuid>-62d437e7:1744e347940:-7d8f</wuid>
  <boy_version>3.2.10.20141111</boy_version>
  <scripts />
  <show_ruler>true</show_ruler>
  <height>600</height>
  <name></name>
  <snap_to_geometry>true</snap_to_geometry>
  <show_grid>true</show_grid>
  <background_color>
    <color red="240" green="240" blue="240" />
  </background_color>
  <foreground_color>
    <color red="192" green="192" blue="192" />
  </foreground_color>
  <widget_type>Display</widget_type>
  <show_close_button>true</show_close_button>
  <width>800</width>
  <rules />
  <show_edit_range>true</show_edit_range>
  <grid_space>6</grid_space>
  <auto_scale_widgets>
    <auto_scale_widgets>false</auto_scale_widgets>
    <min_width>-1</min_width>
    <min_height>-1</min_height>
  </auto_scale_widgets>
  <actions hook="false" hook_all="false" />
  <y>-1</y>
  <x>-1</x>
```

```
<widget typeId="org.csstudio.opibuilder.widgets.Rectangle" version="1.0.0">
  <border_alarm_sensitive>false</border_alarm_sensitive>
  <visible>true</visible>
  <fill_level>0.0</fill_level>
  <line_color>
    <color red="128" green="0" blue="255" />
  </line_color>
  <wuid>-62d437e7:1744e347940:-7d7d</wuid>
  <bg_gradient_color>
    <color red="255" green="255" blue="255" />
  </bg_gradient_color>
  <scripts />
  <height>43</height>
  <anti_alias>true</anti_alias>
  <name>Rectangle_19</name>
  <forecolor_alarm_sensitive>false</forecolor_alarm_sensitive>
  <alpha>255</alpha>
  <scale_options>
    <width_scalable>true</width_scalable>
    <height_scalable>true</height_scalable>
    <keep_wh_ratio>false</keep_wh_ratio>
  </scale_options>
  <transparent>false</transparent>
  <pv_name></pv_name>
  <background_color>
    <color red="255" green="217" blue="255" />
  </background_color>
  <foreground_color>
    <color red="255" green="0" blue="0" />
  </foreground_color>
  <widget_type>Rectangle</widget_type>
  <enabled>true</enabled>
  <fg_gradient_color>
    <color red="255" green="255" blue="255" />
  </fg_gradient_color>
  <backcolor_alarm_sensitive>false</backcolor_alarm_sensitive>
  <font>
```

```
      <opifont.name fontName="Sans" height="10" style="0">Default</opifont.name>
    </font>
    <width>512</width>
    <line_style>0</line_style>
    <border_style>0</border_style>
    <rules />
    <pv_value />
    <border_width>1</border_width>
    <line_width>0</line_width>
    <horizontal_fill>true</horizontal_fill>
    <border_color>
      <color red="255" green="255" blue="255" />
    </border_color>
    <actions hook="false" hook_all="false" />
    <y>54</y>
    <tooltip>$(pv_name)
$(pv_value)</tooltip>
    <x>144</x>
    <gradient>false</gradient>
  </widget>
  <widget typeId="org.csstudio.opibuilder.widgets.Rectangle" version="1.0.0">
    <border_alarm_sensitive>false</border_alarm_sensitive>
    <visible>true</visible>
    <fill_level>0.0</fill_level>
    <line_color>
      <color red="128" green="0" blue="255" />
    </line_color>
    <wuid>-62d437e7:1744e347940:-7d6b</wuid>
    <bg_gradient_color>
      <color red="255" green="255" blue="255" />
    </bg_gradient_color>
    <scripts />
    <height>43</height>
    <anti_alias>true</anti_alias>
    <name>Rectangle_20</name>
    <forecolor_alarm_sensitive>false</forecolor_alarm_sensitive>
    <alpha>255</alpha>
```

```
    <scale_options>
      <width_scalable>true</width_scalable>
      <height_scalable>true</height_scalable>
      <keep_wh_ratio>false</keep_wh_ratio>
    </scale_options>
    <transparent>false</transparent>
    <pv_name></pv_name>
    <background_color>
      <color red="255" green="236" blue="255" />
    </background_color>
    <foreground_color>
      <color red="255" green="0" blue="0" />
    </foreground_color>
    <widget_type>Rectangle</widget_type>
    <enabled>true</enabled>
    <fg_gradient_color>
      <color red="255" green="255" blue="255" />
    </fg_gradient_color>
    <backcolor_alarm_sensitive>false</backcolor_alarm_sensitive>
    <font>
      <opifont.name fontName="Sans" height="10" style="0">Default</opifont.name>
    </font>
    <width>512</width>
    <line_style>0</line_style>
    <border_style>0</border_style>
    <rules />
    <pv_value />
    <border_width>1</border_width>
    <line_width>0</line_width>
    <horizontal_fill>true</horizontal_fill>
    <border_color>
      <color red="255" green="255" blue="255" />
    </border_color>
    <actions hook="false" hook_all="false" />
    <y>102</y>
    <tooltip>$(pv_name)
$(pv_value)</tooltip>
```

<x>144</x>
<gradient>false</gradient>
</widget>
<widget typeId="org.csstudio.opibuilder.widgets.Label" version="1.0.0">
<visible>true</visible>
<vertical_alignment>1</vertical_alignment>
<wuid>-62d437e7:1744e347940:-7d59</wuid>
<auto_size>false</auto_size>
<scripts />
<height>25</height>
<name>Label_12</name>
<scale_options>
<width_scalable>true</width_scalable>
<height_scalable>true</height_scalable>
<keep_wh_ratio>false</keep_wh_ratio>
</scale_options>
<transparent>true</transparent>
<background_color>
<color red="255" green="255" blue="255" />
</background_color>
<foreground_color>
<color red="0" green="0" blue="0" />
</foreground_color>
<widget_type>Label</widget_type>
<enabled>true</enabled>
<text>T300-1</text>

<opifont.name fontName="Sans" height="10" style="1">Default Bold</opifont.name>

<width>129</width>
<border_style>0</border_style>
<rules />
<border_width>1</border_width>
<border_color>
<color red="0" green="128" blue="255" />
</border_color>
<horizontal_alignment>1</horizontal_alignment>

```
  <actions hook="false" hook_all="false" />
  <y>63</y>
  <wrap_words>false</wrap_words>
  <tooltip></tooltip>
  <x>144</x>
</widget>
<widget typeId="org.csstudio.opibuilder.widgets.Label" version="1.0.0">
  <visible>true</visible>
  <vertical_alignment>1</vertical_alignment>
  <wuid>-62d437e7:1744e347940:-7d47</wuid>
  <auto_size>false</auto_size>
  <scripts />
  <height>31</height>
  <name>Label_13</name>
  <scale_options>
    <width_scalable>true</width_scalable>
    <height_scalable>true</height_scalable>
    <keep_wh_ratio>false</keep_wh_ratio>
  </scale_options>
  <transparent>true</transparent>
  <background_color>
    <color red="255" green="255" blue="255" />
  </background_color>
  <foreground_color>
    <color red="0" green="0" blue="0" />
  </foreground_color>
  <widget_type>Label</widget_type>
  <enabled>true</enabled>
  <text>T300-2</text>
  <font>
    <opifont.name fontName="Sans" height="10" style="1">Default Bold</opifont.name>
  </font>
  <width>107</width>
  <border_style>0</border_style>
  <rules />
  <border_width>1</border_width>
  <border_color>
```

```
    <color red="0" green="128" blue="255" />
  </border_color>
  <horizontal_alignment>1</horizontal_alignment>
  <actions hook="false" hook_all="false" />
  <y>108</y>
  <wrap_words>false</wrap_words>
  <tooltip></tooltip>
  <x>155</x>
</widget>
<widget typeId="org.csstudio.opibuilder.widgets.Rectangle" version="1.0.0">
  <border_alarm_sensitive>false</border_alarm_sensitive>
  <visible>true</visible>
  <fill_level>0.0</fill_level>
  <line_color>
    <color red="128" green="0" blue="255" />
  </line_color>
  <wuid>-62d437e7:1744e347940:-7d31</wuid>
  <bg_gradient_color>
    <color red="255" green="255" blue="255" />
  </bg_gradient_color>
  <scripts />
  <height>43</height>
  <anti_alias>true</anti_alias>
  <name>Rectangle_21</name>
  <forecolor_alarm_sensitive>false</forecolor_alarm_sensitive>
  <alpha>255</alpha>
  <scale_options>
    <width_scalable>true</width_scalable>
    <height_scalable>true</height_scalable>
    <keep_wh_ratio>false</keep_wh_ratio>
  </scale_options>
  <transparent>false</transparent>
  <pv_name></pv_name>
  <background_color>
    <color red="30" green="144" blue="255" />
  </background_color>
  <foreground_color>
```

```
    <color red="255" green="0" blue="0" />
  </foreground_color>
  <widget_type>Rectangle</widget_type>
  <enabled>true</enabled>
  <fg_gradient_color>
    <color red="255" green="255" blue="255" />
  </fg_gradient_color>
  <backcolor_alarm_sensitive>false</backcolor_alarm_sensitive>
  <font>
    <opifont.name fontName="Sans" height="10" style="0">Default</opifont.name>
  </font>
  <width>47</width>
  <line_style>0</line_style>
  <border_style>0</border_style>
  <rules />
  <pv_value />
  <border_width>1</border_width>
  <line_width>0</line_width>
  <horizontal_fill>true</horizontal_fill>
  <border_color>
    <color red="0" green="128" blue="255" />
  </border_color>
  <actions hook="true" hook_all="false">
    <action type="OPEN_DISPLAY">
      <path>behnam-test2.opi</path>
      <macros>
        <include_parent_macros>true</include_parent_macros>
      </macros>
      <replace>1</replace>
      <description></description>
    </action>
  </actions>
  <y>150</y>
  <tooltip>$(pv_name)
$(pv_value)</tooltip>
  <x>609</x>
  <gradient>false</gradient>
```

```
</widget>
<widget typeId="org.csstudio.opibuilder.widgets.Rectangle" version="1.0.0">
  <border_alarm_sensitive>false</border_alarm_sensitive>
  <visible>true</visible>
  <fill_level>0.0</fill_level>
  <line_color>
    <color red="128" green="0" blue="255" />
  </line_color>
  <wuid>-62d437e7:1744e347940:-7d1f</wuid>
  <bg_gradient_color>
    <color red="255" green="255" blue="255" />
  </bg_gradient_color>
  <scripts />
  <height>43</height>
  <anti_alias>true</anti_alias>
  <name>Rectangle_22</name>
  <forecolor_alarm_sensitive>false</forecolor_alarm_sensitive>
  <alpha>255</alpha>
  <scale_options>
    <width_scalable>true</width_scalable>
    <height_scalable>true</height_scalable>
    <keep_wh_ratio>false</keep_wh_ratio>
  </scale_options>
  <transparent>false</transparent>
  <pv_name></pv_name>
  <background_color>
    <color red="30" green="144" blue="255" />
  </background_color>
  <foreground_color>
    <color red="255" green="0" blue="0" />
  </foreground_color>
  <widget_type>Rectangle</widget_type>
  <enabled>true</enabled>
  <fg_gradient_color>
    <color red="255" green="255" blue="255" />
  </fg_gradient_color>
  <backcolor_alarm_sensitive>false</backcolor_alarm_sensitive>
```


<opifont.name fontName="Sans" height="10" style="0">Default</opifont.name>

<width>47</width>
<line_style>0</line_style>
<border_style>0</border_style>
<rules />
<pv_value />
<border_width>1</border_width>
<line_width>0</line_width>
<horizontal_fill>true</horizontal_fill>
<border_color>
<color red="0" green="128" blue="255" />
</border_color>
<actions hook="false" hook_all="false" />
<y>150</y>
<tooltip>$(pv_name)
$(pv_value)</tooltip>
<x>563</x>
<gradient>false</gradient>
</widget>
<widget typeId="org.csstudio.opibuilder.widgets.Rectangle" version="1.0.0">
<border_alarm_sensitive>false</border_alarm_sensitive>
<visible>true</visible>
<fill_level>0.0</fill_level>
<line_color>
<color red="128" green="0" blue="255" />
</line_color>
<wuid>-62d437e7:1744e347940:-7d0d</wuid>
<bg_gradient_color>
<color red="255" green="255" blue="255" />
</bg_gradient_color>
<scripts />
<height>43</height>
<anti_alias>true</anti_alias>
<name>Rectangle_23</name>
<forecolor_alarm_sensitive>false</forecolor_alarm_sensitive>

<alpha>255</alpha>
<scale_options>
  <width_scalable>true</width_scalable>
  <height_scalable>true</height_scalable>
  <keep_wh_ratio>false</keep_wh_ratio>
</scale_options>
<transparent>false</transparent>
<pv_name></pv_name>
<background_color>
  <color red="30" green="144" blue="255" />
</background_color>
<foreground_color>
  <color red="255" green="0" blue="0" />
</foreground_color>
<widget_type>Rectangle</widget_type>
<enabled>true</enabled>
<fg_gradient_color>
  <color red="255" green="255" blue="255" />
</fg_gradient_color>
<backcolor_alarm_sensitive>false</backcolor_alarm_sensitive>

  <opifont.name fontName="Sans" height="10" style="0">Default</opifont.name>

<width>47</width>
<line_style>0</line_style>
<border_style>0</border_style>
<rules />
<pv_value />
<border_width>1</border_width>
<line_width>0</line_width>
<horizontal_fill>true</horizontal_fill>
<border_color>
  <color red="0" green="128" blue="255" />
</border_color>
<actions hook="false" hook_all="false" />
<y>150</y>
<tooltip>$(pv_name)

```
$(pv_value)</tooltip>
    <x>517</x>
    <gradient>false</gradient>
  </widget>
  <widget typeId="org.csstudio.opibuilder.widgets.Rectangle" version="1.0.0">
    <border_alarm_sensitive>false</border_alarm_sensitive>
    <visible>true</visible>
    <fill_level>0.0</fill_level>
    <line_color>
      <color red="128" green="0" blue="255" />
    </line_color>
    <wuid>-62d437e7:1744e347940:-7cfb</wuid>
    <bg_gradient_color>
      <color red="255" green="255" blue="255" />
    </bg_gradient_color>
    <scripts />
    <height>43</height>
    <anti_alias>true</anti_alias>
    <name>Rectangle_24</name>
    <forecolor_alarm_sensitive>false</forecolor_alarm_sensitive>
    <alpha>255</alpha>
    <scale_options>
      <width_scalable>true</width_scalable>
      <height_scalable>true</height_scalable>
      <keep_wh_ratio>false</keep_wh_ratio>
    </scale_options>
    <transparent>false</transparent>
    <pv_name></pv_name>
    <background_color>
      <color red="30" green="28" blue="255" />
    </background_color>
    <foreground_color>
      <color red="255" green="0" blue="0" />
    </foreground_color>
    <widget_type>Rectangle</widget_type>
    <enabled>true</enabled>
    <fg_gradient_color>
```

```
    <color red="255" green="255" blue="255" />
   </fg_gradient_color>
   <backcolor_alarm_sensitive>false</backcolor_alarm_sensitive>
   <font>
    <opifont.name fontName="Sans" height="10" style="0">Default</opifont.name>
   </font>
   <width>47</width>
   <line_style>0</line_style>
   <border_style>0</border_style>
   <rules />
   <pv_value />
   <border_width>1</border_width>
   <line_width>0</line_width>
   <horizontal_fill>true</horizontal_fill>
   <border_color>
    <color red="0" green="128" blue="255" />
   </border_color>
   <actions hook="false" hook_all="false" />
   <y>150</y>
   <tooltip>$(pv_name)
$(pv_value)</tooltip>
   <x>471</x>
   <gradient>false</gradient>
  </widget>
  <widget typeId="org.csstudio.opibuilder.widgets.Rectangle" version="1.0.0">
   <border_alarm_sensitive>false</border_alarm_sensitive>
   <visible>true</visible>
   <fill_level>0.0</fill_level>
   <line_color>
    <color red="128" green="0" blue="255" />
   </line_color>
   <wuid>-62d437e7:1744e347940:-7ce9</wuid>
   <bg_gradient_color>
    <color red="255" green="255" blue="255" />
   </bg_gradient_color>
   <scripts />
   <height>43</height>
```

<anti_alias>true</anti_alias>
<name>Rectangle_25</name>
<forecolor_alarm_sensitive>false</forecolor_alarm_sensitive>
<alpha>255</alpha>
<scale_options>
  <width_scalable>true</width_scalable>
  <height_scalable>true</height_scalable>
  <keep_wh_ratio>false</keep_wh_ratio>
</scale_options>
<transparent>false</transparent>
<pv_name></pv_name>
<background_color>
  <color red="30" green="144" blue="255" />
</background_color>
<foreground_color>
  <color red="255" green="0" blue="0" />
</foreground_color>
<widget_type>Rectangle</widget_type>
<enabled>true</enabled>
<fg_gradient_color>
  <color red="255" green="255" blue="255" />
</fg_gradient_color>
<backcolor_alarm_sensitive>false</backcolor_alarm_sensitive>

  <opifont.name fontName="Sans" height="10" style="0">Default</opifont.name>

<width>47</width>
<line_style>0</line_style>
<border_style>0</border_style>
<rules />
<pv_value />
<border_width>1</border_width>
<line_width>0</line_width>
<horizontal_fill>true</horizontal_fill>
<border_color>
  <color red="0" green="128" blue="255" />
</border_color>

```
    <actions hook="true" hook_all="false">
      <action type="OPEN_DISPLAY">
        <path>behnam-test14.opi</path>
        <macros>
          <include_parent_macros>true</include_parent_macros>
        </macros>
        <replace>1</replace>
        <description></description>
      </action>
    </actions>
    <y>150</y>
    <tooltip>$(pv_name)
$(pv_value)</tooltip>
    <x>425</x>
    <gradient>false</gradient>
  </widget>
  <widget typeId="org.csstudio.opibuilder.widgets.Rectangle" version="1.0.0">
    <border_alarm_sensitive>false</border_alarm_sensitive>
    <visible>true</visible>
    <fill_level>0.0</fill_level>
    <line_color>
      <color red="128" green="0" blue="255" />
    </line_color>
    <wuid>-62d437e7:1744e347940:-7cd7</wuid>
    <bg_gradient_color>
      <color red="255" green="255" blue="255" />
    </bg_gradient_color>
    <scripts />
    <height>43</height>
    <anti_alias>true</anti_alias>
    <name>Rectangle_26</name>
    <forecolor_alarm_sensitive>false</forecolor_alarm_sensitive>
    <alpha>255</alpha>
    <scale_options>
      <width_scalable>true</width_scalable>
      <height_scalable>true</height_scalable>
      <keep_wh_ratio>false</keep_wh_ratio>
```

```
    </scale_options>
    <transparent>false</transparent>
    <pv_name></pv_name>
    <background_color>
      <color red="30" green="144" blue="255" />
    </background_color>
    <foreground_color>
      <color red="255" green="0" blue="0" />
    </foreground_color>
    <widget_type>Rectangle</widget_type>
    <enabled>true</enabled>
    <fg_gradient_color>
      <color red="255" green="255" blue="255" />
    </fg_gradient_color>
    <backcolor_alarm_sensitive>false</backcolor_alarm_sensitive>
    <font>
      <opifont.name fontName="Sans" height="10" style="0">Default</opifont.name>
    </font>
    <width>47</width>
    <line_style>0</line_style>
    <border_style>0</border_style>
    <rules />
    <pv_value />
    <border_width>1</border_width>
    <line_width>0</line_width>
    <horizontal_fill>true</horizontal_fill>
    <border_color>
      <color red="0" green="128" blue="255" />
    </border_color>
    <actions hook="false" hook_all="false" />
    <y>150</y>
    <tooltip>$(pv_name)
$(pv_value)</tooltip>
    <x>379</x>
    <gradient>false</gradient>
  </widget>
  <widget typeId="org.csstudio.opibuilder.widgets.Rectangle" version="1.0.0">
```

<border_alarm_sensitive>false</border_alarm_sensitive>
<visible>true</visible>
<fill_level>0.0</fill_level>
<line_color>
  <color red="128" green="0" blue="255" />
</line_color>
<wuid>-62d437e7:1744e347940:-7cc5</wuid>
<bg_gradient_color>
  <color red="255" green="255" blue="255" />
</bg_gradient_color>
<scripts />
<height>43</height>
<anti_alias>true</anti_alias>
<name>Rectangle_27</name>
<forecolor_alarm_sensitive>false</forecolor_alarm_sensitive>
<alpha>255</alpha>
<scale_options>
  <width_scalable>true</width_scalable>
  <height_scalable>true</height_scalable>
  <keep_wh_ratio>false</keep_wh_ratio>
</scale_options>
<transparent>false</transparent>
<pv_name></pv_name>
<background_color>
  <color red="30" green="144" blue="255" />
</background_color>
<foreground_color>
  <color red="255" green="0" blue="0" />
</foreground_color>
<widget_type>Rectangle</widget_type>
<enabled>true</enabled>
<fg_gradient_color>
  <color red="255" green="255" blue="255" />
</fg_gradient_color>
<backcolor_alarm_sensitive>false</backcolor_alarm_sensitive>
<font>
  <opifont.name fontName="Sans" height="10" style="0">Default</opifont.name>

```
    </font>
    <width>47</width>
    <line_style>0</line_style>
    <border_style>0</border_style>
    <rules />
    <pv_value />
    <border_width>1</border_width>
    <line_width>0</line_width>
    <horizontal_fill>true</horizontal_fill>
    <border_color>
      <color red="0" green="128" blue="255" />
    </border_color>
    <actions hook="false" hook_all="false" />
    <y>150</y>
    <tooltip>$(pv_name)
$(pv_value)</tooltip>
    <x>333</x>
    <gradient>false</gradient>
  </widget>
  <widget typeId="org.csstudio.opibuilder.widgets.Label" version="1.0.0">
    <visible>true</visible>
    <vertical_alignment>1</vertical_alignment>
    <wuid>-62d437e7:1744e347940:-7cb3</wuid>
    <auto_size>false</auto_size>
    <scripts />
    <height>20</height>
    <name>Label_15</name>
    <scale_options>
      <width_scalable>true</width_scalable>
      <height_scalable>true</height_scalable>
      <keep_wh_ratio>false</keep_wh_ratio>
    </scale_options>
    <transparent>true</transparent>
    <background_color>
      <color red="255" green="255" blue="255" />
    </background_color>
    <foreground_color>
```

```
    <color red="0" green="0" blue="0" />
  </foreground_color>
  <widget_type>Label</widget_type>
  <enabled>true</enabled>
  <text>PMT1</text>
  <font>
    <opifont.name fontName="Sans" height="10" style="0">Default</opifont.name>
  </font>
  <width>80</width>
  <border_style>0</border_style>
  <rules />
  <border_width>1</border_width>
  <border_color>
    <color red="0" green="128" blue="255" />
  </border_color>
  <horizontal_alignment>1</horizontal_alignment>
  <actions hook="true" hook_all="false">
    <action type="OPEN_DISPLAY">
      <path>Behnam-test10.opi</path>
      <macros>
        <include_parent_macros>true</include_parent_macros>
      </macros>
      <replace>1</replace>
      <description></description>
    </action>
  </actions>
  <y>162</y>
  <wrap_words>false</wrap_words>
  <tooltip></tooltip>
  <x>588</x>
</widget>
<widget typeId="org.csstudio.opibuilder.widgets.Label" version="1.0.0">
  <visible>true</visible>
  <vertical_alignment>1</vertical_alignment>
  <wuid>-62d437e7:1744e347940:-7ca1</wuid>
  <auto_size>false</auto_size>
  <scripts />
```

<height>20</height>
<name>Label_16</name>
<scale_options>
  <width_scalable>true</width_scalable>
  <height_scalable>true</height_scalable>
  <keep_wh_ratio>false</keep_wh_ratio>
</scale_options>
<transparent>true</transparent>
<background_color>
  <color red="255" green="255" blue="255" />
</background_color>
<foreground_color>
  <color red="0" green="0" blue="0" />
</foreground_color>
<widget_type>Label</widget_type>
<enabled>true</enabled>
<text>DIG</text>

  <opifont.name fontName="Sans" height="10" style="0">Default</opifont.name>

<width>80</width>
<border_style>0</border_style>
<rules />
<border_width>1</border_width>
<border_color>
  <color red="0" green="128" blue="255" />
</border_color>
<horizontal_alignment>1</horizontal_alignment>
<actions hook="true" hook_all="false">
  <action type="OPEN_DISPLAY">
    <path>behnam-test12.opi</path>
    <macros>
      <include_parent_macros>true</include_parent_macros>
    </macros>
    <replace>1</replace>
    <description></description>
  </action>

```
  </actions>
  <y>162</y>
  <wrap_words>false</wrap_words>
  <tooltip></tooltip>
  <x>547</x>
</widget>
<widget typeId="org.csstudio.opibuilder.widgets.Label" version="1.0.0">
  <visible>true</visible>
  <vertical_alignment>1</vertical_alignment>
  <wuid>-62d437e7:1744e347940:-7c8f</wuid>
  <auto_size>false</auto_size>
  <scripts />
  <height>20</height>
  <name>Label_17</name>
  <scale_options>
    <width_scalable>true</width_scalable>
    <height_scalable>true</height_scalable>
    <keep_wh_ratio>false</keep_wh_ratio>
  </scale_options>
  <transparent>true</transparent>
  <background_color>
    <color red="255" green="255" blue="255" />
  </background_color>
  <foreground_color>
    <color red="0" green="0" blue="0" />
  </foreground_color>
  <widget_type>Label</widget_type>
  <enabled>true</enabled>
  <text>DIG</text>
  <font>
    <opifont.name fontName="Sans" height="10" style="0">Default</opifont.name>
  </font>
  <width>80</width>
  <border_style>0</border_style>
  <rules />
  <border_width>1</border_width>
  <border_color>
```

```
    <color red="0" green="128" blue="255" />
  </border_color>
  <horizontal_alignment>1</horizontal_alignment>
  <actions hook="true" hook_all="false">
    <action type="OPEN_DISPLAY">
      <path>behnam-test13.opi</path>
      <macros>
        <include_parent_macros>true</include_parent_macros>
      </macros>
      <replace>1</replace>
      <description></description>
    </action>
  </actions>
  <y>162</y>
  <wrap_words>false</wrap_words>
  <tooltip></tooltip>
  <x>501</x>
</widget>
<widget typeId="org.csstudio.opibuilder.widgets.Label" version="1.0.0">
  <visible>true</visible>
  <vertical_alignment>1</vertical_alignment>
  <wuid>-62d437e7:1744e347940:-7c80</wuid>
  <auto_size>false</auto_size>
  <scripts />
  <height>20</height>
  <name>Label_18</name>
  <scale_options>
    <width_scalable>true</width_scalable>
    <height_scalable>true</height_scalable>
    <keep_wh_ratio>false</keep_wh_ratio>
  </scale_options>
  <transparent>true</transparent>
  <background_color>
    <color red="255" green="255" blue="255" />
  </background_color>
  <foreground_color>
    <color red="0" green="0" blue="0" />
```

```
  </foreground_color>
  <widget_type>Label</widget_type>
  <enabled>true</enabled>
  <text>DIG</text>
  <font>
    <opifont.name fontName="Sans" height="10" style="0">Default</opifont.name>
  </font>
  <width>80</width>
  <border_style>0</border_style>
  <rules />
  <border_width>1</border_width>
  <border_color>
    <color red="0" green="128" blue="255" />
  </border_color>
  <horizontal_alignment>1</horizontal_alignment>
  <actions hook="false" hook_all="false" />
  <y>162</y>
  <wrap_words>false</wrap_words>
  <tooltip></tooltip>
  <x>409</x>
</widget>
<widget typeId="org.csstudio.opibuilder.widgets.Label" version="1.0.0">
  <visible>true</visible>
  <vertical_alignment>1</vertical_alignment>
  <wuid>-62d437e7:1744e347940:-7c79</wuid>
  <auto_size>false</auto_size>
  <scripts />
  <height>20</height>
  <name>Label_19</name>
  <scale_options>
    <width_scalable>true</width_scalable>
    <height_scalable>true</height_scalable>
    <keep_wh_ratio>false</keep_wh_ratio>
  </scale_options>
  <transparent>true</transparent>
  <background_color>
    <color red="255" green="255" blue="255" />
```

```
  </background_color>
  <foreground_color>
    <color red="0" green="0" blue="0" />
  </foreground_color>
  <widget_type>Label</widget_type>
  <enabled>true</enabled>
  <text>DIG</text>
  <font>
    <opifont.name fontName="Sans" height="10" style="0">Default</opifont.name>
  </font>
  <width>80</width>
  <border_style>0</border_style>
  <rules />
  <border_width>1</border_width>
  <border_color>
    <color red="0" green="128" blue="255" />
  </border_color>
  <horizontal_alignment>1</horizontal_alignment>
  <actions hook="true" hook_all="false">
    <action type="OPEN_DISPLAY">
      <path>behnam-test15.opi</path>
      <macros>
        <include_parent_macros>true</include_parent_macros>
      </macros>
      <replace>1</replace>
      <description></description>
    </action>
  </actions>
  <y>162</y>
  <wrap_words>false</wrap_words>
  <tooltip></tooltip>
  <x>372</x>
</widget>
<widget typeId="org.csstudio.opibuilder.widgets.Label" version="1.0.0">
  <visible>true</visible>
  <vertical_alignment>1</vertical_alignment>
  <wuid>-62d437e7:1744e347940:-7c67</wuid>
```

<auto_size>false</auto_size>
<scripts />
<height>20</height>
<name>Label_21</name>
<scale_options>
  <width_scalable>true</width_scalable>
  <height_scalable>true</height_scalable>
  <keep_wh_ratio>false</keep_wh_ratio>
</scale_options>
<transparent>true</transparent>
<background_color>
  <color red="255" green="255" blue="255" />
</background_color>
<foreground_color>
  <color red="0" green="0" blue="0" />
</foreground_color>
<widget_type>Label</widget_type>
<enabled>true</enabled>
<text>PMT2</text>

  <opifont.name fontName="Sans" height="10" style="0">Default</opifont.name>

<width>80</width>
<border_style>0</border_style>
<rules />
<border_width>1</border_width>
<border_color>
  <color red="0" green="128" blue="255" />
</border_color>
<horizontal_alignment>1</horizontal_alignment>
<actions hook="true" hook_all="false">
  <action type="OPEN_DISPLAY">
    <path>behnam-test11.opi</path>
    <macros>
      <include_parent_macros>true</include_parent_macros>
    </macros>
    <replace>1</replace>

```
    <description></description>
   </action>
  </actions>
  <y>162</y>
  <wrap_words>false</wrap_words>
  <tooltip></tooltip>
  <x>317</x>
 </widget>
 <widget typeId="org.csstudio.opibuilder.widgets.Label" version="1.0.0">
  <visible>true</visible>
  <vertical_alignment>1</vertical_alignment>
  <wuid>-62d437e7:1744e347940:-454</wuid>
  <auto_size>false</auto_size>
  <scripts />
  <height>31</height>
  <name>Label</name>
  <scale_options>
   <width_scalable>true</width_scalable>
   <height_scalable>true</height_scalable>
   <keep_wh_ratio>false</keep_wh_ratio>
  </scale_options>
  <transparent>true</transparent>
  <background_color>
   <color red="255" green="255" blue="255" />
  </background_color>
  <foreground_color>
   <color red="0" green="0" blue="0" />
  </foreground_color>
  <widget_type>Label</widget_type>
  <enabled>true</enabled>
  <text>ICARUS Top Level Slow Control</text>
  <font>
   <opifont.name fontName="Sans" height="10" style="1">Default Bold</opifont.name>
  </font>
  <width>487</width>
  <border_style>0</border_style>
  <rules />
```

```
  <border_width>1</border_width>
  <border_color>
    <color red="0" green="128" blue="255" />
  </border_color>
  <horizontal_alignment>1</horizontal_alignment>
  <actions hook="false" hook_all="false" />
  <y>18</y>
  <wrap_words>false</wrap_words>
  <tooltip></tooltip>
  <x>186</x>
</widget>
<widget typeId="org.csstudio.opibuilder.widgets.Rectangle" version="1.0.0">
  <border_alarm_sensitive>false</border_alarm_sensitive>
  <visible>true</visible>
  <fill_level>0.0</fill_level>
  <line_color>
    <color red="128" green="0" blue="255" />
  </line_color>
  <wuid>-21a7a3ea:175547e04f9:-6fd8</wuid>
  <bg_gradient_color>
    <color red="255" green="255" blue="255" />
  </bg_gradient_color>
  <scripts />
  <height>55</height>
  <anti_alias>true</anti_alias>
  <name>Rectangle</name>
  <forecolor_alarm_sensitive>false</forecolor_alarm_sensitive>
  <alpha>255</alpha>
  <scale_options>
    <width_scalable>true</width_scalable>
    <height_scalable>true</height_scalable>
    <keep_wh_ratio>false</keep_wh_ratio>
  </scale_options>
  <transparent>false</transparent>
  <pv_name></pv_name>
  <background_color>
    <color name="Minor" red="255" green="128" blue="0" />
```

```
    </background_color>
    <foreground_color>
      <color red="255" green="0" blue="0" />
    </foreground_color>
    <widget_type>Rectangle</widget_type>
    <enabled>true</enabled>
    <fg_gradient_color>
      <color red="255" green="255" blue="255" />
    </fg_gradient_color>
    <backcolor_alarm_sensitive>false</backcolor_alarm_sensitive>
    <font>
      <opifont.name fontName="Sans" height="10" style="0">Default</opifont.name>
    </font>
    <width>103</width>
    <line_style>0</line_style>
    <border_style>0</border_style>
    <rules />
    <pv_value />
    <border_width>1</border_width>
    <line_width>0</line_width>
    <horizontal_fill>true</horizontal_fill>
    <border_color>
      <color name="Minor" red="255" green="128" blue="0" />
    </border_color>
    <actions hook="false" hook_all="false" />
    <y>18</y>
    <tooltip>$(pv_name)
$(pv_value)</tooltip>
    <x>18</x>
    <gradient>false</gradient>
  </widget>
  <widget typeId="org.csstudio.opibuilder.widgets.Rectangle" version="1.0.0">
    <border_alarm_sensitive>false</border_alarm_sensitive>
    <visible>true</visible>
    <fill_level>0.0</fill_level>
    <line_color>
      <color red="128" green="0" blue="255" />
```

```
</line_color>
<wuid>-21a7a3ea:175547e04f9:-6fce</wuid>
<bg_gradient_color>
  <color red="255" green="255" blue="255" />
</bg_gradient_color>
<scripts />
<height>55</height>
<anti_alias>true</anti_alias>
<name>Rectangle_29</name>
<forecolor_alarm_sensitive>false</forecolor_alarm_sensitive>
<alpha>255</alpha>
<scale_options>
  <width_scalable>true</width_scalable>
  <height_scalable>true</height_scalable>
  <keep_wh_ratio>false</keep_wh_ratio>
</scale_options>
<transparent>false</transparent>
<pv_name></pv_name>
<background_color>
  <color name="Minor" red="255" green="128" blue="0" />
</background_color>
<foreground_color>
  <color red="255" green="0" blue="0" />
</foreground_color>
<widget_type>Rectangle</widget_type>
<enabled>true</enabled>
<fg_gradient_color>
  <color red="255" green="255" blue="255" />
</fg_gradient_color>
<backcolor_alarm_sensitive>false</backcolor_alarm_sensitive>
<font>
  <opifont.name fontName="Sans" height="10" style="0">Default</opifont.name>
</font>
<width>103</width>
<line_style>0</line_style>
<border_style>0</border_style>
<rules />
```

```
    <pv_value />
    <border_width>1</border_width>
    <line_width>0</line_width>
    <horizontal_fill>true</horizontal_fill>
    <border_color>
      <color name="Minor" red="255" green="128" blue="0" />
    </border_color>
    <actions hook="false" hook_all="false" />
    <y>150</y>
    <tooltip>$(pv_name)
$(pv_value)</tooltip>
    <x>18</x>
    <gradient>false</gradient>
  </widget>
  <widget typeId="org.csstudio.opibuilder.widgets.Rectangle" version="1.0.0">
    <border_alarm_sensitive>false</border_alarm_sensitive>
    <visible>true</visible>
    <fill_level>0.0</fill_level>
    <line_color>
      <color red="128" green="0" blue="255" />
    </line_color>
    <wuid>-21a7a3ea:175547e04f9:-6fc7</wuid>
    <bg_gradient_color>
      <color red="255" green="255" blue="255" />
    </bg_gradient_color>
    <scripts />
    <height>55</height>
    <anti_alias>true</anti_alias>
    <name>Rectangle_30</name>
    <forecolor_alarm_sensitive>false</forecolor_alarm_sensitive>
    <alpha>255</alpha>
    <scale_options>
      <width_scalable>true</width_scalable>
      <height_scalable>true</height_scalable>
      <keep_wh_ratio>false</keep_wh_ratio>
    </scale_options>
    <transparent>false</transparent>
```

```
    <pv_name></pv_name>
    <background_color>
      <color name="Minor" red="255" green="128" blue="0" />
    </background_color>
    <foreground_color>
      <color red="255" green="0" blue="0" />
    </foreground_color>
    <widget_type>Rectangle</widget_type>
    <enabled>true</enabled>
    <fg_gradient_color>
      <color red="255" green="255" blue="255" />
    </fg_gradient_color>
    <backcolor_alarm_sensitive>false</backcolor_alarm_sensitive>
    <font>
      <opifont.name fontName="Sans" height="10" style="0">Default</opifont.name>
    </font>
    <width>103</width>
    <line_style>0</line_style>
    <border_style>0</border_style>
    <rules />
    <pv_value />
    <border_width>1</border_width>
    <line_width>0</line_width>
    <horizontal_fill>true</horizontal_fill>
    <border_color>
      <color name="Minor" red="255" green="128" blue="0" />
    </border_color>
    <actions hook="false" hook_all="false" />
    <y>87</y>
    <tooltip>$(pv_name)
$(pv_value)</tooltip>
    <x>18</x>
    <gradient>false</gradient>
  </widget>
  <widget typeId="org.csstudio.opibuilder.widgets.Label" version="1.0.0">
    <visible>true</visible>
    <vertical_alignment>1</vertical_alignment>
```

<wuid>-21a7a3ea:175547e04f9:-6dac</wuid>
<auto_size>false</auto_size>
<scripts />
<height>55</height>
<name>Label_24</name>
<scale_options>
<width_scalable>true</width_scalable>
<height_scalable>true</height_scalable>
<keep_wh_ratio>false</keep_wh_ratio>
</scale_options>
<transparent>true</transparent>
<background_color>
<color red="255" green="255" blue="255" />
</background_color>
<foreground_color>
<color red="0" green="0" blue="0" />
</foreground_color>
<widget_type>Label</widget_type>
<enabled>true</enabled>
<text> PMT
HV
distribution</text>

<opifont.name fontName="Sans" height="10" style="1">Default Bold</opifont.name>

<width>103</width>
<border_style>0</border_style>
<rules />
<border_width>1</border_width>
<border_color>
<color red="0" green="128" blue="255" />
</border_color>
<horizontal_alignment>1</horizontal_alignment>
<actions hook="true" hook_all="false">
<action type="OPEN_DISPLAY">
<path>Behnam-test22.opi</path>
<macros>

<include_parent_macros>true</include_parent_macros>
</macros>
<replace>1</replace>
<description></description>
</action>
</actions>
<y>87</y>
<wrap_words>false</wrap_words>
<tooltip></tooltip>
<x>18</x>
</widget>
<widget typeId="org.csstudio.opibuilder.widgets.Label" version="1.0.0">
<visible>true</visible>
<vertical_alignment>1</vertical_alignment>
<wuid>-21a7a3ea:175547e04f9:-6cdc</wuid>
<auto_size>false</auto_size>
<scripts />
<height>55</height>
<name>Label_25</name>
<scale_options>
<width_scalable>true</width_scalable>
<height_scalable>true</height_scalable>
<keep_wh_ratio>false</keep_wh_ratio>
</scale_options>
<transparent>true</transparent>
<background_color>
<color red="255" green="255" blue="255" />
</background_color>
<foreground_color>
<color red="0" green="0" blue="0" />
</foreground_color>
<widget_type>Label</widget_type>
<enabled>true</enabled>
<text>PMT
Digitizers</text>
<font>
<opifont.name fontName="Sans" height="10" style="1">Default Bold</opifont.name>

```
  </font>
  <width>103</width>
  <border_style>0</border_style>
  <rules />
  <border_width>1</border_width>
  <border_color>
    <color red="0" green="128" blue="255" />
  </border_color>
  <horizontal_alignment>1</horizontal_alignment>
  <actions hook="true" hook_all="false">
    <action type="OPEN_DISPLAY">
      <path>Behnam-test23.opi</path>
      <macros>
        <include_parent_macros>true</include_parent_macros>
      </macros>
      <replace>1</replace>
      <description></description>
    </action>
  </actions>
  <y>150</y>
  <wrap_words>false</wrap_words>
  <tooltip></tooltip>
  <x>18</x>
</widget>
<widget typeId="org.csstudio.opibuilder.widgets.Label" version="1.0.0">
  <visible>true</visible>
  <vertical_alignment>1</vertical_alignment>
  <wuid>-21a7a3ea:175547e04f9:5ea3</wuid>
  <auto_size>false</auto_size>
  <scripts />
  <height>55</height>
  <name>Label_26</name>
  <scale_options>
    <width_scalable>true</width_scalable>
    <height_scalable>true</height_scalable>
    <keep_wh_ratio>false</keep_wh_ratio>
  </scale_options>
```

<transparent>true</transparent>
<background_color>
<color red="255" green="255" blue="255" />
</background_color>
<foreground_color>
<color red="0" green="0" blue="0" />
</foreground_color>
<widget_type>Label</widget_type>
<enabled>true</enabled>
<text>PMT
Primary
HV</text>

<opifont.name fontName="Sans" height="10" style="1">Default Bold</opifont.name>

<width>103</width>
<border_style>0</border_style>
<rules />
<border_width>1</border_width>
<border_color>
<color red="0" green="128" blue="255" />
</border_color>
<horizontal_alignment>1</horizontal_alignment>
<actions hook="true" hook_all="false">
<action type="OPEN_DISPLAY">
<path>behnam-test21.opi</path>
<macros>
<include_parent_macros>true</include_parent_macros>
</macros>
<replace>1</replace>
<description></description>
</action>
</actions>
<y>18</y>
<wrap_words>false</wrap_words>
<tooltip></tooltip>
<x>18</x>

</widget>
</display>

In the following part, some extra and new layouts regarding to functionality have been represented explicitly.

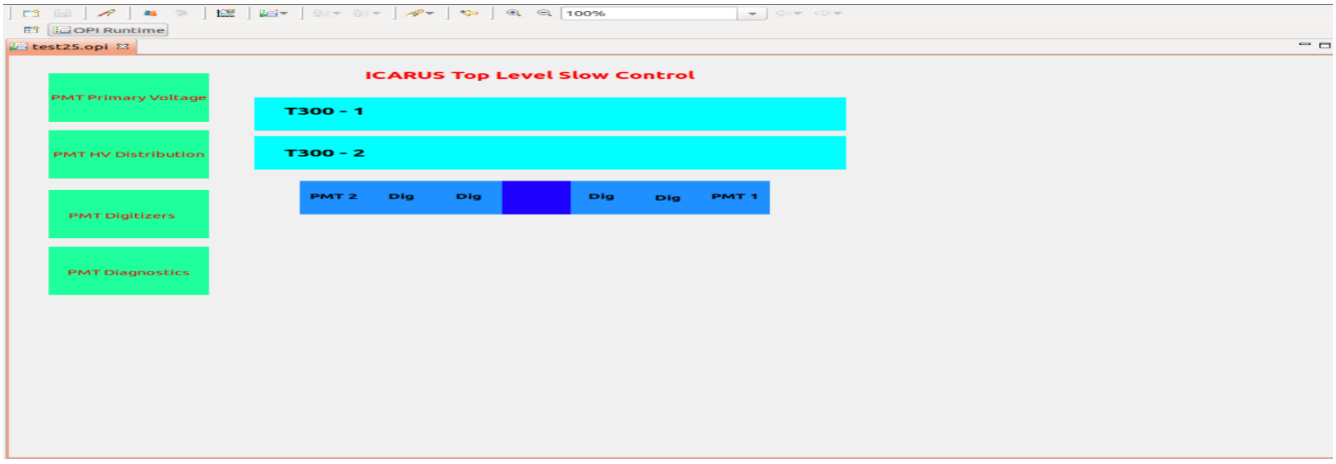

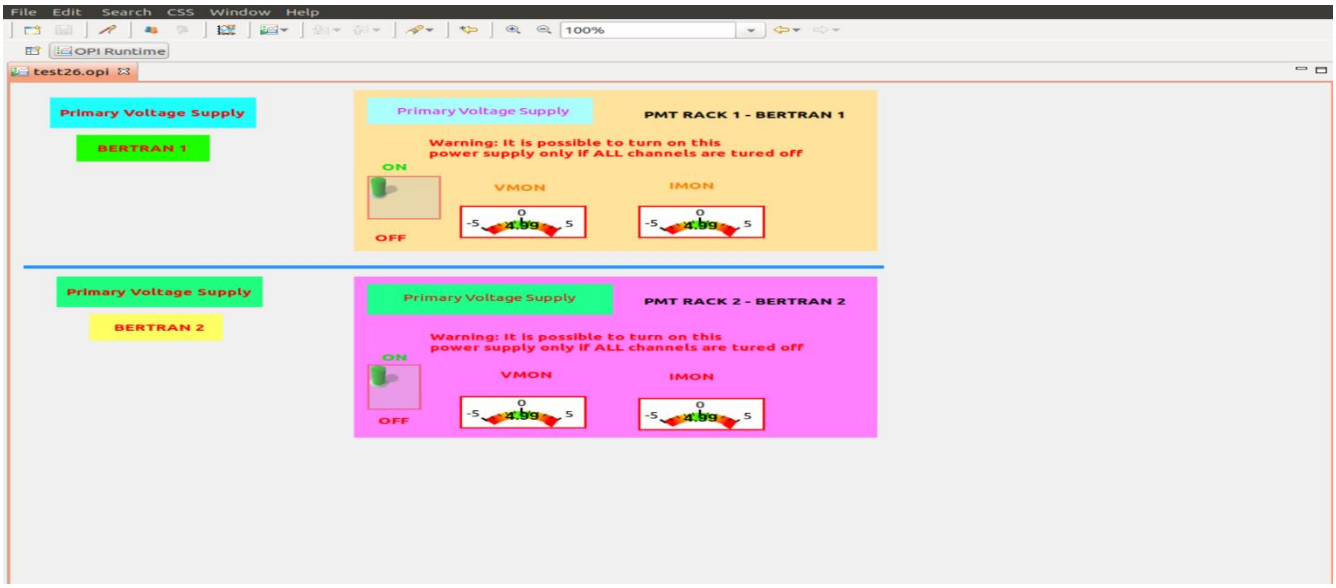

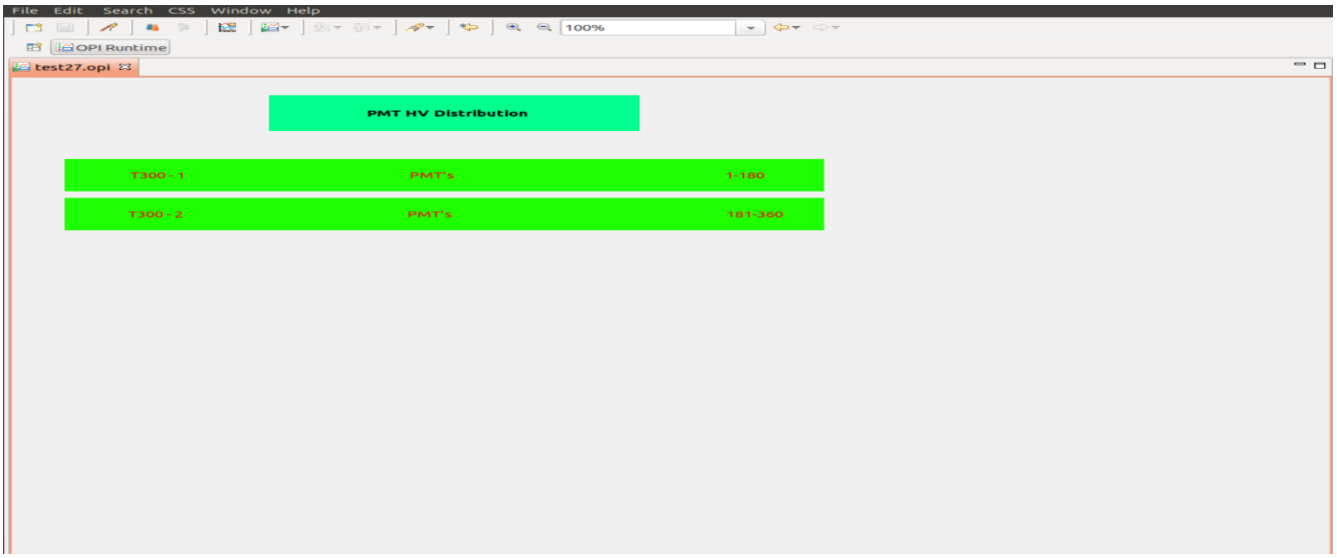
File Edit Search CSS Window Help
100%
OPI Runtime
test27.opi
PMT HV Distribution
T300 - 1
PMT's
1-180
T300 - 2
PMT's
181-360

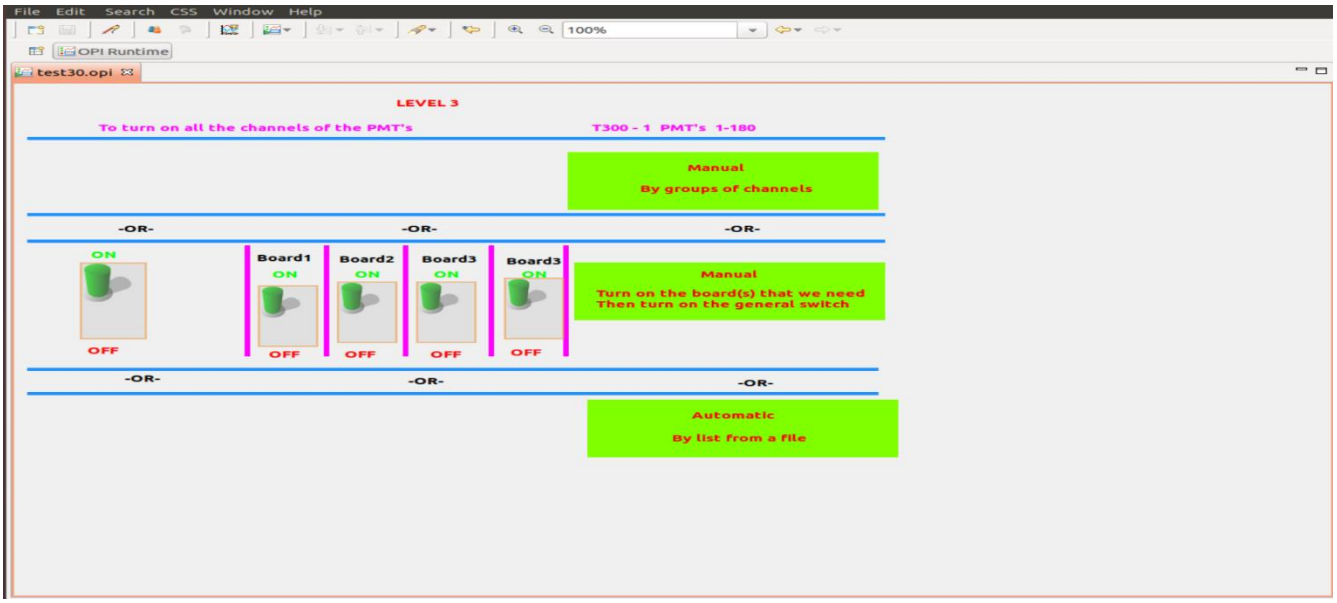
File Edit Search CSS Window Help
100%
OPI Runtime
test30.opi
LEVEL 3
To turn on all the channels of the PMT's
T300 - 1 PMT's 1-180
Manual
By groups of channels
-OR-
-OR-
-OR-
ON
OFF
Board1
Board2
Board3
Board3
ON
OFF
Manual
Turn on the board(s) that we need
Then turn on the general switch
-OR-
-OR-
-OR-
Automatic
By list from a file

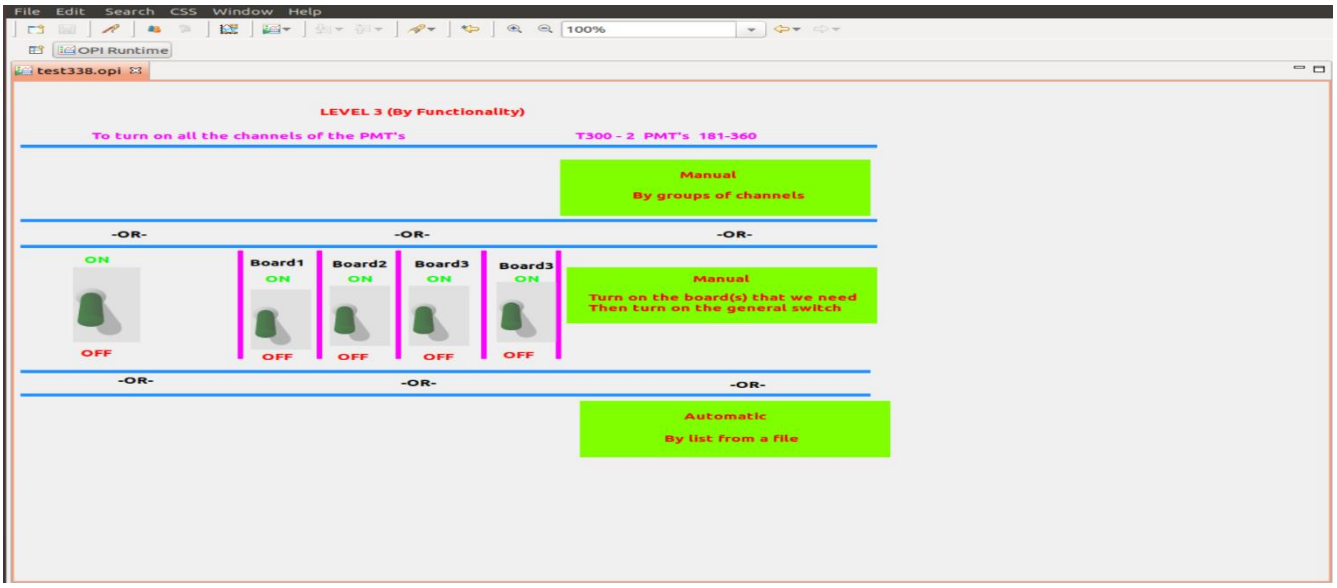
File Edit Search CSS Window Help
100%
OPI Runtime
test338.opi
LEVEL 3 (By Functionality)
To turn on all the channels of the PMT's
T300 - 2 PMT's 181-360
Manual
By groups of channels
-OR-
-OR-
-OR-
ON
OFF
Board1
Board2
Board3
Board3
Manual
Turn on the board(s) that we need
Then turn on the general switch
-OR-
-OR-
-OR-
Automatic
By list from a file


File Edit Search CSS Window Help
100%
OPI Runtime
test29.opi
ICARUS - 8 VME Crates with PMT Digitizers
Top Dig - WW Bot
Top Dig - WE Bot
Top Dig - EW Bot
Top Dig - EE Bot

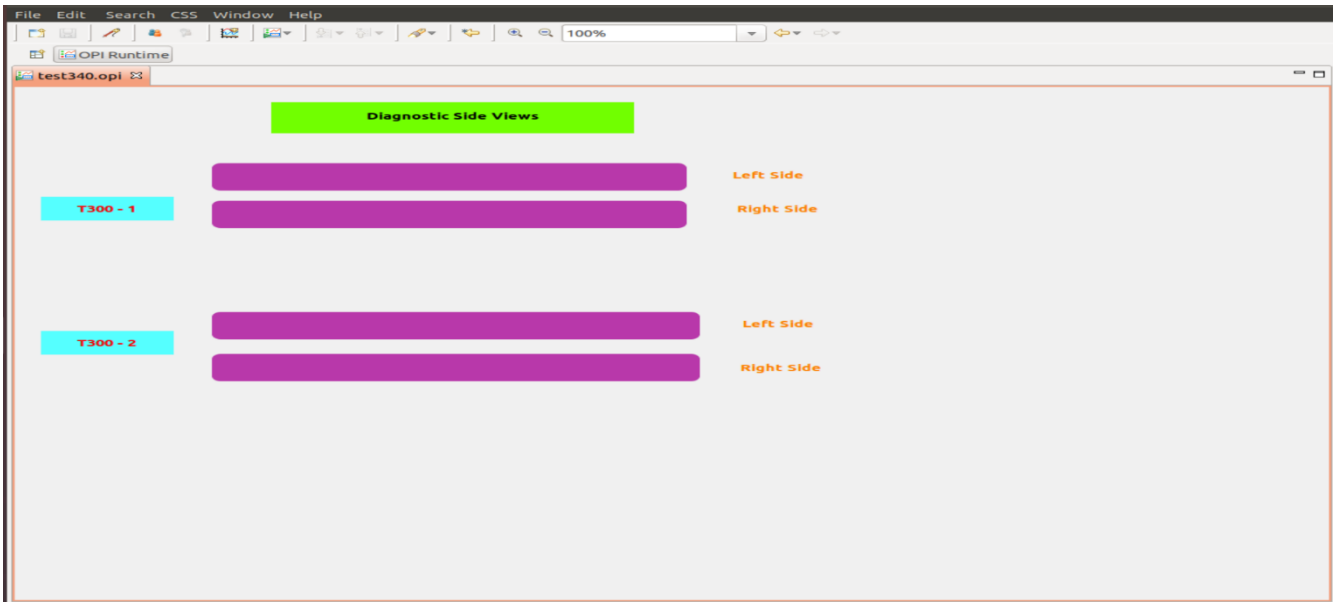
File Edit Search CSS Window Help
100%
OPI Runtime
test340.opi
Diagnostic Side Views
T300 - 1
Left Side
Right Side
T300 - 2
Left Side
Right Side

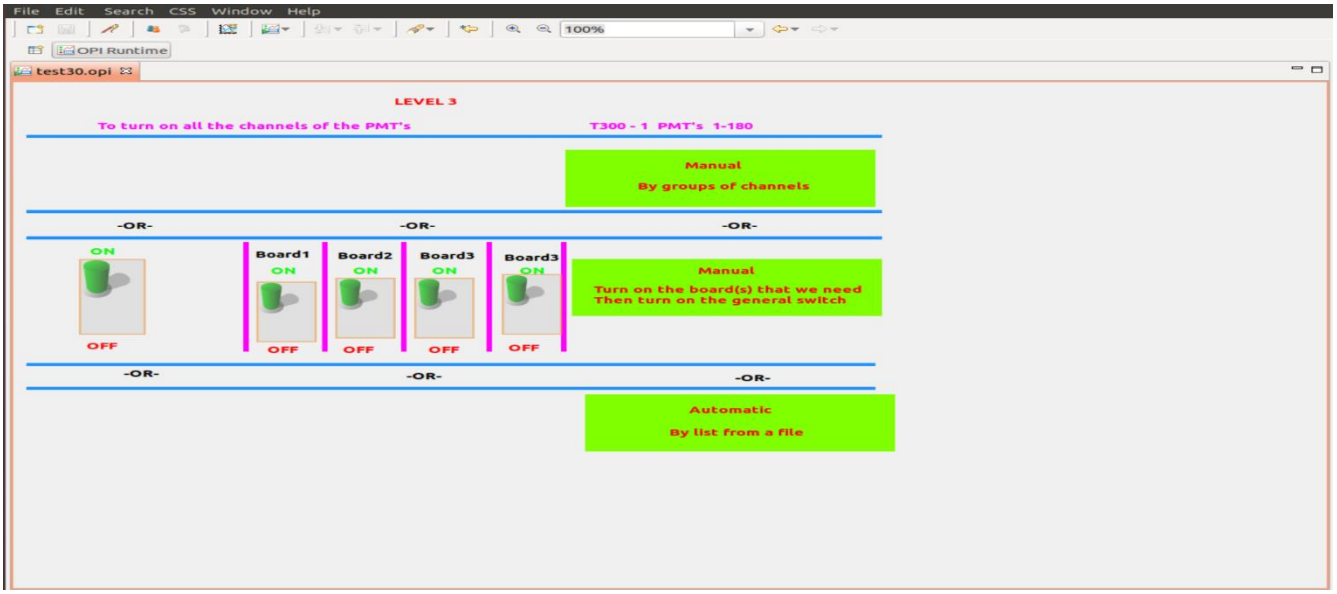
File Edit Search CSS Window Help
100%
OPI Runtime
test30.opi
LEVEL 3
To turn on all the channels of the PMT's
T300 - 1 PMT's 1-180
Manual
By groups of channels
-OR-
-OR-
-OR-
ON
OFF
Board1
Board2
Board3
Board3
Manual
Turn on the board(s) that we need
Then turn on the general switch
-OR-
-OR-
-OR-
Automatic
By list from a file

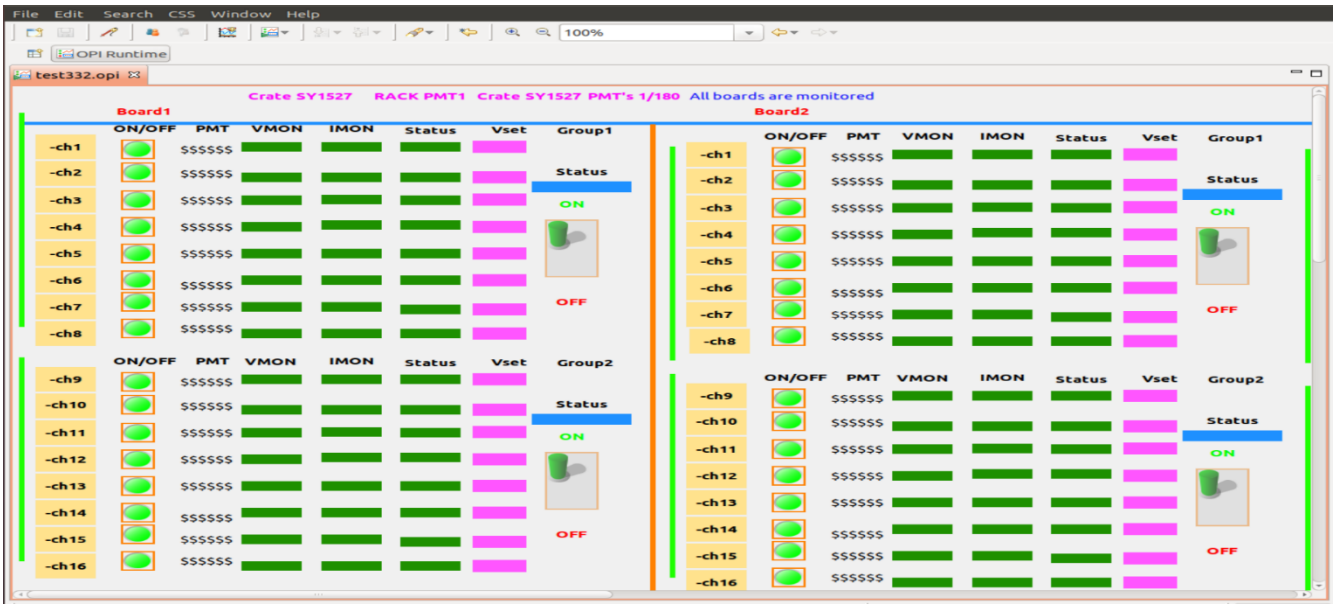
File Edit Search CSS Window Help
100%
OPI Runtime
test332.opi
Crate SY1527 RACK PMT1 Crate SY1527 PMT's 1/180 All boards are monitored
Board1
Board2
ON/OFF PMT VMON IMON Status Vset Group1
ON/OFF PMT VMON IMON Status Vset Group2
-ch1 -ch2 -ch3 -ch4 -ch5 -ch6 -ch7 -ch8
-ch9 -ch10 -ch11 -ch12 -ch13 -ch14 -ch15 -ch16
$$$$$$
Status
ON
OFF

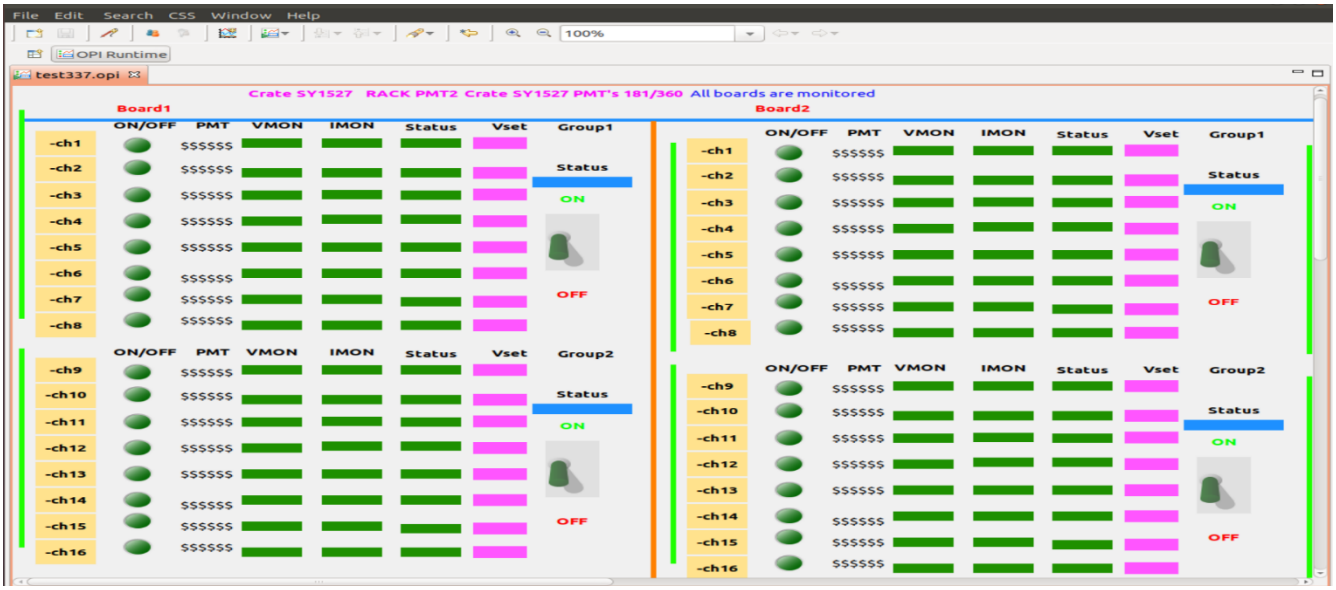
File Edit Search CSS Window Help
100%
OPI Runtime
test337.opi
Crate SY1527 RACK PMT2 Crate SY1527 PMT's 181/360 All boards are monitored
Board1
Board2
ON/OFF PMT VMON IMON Status Vset Group1
ON/OFF PMT VMON IMON Status Vset Group2
-ch1 -ch2 -ch3 -ch4 -ch5 -ch6 -ch7 -ch8
-ch9 -ch10 -ch11 -ch12 -ch13 -ch14 -ch15 -ch16
$$$$$$
Status
ON
OFF

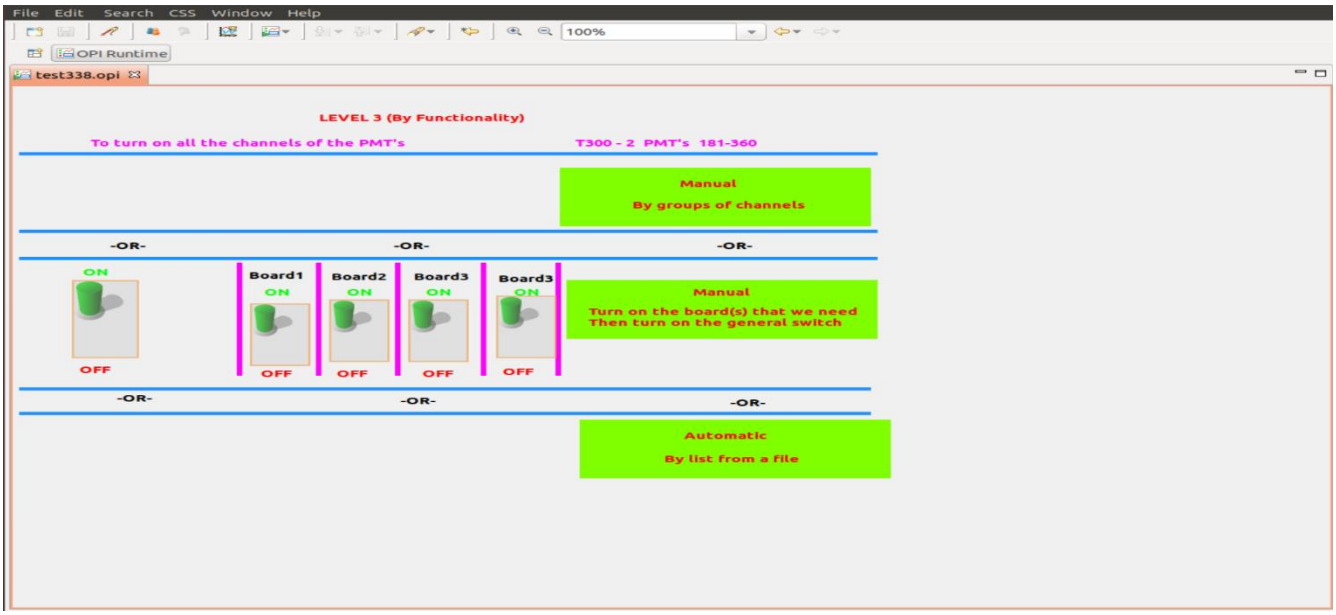
File Edit Search CSS Window Help
100%
OPI Runtime
test338.opi
LEVEL 3 (By Functionality)
To turn on all the channels of the PMT's
T300 - 2 PMT's 181-360
Manual
By groups of channels
-OR-
-OR-
-OR-
ON
OFF
Board1
ON
OFF
Board2
ON
OFF
Board3
ON
OFF
Board3
ON
OFF
Manual
Turn on the board(s) that we need
Then turn on the general switch
-OR-
-OR-
-OR-
Automatic
By list from a file

Acknowledgements

So many thanks to my kind wife and her warm presence in every moment of my thesis. Special thanks to all my family members in which they accompanied me in my PhD studies warmly.

I would like to express my special thankfulness to my supervisors, Prof. Vincenzo Bellini, Prof. Giuseppe Andronico and Prof. Corrado Santoro, which provided very kind guidance, leading me to the results of this PhD research project. I really appreciate their accurate and uninterrupted supervision, even at the time of the COVID19 pandemic.

I would also like to express my appreciations to Mr. Giuseppe Sava as an expert of slow control for his kind collaboration and the dedicated time to this project. Special thanks to Dr. Francesco Tortorici for his kind help.